PB-245 829

OUTDOOR SMOG CHAMBER STUDIES. EFFECT OF HYDROCARBON REDUCTION ON NITROGEN DIOXIDE

Harvey Jeffries, et al

North Carolina University at Chapel Hill

Prepared for:

Environmental Science Research Laboratory

June 1975

DISTRIBUTED BY:

NTIS

National Technical Information Service
U. S. DEPARTMENT OF COMMERCE

301011

PB 245 829

EPA-650/3-75-011

June 1975

Ecological Research Series

OUTDOOR SMOG CHAMBER STUDIES

EFFECT OF HYDROCARBON REDUCTION ON NITROGEN DIOXIDE

Reproduced by
NATIONAL TECHNICAL
INFORMATION SERVICE
US Department of Commerce
Springfield, VA. 22151

U.S. Environmental Protection Agency
Office of Research and Development
Washington, D.C. 20460

TECHNICAL REPORT DATA

(Please read Instructions on the reverse before completing)

1. REPORT NO.
EPA-650/3-75-011

2.

3. RECIPIENT'S ACCESSION NO.

4. TITLE AND SUBTITLE
Outdoor Smog Chamber Studies: Effect of Hydrocarbon Reduction on Nitrogen Dioxide

5. REPORT DATE
June 1975

6. PERFORMING ORGANIZATION CODE

7. AUTHOR(S)
Jeffries, Harvey E.
Fox, Donald L.
Kamens, Richard M.

8. PERFORMING ORGANIZATION REPORT NO.

9. PERFORMING ORGANIZATION NAME AND ADDRESS
Department of Environmental Sciences & Engineering
School of Public Health
University of North Carolina
Chapel Hill, NC 27514

10. PROGRAM ELEMENT NO.
1AA008

11. CONTRACT/GRANT NO.
800916

12. SPONSORING AGENCY NAME AND ADDRESS
Environmental Sciences Research Laboratory
Environmental Protection Agency
Research Triangle Park, NC 27711

13. TYPE OF REPORT AND PERIOD COVERED
Interim Report (6/15/72-1/31/75)

14. SPONSORING AGENCY CODE

15. SUPPLEMENTARY NOTES

16. ABSTRACT

A 312 m^3 (11,018 ft^3) Teflon film outdoor smog chamber was constructed in rural North Carolina. The chamber was operated with natural conditions of solar radiation, termperature and relative humidity which existed at the time of a run. Ninety-two 12-hour runs using propylene and oxides of nitrogen were conducted to assess the performance of the system. A photochemical model, in which only the light intensity magnitude and pattern and the rate of heterogeneous surface reactions were changed, was used to compare the outdoor results with those of three indoor chambers. Good agreement was found in all cases. One-hundred-thirty 12-hour runs were conducted using a simulated urban hydrocarbon mix and oxides of nitrogen. Reduction of the hydrocarbon concentration resulted in reductions of nitrogen dioxide (NO_2) maximum concentration and, for large reductions, the daytime NO_2 dosage. Other factors investigated included NO_2 to NO ratio at constant NO_x, effect of slow dilution, and results of extended 24-hour and 36-hour runs.

17. KEY WORDS AND DOCUMENT ANALYSIS

a. DESCRIPTORS	b. IDENTIFIERS/OPEN ENDED TERMS	c. COSATI Field/Group
Smog *Smog Chambers* *Hydrocarbons* *NO_2 (Nitrogen Dioxide)* *Photochemical Reactions* *Model* *Photochemical*		

PRICES SUBJECT TO CHANGE

18. DISTRIBUTION STATEMENT
Release Unlimited

19. SECURITY CLASS *(This Report)*
Unclassified

20. SECURITY CLASS *(This page)*
Unclassified

21. NO. OF PAGES
223

22. PRICE
7.25 - 2.25

1.

EPA-650/3-75-011

OUTDOOR SMOG CHAMBER STUDIES

EFFECT OF HYDROCARBON REDUCTION ON NITROGEN DIOXIDE

by

Harvey Jeffries, Donald Fox, and Richard Kamens

University of North Carolina
Chapel Hill, North Carolina 27514

Grant No. 800916
ROAP No. 21AZJ-008
Program Element No. 1AA008

EPA Project Officer: Basil Dimitriades

Chemistry and Physics Laboratory
National Environmental Research Center
Research Triangle Park, North Carolina 27711

Prepared for

U.S. ENVIRONMENTAL PROTECTION AGENCY
Office of Research and Development
Washington, D. C. 20460

June 1975

ia

EPA REVIEW NOTICE

This report has been reviewed by the National Environmental Research Center - Research Triangle Park, Office of Research and Development, EPA, and approved for publication. Approval does not signify that the contents necessarily reflect the views and policies of the Environmental Protection Agency, nor does mention of trade names or commercial products constitute endorsement or recommendation for use.

RESEARCH REPORTING SERIES

Research reports of the Office of Research and Development, U.S. Environmental Protection Agency, have been grouped into series. These broad categories were established to facilitate further development and application of environmental technology. Elimination of traditional grouping was consciously planned to foster technology transfer and maximum interface in related fields. These series are:

1. ENVIRONMENTAL HEALTH EFFECTS RESEARCH
2. ENVIRONMENTAL PROTECTION TECHNOLOGY
3. ECOLOGICAL RESEARCH
4. ENVIRONMENTAL MONITORING
5. SOCIOECONOMIC ENVIRONMENTAL STUDIES
6. SCIENTIFIC AND TECHNICAL ASSESSMENT REPORTS
9. MISCELLANEOUS

This report has been assigned to the ENVIRONMENTAL PROTECTION TECHNOLOGY series. This series describes research performed to develop and demonstrate instrumentation, equipment and methodology to repair or prevent environmental degradation from point and non-point sources of pollution. This work provides the new or improved technology required for the control and treatment of pollution sources to meet environmental quality standards.

This document is available to the public for sale through the National Technical Information Service, Springfield, Virginia 22161.

Publication No. EPA-650/3-75-011

ABSTRACT

A 312 m^3 (11,018 ft^3) Teflon film outdoor smog chamber was constructed in rural North Carolina. The chamber was operated with natural conditions of solar radiation, temperature and relative humidity which existed at the time of a run. Ninety-two 12-hour runs using propylene and oxides of nitrogen were conducted to assess the performance of the system. A photochemical model, in which only the light intensity magnitude and pattern and the rate of heterogeneous surface reactions were changed, was used to compare the outdoor results with those of three indoor chambers. Good agreement was found in all cases. One-hundred-thirty 12-hour runs were conducted using a simulated urban hydrocarbon mix and oxides of nitrogen. Reduction of the hydrocarbon concentration resulted in reductions of nitrogen dioxide (NO_2) maximum concentration and, for large reductions, the daytime NO_2 dosage. Other factors investigated included NO_2 to NO ratio at constant NO_x, effect of slow dilution, and results of extended 24-hour and 36-hour runs.

CONTENTS

Page

Abstract iii

Table of Contents v

List of Figures vi

List of Tables xi

Acknowledgments xiii

Sections

I Summary and Conclusions 1

II Recommendations 5

III Introduction 7

IV Design and Construction of Smog Chamber Facility 14

V Experimental Methods and Procedures 25

VI Results and Discussion, Part I: Facility Performance 53

VII Results and Discussion, Part II: Effects of Hydrocarbon Reduction on Nitrogen Dioxide Concentrations 121

VIII Other Results and Observations 165

IX References 177

X Glossary 182

XI Appendices 186

Preceding page blank

LIST OF FIGURES

No.		Page
1	Dependence of nitrogen dioxide maximum concentration on initial nitrogen oxides and nonmethane hydrocarbon in the Bureau of Mines study by Dimitriades	9
2	Idealized representation of NO, NO_2, O_3, aerosol and PAN profiles for various initial conditions	10
3	The University of North Carolina outdoor smog chamber	18
4	Schematic of UNC outdoor smog chamber	19
5	Orientation of UNC outdoor smog chamber with respect to seasonal sunrise and sunset positions	21
6	Solar altitude and zenith angle at noon at the UNC outdoor smog chamber for each month	21
7	Flowchart of on-site data treatment procedures	30
8	Flowchart of preliminary off-site data treatment procedures	31
9	Flowchart of final off-site data treatment procedures	32
10	CAPI-6 definition of NO_2 formation rate applied to typical indoor and outdoor smog chamber profiles	41
11	Average daily solar radiation on a horizontal surface in the USA for January	49
12	Average daily solar radiation on a horizontal surface in the USA for July	49
13	Theoretical solar radiation on a surface normal to the solar beam as a function of month	51
14	Theoretical solar radiation on a horizontal surface as a function of month	51
15	Specific photolysis rate for nitrogen dioxide and incident total solar radiation and ultraviolet radiation as a function of time for September 18, 1974	58
16	Specific photolysis rate for nitrogen dioxide and incident total solar radiation and ultraviolet radiation as a function of time for September 19, 1974	59

LIST OF FIGURES (CONTINUED)

No.		Page
17	Selected air temperature profiles in outdoor smog chamber	61
18	Selected dewpoint profiles in outdoor smog chamber	61
19	Comparison of three different NO_2 measurement methods in a propylene/NO_x system in the outdoor smog chamber	64
20	Calibration and correction technique for environmental chromatograph	67
21	Sample gas chromatogram of hydrocarbon mix from chamber air immediately after injection	73
22	Example of NO oxidation run in background air	76
23	Example of reproducibility between two chamber halves for propylene	80
24	Example of reproducibility between two chamber halves for urban hydrocarbon mix	80
25	Example of reproducibility between two chamber halves for urban hydrocarbon mix	81
26	Effect of hydrocarbon reduction and solar radiation	82
27	Effect of hydrocarbon and solar radiation	82
28	Comparison of total solar radiation for a totally clear day and a partly cloudy day	83
29	Comparison of mix (olefins and paraffins) and mix with toluene	85
30	Comparison of mix (olefins and paraffins) and mix with toluene	86
31	Comparison of (mix with toluene) with (mix, toluene and m-xylene)	87
32	Comparison of mix and mix with m-xylene as nonmethane hydrocarbon	87
33	Comparison of mix and propylene as nonmethane hydrocarbon	89

LIST OF FIGURES (CONTINUED)

No.		Page
34	Comparison of mix and propylene as nonmethane hydrocarbon	89
35	Variable light intensity model of May 25, 1974	94
36	Dual matched propylene run in UNC outdoor smog chamber	94
37	Actual solar radiation for May 25, 1974	95
38	Variable light intensity model of May 7, 1974	96
39	Dual matched propylene run in UNC outdoor chamber	96
40	Actual solar radiation for May 7, 1974	97
41	Constant light intensity model	99
42	Ramping light intensity model	99
43	Fast HNO_2 reaction model	100
44	Fast HNO_2 reaction model	100
45	Actual profiles for EPA-325	104
46	UNC model of EPA-325	105
47	Actual profiles of run EC-17 in SAPRC chamber at Riverside, California	106
48	UNC model of EC-17	107
49	Actual profiles of run EC-17 in SAPRC chamber at Riverside, California	108
50	UNC model of run EC-17	109
51	Actual profiles of EC-18 in SAPRC chamber at Riverside, California	110
52	UNC model of EC-18	111
53	Actual profiles of EC-18 in SAPRC chamber at Riverside, California.	112
54	UNC model of run EC-18	113

LIST OF FIGURES(CONTINUED)

No.		Page
55	Actual profiles of a Lockheed run	116
56	UNC model of a Lockheed run	117
57	Actual profiles of Bureau of Mines run	119
58	Mix run for comparison with BOM run	120
59	Mean nitrogen dioxide concentration as a function of mean initial oxides of nitrogen for urban hydrocarbon mix in UNC outdoor smog chamber	125
60	Nitrogen dioxide maximum concentration as a function of initial oxides of nitrogen for individual runs for urban hydrocarbon mix in UNC outdoor chamber	126
61	Effect of single light pulse on nitrogen oxides conversion rate in a system initially containing NO_x/propylene	133
62	Example of rapid changes in solar radiation accelerating occurrence of nitrogen dioxide maximum	133
63	Nitrogen dioxide profiles at constant initial NO_x of 0.51 ppm	136
64	Nitrogen dioxide profiles at constant initial NO_x of 0.36 ppm	137
65	Nitrogen dioxide profiles at constant initial NO_x of 0.24 ppm	138
66	Nitrogen dioxide profiles for October 5 and 6, 1974	139
67	Total solar radiation for a clear summer and a clear fall day	140
68	Profiles for dual run	141
69	Profiles for dual run	142
70	Mean nitrogen dioxide 10-hour average concentration as a function of mean initial oxides of nitrogen for urban hydrocarbon mix in UNC outdoor chamber	144
71	Extended run of June 16-17, 1974	154
72	Total solar radiation for June 16, 1974	155

LIST OF FIGURES(CONTINUED)

No.		Page
73	Extended dual run of June 12-13, 1974	156
74	Total solar radiation for June 12, 1974	157
75	Extended dual run of September 20-21, 1974	158
76	Total solar radiation for September 20, 1974	159
77	Differential percentage NO_2 run under clear sky	166
78	Differential percentage NO_2 run under clear sky	166
79	Differential percentage NO_2 run under erratic solar radiation	167
80	Differential percentage NO_2 run under erratic solar radiation	167
81	Example of dilution in a reactive system	169
82	Example of dilution in a less reactive system	169
83	Extended 36-hour run of June 12-13, 1974	172
84	Total solar radiation for June 12-13, 1974	173
85	Effect of air temperature at maximum rate on maximum nitric oxide disappearance for clear days for November 1973 and NO_x/mix in UNC outdoor smog chamber	175
86	Formaldehyde photolysis chemistry	196
87	Flow diagram of one liter quartz globe CSTR for nitrogen dioxide photolysis rate measurements	205

LIST OF TABLES

No.		Page
1	Instrument Characteristics	26
2	Calibration Sources for Gases	27
3	Simulated Urban Hydrocarbon Mixture	44
4	Selected Climatological Data for Piedmont North Carolina	46
5	Number of Days in which Percentage Maximum Possible Sunshine was Greater than or Equal to a Given value. Tuesdays and Thursdays in 1969-1971 (313 Days) bymonth	48
6	Actual Physical and Chemical Characteristics of the Chamber	54
7	Specific Photolysis Rate for Nitrogen Dioxide in Outdoor Smog Chamber During September, 1973	57
8	Relative Distribution of Individual Compounds of the Hydrocarbon Mix in Tanks and in Chamber Air After Injection	72
9	Rates of Ozone Decay in UNC Outdoor Chamber Using Background Air	75
10	Rate of NO Loss and NO_2 Formation in UNC Outdoor Chamber Using Background Air. (Initial)	77
11	Mix Performance With and Without Aromatics (Side to Side Comparison)	84
12	Mean Values of Nitrogen Dioxide Maximum and Average Concentration, Average Daily Solar Radiation as a Function of Mean Initial Nitrogen Oxides and Mean Initial Hydrocarbons	122
13	Nitrogen Dioxide Maximum Concentrations, Time to NO-NO_2 Crossover, Net NO_2 Formed, Average Solar Radiation at Initial NO_x Average Concentration of 0.361 ppm Broken Down by Initial Hydrocarbon Average Concentrations Average Solar Radiation Values	128

LIST OF TABLES (cont)

14 Pairwise Comparison of Effects of Reducing Initial Hydrocarbon Concentration on Nitrogen Dioxide Maximum Concentrations for Selected Dual Runs with Urban Hydrocarbon Mix in UNC Outdoor Chamber 135

15 Mean Nitrogen Dioxide 10 Hour Average Concentration and Mean Average to Maximum Nitrogen Dioxide Ratio Broken Down by Mean Initial Oxides of Nitrogen and Mean Initial Hydrocarbon for Urban Hydrocarbon Mix in UNC Outdoor Chamber 146

16 Pairwise Comparison of Effects of Reducing Initial Hydrocarbon Concentration on Nitrogen Dioxide Average Concentration and Dosage for Selected Dual Runs with Urban Hydrocarbon Mix in UNC Outdoor Chamber 147

17 Magnitudes of Terms in Nitrogen Dioxide Maximum Regression Equation 150

18 Pairwise Comparison of Effects of Reducing Initial Hydrocarbon Concentration on Final Nitrogen Dioxide Concentration for Selected Dual Runs with Urban Hydrocarbon Mix in UNC Outdoor Chamber 152

19 Comparison of Daytime and Nighttime Nitrogen Dioxide Dosages for Extended Dual Runs with Urban Hydrocarbon Mix in UNC Outdoor Chamber 160

20 Number of Hours Exceeding Various NO_2 Concentrations 163

21 Air Temperature Statistics at Various Chemical Events in Outdoor Chamber 175

22 Organic Symbols Used in Mechanism 197

23 Confidence Intervals on Accuracy of Measurement of Ozone at 8 PPHM 203

ACKNOWLEDGEMENTS

Several people at the Department of Environmental Sciences and Engineering, School of Public Health, University of North Carolina (UNC), and at the Environmental Protection Agency, National Environmental Research Center, Research Triangle Park (EPA), contributed substantially to the work performed on this project. Laura Alexander (UNC) served as data management assistant and masterly handled the many details of day-to-day operation. Dr. Robert Baker (UNC) was primarily responsible for experimental and data processing program development and also performed statistical analysis of data. The experimental facility was constructed by Jack Brown and Wallace Pendergraft of the UNC School of Public Health Shop under the management of Frank Malcolm. Many of the experiments were performed by UNC graduate students George Siple, Dennis Stotts, Surendra Joshi, and Charles Feigley. Charles Feigley also performed the detailed statistical analysis of instrument calibration and the majority of the statistical analysis of results. Much of the detail of the data processing was performed by UNC graduate students Chingman Kwan, Glen Sims, and Mary Witul. Robert Jones implemented most of the computer-instrument interface and the automatic control systems for the chamber. Joseph Sickles developed the theory and design of the continuous NO_2 chemical actinometer used to make chemically meaningful light intensity measurements.

In addition, Joseph Sickles and Bruce Gantner were instrumental in developing the photochemical models used. Messrs Jones, Sickles, and Gantner were also graduate students of UNC.

Drs. Marcia Dodge and John Overton of EPA's Chemistry and Physics Laboratory supplied a copy of EPA's kinetics simulation program and smog chamber data from several of the chambers modeled in this report. William Lonneman, also of EPA, implemented the gas chromatographic system used in this study.

Dr. Basil Dimitriades and other members of the Chemistry and Physics Laboratory of EPA spent many hours in discussion and planning meetings with the UNC staff throughout the project. Dr. Dimitriades' comments were especially appreciated.

Dr. Lyman Ripperton, presently associated with the Research Triangle Institute provided valuable guidance during the initial phases of the project.

SECTION I

SUMMARY AND CONCLUSIONS

One hundred thirty 12-hour runs were conducted in a large dual, outdoor smog chamber utilizing ambient conditions of solar radiation, temperature and relative humidity, and using a chemical system consisting of a simulated urban hydrocarbon mix and oxides of nitrogen (NO_x). These experiments were performed over an initial hydrocarbon range of 0.22 to 4.2 parts per million carbon (ppmC) and an initial oxides of nitrogen concentration range of 0.007 to 0.7 parts per million (ppm). The initial NO_x concentration consisted of 80% nitric oxide (NO) and 20% nitrogen dioxide (NO_2) in all but a few experiments. Data were obtained by performing runs in pairs, with the same initial NO_x on both sides of the dual chamber, but different initial nonmethane hydrocarbon (NMHC). This allowed a direct determination of the effect of reducing NMHC on NO_2 maximum concentrations and dosages. Relevant evidence was also obtained from comparison of runs conducted on different days, with different ambient atmospheric conditions.

A non-linear multiple regression equation for NO_2 maximum concentration accounted for 92% of the total variance in NO_2 maximum. The independent variables were initial NO_x, initial NMHC, average solar radiation between sunrise and the NO-NO_2 crossover, the average solar radiation near the NO_2 peak. In the equation, NO_2 maximum was primarily dependent upon initial NO_x; the functional dependence upon initial hydrocarbon concentration could cause a ± 20% variation in the initial NO_x dependence; the functional dependence upon solar radiation measures could also cause a further ±5% non-linear variation in the initial NO_x dependence.

Comparison of results from dual runs conducted on the same day, under the same solar radiation and initial NO_x conditions, clearly showed a decrease in NO_2 maximum concentrations with decreasing initial NMHC for all cases. For example, at an initial NO_x concentration of 0.51 ppm, a 72% reduction of NMHC, from 2.58 ppmC to 0.70 ppmC, reduced both the

NO_2 maximum and the NO_2 dosage by 35%.

Comparison of results from runs conducted on different days, under different solar radiation and constant initial NO_x conditions, showed a decrease in NO_2 maximum concentrations with decreasing initial NMHC, but the decrease was also a function of exact solar radiation conditions during each run. For example, at an initial NO_x concentration of 0.36 ppm on different days, a 56% reduction in NMHC, from 3.2 ppmC to 1.4 ppmC, reduced the NO_2 maximum by 20%.

Overall, for initial NMHC and NO_x levels similar to those typically present in current urban atmospheres, reduction of the NMHC reactant by 60-90% caused a 20-35% reduction in both NO_2 dosage and maximum NO_2 concentrations.

These results are from runs which were started before sunrise and terminated at 1700 hours EDT and were conducted under static conditions. To explore the possible effects of conditions more closely simulating the real atmosphere, several runs were extended to 24 or 36 hours. Other runs were diluted at rates of 7-10% per hour from early morning until 1700 hours.

In the 24-hour extended runs, high concentrations of NO_2 sometimes occurred throughout the nighttime period. These high nighttime NO_2 concentrations were the result of high NO_2 and low O_3 at the end of the solar day. Those runs which resulted in high (> 0.1 ppm) ozone concentrations at sunset had much lower nighttime NO_2 concentrations because the NO_2 was consumed either during the day or during the nighttime period by reaction with O_3. Because various solar radiation conditions could lead to different O_3 concentrations at the end of the solar day from the same initial NO_x and NMHC, the nighttime occurrence of NO_2 was a function of the exact solar radiation conditions during the daylight period. For those runs that had high nighttime NO_2 concentrations the nighttime contribution to the total 22-hour NO_2

dosage was as high as 60%. For those runs in which NO_2 disappeared during the night, the nighttime contribution to total NO_2 dosage was only 25-28%.

One extended experiment was performed which indicated, that although hydrocarbon reduction would be capable of reducing both O_3 and NO_2 maximum concentrations during the first daylight period, it might have little effect on O_3 and NO_2 maximum concentrations in the second daylight period. For example, in a 36-hour static experiment, a 50% reduction in NMHC (from 2.9 ppmC to 1.3 ppmC at initial NO_x of 0.36 ppm) resulted in a 10% reduction in NO_2 maximum concentration and a 74% reduction (from 0.392 to 0.103 ppm) in O_3 maximum concentration in the first daylight period. In the nighttime period, NO_2 in both sides decreased to approximately 0.05 ppm while the ozone decreased to 0.24 and 0.04 ppm; the NO concentration was expected to be essentially zero. In the second daylight period, the NO_2 remained relatively constant at 0.045 ppm while the ozone increased in both sides with no additional material added to a value near that of the higher NMHC run on the first day (0.40 and 0.37 ppm O_3). This occurred even though the NO_2 concentrations remained below 0.05 ppm and the "reactive" hydrocarbons in the mix had presumably been consumed the previous day.

Slow dilution of relatively reactive propylene/NO_x systems led to lower NO_2 and O_3 maximum concentrations than occurred in the same undiluted chemical system. Dilution of lower reactivity hydrocarbon mix/NO_x systems led to lower NO_2 concentrations, but higher O_3 concentrations than occurred in the same system without dilution. This was primarily due to more rapid achievement of higher NO_2/NO ratios in the diluted system at the most optimum time in the solar day for O_3 generation.

The concept of a large outdoor chamber, which used ambient conditions of solar radiation, temperature, and relative humidity, was very useful in studying photochemical systems representative of urban environments. The data from such a chamber were more difficult to interpret than that from more traditional (artifically illuminated) smog chambers because of the day-to-day variations in solar radiation and other meteorological factors. The advantages of performing a large number of experiments under essentially "real" conditions, however, proved to be significant. The results under these real conditions differed from those which had been previously obtained in indoor chambers with constant conditions of light, temperature, and humidity. The experimental approach adopted in this study represents somewhat of a half-way point between the traditional smog chamber approach and that based on direct observation of the real atmosphere.

SECTION II
RECOMMENDATIONS

These experiments were conducted under essentially static conditions. Work reported in this document would suggest that the static situation may not always be the "worst case" condition because of interaction between the chemical system and the natural diurnal light-intensity and physical operating conditions. There was a solar radiation effect in the results reported. Any factor which changes the speed of NO to NO_2 conversion will probably affect the NO_2 maximum concentration and most definitely will affect the O_3 formation. It is recommended that such factors as rapid dilution and continued injection of fresh materials just after the early morning peak be examined.

The information content of the present data set has not been exhausted. It is recommended that further data analysis be done, especially in relating solar radiation variations to outcomes in experiments. This analysis will also require further specialized experimental runs to support findings. The formation of O_3 under outdoor conditions is very much a function of the photochemically weighted light-history. These factors need to be determined and have not been addressed in this report.

Factors relating rate of NO_2 photolysis to total solar radiation and ultraviolet radiation need further exploration, especially on days which exhibit rapid increases and decreases in light intensity, and on thinly overcast days.

The roles of nitrous acid and other photoacceptors such as aldehydes at the very beginning of irradiation require clarification since the presence of these photoacceptors determines the initial speed of NO to NO_2 conversion and therefore affects the subsequent formation of O_3 under outdoor light conditions. A similar situation exists with respect to the initial NO_2/NO_x ratio. It is recommended that direct comparison experiments be conducted in which runs with added nitrous acid and aldehydes are compared to runs with only hydrocarbon/NO_x.

Further experimental runs should measure specific NO_2, nitric acid, PAN, specific hydrocarbons and aldehydes. This data would be needed to validate future photochemical models and aid in determining the factors leading to O_3 generation.

The modeling program should be modified to allow variable temperature and dewpoint profiles to continuously adjust those rate constants that are known to be temperature dependent or include water concentration.

The second and third day irradiation of so-called "spent" reaction systems requires a detailed exploration. Results reported herein would suggest that although hydrocarbon reduction might be beneficial, in terms of controlling NO_2 and ozone concentrations on the first day of irradiation, it may not be successful on the second and subsequent days. The ozone concentration in the downwind air parcel on these days may be primarily a function of dilution and two or three day weather patterns.

The precursor-pollutant relationship found in this study was different than that which had been found under constant light-intensity conditions in a previous study. This has been attributed to the diurnal variation in solar radiation and other natural phenomena associated with solar radiation. Because of this outcome, it is recommended that other precursor-pollutant relationships that have been or will be determined in smog chamber studies should be examined to determine if real solar radiation conditions will affect the relationship.

SECTION III
INTRODUCTION

BACKGROUND

On April 30, 1971, the Environmental Protection Agency promulgated national ambient air quality standards (NAAQS) for photochemical oxidants (O_x), nitrogen dioxide (NO_2), and nonmethane hydrocarbons (NMHC)[1]. As put forth in the Federal Register, NMHC at an ambient level of 160 $\mu g/m^3$ (0.24 ppm as methane, 6-9 a.m. average not to be exceeded more than once per year) would serve as a guide to achieve the one hour oxidant standard of 0.08 ppm (not to be exceeded more than once per year). Reduction in nitrogen oxide emissions was employed as the most effective way of controlling NO_2. The NO_2 standard, which is an annual average of 0.05 ppm, was developed from NO_2 health effects studies,[2,3] independently of O_x control strategy.

At the time the standards were set, it was not possible to fully assess the complex short-term photochemical relationships between oxides of nitrogen (NO_x), NMHC, and O_x. Hence, the national control strategy for ambient ozone consisted of reducing only the hydrocarbon precursor based on an upper limit relationship between nonmethane hydrocarbon and ozone. This relationship was developed from aerometric data only. Such a relationship did not take into account the role played by the oxides of nitrogen and the potential effects that NMHC reduction may have on NO_2 concentrations.

Early chamber findings of Korth, et al.[4], were able to show, by using dilute auto exhaust, that a decrease in initial hydrocarbons resulted in a proportional decrease in the rate of NO_2 formation (at constant initial NO_x). Dimitriades[5] in the Bureau of Mines (BOM) smog chamber using NO_x (90% NO, 10% NO_2) and auto exhaust, irradiated at constant light intensity, demonstrated that maximum NO_2 concentrations (NO2M) were essentially independent of initial NMHC concentrations in the range of 0.0 to 1 ppm initial NO_x (INOX) and 0 to 4.6 ppmC initial NMHC (IHC). Dimitriades' data are shown in Figure 1; from these data he estimated a value of 0.63 for the ratio of NO2M to INOX. Possible difficulties with various control strategies involving both NO_x and NMHC were later succintly illustrated by Stephens[6]. Although Stephens intentionally does not quantify his axes (Figure 2), his diagram suggests that excessive hydrocarbon control compared to NO_x control could have the tendency of shifting high NO_2 concentrations to a later time in the day with a possibility of greater NO_2 dosages.

Altshuller[7] has stated in summary that "the formation of nitrogen dioxide can be slowed up by a high degree of control of hydrocarbons". However he also points out that "the way irradiation chambers are operated starting at near midday light intensities and temperatures accelerates the early stages of the reaction unrealistically rapidly compared to atmospheric conditions". For this reason it is important to determine if a relationship like the one in Figure 1 would hold under more realistic conditions of natural solar radiation, temperature, and relative humidity. Large reductions in NMHC could lead to higher NO_2 dosages with potentially, worse NO_2 health effects, while achieving the oxidant standard. This would require more rigid emission standards for NO_x.

Thus, while the effect of reducing NMHC on oxidant formation is considered beneficial, the effect of this reduction on NO_2 concentrations in the ambient atmosphere is not clear. Will NO_2 peaks be lower, higher, or the same? Will NO_2 dosages increase? Will it be more difficult to meet the annual standard for NO_2? Is the formation of NO_2 slowed so significantly that large NO_2 concentrations occur at the end of the day? If so, what might be the fate of this remaining NO and NO_2?

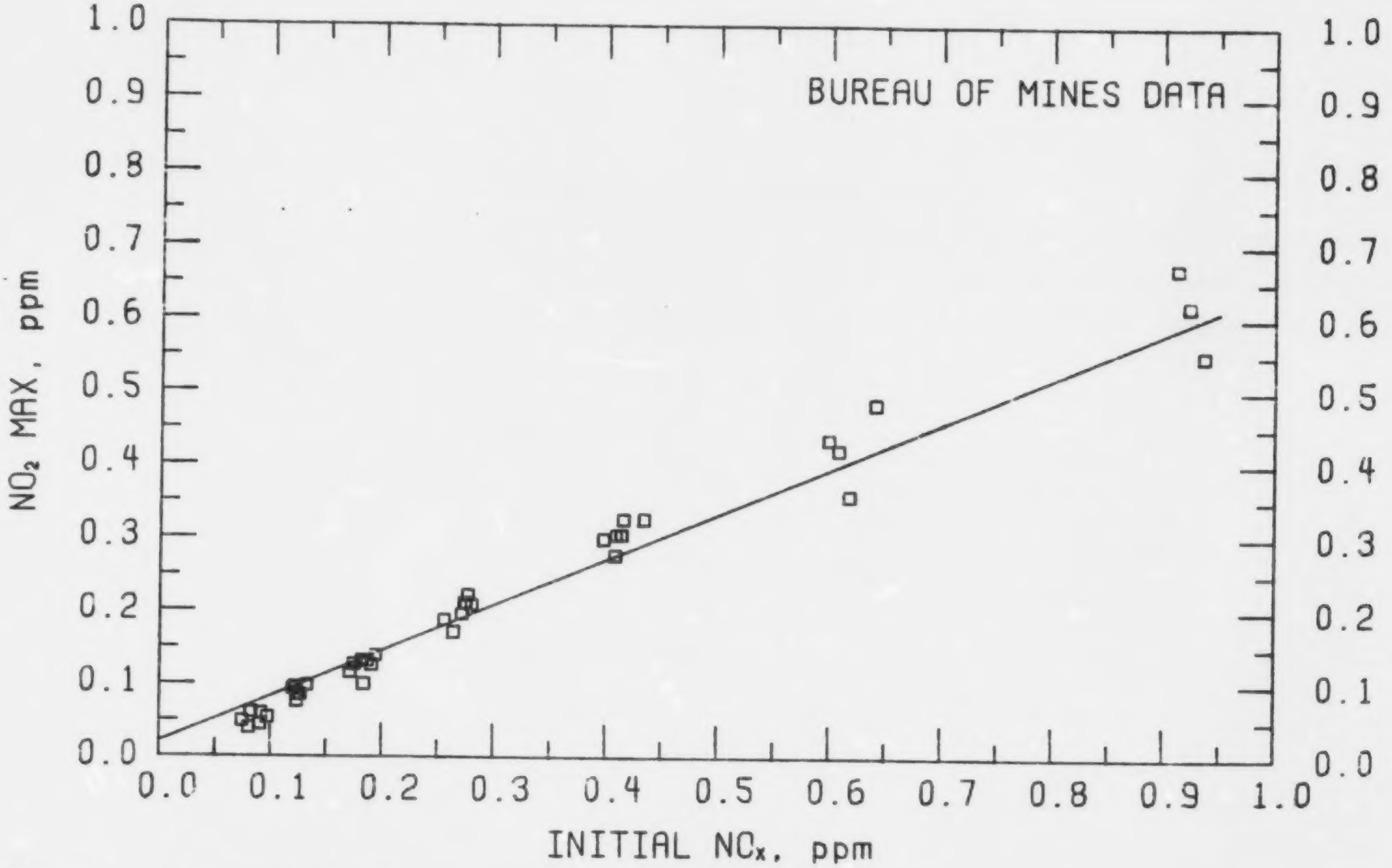

Figure 1. Dependence of nitrogen dioxide maximum concentration on initial nitrogen oxides and nonmethane hydrocarbon in the Bureau of Mines study by Dimitriades. Equation of regression line: $[NO_2]max = 0.6216[NO_x]_o + 0.021$.

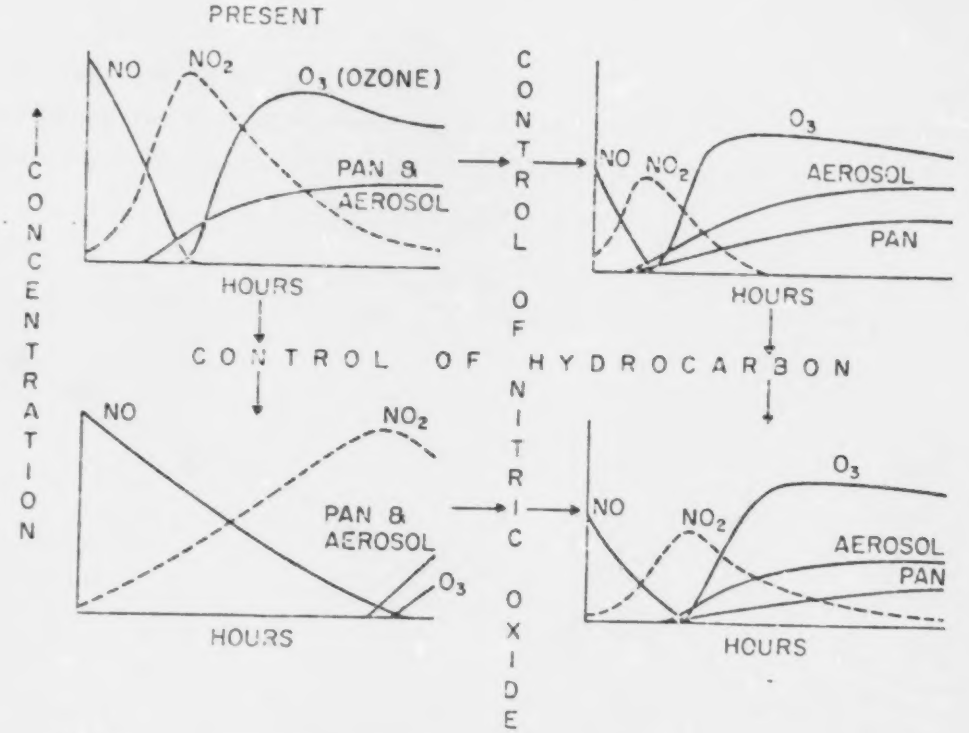

Figure 2. Idealized representation of NO, NO$_2$,O$_3$, aerosol and PAN (peroxyacylnitrate) profiles for various initial conditions. The coordinates of concentration and time are deliberately left unnumbered. (from reference 6).

There are three investigative methods for finding answers to these questions, each with inherent advantages and disadvantages. These are: 1) examine existing ambient air monitoring data (aerometric data) and collect new aerometric data, 2) use models of chemical and physical ambient air processes, and 3) perform new smog chamber experiments.

While the aerometric data approach has potential for giving answers to the questions posed above, the existing data is inadequate. Collection of new data is expensive and long term. Since we cannot control the conditions observed in the atmosphere, the most interesting conditions might not actually exist in the present atmosphere. Any relationship that might be determined would probably be a correlative or statistical one and not a causative one. Aerometric data could, perhaps, provide validation of results derived from the other two approaches.

The modeling approach could give a detailed mechanistic or physical understanding of the effect of hydrocarbon reduction on NO_2 behavior. Any combination of conditions and strategies could be tested and the conditions would be easily manipulated. The difficulty with this approach, at the present time, is that vital information is missing or untested. The model must be validated.

The traditional smog chamber approach suffers from the fact that conditions in the chamber are not necessarily very representative of those in ambient air. Factors such as surface effects, constant light intensity, unrealistic spectral distribution, constant temperature and relative humidity, static operating conditions, and reactant identity usually differ from actual urban air and thus would make it very difficult to extrapolate results obtained in smog chambers to ambient air behavior. On the other hand, within the limits of the operating conditions, a properly designed smog chamber system could provide answers to the questions asked above. Compared to the other two approaches these could be obtained relatively inexpensively and quickly. Like the modeling approach, conditions not found in the ambient air could be tested and although a mechanistic understanding would not necessarily result, cause and effect relationships could be found.

PURPOSE

The purpose of the work performed in this study was to determine, in a smog chamber operated under conditions typical of ambient air, the effects of hydrocarbon reduction on nitrogen dioxide concentrations in chemical systems reasonably representative of urban conditions. In addition, because the chamber would be located outdoors, an assessment was to be made of operating characteristics and performance of the chamber. Results were to be compared with those from indoor chambers.

APPROACH

To obtain physical operating conditions in a smog chamber that are typical of ambient atmospheric conditions, a smog chamber can be built outdoors. The daily variations in outdoor conditions present difficulties not found with indoor chambers. On the other hand, these variations exist in nature and are therefore useful in the experiment. The effects of these variations can be treated by proper experimental design and analysis. Using these concepts, an overall approach was devised that consisted of four major steps. These were:

1) The design and construction of a dual outdoor smog chamber which was capable of operating under conditions of light, temperature, and humidity typical of urban ambient situations.

2) The testing of the chamber and associated facility. This consisted of determining if the chamber design was physically sound and durable, and if it exhibited reasonable performance characteristics with respect to generally accepted smog chamber measures.

3) The performance of a series of 12 hour experimental runs in which the initial starting conditions of NO_x and NMHC were varied over a range typical of morning urban atmospheric concentrations, before and after hydrocarbon control.

4) The limited exploration of the effects of variations in operating conditions on the outcome of the experiments in 3) above. These consisted of:
    a) different initial percentage of NO_2,
    b) extended run times (24 and 36 hours durations), without additional material injected, and
    c) slow dilution of the reactive system with clean air.

In addition, numerous supportive tasks that could affect data quality or understanding were performed. Some of these tasks were instrument performance testing, development of a chemically meaningful light intensity measurement system, development of computer programs and hardware needed to operate the project effectively, analysis of any existing data that would be of benefit to the overall project goals, and the investigation of current modeling technology.

SECTION IV

DESIGN AND CONSTRUCTION OF SMOG CHAMBER FACILITY

DESIGN CRITERIA

Having made the decision to build a chamber outdoors for the purpose of achieving a more realistic simulation of urban ambient conditions, the choice of location, size, construction materials and methods, air handling or air movement, pollutant introduction, orientation, and type of supporting facilities remained. Boundaries on these choices were introduced by identifying desired characteristics and physical, chemical, or financial limitations. Several of these factors affected more than one of the areas of choices listed above; therefore, these factors will be discussed first.

Besides being located outdoors, it was desired that the chamber exhibit low surface effects. This implied a very large volume and choice of inert materials (few metal surfaces). This large volume requirement introduced other design requirements, such as: 1) finding a location that had background air that would be suitable for use without clean up because it would be prohibitively expensive to clean 350,000 ℓ for every run, 2) providing for relatively short purging times so that runs could be performed every day if necessary, 3) assuring that the volume was well mixed to avoid the problems associated with inhomogeneous chemistry, and 4) selecting arrangements so as to provide adequate laboratory space near chamber without shadowing but still allow easy access to chamber contents.

Because we recognized that outdoor conditions can vary from day to day, the chamber design had to provide some method of experimental control over these effects. This requirement suggested a dual chamber arrangement or dual compartment system. This meant doubling the air handling system hardware and required either two or each instrument type or timesharing of each instrument between the two chamber compartments.

Since the purpose of operating outdoors was to use atmospheric light and temperature conditions, the chamber design had to allow for full solar intensity and reasonable solar spectrum fidelity, but had to avoid a large "greenhouse effect" for air temperature. These desired characteristics affected chamber orientation, wall materials, and the physical arrangements of the chamber.

The varying ambient conditions, the long run times, the number of variables to be measured, and the need to timeshare the instruments suggested that it would be necessary to fully automate the data collection and processing. More than 10,000 numbers would be required for each dual run, primarily because of varying ambient conditions. A minicomputer data acquisition and control system would greatly increase the project productivity.

Finally, the entire chamber facility had to be constructed at a reasonable cost (less than $20,000). This meant that, where possible, wood was used as opposed to metal. Techniques that could be implemented by project staff were used extensively as opposed to those that required commercial hardware or personnel.

FACILITY DESCRIPTION AND CONSTRUCTION METHODS

Location

A site was chosen approximately 32 kilometers from the University of North Carolina at Chapel Hill. It is in Chatham County, North Carolina and is approximately 10 kilometers from the small town of Pittsboro. Chatham County is one of the most rural, least industrialized counties in North Carolina and is heavily wooded. The background concentrations of NO_x and nonmethane hydrocarbons were usually less than 0.025 ppm and less than 0.20 ppmC. More importantly, the air exhibited very low reactivity in the chamber.

Materials

The most important factors that influenced the choice of materials were that the chamber surfaces had to be chemically inert, durable, and have a very high transmission for the entire solar spectrum. Glass was unsatisfactory because of its spectral properties in the infrared (IR) and short wave length ultraviolet (UV) regions. Most films exhibit undesirable surface effects at low concentrations of trace gases. Fluorinated ethylene propylene (FEP) Teflon film however, had been used in many laboratories for years to make bags for photochemical experiments and seemed to be the most acceptable material. Its transmission in the UV and visible regions of the solar spectrum is excellent[8,9] and it has only a few absorption bands in the IR, a property necessary to reduce the "greenhouse effect". It has a very low permeability for most chemical species[9,10] and can be heat sealed to form large durable panels. For this application its worst property was its ability to hold a static charge for long periods of time. Type A film, 0.13 mm thick was chosen since film suppliers had indicated that Type C film would not hold a heat seal when exposed to sunlight[11]. This film is available in widths of 117 cm and in rolls of 34.4 m. To facilitate the replacement of a damaged section, the technique for enclosing the volume had to be one that would accommodate individual 117 cm wide Teflon panels for the sides. Other large areas that would not be as subject to wear could be fabricated from 117 cm wide panels commercially heat sealed together to form one piece, leakfree panels.

Physical Design and Construction Techniques

Because inlet and outlet doors, stirring fans, manifolds and other fittings had to enter the film in an airtight manner, it was decided early in the design that these fittings would be inserted through a solid floor. This left the sides free for light entry. The floor of the chamber was elevated approximately 1.2 m to allow for easy access.

Several shapes were considered for the chamber: spherical, half cylinder, box, dome, and A-frame. All but the A-frame were eliminated because of either difficulties in achieving a watertight structure or prohibitive costs. The final design was an A-frame 9.14 m wide, 12.19 m long and 6.10 m high at the peak on a plywood floor 1.22 m above the ground. Wooden beams, 5.08 cm by 20.32 cm, located on edge at 99.1 cm centers formed an exterior framework on top of the plywood floor. Continuous 16.46 m lengths of film were attached to the inside of the beams with a 0.61 m overlap on the floor at each side. The film was held in place from the inside by aluminum u-channels, nailed firmly to the wooden beams compressing the film against the external support. See Figures 3 and 4.

One piece, heat sealed Teflon film panels were used in such places as the triangular end panels and floors. The floor to side seals were achieved by a 0.61 m overlap of side panel film over floor panel film. A rubber strip under the film and an aluminum strip on top of the film completed the seal. All other seals were Teflon to Teflon under pressure of the aluminum u channel. A single unsupported heat sealed Teflon panel similar to the end panels was used to separate the chamber into two halves of equal volume. It was sealed to the floor and side panels in the same manner as described above The film was stretched as tight as possible during hanging, but enough flexing occurred to compensate for small volume changes due to temperature changes from cloud passage or wind pressure changes.

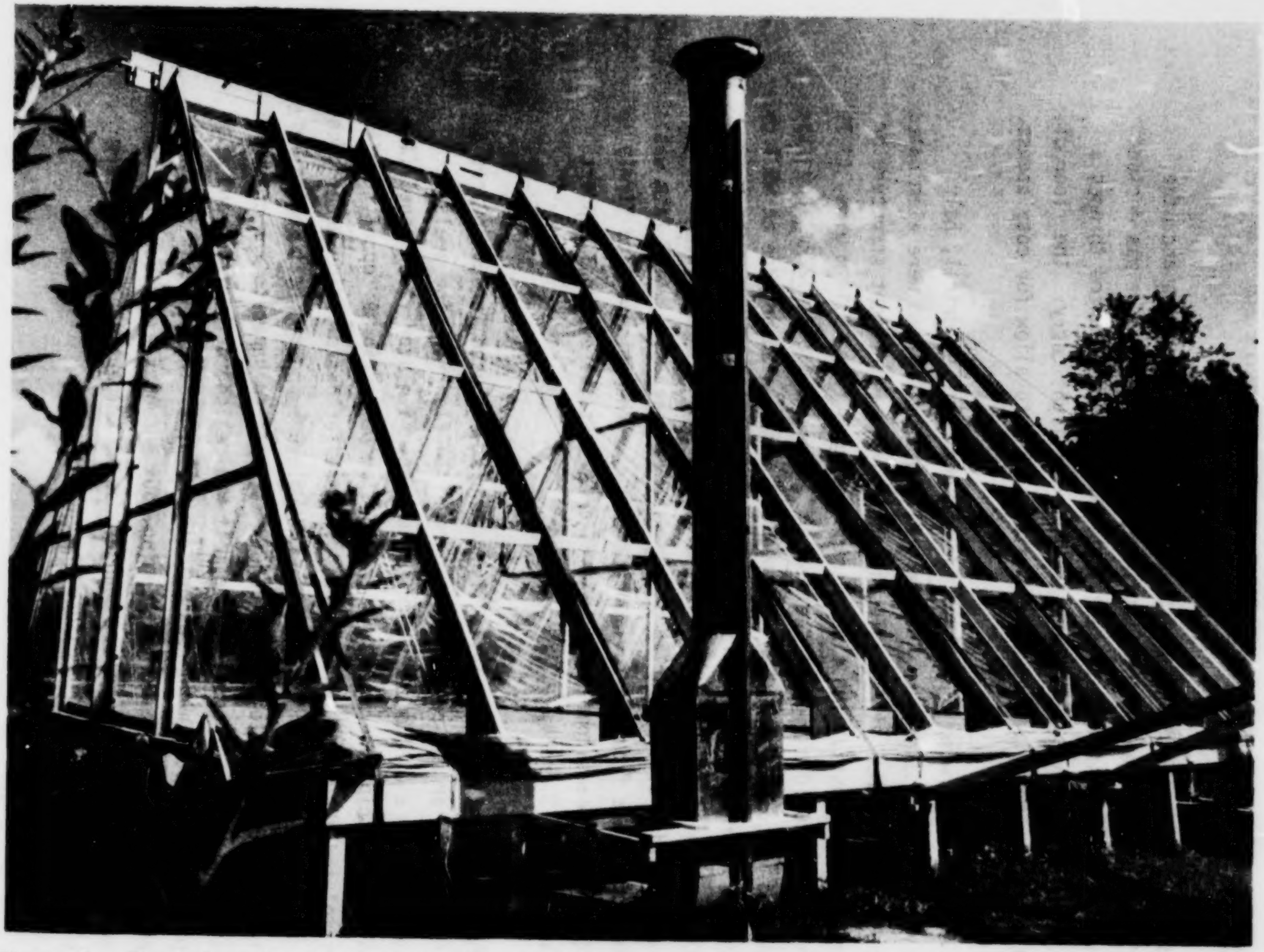

Figure 3. The University of North Carolina outdoor smog chamber. Courtesy of the Greensboro Daily News.

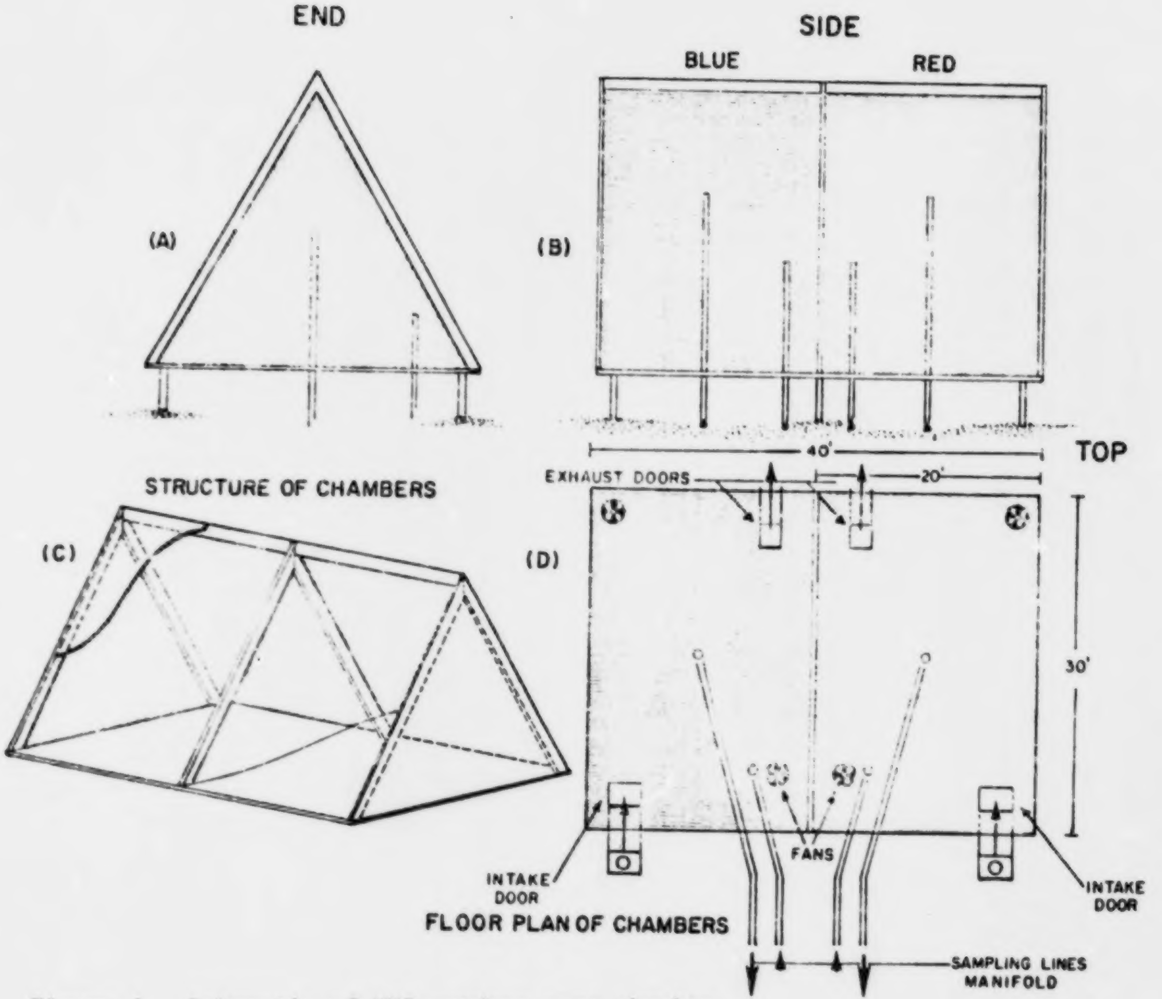
END
(A)
SIDE
BLUE
RED
(B)
STRUCTURE OF CHAMBERS
(C)
40'
20'
TOP
EXHAUST DOORS
(D)
30'
FANS
INTAKE DOOR
INTAKE DOOR
FLOOR PLAN OF CHAMBERS
SAMPLING LINES MANIFOLD

Figure 4. Schematic of UNC outdoor smog chamber.

Aluminum foil was placed under the film on the floor to reflect the light and heat backup through the chamber. This was necessary to reduce solar heating of the air to a value that was within normal urban environments and to compensate for transmission losses through the Teflon film.

Orientation

The chamber was oriented with its long axis approximately north to south. The actual long axis orientation is along a 27° - 207° true heading. The orientation with respect to the sunrise and sunset at different times of the year and the altitude of the sun at noon for different times of the year are illustrated in Figures 5 and 6.

It was expected that the reflective chamber floor would interact with the sun to increase the photon flux in the chamber and thus compensate for transmission losses through the film. Multiple reflections in the two chamber sides would probably help to equalize overall solar exposure.

Air Handling Systems

There were three air handling systems in each half of the chamber, one for exhausting, one for sampling, and one for mixing. The exhaust system consisted of two intake stacks, 0.61 m x 0.91 m intake doors, 0.61 m x 0.61 m exhaust doors, and an exhaust blower. The exhaust blower was a dual blower on a single shaft driven by a 1.5 horsepower motor. Air entered the system through the two 5.49 m high by 30.5 cm diameter stacks. This system was designed to permit rapid exhausting of chamber contents and replacement with ambient air. The filling rate was 7190 l/min. The chamber could be flushed to a 99.6% decay of initial contents in 2 hours.

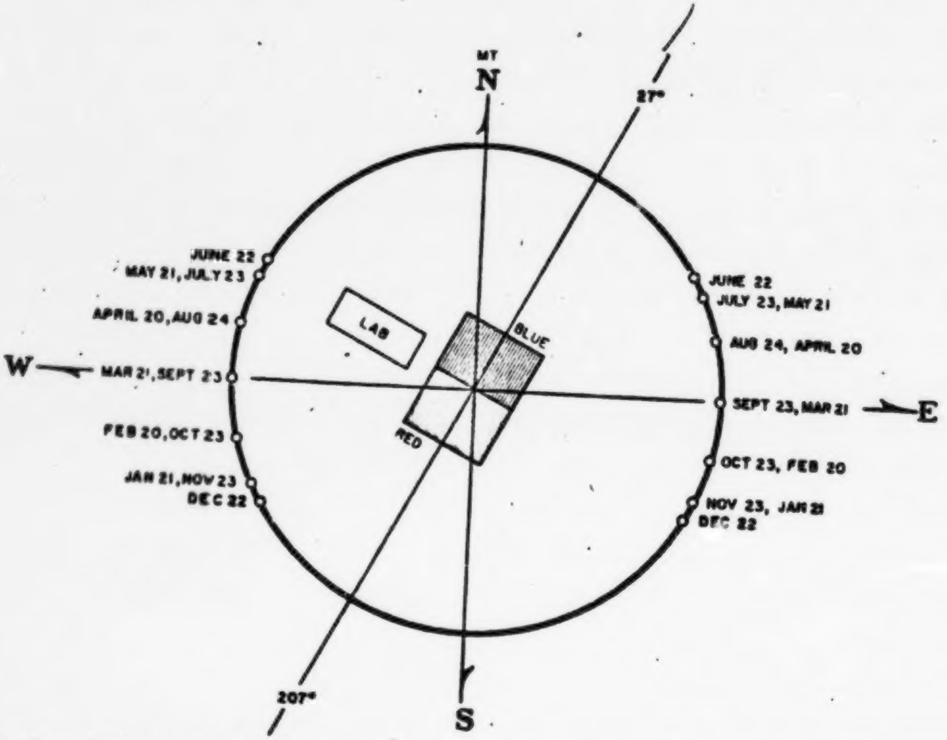
MT
N
27°
JUNE 22
MAY 21, JULY 23
APRIL 20, AUG 24
MAR 21, SEPT 23
FEB 20, OCT 23
JAN 21, NOV 23
DEC 22
W
LAB
BLUE
RED
JUNE 22
JULY 23, MAY 21
AUG 24, APRIL 20
SEPT 23, MAR 21
E
OCT 23, FEB 20
NOV 23, JAN 21
DEC 22
207°
S

Figure 5. Orientation of UNC outdoor smog chamber with respect to seasonal sunrise and sunset positions.

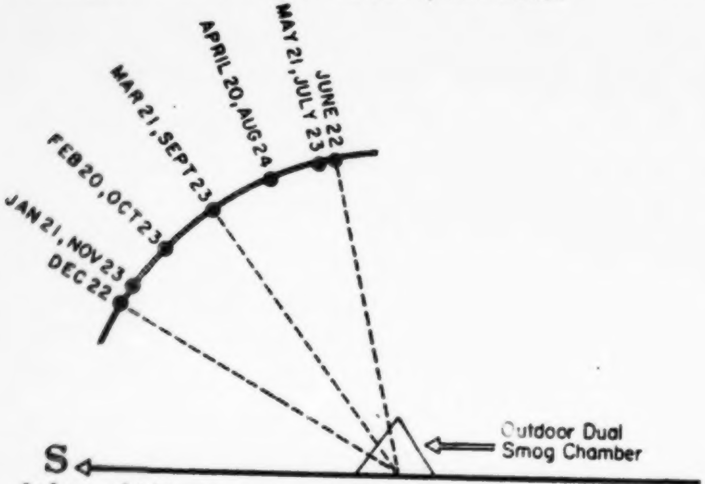
JUNE 22
MAY 21, JULY 23
APRIL 20, AUG 24
MAR 21, SEPT 23
FEB 20, OCT 23
JAN 21, NOV 23
DEC 22
Outdoor Dual Smog Chamber
S

Figure 6. Solar altitude and zenith angle at noon at the UNC outdoor smog chamber for each month.

The second air handling or manifold system was for sampling and injection of pollutant materials into the chamber halves. To insure representative sampling, a 3.17 cm I.D. glass manifold ran from a point 1.83 m above the floor in the center of each chamber half down through the floor and over to a sampling laboratory. The sampling volumes required by all the instruments did not exceed 5 l/min but to reduce losses due to long resident times it was necessary to have higher flows in the manifold. The flow rate in the manifold was 60 lpm. Over the duration of a 12 hour experiment, this could have exhausted 28% of the chamber volume. To avoid the necessity of makeup air, the sampling manifold was made as a closed loop. Squirrel cage blowers with housings and fans that were Teflon coated were used to circulate air through the manifolds. The unused sample air was then returned through a 3.17 cm I.D. glass manifold to the chamber. These return manifolds provided a convenient method for injecting the initial reactants.

Inside each chamber half were two mixing fans located in opposite corners. These provided circulation and mixing of the chamber contents. The fans were 50.8 cm diameter cast aluminum units that had been FEP Teflon coated. They operated in a horizontal position, 0.76 m above the floor on 2.54 cm diameter Teflon coated steel shafts that extended through the chamber floor. Under the floor, 1/4 horsepower, 1750 rpm motors provided power through a belt and pulley system to each fan. Each fan operated at approximately 31.15 m^3/min.

Laboratory

A laboratory was built adjacent to the chamber. It was a 3.66 m W x 15.24 m L x 3.05 m H wooden structure oriented perpendicular to the chamber and 3.66 m away from it to avoid any shadowing. The first 5.49 m nearest the chamber contained the instrumentation, manifolds, and calibration systems. The next 5.49 m contained the data acquisition computer system and the operations area. The last 4.27 m of the laboratory was a utility area with running water and storage facilities. Gas tanks necessary to operate the instruments and perform calibration were located in a 1.22 m x 1.83 m room completely closed-off from, but attached to the laboratory. The injection system gas tanks and valves were housed in a second 1.52 m x 1.52 m well-insulated, heated room adjacent to the end of the laboratory nearest the chamber.

Injection System

Pollutants were injected into the chamber sides via the return side of the sampling manifolds. The return manifolds entered the chamber sides under one of the mixing fans. The injection process used gas cylinders containing pollutants at high concentrations (1000-10,000 ppm range), two stage, stainless steel diaphragm regulators, on-off solenoid valves, and capillary flow restrictors or precision needle valves with vernier handles. The flow rate of injected material into the manifolds could be well established for a given pressure and length of capillary tubing or needle valve setting; the total injection volume could be accurately controlled as a function of the time the solenoid valve was open. Conditions could be varied sufficiently to have the injection time range from a few minutes for each component to 1-2 hours for a programmed injection used to simulate the buildup of pollutants in urban areas.

Data Acquisition System

A computer based data acquisition and control system (DAS) was used to acquire, process, and record data for the chamber instrument system. The DAS consisted of: 1) a PDP 11/40 computer with 32 kilobytes of core memory, 2) a high speed papertape reader/punch, 3) a 2.4 million byte cartridge disk system, 4) thirty character per second keyboard/-printer terminal, 5) time-of-day clock, 6) 5-1/2 digit, digital voltmeter, and 7) a 200-channel, 3-wire crossbar scanner.

Output signals from each instrument were wired to the crossbar scanner (or analog signal multiplexer). Under control of programs in the computer, the scanner connected the selected signal leads to the input of the digital voltmeter. The digital voltmeter, which had excellent noise and spurious signal suppression and could measure a 1 volt signal with a resolution of 10 microvolts, was triggered to acquire a reading and to supply the binary coded decimal, 5-1/2 digit number to the computer. The computer processed the information and then commanded the scanner to move to the next channel and repeat the process. The data processing will be described in a later chapter. The timing of the computer processes was under the control of a digital date and time-of-day clock which signaled event times to the computer. Another digital timer operated Teflon solenoid valves on the inlet of each instrument to connect the instruments to one chamber half during a given cycle of data acquisition.

This system provided fully automatic acquisitions and processing of data during a run and provided the operator with immediate, full data in physical units. Given this information about what was happening, the operator could then concentrate on what he wanted to do. It also allowed the massive amount of information generated during a run to be processed in a more effectual manner after the run was over.

SECTION V

EXPERIMENTAL METHODS AND PROCEDURES

MEASUREMENT METHODS

Instrumentation

The instrumentation was located in the temperature-controlled laboratory adjacent to the chamber. Gas instrumentation included equipment for measuring total hydrocarbons, methane, carbon monoxide, nitric oxide, nitrogen dioxide, and ozone. Standard meteorological instruments were used to measure solar radiation, ultra-violet radiation, air temperature, and dew point. A temperature-programable, dual, flame ionization gas chromatograph was used for detailed hydrocarbon analysis. Table 1 lists the instrument models and their characteristics.

At the sample inlet of each gas instrument was a 3-way Teflon ac solenoid valve. Since there were two intake manifolds (one for each chamber half), air from either manifold could be drawn through a 3-way valve and into the instrument. In this manner timesharing of one instrument between the two chamber halves was possible.

Calibration

The techniques used to calibrate the continuous monitoring instruments closely followed the procedures set forth by EPA[1], although other methods were used as needed (see Table 2). An attempt was made to interlock the NO_x and O_3 calibration apparatus so that each specific method could be used as a check against the others. That is, ozone, from a neutral buffered potassium iodide calibrated ozone generator was used in combination with a standard tank source of NO to produce an equivalent amount of NO_2 by a $NO-O_3$ titration.[12] This calibration

Table 1. INSTRUMENT CHARACTERISTICS

Substance	Method	Manf. Model	MDC[a]	Range	Mode	Time Shared
O_3	Chemiluminescent	Bendix 8002	0.001 ppm	0-1 ppm	Continuous	Yes
NO NO_2 NO_x	Chemiluminescent	Bendix 8101-B	0.005 ppm each	0-1 ppm	Cyclic 30 sec each	Yes
THC CH_4 CO	Flame Ionization	Byron 233A Environmental Chromatograph	<0.01 ppm each	0-300 ppm	Cyclic 4 mins	Yes
Dewpoint	Cooled mirror	Cambridge Model 880	0.1°F	-40°F - 120°F	Continuous	Yes
Total Solar Radiation	Pyranometer	Eppley Black and White	7.5 mv/cal/ cm^2-min	0-2 cal/cm^2-min	Continuous	No
UV Radiation	Pyranometer	Eppley UV	0.2 mv/millical/ cm^2-min	0-0.1 cal/ cm^2min	Continuous	No
Temperature	Thermistor	YSI	0.2°F	20-110°F	Continuous	No
UV-VIS-IR Spectrophotometer	---	Heath	0.1% T		Manual	
Detailed HC	Flame Ionization	P.E. 900	0.002 ppmC	---	Manual	No

[a] Minimum detectable concentration.

Table 2. CALIBRATION SOURCES FOR GASES

Gaseous Species	Source	Calibration Method	References
O_3	Ozone Generator	Neutral Buffered KI	Fed. Reg. (1971)[1]
NO	Cylinder	Certified Commercial Analysis	
NO_2	a) Permeation Tube	Volumetric	Saltzman (1971)[13]
	b) Cylinders	Certified Commercial Analysis	
	c) Oxidation of NO	Gas Phase Titration	Rehme _et_ _al_. (1974)[12]
CH_4,CO,and Butane	Cylinder	Certified Commercial Analysis	Fed. Reg. (1971)[1]
Propane	Permeation Tube	Volumetric	Saltzman (1971)[13]

factor for NO_2 was compared with those obtained from a volumetrically calibrated permeation tube[13], standard bubbler method[14] and from certified NO_2 commercial cylinders. The total hydrocarbon (THC), methane (CH_4) and carbon monoxide (CO) modes of the environmental chromatograph were calibrated using commercially prepared gases in the 1-15 ppmC range in HC-free air (< 0.1 ppmC). The response factor for the THC mode of the instrument for nonmethane hydrocarbon (NMHC) was determined by additional calibration with commercially prepared cylinders of butane and hexane. These calibrations were also compared with a volumetrically calibrated propane permeation tube. Thus, multiple methods were employed to insure as accurate a calibration as possible. Initially, a complete calibration of all instruments was performed prior to each run until instrument-calibration familiarity and general drift patterns were established. Subsequently, it was found that the environmental chromatograph required daily calibration; the NO_x and O_3 meters, however, only required calibration approximately once a week.

STANDARD OPERATING PROCEDURE

Prior to an experimental run, the chamber was purged overnight with background ambient air. At precisely 0500 hours EDT the DAS began recording measurements of the background concentrations of THC, CH_4, CO, NO, NO_2 and O_3. Single instruments were timeshared on an alternating four minute cycle between the two sides. The chamber intake and exhaust doors were sealed before sunrise. The hydrocarbon analyzer was calibrated. The background concentrations of NMHC and NO_x were then subtracted from the desired pollutant concentrations to determine the injection concentrations. The starting concentrations of NO, NO_2 and NMHC were injected, in the order given, as a slug injection by the use of high concentration gas tanks, electric on-off solenoid valves and precision needle valves. Depending on the pollutant to be injected, the on-off solenoid valves were actuated from inside the laboratory for predetermined periods of 1-7 minutes. Time-flow relationships and instrument readings verified the injection concentrations. Automatic monitoring of the pollutants occurred until 1700 hours EDT when the run was terminated. The chamber doors were then opened and the chamber contents were purged with ambient air. Data was printed out and punched from the computer disk and the computer was programmed to initiate another run at 0500 hours the following day.

DATA TREATMENT PROCEDURES

General

Figures 7, 8, and 9 are flowcharts of the processes used to treat the data collected. The processes are divided into those that occurred during a run, those performed immediately after a run, and those that were done later. The operations were carried out on three different computers and a programmable calculator with plotter. The steps in Figure 7 occurred on the PDP 11/40 at the chamber site and on a Hewlett-Packard 9810 programmable calculator with plotter at UNC. The steps in Figure 8 occurred on a PDP 11/40 at EPA which was equipped with a compatible disk drive and nine track magnetic tape unit. The major data manipulation steps illustrated in Figure 9 were performed on an IBM S370/165 at the Triangle Universities Computational Center (TUCC) which supports a wide range of statistical programs, teleprocessing operations for graphical processing, and large on-line and off-line storage facilities.

During Run

The operator began data acquisition operations by answering questions from the keyboard (Step 1A, Figure 7). These included supplying the starting day and time and the finishing day and time. With this information, the acquisition program would initiate and cease data

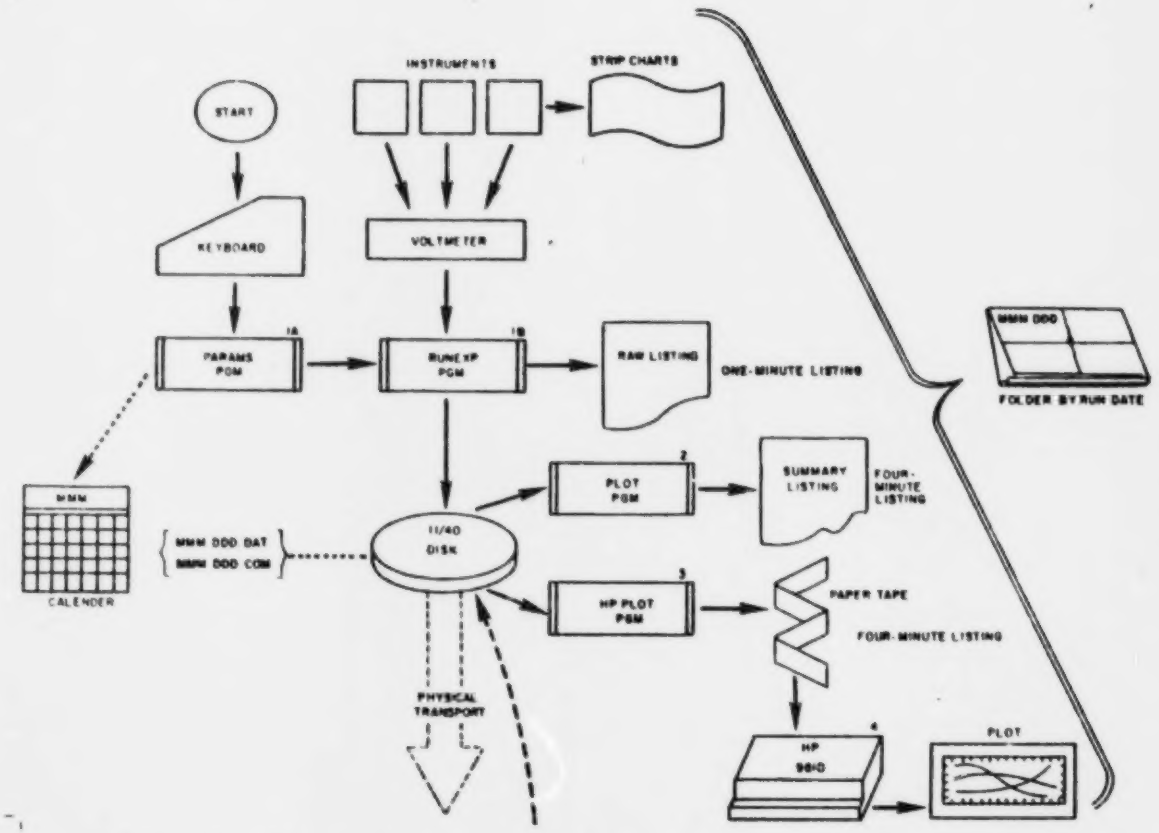
START
KEYBOARD
INSTRUMENTS
STRIP CHARTS
VOLTMETER
1A
PARAMS PGM
1B
RUNEXP PGM
RAW LISTING
ONE-MINUTE LISTING
MMM DDD
FOLDER BY RUN DATE
MMM
CALENDER
MMM DDD DAT
MMM DDD COM
11/40 DISK
2
PLOT PGM
SUMMARY LISTING
FOUR-MINUTE LISTING
3
HP PLOT PGM
PAPER TAPE
FOUR-MINUTE LISTING
PHYSICAL TRANSPORT
4
HP 9810
PLOT

Figure 7. Flowchart of on-site data treatment procedures.

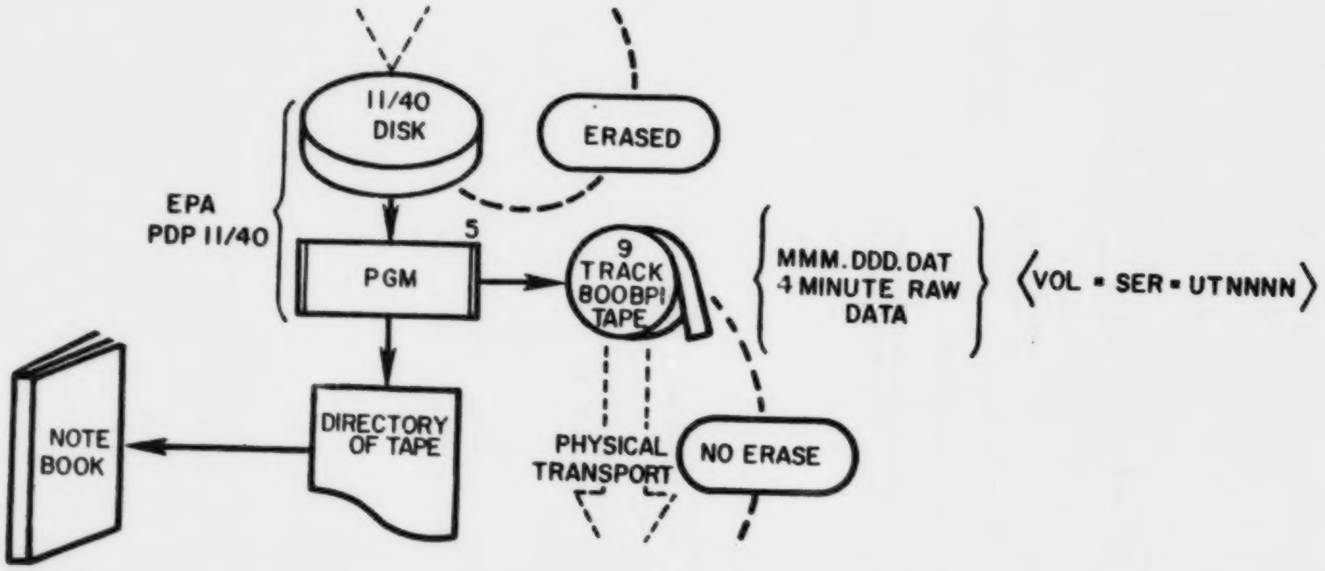
11/40
DISK
ERASED
EPA
PDP 11/40
5
PGM
9
TRACK
800BPI
TAPE
MMM.DDD.DAT
4 MINUTE RAW
DATA
⟨VOL = SER = UTNNNN⟩
NOTE
BOOK
DIRECTORY
OF TAPE
PHYSICAL
TRANSPORT
NO ERASE

Figure 8. Flowchart of preliminary off-site data treatment procedures.

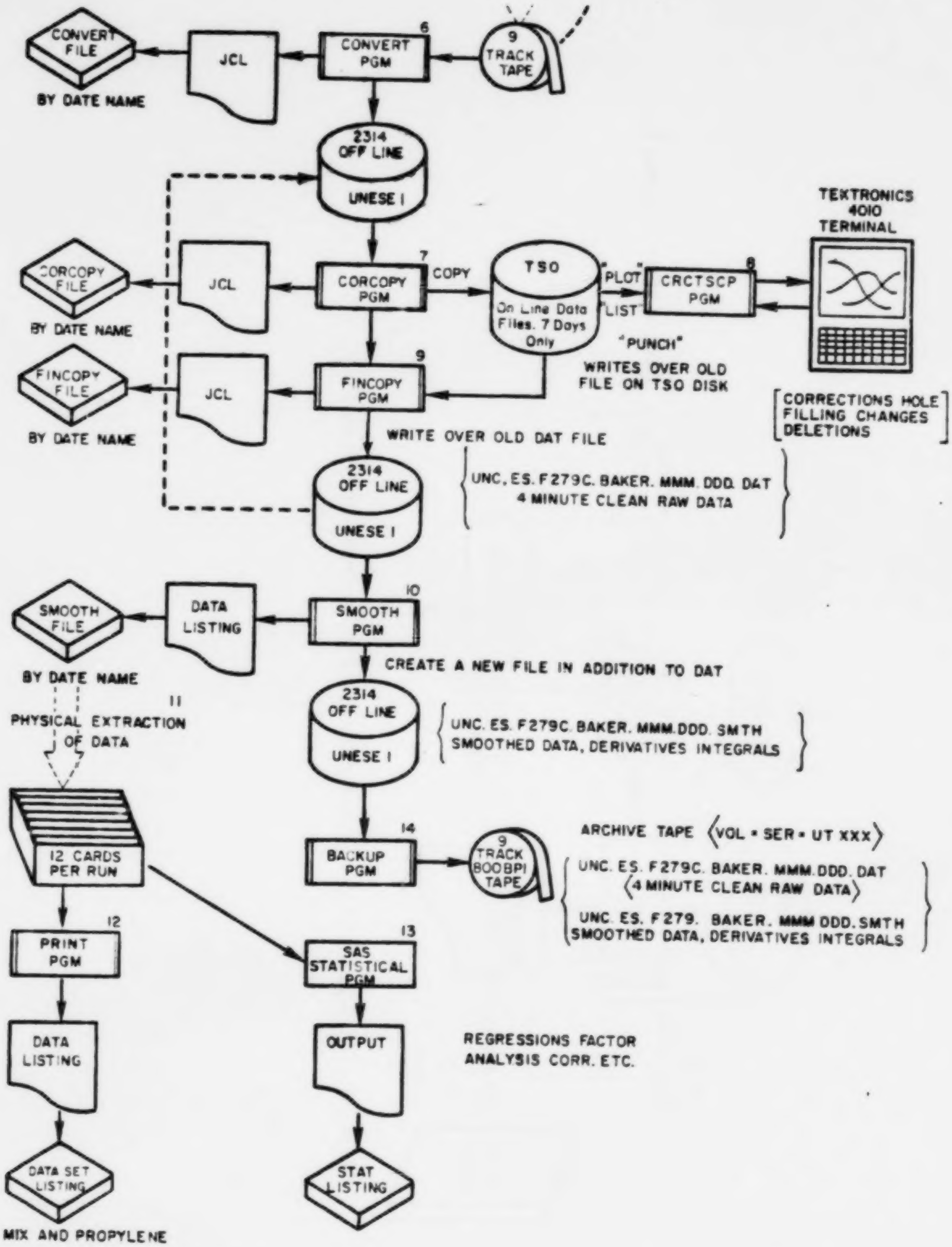
CONVERT FILE
BY DATE NAME
JCL
6
CONVERT PGM
9 TRACK TAPE
2314 OFF LINE
UNESE I
TEXTRONICS 4010 TERMINAL
CORCOPY FILE
BY DATE NAME
JCL
7
CORCOPY PGM
COPY
TSO
On Line Data Files. 7 Days Only
"PLOT"
"LIST"
8
CRCTSCP PGM
"PUNCH"
WRITES OVER OLD FILE ON TSO DISK
FINCOPY FILE
BY DATE NAME
JCL
9
FINCOPY PGM
CORRECTIONS HOLE FILLING CHANGES DELETIONS
WRITE OVER OLD DAT FILE
2314 OFF LINE
UNESE I
UNC, ES. F279C. BAKER. MMM. DDD. DAT
4 MINUTE CLEAN RAW DATA
SMOOTH FILE
DATA LISTING
10
SMOOTH PGM
BY DATE NAME
CREATE A NEW FILE IN ADDITION TO DAT
11
PHYSICAL EXTRACTION OF DATA
2314 OFF LINE
UNESE I
UNC. ES. F279C. BAKER. MMM.DDD. SMTH
SMOOTHED DATA, DERIVATIVES INTEGRALS
12 CARDS PER RUN
14
BACKUP PGM
9 TRACK 800BPI TAPE
ARCHIVE TAPE ⟨VOL = SER = UT XXX⟩
UNC. ES. F279C. BAKER. MMM.DDD. DAT
⟨4 MINUTE CLEAN RAW DATA⟩
UNC. ES. F279. BAKER. MMM DDD. SMTH
SMOOTHED DATA, DERIVATIVES INTEGRALS
12
PRINT PGM
13
SAS STATISTICAL PGM
DATA LISTING
OUTPUT
REGRESSIONS FACTOR ANALYSIS CORR. ETC.
DATA SET LISTING
STAT LISTING
MIX AND PROPYLENE

Figure 9. Flowchart of final off-site data treatment procedures.

collection automatically at the appropriate times. This allowed the operator to have considerable background level information available when he arrived at the site to make the injections. The operator was responsible for entering information about the run on a calendar-type log which served as one type of key to data retrieval since all runs had the run date as part of their names.

A 12-hour run was divided into four minute intervals. A digital timer operated Teflon solenoid valves on the inlet of each instrument to connect the instruments to one chamber half during each four minute period. The DAS acquired the signal outputs every minute and converted the voltage readings to physical units using calibration equations stored in memory. At the end of each four minute period, the valves were switched and the physical data was written onto the disk system for subsequent data processing.

Several options were available to the operator concurrent with data acquisition. He could 1) request a minute by minute data listing to be generated, 2) request that a line printer type plot be generated of any data on the disk, including old runs, 3) request that a comment be entered and stored along with the current time-of-day in a comment file on the disk, 4) request a listing of system status information, 5) request that data from an instrument not be stored on the disk if the instrument was defective or being calibrated, and 6) alter the calibration equations for each substance. Each substance was assigned a default calibration equation (see Appendix B). Instrument performance was susceptible to change from one day to the next; altering the calibration equations provided a means of compensating for such a change rather than having to make daily adjustments to the instrument.

After Run

Because the instrument response time was not immediate at the valve switching, the readings made in the first minute, and for some instruments the second minute, of a four minute cycle could have been based on a mixture of air from both chambers. In addition, certain instruments provided an update in their readings only once every minute or once every four minutes. Consequently, the two processing programs (steps 2 and 3, Figure 7) that operated on these minute-by-minute data files were designed to use only the one reading out of four (usually from the third minute of the cycle) that was appropriate for each substance. The first of these programs (step 2, Figure 7) could generate three different outputs: 1) a formated, four minute, summary listing of the data, 2) a line printer plot of the data with a resolution of 0.8% full scale, and 3) a file in which the data and comments were combined and stored as though they were punched on cards. The second processing program (step 3, Figure 7) generated a paper tape which could be read by a Hewlett-Packard programmable calculator with plotter (HP). Thus, after each run, plots and listings of all the substances were immediately available. The strip charts from each instrument, the one minute listing with operator comments that was generated during the run, the formated, four minute summary listing, the paper tape, and the HP plot were filed together in folders and indexed by run date. These became the basic information source for a run. The card image file described above was stored on magnetic tape so that it could be read by an IBM computer for later analysis.

The creation of the card image tape files was delayed until the UNC disk cartridge could be transferred to another PDP 11/40 computer at EPA which had a magnetic tape unit and a disk cartridge unit among its peripheral devices (Figure 8). This was usually done after 20 runs had been accumulated.

Other than the plots and listings, no other data treatment procedures were normally attempted on the site computer. There were several reasons for this, among them: limitations on program size, the presence of extensive statistical packages on other computers, and primarily a shortage of available time when the computer would not be collecting data.

After the tape files were created, the tape was carried to TUCC. This installation has an IBM S/370 computer with extensive programming support and statistical packages available. The tape files were input to a project-generated program called CONVERT which created files on a project-owned IBM disk pack resident at TUCC (Step 6, Figure 9). Besides converting from ASCII (the character code used by PDP computers) to EBCDIC (the character code used by IBM computers), CONVERT formated the data so that each record of the output file contained the last time of a four minute cycle, the reading collected in that cycle for each of the 12 substances, the chamber side from which the readings in that cycle were taken, and the year, month, and day of the run. These files had names composed of the month, year, and day on which the run was started followed by the extension ".DAT". For purposes of uniformity, each file contained 180 data records, sufficient to hold 12 hours of data between 0500 and 1700 hours. If a run was less than 12 hours, a missing data code was inserted in each record where necessary. The data records were followed by a varying number of comment records containing the date and time of the comment as well as the comment itself.

The raw data in these files could contain various errors: the readings might have come from a calibration period when the suppress option was forgotten, the sensitivity of an instrument was changed without an appropriate calibration equation change, or data were missing due to hardware failure or operation suppression.

To correct these errors, personnel used a project-generated program called CRCTSCP (Step 8, Figure 9). The .DAT file was copied to an online system pack so that it would be accessible under an IBM supplied interactive timesharing system called TSO. This is labeled in Figure 9 as the "CORCOPY" step. Personnel then entered the TSO system using a Tektronix 4010 graphics display terminal as the input/output device.

Using the 4010 offered several advantages: first, data could be rapidly plotted on the screen; second, the interactive nature of the system allowed the user to select a section of the plot and have it expanded to full screen size so that fine detail could be examined; third, the 4010 has adjustable crosshairs that allow the user to select a point on the screen and have its coordinates supplied to the computer. Thus the data could be graphically edited to correct spurious values and to remove gaps. Removal of gaps was necessary to make the data continuous across time so that subsequent numerical calculation of integrals and derivatives would be possible. Data were plotted on the screen and the crosshairs were used to edit the data in two ways: either to supply a specific data value at a certain time, or to supply the starting and finishing values over a period of time and have the intervening values computed by the program using linear interpolation. When all necessary editing had been performed, the edited data file on the on-line disk was copied over the old .DAT file on the project-owned, off-line disk. The .DAT extension was retained. The original raw data (that is, unedited data) remained available on the magnetic tape. This is labeled in Figure 9 as the "FINCOPY" step. The edited .DAT files were then passed through a high-frequency cut-off filter program called SMOOTH. The function of this program was to attenuate any high frequency noise spikes in the data so that meaningful derivatives could be calculated. The output of this program was 1) a formated listing of the raw data, 2) the r^2 resulting from a moving, least squares parabola fitted to five sequential points, 3) the value of the mid-point of the fitted parabola taken as the smooth data, 4) the derivative of the curve at each point, computed by a least squares, numerical procedure, based on five points, and 5) the integral of the curve from the start of data collection to the point under consideration. In general, the filtering was not necessary for the O_3 and NO_x data, but a fair amount of high frequency noise was present in the THC, NMHC, and CO data. The smoothed data along with the computed derivatives and integrals for each variable were written onto the project-owned disk with a name composed of the month, year, and day, as with the original raw data file, but with the extension ".SMTH". These .SMTH files became the final working files for a run.

A project-generated program called SMTHPLT was used to plot data in the .SMTH files on a Broomall plotter using the TUCC computer. These are the plots used as figures in this report. The .SMTH file listings were examined by project personnel and the actual (rather than the intended) initial conditions, peak concentrations, maximum rates, meteorological conditions, and dosages were extracted and key punched on cards. A total of 135 measures were extracted or computed from each side of each dual run. These data were used to generate plots for graphical analysis and as input to statistical analyses for what was called initial condition analysis. The key punched data were input to a project-generated PRINT program which listed the data from all runs using various groupings such as the same substance measured at various times in a run, and the values of different substances at the same time in a run. Times of importance included crossover times and times at which peak concentrations and peak rates were achieved. The key-punched data were also used as input to the non-linear, least-squares, multiple regression program (NLREG) available in the TUCC library.

The TUCC installation has several comprehensive statistical packages available, including the Statistical Analysis System (SAS) and the Statistical Package for the Social Sciences (SPSS). These programs were used to create an SPSS data file and an SAS data file from the cards. SAS was used to generate scattergrams from variable pairs and to perform selected regression analyses. SPSS analyses included descriptive statistics (means, standard deviations, etc.) of the variables, factor analyses, and joint frequency distributions for groups as well as pairs of variables.

All the runs over the two year data period occupy approximately 8 million bytes (characters) of storage on the project disk pack. In addition, there is one magnetic tape of raw data holding 4.9 million bytes, and more than 500 computer listings of data in various forms.

STANDARD NOMENCLATURE AND CONVENTIONS

During the grant period a system of nomenclature developed. Thus, certain terms used in this report have meanings specifically related to this project. The purpose of this section is to present and define the most important conventions used in this report. A more complete list, defining names and abbreviations, is contained in the glossary and a detailed description of the nomemclature conventions is given in Appendix A.

During the construction and operation of the smog chamber, conventions were adopted for naming parts of the facility and for naming experimental procedures. The chamber itself was divided into 169.9 m^3 (6000 ft^3) halves, each half was designated as a "side". For purposes of identification, one side was called the "BLUE" side and the other was called the "RED" side (see Figure 5). Manifolds and instrument sample lines were color coded and the color designation was used in data handling, from acquisition through final analysis. An experiment in a single chamber side was designated as a "run". A "dual run" was an experiment using both sides of the chamber to compare the effects of differences in controlled variables (such as initial concentrations) under identical solar radiation and temperature conditions. Data was collected by computer for each run from 0500 to 1700 Eastern Daylight Time. For purposes of defining starting conditions, however, the initial time was considered to be the time at which the hydrocarbon injection was completed.

In analyzing data from the smog chamber it was necessary to establish names for measures of reactivity and experimental variables which were consistant with requirements of the computer programs used. In general, these names had to consist of only alphanumeric characters, to begin with a letter of the alphabet, and to be no longer than eight characters. The names were composed of the abbreviation for the chemical or physical quantity to which the name applies, plus prefixes and suffixes describing the type of measure and the time of measurement. The types of measures considered included concentrations (____) (no special prefix or suffix), dosage (D___), rate of change of concentration (___R), differences (__ DIF__), maximum concentrations (__M) and averages (__AV__). The times of measurement correspond to various uniquely defined events in the course of a run. The events which were of interest included time at which initial conditions were achieved (I__), crossover (X__), the maximum rate of NO disappearance (__NOR), the maximum rate of NO_2 formation (__NO2R), the maximum rate of O_3 formation (__O3R), the maximum O_3 concentration (__O3M), and the end of run (__FIN). To name measures computed between the above events, the periods of time between events were given a numeric designation. The time between achieving initial conditions and crossover is "1", between crossover and NO2R is "2", between NO2R and NO2M is "3", between NO2M and O3R is "4", and between O3R and O3M is "5". For example, "HCAV3" is the average nonmethane hydrocarbon concentration between the times of the maximum rate of NO_2 formation and the maximum NO_2 concentration. "O3AV35" is the average ozone concentration between the times of NO2M and the ozone maximum concentration.

Some of the measures used in data analysis are different from the measures considered when analyzing indoor chamber data. Measures of reactivity as defined by the Coordinating Research Council project CAPI-6[15] often are not clearly applicable to outdoor chamber data. An example of an ambiguous definition is that of NO_2 formation rate. CAPI-6 defines NO_2 formation rate as

$$\text{Rate} = [\text{NO}]_i \ / \ 2T_{1/2}$$

That is, half the initial NO divided by the time to form an amount of NO_2 equal to 1/2 the initial NO. The broken line in Figure 10(a) shows such a rate on data from a typical indoor chamber. The slope of the NO_2 concentration line is quite close to the straight-line slope at any instant. Examining the data from a hypothetical run in an outdoor smog chamber in Figure 10(b), it will be noted that the instantaneous rate of NO_2 formation differs markedly from the straight-line slope. This is mainly a result of constantly increasing light intensity in the morning. The length of the initial period with zero light intensity is a function of injection time and sun rise, not a characteristic of system reactivity as would be desirable.

One means of avoiding this is to consider the maximum instantaneous rate instead of some average rate. The maximum rate is uniquely defined for nearly all NO_2 curves. It may be calculated by hand, or a computer can easily calculate and output the maximum rates. Because of the difficulties in applying CAPI-6 definitions to outdoor chamber data, other measures were adopted. The principal measures of reactivity used in the analysis were the following:

1. Time to crossover, when the NO_2 concentration equals the NO concentration (TIMEX).
2. Maximum rate of NO_2 formation (NO2R).
3. Maximum rate of NO disappearance (NOR).
4. Maximum rate of O_3 formation (O3R).
5. Maximum NO_2 concentration (NO2M).
6. Maximum O_3 concentration (O3M).
7. Average rates of concentration change between events in the system, e.g., NO2RAV3.

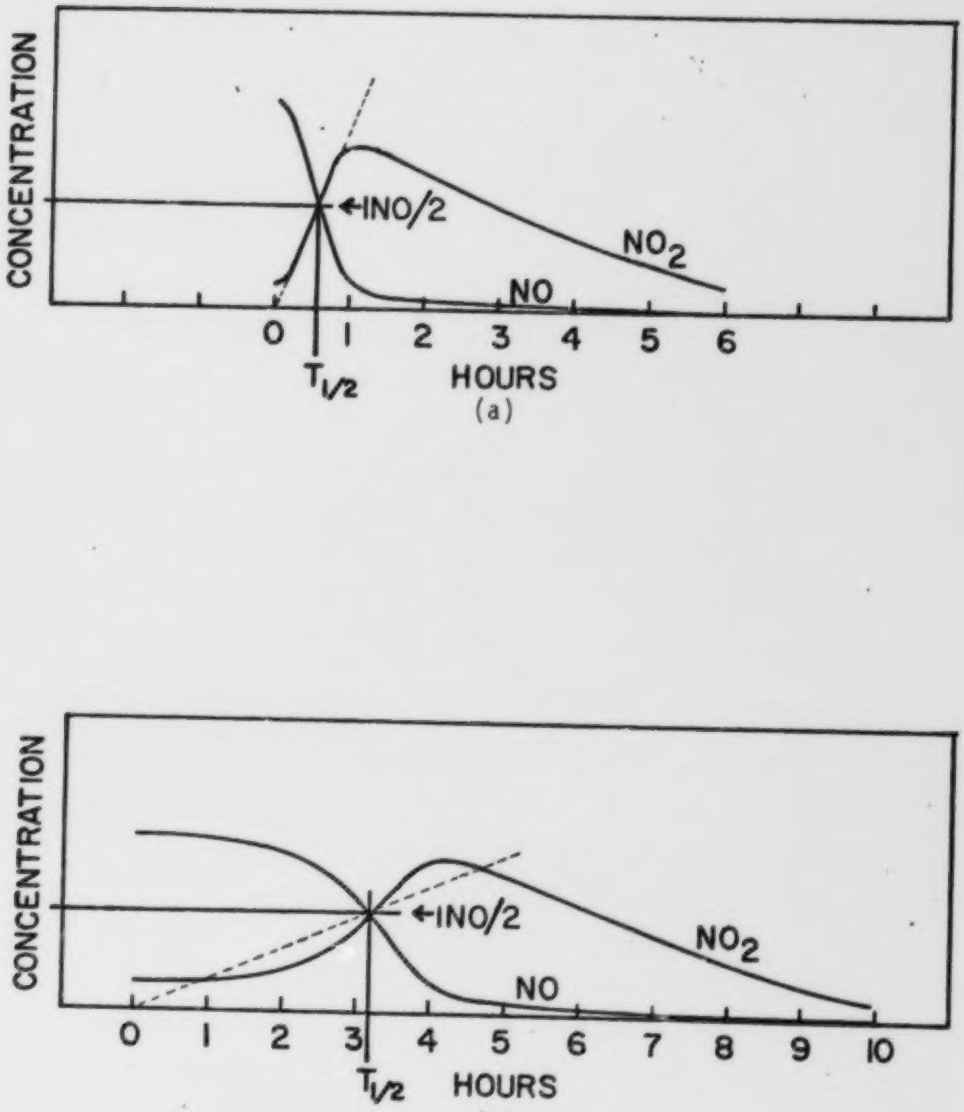

Figure 10. CAPI-6 definition of NO_2 formation rate applied to typical indoor(a) and outdoor(b) smog chamber profiles.

EXPERIMENTAL DESIGN

General

There were five factors considered in the experimental design: the reactant identity, the reactant concentrations, the purpose of the run, the climatology and the distribution of illumination, and the time period available. The first three factors were subject to choice; the last two imposed limitations.

Basic Program Plan

Two different types of hydrocarbons were used. Because of the large amount of previous smog chamber and modeling work that had been performed with propylene, experiments used to test the chamber, those intended for comparison with previous indoor work, and those to be used for modeling purposes were designed with propylene as the only NMHC. To determine the effect of NMHC control on the behavior of NO_2, a hydrocarbon mixture that was reasonably representative of urban conditions was needed. The design and composition of this mixture will be discussed in detail in a subsequent section.

Since the primary effect under investigation was hydrocarbon reduction, the primary variable between the two chamber halves was the initial NMHC concentration, while the INOX concentrations and the percentage of INOX that was NO_2 (PCTNO2) were to be the same in the two chamber sides. Runs were always performed in pairs.

A relatively few INOX values were planned while a larger number of IHC values were to be explored. Although a large range of concentrations was used, no attempt was made to obtain a balanced design in terms of number of runs at each concentration because of the variation in meteorological factors expected (see discussion below). With respect to the choices for INOX, a large number of runs was planned at a value which, according to Dimitriades' work[5,16], would result in a maximum NO_2 value that would achieve the annual air quality standard for NO_2 using Larsen's technique to transform a one hour average value to an annual mean value[17,18].

Fewer runs were planned at INOX values above and below this standard value with the number of runs at each value decreasing as the value became further removed from the standard. The range of INOX was chosen from background (~ 0.007 ppm) to ~ 1.0 ppm. The choice of IHC values was more arbitrary than the INOX; because of the background air concentrations, it was difficult to do experiments at or below 0.22 ppmC and no runs were performed above approximately 4.2 ppmC. Within this range IHC were spaced at approximately 0.5 ppmC intervals.

Some runs were planned in a 2 x 2 pattern. That is, all combinations of two sides of the chamber and two IHC with constant INOX and PCTNO2 were designated, yielding four runs at each IHC level on three different days. Runs and run pairs were planned in a somewhat random fashion within sets as were INOX concentrations where possible; runs were not performed in random order if certain matches of weather conditions were needed.

In all basic experiments, the initial percentage NO_2 was chosen to be 10% of the INOX for the propylene runs and 20% of the INOX for the hydrocarbon mix runs. Some experiments were planned to investigate the effects of different PCTNO2 levels. In these paired runs, the IHC and INOX was to be the same in each chamber half with the only difference between sides being the PCTNO2 value.

Table 3. SIMULATED URBAN HYDROCARBON MIXTURE

Class/Compound	Relative Concentrations		Mole Fraction	
	ppm	ppmC	Total Mix	Without Aromatics
1. Acetylenic				
acetylene	265	530	0.131	0.171
Subtotal	265	530	0.131	0.171
2. Paraffins				
isopentane	172	860	0.085	0.111
n-pentane	286	1430	0.141	0.184
2-methyl-pentane	85	510	0.042	0.055
2,4-dimethyl pentane	69	483	0.034	0.044
2,2,4-trimethylene pentane	76	608	0.038	0.049
Subtotal	688	3891	0.340	0.444
Average carbon number = 5.7				
3. Olefins				
butene-1	40	160	0.020	0.026
cis-2-butene	43	172	0.021	0.028
2-methyl-1-butene	26	130	0.013	0.017
2-methyl-2-butene	32	160	0.016	0.021
ethylene	360	720	0.178	0.232
propylene	97	291	0.048	0.062
Subtotal	598	1633	0.296	0.385
Average carbon number = 2.7				
4. Aromatics				
toluene	140	980	0.069	
m-xylene	90	720	0.044	
n-propyl-benzene	60	540	0.030	
sec-butyl-benzene	60	600	0.030	
1,2,4,trimethyl-benzene	123	1107	0.061	
Subtotal	473	3947	0.234	
Average carbon number = 8.3				
TOTAL with aromatics	2024	10,001	1.000	
without aromatics	1551	6,054		1.000

Urban Hydrocarbon Mixture

The chemical composition of the NMHC had to be reasonably representative of urban conditions. The Chemistry and Physic Laboratory of EPA had developed a mix based on field sampling by the Environmental Protection Agency in Los Angeles and Cincinnati which was selected for use in this study[19]. This mix was a compromise between actual urban early morning analysis and what could be easily analyzed with a gas chromatograph. Percentage distributions by mole fraction and average carbon number were balanced in the makeup of the mix (see Table 3). As originally proposed the mix consisted of 13% acetylene, 34% paraffins (average carbon number 5.7), 30% olefins (average carbon number 2.7) and 23% aromatics (average carbon number 8.3). It was very difficult to operate with the full aromatic content of the mix because of the retention of the heavier compounds from one day's run to the next either in the chamber or the sample lines. Experiments were performed with only toluene as 23% of the mix, with 23% of the mix as toluene and m-xylene, and with no aromatics at all. These experiments are described in the discussion of Chamber Chemical Performance in this report. Essentially no difference was found in NO, NO_2, and O_3 profiles in dual matched runs in which the same NMHC-ppmC concentration was used but the relative percentage of the toluene was 0% and 23%. Slight differences were found in dual runs with mix verses mix, toluene, and m-xylene. The observed differences could have been due to at least two factors. 1) different reactivity of the aromatic that replaces some of the paraffins and olefins, and 2) fewer molecules being present in the mix and aromatic runs, because the same ppmC was used on each side and the average carbon number of the aromatics was higher than that of the mix. Because there were no significant differences in the mix and toluene runs and mix only runs, and because the mole fraction weighted reactivity of the five aromatic compounds was very close to that of toluene, the aromatics were omitted from the full mixture entirely. Therefore, the hydrocarbon mix adopted for

Table 4. SELECTED CLIMATOLOGICAL DATA FOR PIEDMONT NORTH CAROLINA

	Mean	Range
Maximum Temperature	69°F	20°-95°F
Average Temperature	58°F	14°-82°F
Minimum Temperature	47°F	0°-72°F
Average Dewpoint	46°F	-3°-73°F
Average Wind Speed	9.2 mph	3.5-73°F
Hours Sunshine	7.86 hours	0-14.2 hrs.
% Possible Sunshine[a]	64.2%	31.5%=SD[c]
Sky Cover[b]	0.59	0.34=SD[c]

[a] The (daylight hours which had full direct sun)/(total daylight hours) x 100%.

[b] Fraction of the total sky hemisphere which had clouds.

[c] Standard deviation.

the experimental runs was 17% acetylene, 44% paraffins, and 39% olefins, as listed in the last column of Table 3, although there were some runs with aromatics added to the mix. In the latter case, the mixture composition was as in column 3 of Table 3 with 23% aromatics (i.e.. toluene).

Climatology and Solar Factors

The general climate of piedmont North Carolina is described by Petterssen[20] as a warm temperate, rainy climate, without dry seasons, and with hot summers. The piedmont has an average rainfall of 45 inches. Selected climatological data are given in Table 4. These data were calculated from data obtained from U.S. Commerce Department[21] for Tuesdays and Thursdays for 1969-1971 (313 days). From Table 4 one can see that, although on the average 60% of the sky was covered by clouds, 64% of the possible sunshine hours were hours of direct, full sun.

In Table 5, the number of Tuesdays and Thursdays in the period 1969-1971 which had various percentages of possible direct sunshine values are broken down by month. This table suggests that the periods of greatest sunshine would be in the spring and fall and that the middle summer months would be characterized by cumulus cloud formation that reduced the total time of direct sunshine. Figures 11 and 12 report the average daily solar radiation on a horizontal surface in the United States for January and July respectively[22]. These figures show that, although the chamber site and Los Angeles are approximately on the same latitude and should receive essentially the same solar radiation, the chamber site receives, on the average, approximately 10-12% less solar radiation in July and approximately the same solar radiation in the winter. Considering the information in Table 5, this result is most probably due to more partly cloudy days in July at the chamber site while Los Angeles has more clear days. In the winter, both locations must have approximately the same sky cover.

Table 5. NUMBER OF DAYS IN WHICH PERCENTAGE MAXIMUM POSSIBLE SUNSHINE WAS GREATER THAN OR EQUAL TO A GIVEN VALUE. TUESDAYS AND THURSDAYS IN 1969-1971 (313 DAYS) BY MONTH. (number of days)

	Percentage Maximum Possible Sunshine			
	100%	<90%	<75%	<50%
January	2	6	11	13
February	8	15	17	19
March	6	12	13	19
April	3	11	17	23
May	3	6	15	20
June	0	3	9	19
July	0	1	7	14
August	2	5	9	20
September	2	8	15	21
October	2	4	7	14
November	5	11	15	21
December	2	7	12	19
Total	35	89	147	222
Summation Percentage	11.2%	28.4%	47%	71%
Actual Percentage	11.2%	17.2%	18.6%	24%

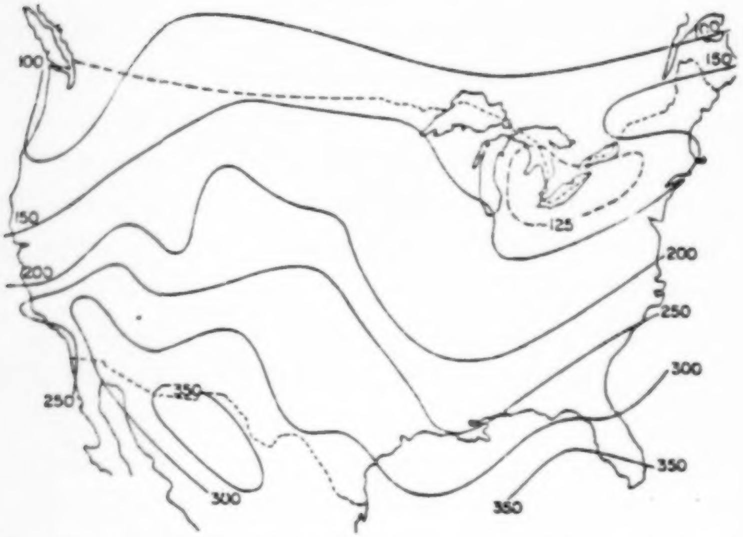
100
100
150
150
125
150
200
200
250
250
300
350
350
300
350
350

Figure 11. Average daily solar radiation on a horizontal surface in the USA for January. The units are cal-cm^{-2}-day. (Sellers[22]).

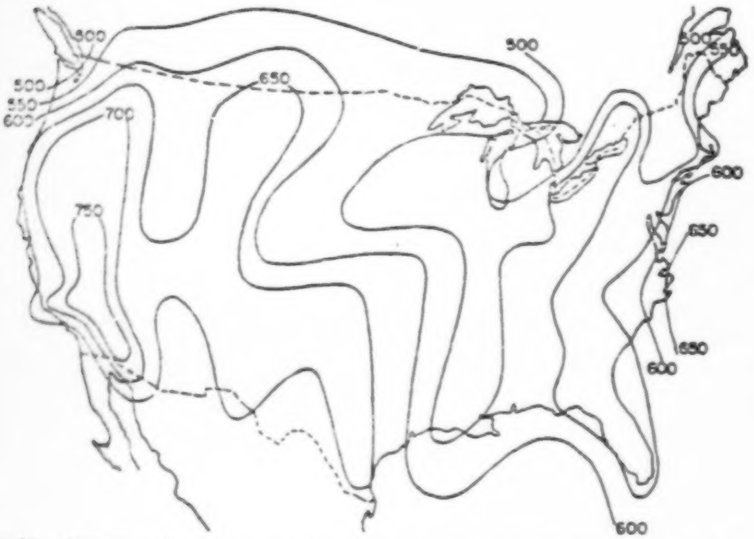
500
500
550
600
650
700
750
500
500
550
600
650
650
600
600

Figure 12. Average daily solar radiation on a horizontal surface in the USA for July. The units are cal-cm^{-2}-day. (Sellers[22])

It is possible by making assumptions about the average dust concentration, water vapor concentration, and ozone concentration aloft, to calculate the theoretical total solar radiation reaching any point on the earth's surface. Figures 13 and 14 illustrate the variation in solar radiation as a function of time and month on a surface normal to the beam and horizontal to the ground. These data are also corrected for atmospheric path length absorption. The cosine view factor is the principal difference between the data in Figure 13 and Figure 14. The major effect of season on intensity normal to the beam is on duration of daylight which can vary from a minimum in December of 9 hours, 34 minutes to a maximum in June of 14 hours, 25 minutes. The seasonal effects on intensity on a horizontal surface include not only the duration of the daylight but also a variation in maximum daily intensity which varies from 0.6 to 1.4 cal-cm^{-2}-min^{-1}. The data of Figure 14 can be compared with actual solar radiation profiles presented in subsequent sections of this report. The agreement was found to be very good for totally clear days (the time axis in Figure 14 is Eastern Standard Time).

The above discussion would suggest that there would be essentially unpredictable variations in solar radiation and temperature in any outdoor experimental design. The obvious method of dealing with these variations would be to run sufficient replicates at the critical locations in the experimental design so as to assure a wide range of solar radiation conditions including totally clear skies. The dual chamber design would assist in achieving a degree of control over these variations. Also to the extent possible, runs should be performed across seasons.

Time Period Available

Weather conditions in piedmont North Carolina do not become satisfactory for outdoor runs until approximately the third week in April. In this

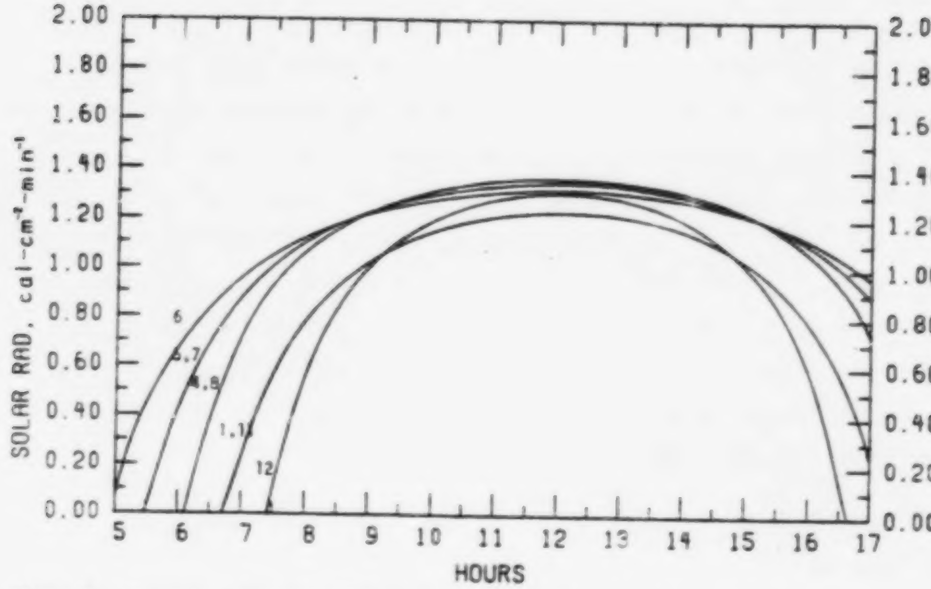

Figure 13. Theoretical solar radiation on a surface normal to the solar beam as a function of month. Numbers correspond to month.

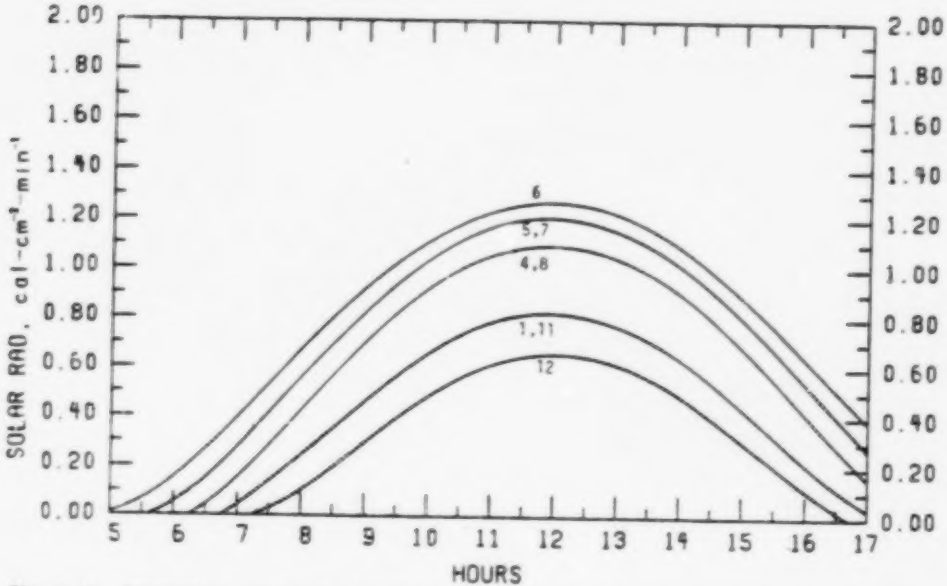

Figure 14. Theoretical solar radiation on a horizontal surface as a function of month. Numbers correspond to month.

period the last freeze, the last high winds, and the last cool days occur. Piedmont North Carolina usually has a rather long "Indian summer" in the fall months of late September and October, sometimes extending through the second week of November. These periods are characterized by cool to cold nights and totally clear days with temperatures reaching 30°C (85°F). Thus, the period from May through early November (approximately six and one half months) is available for outdoor runs. Under ideal conditions, approximately twenty dual runs per month could be performed, giving an upper limit of 260 runs or 130 dual runs per season. Unexpected maintenance or bad weather can reduce this number substantially.

SECTION VI

RESULTS AND DISCUSSION
PART I: FACILITY PERFORMANCE

Because of the uniqueness of this chamber, extensive testing was performed to assess its operating characteristics. These tests were to determine if the chamber design was physically sound and durable, and if it exhibited reasonable performance characteristics with respect to generally accepted smog chamber measures. The actual testing consisted of performing standard runs, comparing results with other chambers, demonstrating that generally accepted photochemical modeling approaches could be applied to the chamber results, and determining if the chamber facility produced data that was consistent and interpretable, even though it was sometimes subject to fluctuations in physical factors such as solar radiation, temperature, and relative humidity.

CHAMBER PHYSICAL PERFORMANCE

Design

The wooden A-frame and Teflon wall chamber was extremely durable. It withstood high winds, snow, freezing rain, and below freezing temperatures without any obvious weakness or stress. One panel had to be replaced in April 1974 after a tornado passed through the southern piedmont area of North Carolina; this replacement was accomplished in two days. The actual chamber volume and surface area that resulted and other physical and chemical data of interest are given in Table 6.

Mixing

Of concern in any study of this nature are the mixing characteristics

Table 6. ACTUAL PHYSICAL AND CHEMICAL CHARACTERISTICS OF THE CHAMBER

Item	Data for each side of chamber
Dimensions	9.14 m W x 6.10 m L x m L x 6.10 m W A-Frame (30 ft.) x (20 ft.) x (20 ft.)
Volume	156 m^3 (5509 ft^3)
Surface Area	204.4 m^2 (2200 ft^2)
Surface/Volume	1.31 m^{-1} (0.40 $ft.^{-1}$)
Moles Air @25°C (77°F)	6380 Moles
Volume of gas from 1% tank to yield 1 ppm in chamber @ 25°C	15.6 ℓ
Volume increase caused by 14°C temperature increase (base temperature - 25°C)	4.49 m^3 (4.7% total volume)
Exhaust and filling rate	7208 ℓ/min (255 ft^3-min^{-1})
Residence time on exhausting	21.6 mins
Time to 99.6% turnover	2.0 hrs
Sampling manifold flow rate	60 ℓ/min
Sampling manifold resident time	<14 sec
Injection manifold resident time	<5 sec
Mixing time in chamber	<3 min to stable reading
Sampling instrument consumption of volume for 12 hours operation	1588 ℓ (1.0% total volume)

of the chamber. This pertains to the rapid ability to achieve a steady concentration immediately after injection and ability to maintain a homogeneous mixture in the chamber for the duration of the run. Mixing in each chamber side was accomplished in three ways: two mixing fans, small constant movement of the Teflon walls from outside breezes, and thermal currents from slight temperature gradients which developed from floor to peak of chamber. No discernible changes in concentrations could be observed in either NO, NO_2, O_3 or NMHC when the mixing fans were turned on for one hour, off for two hours, and then on once more. Injection information over the past two years has consistantly shown that no more than 2 1/2 minutes were required to achieve a constant concentration (within the precision of the NO_x analyzer $\pm$ 0.002 ppm) after the completion of the injection process. In order to insure that the sample air from the center of the chamber was representative of other air in various parts of the chamber, the sample and return manifolds were switched during an experiment. This permitted sampling from the corner of the chamber (0.5 m from the floor) under one of the mixing fans; again no difference could be seen in the measurements just prior to and after the change in sampling location.

Air Handling Systems

Tracer experiments using ozone demonstrated the chamber could be purged to 0.1% of its original concentration with clean background air in approximately 1.5 hours. The decay profile followed that of an exponential dilution system. The purge rate was adjusted downward however, to prevent excessive stress on the Teflon walls and floor. This meant that a minimum of 3 hours of chamber purging was required before the startup of a new experiment.

Flow measurements taken inside the sampling manifold with a hot wire anemometer were 60 l/min; with an average manifold length of 9.14 m, thus less than 14 seconds were required for air in the chamber to reach the instruments. Since the chamber air on summer days was warmer than the manifolds inside the laboratory, heating tapes had to be installed on the entire manifold length to prevent condensation.

Chamber Tightness

It was impossible to expect that a 12,000 ft^3 Teflon film structure would be entirely leak free. The rate of dilution by exchange with outside air tended to be small according to CO tracer experiments. Material expanded out of the chamber when the temperature was rising and this did not result in any change in mixing ratio. When the temperature decreased, the volume decreased and outside air was drawn into the chamber, which caused dilution. Generally, air temperatures tended to rise throughout the course of the experiment, causing little dilution by this mechanism. Another mechanism for exchange was the compression and expansion of the film due to wind gusts which "pumped" the chamber walls. This was the predominant mechanism for exchange, since the looseness in the walls absorbed the small volume changes due to solar radiation changes which caused air heating and cooling. The overall mass loss during the course of a 12 hour run was never more than 12%, according to CO data mostly on windy days (see ozone and NO decay tests in a later discussion for other species loss rates). No correction was made for any mass loss by exchange.

Solar Radiation, Temperature, and Humidity

It has been stressed throughout this report that natural outdoor conditions made these smog experiments unique and more realistic. Materials were carefully selected to insure that these natural conditions would exist inside the chamber. Upon completion of the chamber, various tests were run. A comparison of the light in the chamber with that outside showed that approximately 85% of the total solar and UV radiation was transmitted inward through the Teflon. These data were

Table 7. SPECIFIC PHOTOLYSIS RATE FOR NITROGEN DIOXIDE IN OUTDOOR SMOG CHAMBER DURING SEPTEMBER, 1973.

Incident total solar radiation, $cal\text{-}cm^{-2}\text{-}min^{-1}$	Φka inside chamber 2 ft. above floor, min^{-1}
0.63	0.22
0.78	0.28
1.09	0.37

recorded by Eppley total solar radiation and UV sensors which do not measure through a full 360° volume, but only 180°. Further comparisons were made by measuring the specific rate of photodissociation (Φk_a) of NO_2 (in nitrogen in Teflon bags) inside the chamber. These measurements were made approximately 2 feet above chamber floor and are reported in Table 7. At all of the outdoor solar conditions in which these comparisons were performed (solar radiation between 0.7 and 1.1 $cal\text{-}cm^{-2}\text{-}min^{-1}$ outside of chamber), the Φk_a for NO_2 was always higher inside the chamber than outside. The reflective aluminum floor was responsible for this difference.

In September 1974, a continuous quartz globe NO_2 actinometer (QGA) was designed and built by Sickles and Jeffries[23]. This device is described in Appendix E. Two days of comparison data for TSR by Eppley sensor and QGA were generated and are reported in Figures 15 and 16. Essentially the same ratio of Φk_a/TSR (that is 0.36 to 0.37 $min^{-1}/cal\text{-}cm^{-2}\text{-}min^{-1}$) was found with the QGA as had been determined in 1973 with NO_2 bag experiments inside the chamber.

In addition to raising the light flux (and thereby compensating for the light losses through the Teflon), the reflective aluminum floor helped prevent large temperature increases inside the chamber. Before

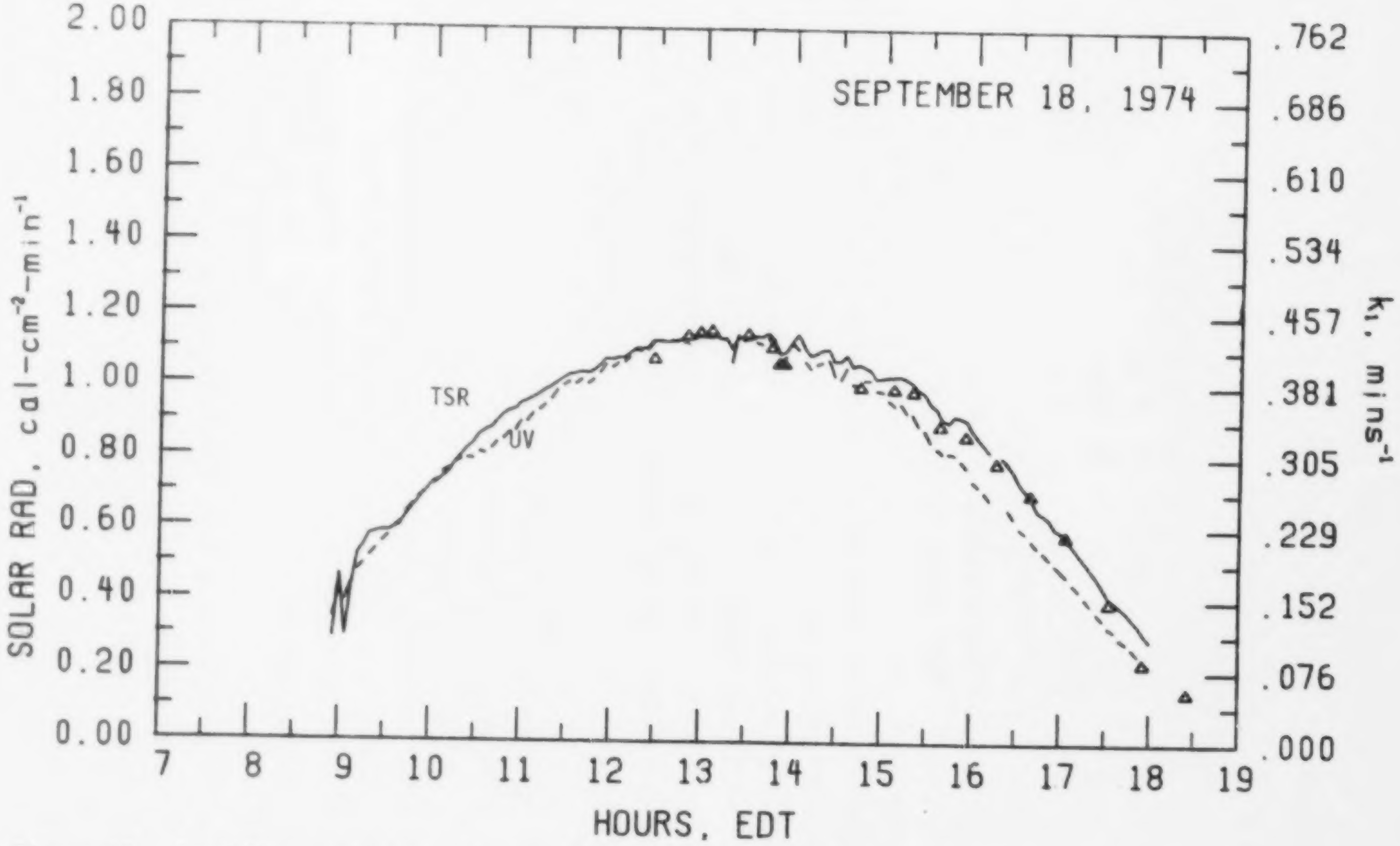

Figure 15. Specific photolysis rate for nitrogen dioxide and incident total solar radiation and ultraviolet radiation as a function of time for September 18, 1974. Solid line is total solar radiation; dashed line is ultraviolet radiation (full scale is 69.08×10^{-3}cal-cm^{-3}-min) and Δ are k_1.

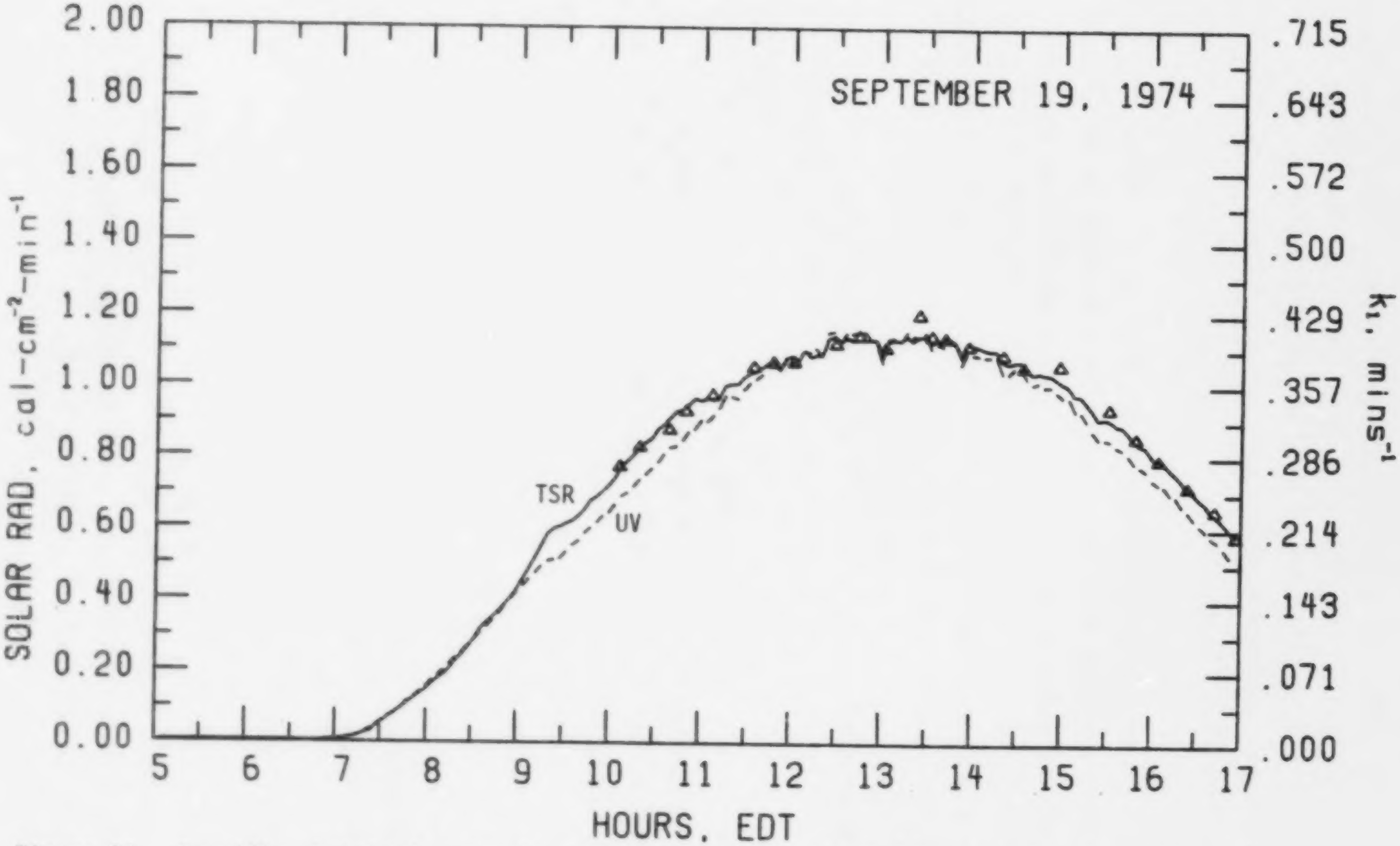

Figure 16. Specific photolysis rate for nitrogen dioxide and incident total solar radiation and ultraviolet radiation as a function of time for September 19, 1974. Solid line is total solar radiation; dashed line is ultraviolet radiation (full scale is 67.45×10^{-3} cal-$^{-2}$-min) and Δ are k_1.

the aluminum floor was installed, a 20°F air temperature rise in the chamber occurred on sunny days with outside temperatures of 85° to 90°F. With the aluminum floor, the air temperature inside the chamber was only 4.5° to 5.6°C (8-10°F) higher than the outside ambient temperature with full summertime solar radiation conditions. Typical air temperature profiles for several days are shown in Figure 17.

No attempt was made to control the relative humidity in the chamber. During the evening and early morning purging procedure (1700 to 0500 hours), condensation would sometimes form on the inside walls of the chamber. In experiments run on mornings after this had happened it could take until approximately 0900 hours for this condensation to evaporate. Typical dew point profiles are shown in Figure 18.

INSTRUMENT PERFORMANCE

Ozone Meter

The chemiluminescent ozone meter used in this study has performed without any failure for the past 24 months. The Teflon particulate filter in the sample line had to be replaced every 2 months and the rotometer setting on the sample and ethylene adjusted weekly to the correct value. The zero and span drifts over the course of a week were usually less than 3 ppb and 20 ppb on the 1 ppm scale. The ozone calibration was studied in detail and this study is reported in Appendix D. This study placed a 95% confidence limit on the overall calibration of the ozone meter of less than ± 0.008 ppm at the NAAQS of 0.08 ppm.

Oxides of Nitrogen Meter

The chemiluminescent NO-NO_x monitor did not have major maintenance or mechanical problems. During calibration, the efficiency of the NO_2 converter was always greater than 99%. After 2 months of constant use, the vacuum pump was routinely rebuilt, the O_3 generator cleaned

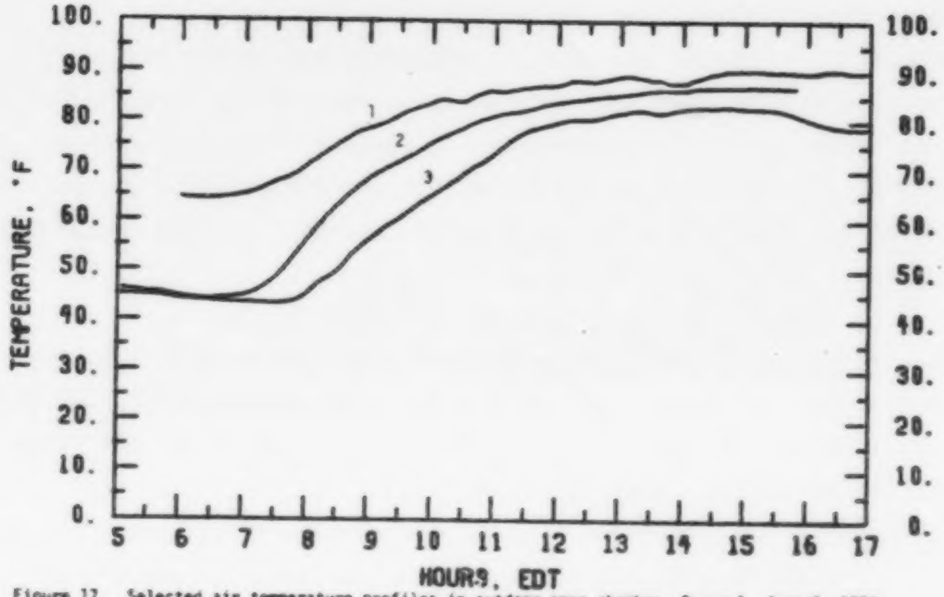

Figure 17. Selected air temperature profiles in outdoor smog chamber. Curve 1, June 9, 1974; curve 2, May 14, 1974; curve 3, October 12, 1974.

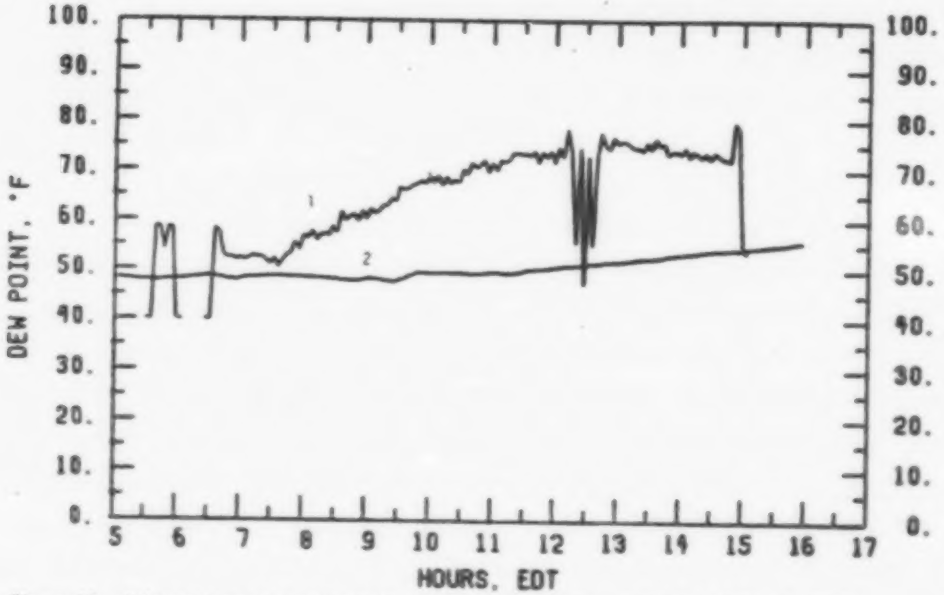

Figure 18. Selected dewpoint profiles in outdoor smog chamber. Curve 1, October 4, 1973; curve 2, May 16, 1974.

and the Teflon filter in the sample line replaced. Because of long continuous operation the NO_2 catalyst exhibited "converter fatigue". This problem manifested itself in a decaying response to high NO_2 concentrations when the meter was used to measure short term high NO_2 (~4 ppm) concentrations. The problem was solved by operating the NO_2 reactor at 325°C while purging with helium overnight and then returning the reactor temperature to 265°C.

Two very important interference characteristics were exhibited by the NO_x monitor used in this study. Initially, this instrument was operated with a gold wire catalyst to reduce NO_2 to NO. It was observed[24] that in propylene runs which generated high oxidant (0.2 to 1 ppm), an increasing positive interference to NO_2 coincided with oxidant buildup; also inordinately high NO concentrations were observed at the end of these smog runs. Neither interference was observed in specially prepared clean air systems of $O_3/NO_2/NO$. Generally, it was found that until the NO_2 peak was reached, NO_2 concentrations reported by the chemiluminescent meter were in good agreement with Saltzman NO_2 bubbler measurements. The interference became most pronounced after the NO_2 peak was reached and oxidant formation began to exceed 0.2 ppm.

A new carbon catalyst, furnished by the manufacturer, was installed in the NO_x instrument in November 1973. Subsequent smog profiles from the chamber still exhibited high NO_x values after the peak, but they did not exhibit the high residual of NO that previously occurred in instrument readings from the spent smog system. Nevertheless, it is strongly suspected that although NO levels in the middle of the run are in closer agreement with those predicted by photostationary equilibrium for coexisting NO, NO_2, and O_3 concentrations[25], near the end of the run there is a minimum concentration (0.01-0.03 ppm) below which the instrument will not read correctly. Therefore it is difficult to make photostationary equilibrium calculations near the end of the run when NO concentrations should be approximately .003 ppm. The NO_2 interference in the NO_x mode of the chemiluminescent analyzer was probably caused by reduction of organic and inorganic nitrogen compounds such as PAN and nitric acid ($HONO_2$) to nitric oxide in the NO_2 converter. The catalytic reactor was run at lower temperatures to reduce the possibility of reducing interfering compounds. Lower converter temperatures (~200°C) did not yield a linear NO_2 conversion efficiency.

Shortly after these tests had been conducted at the UNC chamber, two other smog chamber groups at the EPA Smog Chamber Conference[26], described more detailed experiments relating to the interference characteristics of the Bendix NO_x analyzer. The Riverside group presented data to show essentially a 100% response to PAN and methyl nitrate, but they found an erratic response to $HONO_2$. This data was subsequently published.[27] The Battelle group presented data which indicated a 100% response to $HONO_2$, but they found an erratic response to PAN[28]. It was not clear how the experiments were performed or if the usual Teflon in-line sample filter was used in either experiment.

It is clear from NO_2 data produced by the UNC chemiluminescent NO_x analyzer that either the UNC analyzer was not responding with 100% efficiency to both $HONO_2$ and PAN or that one of these compounds was not present in the sampling lines, because in high concentration (4-5 ppmC) propylene runs, 60% of the initial NO_x was not measured near the end of the run (see Figure 19). The Battelle group has developed a technique for measuring $HONO_2$ based on its selective removal by fine nylon fibers.[29] A propylene/NO_x experiment was conducted using two Bendix chemiluminescent NO_x analyzers. The project analyzer was operated in its normal manner with a Teflon in-line sample filter; the second NO_x analyzer had a nylon fiber $HONO_2$ scrubber installed in front of the Teflon in-line filter so that it would not respond to $HONO_2$. Manual Saltzman bubbler data were also taken. The results of this test run are shown in Figure [illegible].

All three measurements agreed well until 30-60 minutes after the NO_2

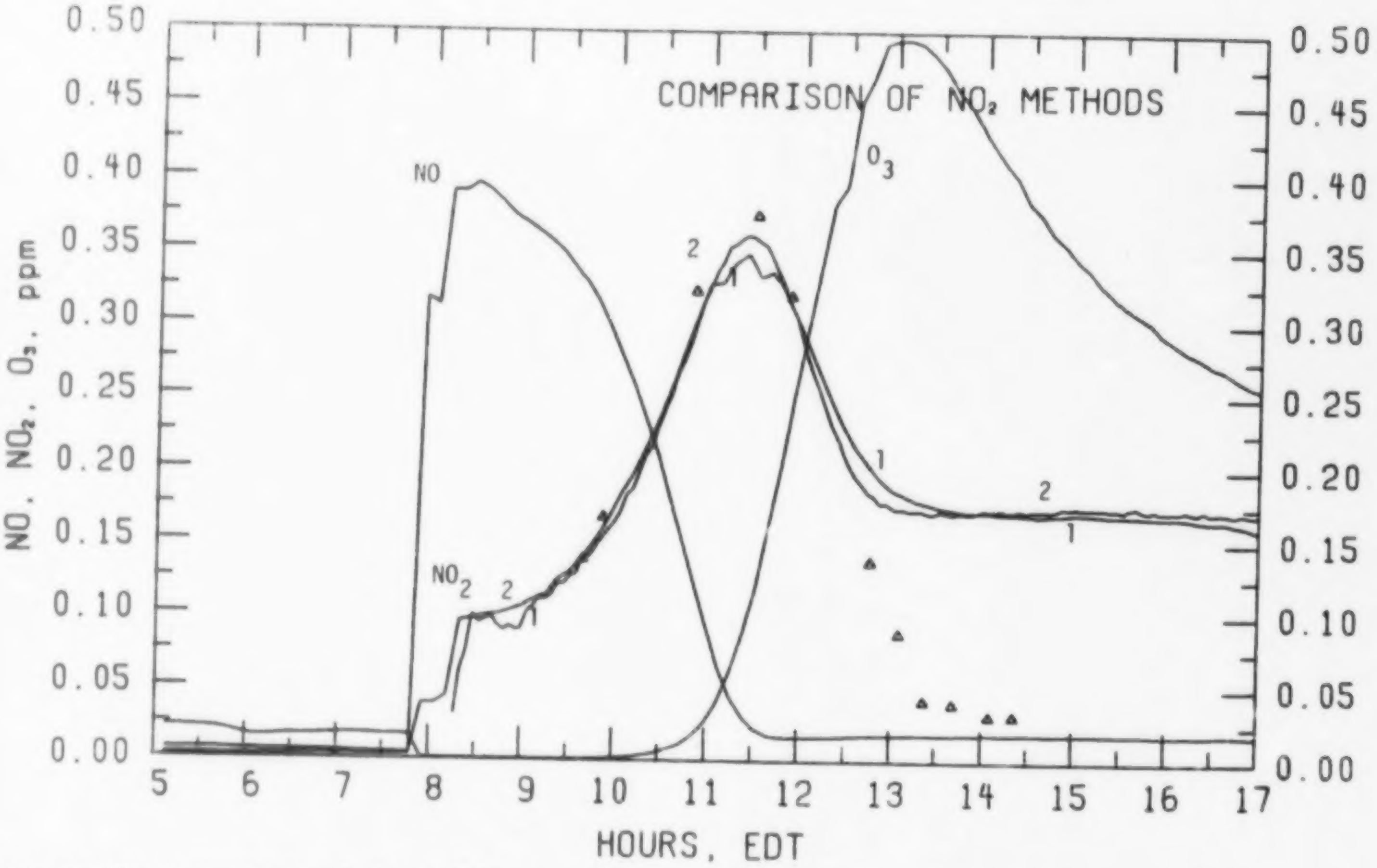

Figure 19. Comparison of three different NO_2 measurement methods in a propylene/NO_x system. Curve 1 - Bendix NO_x analyzer with Teflon filter. Curve 2 - Bendix NO_x analyzer with nylon HNO_3 scrubber. Δ - Saltzman bubbler measurements. NMHC concentration 4.06 ppmC.

peak. This was the time of maximum formation of PAN and $HONO_2$. The two chemiluminescent instruments agreed almost perfectly the entire run, indicating that the project analyzer was not measuring $HONO_2$. Subsequent measurements of $HONO_2$ using the Battelle method have shown that $HONO_2$ was present in the sampling manifold at approximately the expected concentrations during the propylene/NO_x experiments. We have concluded that the particular sampling arrangement probably influences whether the Bendix NO_x analyzer can measure $HONO_2$, and that in our arrangement, the analyzer does not detect $HONO_2$, but does respond to PAN, probably at 100% efficiency. Therefore, NO_2 data from the project NO_x analyzer after the NO_2 peak was actually NO_2 + PAN.

Since PAN does not begin to form in appreciable quantities until after the NO_2 has reached its peak (or more properly, the NO/NO_2 ratio has become very small), the NO_2 peak measurements reported in this study are valid measurements of the NO_2 maximum concentration. This is supported by Saltzman bubbler data taken on a number of runs at various concentrations (an example is shown in Figure 19). In propylene experiments, where the most interference would be expected, the Saltzman and chemiluminescent NO_2 data agreed until 30-60 minutes after the NO_2 peak. The mix contained only a small amount of compounds capable of forming the peroxyacyl radical needed for PAN formation, so therefore the interference in mix experiments would have been very small. In the auto exhaust experiments of Dimitriades[5], the PAN formation ranged from .001 to .08 ppm over a hydrocarbon range of .1 to 4.8 ppmC. Saltzman bubbler data in the mix runs were also in good agreement with the NO_x analyzer near the peak.

Only runs employing the hydrocarbon mix were used in assessing the effects of hydrocarbon reduction on NO_2 concentrations. No corrections were applied to the NO_2 data in these experiments. Nitrogen dioxide maximum concentrations were considered to be valid based on the studies described above. Nitrogen dioxide dosages in the high hydrocarbon runs could have been high by 3-5% due to PAN interference in the afternoon.

Runs employing propylene as the hydrocarbon were used for testing and modeling purposes. The NO_2 data in these runs were also not corrected for the PAN interference and in the figures in this report which show propylene data, the NO_2 data after the peak should be taken as NO_2 plus PAN.

ENVIRONMENTAL CHROMATOGRAPH

The environmental chromatograph required more attention than the other instruments. Columns were replaced or reactivated monthly. Daily calibrations were required; the reproducibility on a 3 ppm calibration source was ± 3%. Thus, for a single measurement, it was possible for the CH_4 to be low by 0.05 ppmC and the total hydrocarbon (THC) high by 0.05 ppmC. For this reason, the NMHC curves (difference between THC and CH_4) for a given run appear to be more noisy than the O_3, NO, or NO_2 profiles.

The environmental chromatograph is not subject to interference, per se, but can exhibit different responses to different hydrocarbon compounds. The Federal Register[1] method indicates that both the CH_4 and THC modes of the instrument be calibrated with CH_4 gas mixtures, as in Figure 20a. This calibration method will work only when the detector response to CH_4 and to higher hydrocarbon compounds is the same; that is, each carbon giving the same increment in signal whether it is CH_4 (increment of 1 unit) or the carbons in C_2H_6 (increment of 2 units) or C_3H_8 (increment of 3 units). This was found not to be true for this environmental chromatograph.

When both modes, THC and CH_4, were calibrated with gas mixtures containing only CH_4, as in Figure 20a, the response to a nonmethane hydrocarbon, such as butane, hexane, or toluene (when present alone or in mixtures

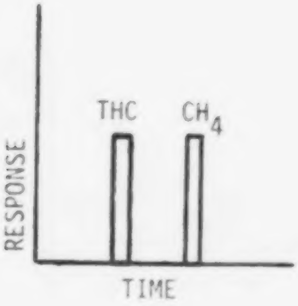
THC
CH_4
RESPONSE
TIME

a) THC and CH_4 outputs calibrated with CH_4 only

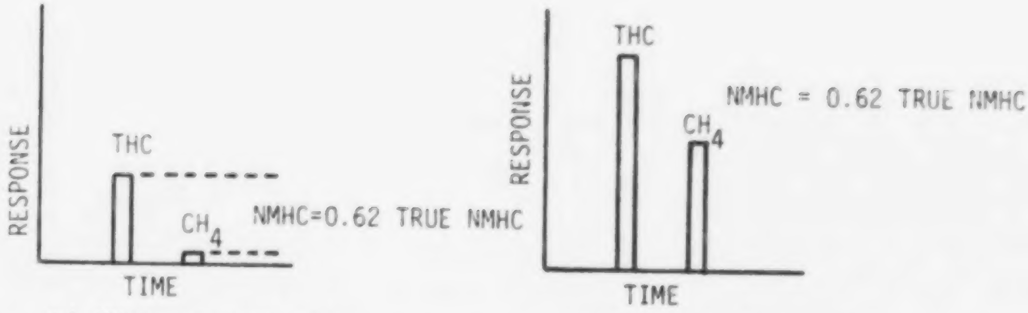
THC
RESPONSE
CH_4
NMHC=0.62 TRUE NMHC
TIME
THC
RESPONSE
NMHC = 0.62 TRUE NMHC
CH_4
TIME

b) NMHC standard only

c) CH_4 + NMHC standard

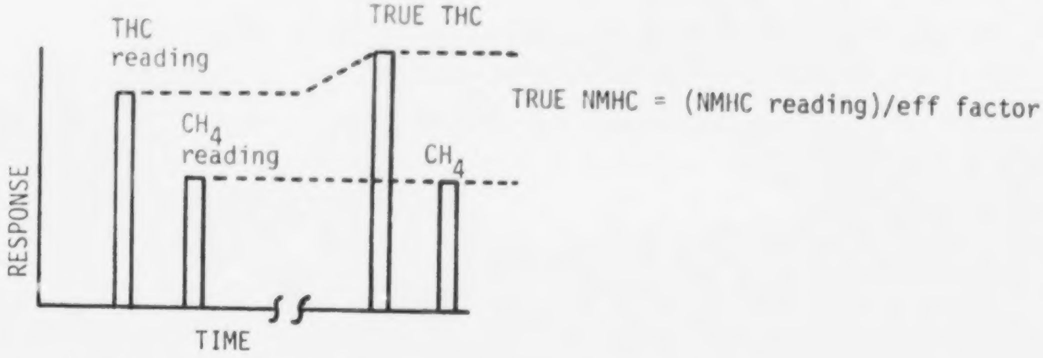
THC reading
TRUE THC
TRUE NMHC = (NMHC reading)/eff factor
CH_4 reading
CH_4
RESPONSE
TIME

d) calibration or efficiency factor applied to (THC - CH_4) reading

Figure 20. Calibration and correction of environmental chromatograph.

with CH_4) was only 62% of the expected value, as in Figure 20b. When NMHC was added to CH_4 mixtures, the THC mode responded 100% to the CH_4 and only 62% to the NMHC as in Figure 20c. The response factor to NMHC could be improved by increasing the hydrogen to air ratio in the detector, but this was at a sacrifice to sensitivity and precision.

The response difference was only between CH_4 and hydrocarbon compounds with more than one carbon, that is, CH_4 was detected with one efficiency and other hydrocarbon compounds were detected with another efficiency. It is not unusual for the first member of a homologous series to be different from higher members. Since CH_4 was measured by itself, it was possible to correct the NMHC after calibrating both modes with CH_4 only, as shown in Figure 20d.

Each week an average efficiency factor was determined by measuring the response to individual known concentrations of butane, hexane, and toluene. This efficiency was always 62% ± 2% of the response to CH_4 only. As the data were acquired during an experiment, the difference between the THC and the CH_4 readings was computed. This gave a value for NMHC that was 62% of the true concentration. It was therefore multiplied by 1.6129 to arrive at the true NMHC concentration. These calculations were performed by the computer for each reading. This method is the only way valid data can be obtained from instruments which exhibit the above characteristics because the THC data is a mixture of material with 100% response and materials with 62% response.

To determine if the response characteristics described above were peculiar to the environmental chromatograph used in this study, two other instruments , one produced by a different manufacturer (Beckman), were tested. The Beckman chromatograph had a 74% response to NMHC when both the THC and CH_4 modes were calibrated with CH_4. The other instrument also had a 60-64% response to NMHC. We would therefore, caution other users of environmental chromatographs to determine the actual response efficiency to NMHC rather than assume it is the same as CH_4.

GAS CHROMATOGRAPH

A gas chromatographic system was designed and developed by William Lonneman of the U.S. Environmental Protection Agency using a Perkin Elmer 900. The original intent of this system was to obtain a qualitative spectrum analysis of the hydrocarbon mixture in the chamber after the completion of the injection process. Chamber air was introduced into a 25 cc sample loop and then concentrated in an associated liquid nitrogen freeze out trap. Hydrocarbon separation and detection were accomplished with a 200 ft. S.C.O.T. column and a flame ionization detector. The analysis was temperature programmed from 30°C to 110°C at 16°/min, with an initial time of 2 minutes and a final temperature of 110°C for 10 minutes.

This system did not permit the separation of C_1-C_3 compounds and 2-methyl-butene-1 from 2-methyl-butene-2. Although this method was used as a qualitative tool, it was possible to obtain some quantitative information on the compounds above by use of hexane as an internal standard.

INJECTION SYSTEM

Of the many different methods initially considered to introduce pollutants into each half of the 312 m^3 smog chamber, concentrated commercially prepared tank and associated valving proved to be most satisfactory. Nitric oxide and NO_2 injections were accomplished in less than one minute with an additional 8 to 12 minutes required to bring these pollutants up to the desired concentrations. Injection rates from the concentrated NO and NO_2 tanks did not vary by more than ± 5% from day to day.

Vapor pressure considerations placed an upper limit on the individual concentrations in the hydrocarbon mix tank(s). The original mix was prepared in two cylinders. Experience in preparation by the manufacturer and storage and injection at the UNC smog chamber permitted a subsequent blend of the same mix to be prepared in one cylinder. A comparison of typical relative concentrations at the beginning of runs on July 28, 1973 (two cylinder injection) and September 18, 1974 (one cylinder injection) is given in Table 8 and a typical chromatogram is shown in Figure 21. These data demonstrated the ability to inject the same general distribution of hydrocarbon species over the course of two smog data periods and at different initial hydrocarbon concentrations. Although there were differences in the actual butene concentrations between the two injections (tanks), the total butenes were 8.89 and 8.66% carbon. The chromatograms in Figure 21 show that the areas for these peaks are quite small and measurement errors were possible.

CHAMBER CHEMICAL PERFORMANCE

Natural Background Air

The natural background air used to purge the chamber was not entirely free from NMHC and oxides of nitrogen. In the spring and early summer months the background NMHC ranged from 0.10 to 0.30 ppmC. During the fall this background could increase from 0.30 to 0.55 ppmC. Oxides of nitrogen in the spring were usually <0.01 ppm. Most of the time this NO_x background was equally divided between NO and NO_2. During a two week inversion period in July 1974, values as high as 0.035 ppm NO_x were measured in the early morning air. To minimize the effects of this background, experiments with high IHC and INOX were performed on these days. Carbon monoxide background varied between 0.3 and 0.6 ppm. Early morning ambient O_3 concentrations were usually below 0.02 ppm with 1 hour daytime maximums falling between 0.03 and 0.05 ppm. A few times during the summer ambient O_3 maximum concentrations were above 0.08 ppm.

To test the oxidant potential of the background in the chamber, experiments were performed by closing the chamber with only background air inside. On April 30, 1974, the maximum 1 hour ambient ozone measured outside the chamber was 0.082 ppm. At this time, 1440 EDT, the oxidant inside the chamber was 0.137 ppm. Data for NMHC and NO_x were not available on this day. A similar run on July 7, 1974, produced 0.167 ppm in the chamber while ambient ozone just outside the chamber was 0.066 ppm. During the course of this experiment, NO_x in the chamber increased from 0.009 ppm to 0.020 ppm (NO was 0.09 ppm and NO_2 was 0.011 ppm), and NMHC increased from 0.1 to 0.2 ppmC. This increase in NO_x and NMHC was apparently due to the degassing of materials from the Teflon film after an experiment the previous day with mix and NO_x.

Ozone Decay in Background Air

The average nighttime rate of destruction of O_3 in rural North Carolina air is approximately 0.11 ppb/min[30]. UNC chamber tests with starting O_3 concentrations of 0.85 and 0.54 ppm in background air show daytime destruction rates of approximately 0.33 to 0.50 ppb/min depending upon the time of day. The average nighttime rate (initial O_3 = 0.6 ppm) was approximately 0.13 ppb/min, very close to the rate reported for rural air.

Assuming that the photolysis of O_3 produces 14% O^1D and 86% O^3P oxygen atoms at a specific rate of 5.1×10^{-2} times the NO_2 photolysis specific rate (ϕka), and that the O^1D oxygen atoms react primarily with water to yield 22% hydroxyl radicals and 89% O^3P atomic oxygen, then only 3% of the ozone photolyzed is lost by this route because the primary fate of O^3P oxygen atoms is to react with O_2 to form O_3. Using a maximum value of 0.55 min^{-1} for ϕka, the net O_3 loss rate due to photolysis would be a maximum of 0.7 ppb/min. For the data in Table 9, the maximum ϕka for NO_2 would be approximately 0.28 min^{-1} using the relationship for ϕka and solar radiation given in Figure 16 and the maximum solar radiation for November given in Figure 14. A ϕka of 0.28 min^{-1} corresponds to an O_3 instantaneous photolysis rate of 12.4 ppb/min at $[O_3]$ = 0.85 ppm. If the net loss of O_3 by photolysis is

Table 8. RELATIVE DISTRIBUTION OF INDIVIDUAL COMPOUNDS OF THE HYDROCARBON MIX IN TANKS AND IN CHAMBER AIR AFTER INJECTION[a]

(percent carbon)

Compound	specified[b] HC mix	Two tank[c] injection of July 28, 1973	One tank[d] injection of Sept. 18, 1974
acetylene	---	---	---
ethylene	---	---	---
propylene	---	---	---
butene-1	3.57	4.01	2.93
cis-2-butene	3.81	2.01	3.20
2-methyl-butene-1	2.91	2.87[e]	2.53[e]
2-methyl-butene-2	3.57		
isopentane	19.20	21.20	18.66
n-pentane	31.96	30.60	37.60
2-methyl-pentane	11.41	13.18	12.00
2,4-dimethyl-pentane	10.73	12.32	9.60
2,2,4-trimethyl-pentane	13.65	13.75	13.50
TOTAL	100.81	99.94[f]	100.02[f]

[a] Data for injections based on area under peak from chromatograms generated by freeze-out of multiple 25 cc air samples and analysis on Perkin-Elmer 900 Gas chromatograph with 200' SCOT column coated with OV-101. See Figure 21 for chromatograph example.

[b] Methane from background air and acetylene, ethylene, propylene from mix were inseparable under the conditions of analysis, therefore the relative distribution was computed omitting these components.

[c] Total non-methane hydrocarbon concentration was 0.7 ppmC injected from two tanks each contain only part of the mixture.

[d] Total non-methane hydrocarbon concentration was 2.0 ppmC injected from one tank containing the entire mixture.

[e] These compounds were not resolvable from each other.

[f] Total butenes in each injection was 8.89% and 8.66% for two tank and one tank injections.

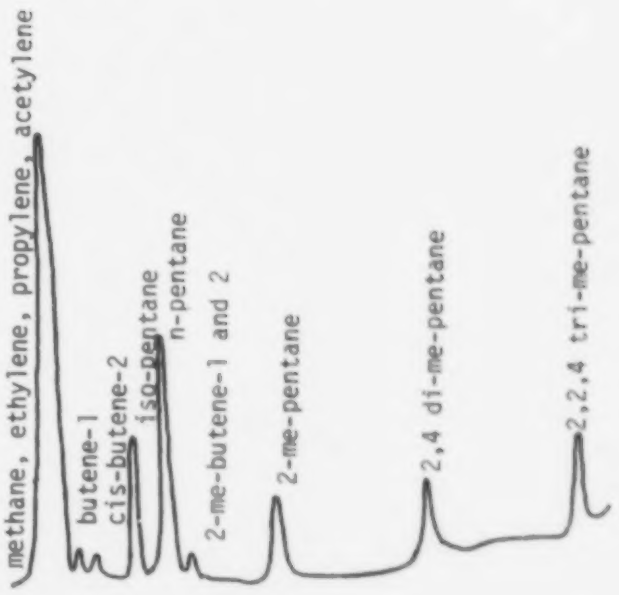

Figure 21. Sample gas chromatogram of hydrocarbon mix from chamber air immediately after injection.

only 3% of the instantaneous rate as described above, the O_3 disappearance rate would be 0.4 ppb/min. Assuming that the nighttime rate of O_3 loss in the chamber (0.13 ppb/min) was due to thermal reactions with the walls and other materials and that it was of the same magnitude during the daytime, then the net theoretical loss rate of O_3 at 1300 hours (solar noon) would be 0.53 ppb/min, in very close agreement with the actual rate measured (0.533 ppb/min). This rate excludes any reactions of O_3 with photochemically generated reactants.

The O_3 loss rate in the chamber decreases with decreasing light intensity. Of course, any O_3 generation due to photochemical processes would decrease the net O_3 loss rate. The O_3 data in Table 9 agree well enough with theory, that any O_3 generation would have to be less than 0.1 ppb/min. This rate of O_3 generation would create 0.06 ppm O_3 in the chamber in 10 hours which is approximately what occurred when background air was irradiated in the chamber. The nighttime O_3 loss rates yield a half-life of 48 to 70 hours and the daytime loss rates yield a half-life of approximately 18 hours.

Oxidation of NO in Background Air

Nitric oxide oxidation tests were conducted by injecting 90% NO and 10% NO_2 into the chamber with background air. During the daytime the average rate of NO disappearance was approximately 0.2 to 0.3 ppb/min for starting NO concentrations ranging from 0.45 to 0.65 ppm. A typical NO/Background dual run is shown in Figure 22. The diurnal trends for two NO oxidation runs are given in Table 10. On November 3, 1973 an initial rate of 0.09 ppb/min was computed for the early morning (the theoretical thermal rate would be 0.06 ppb/min); this was followed by a midday rate of 0.31 ppb/min (thermal rate = 0.051 ppb/min) and an afternoon value of 0.24 ppb/min (thermal rate = 0.040 ppb/min), thus these rates appear to be a function of light intensity. The rates of NO_2 formation, also included in Table 10, show that the NO decay rate is almost twice the NO_2 formation rate, indicating that the

Table 9. RATES OF OZONE DECAY IN UNC OUTDOOR CHAMBER USING BACKGROUND AIR

Date	Time, EST	O_3 Change, RED ppm, Start	O_3 Change, RED ppm, End	O_3 Change, Blue ppm, Start	O_3 Change, Blue ppm, End	O_3 Rate RED, ppb/min	O_3 Rate BLUE, ppb/min
Nov. 4, 1973	1028-1404	0.8514	0.7363	0.8485	0.7481	0.533	0.465
and	1404-2102	0.7363	0.5812	0.7481	0.6060	0.371	0.340
Nov. 5, 1973	2102-0500	0.5812	0.5187	0.6060	0.5434	0.131	0.131
Dec. 6, 1973	1301-1501	0.8676	0.7984	0.8604	0.7997	0.577	0.506
	1501-1701	0.7984	0.7340	0.7997	0.7354	0.537	0.536
	1701-1901	0.7340	0.7007	0.7354	0.6937	0.278	0.348
	1901-2358	0.7007	0.6624	0.6937	0.6625	0.129	0.105
Dec. 7, 1973	2358-1313	0.6624	0.4976			0.207	
	1313-1517	0.4976	0.4573			0.325	

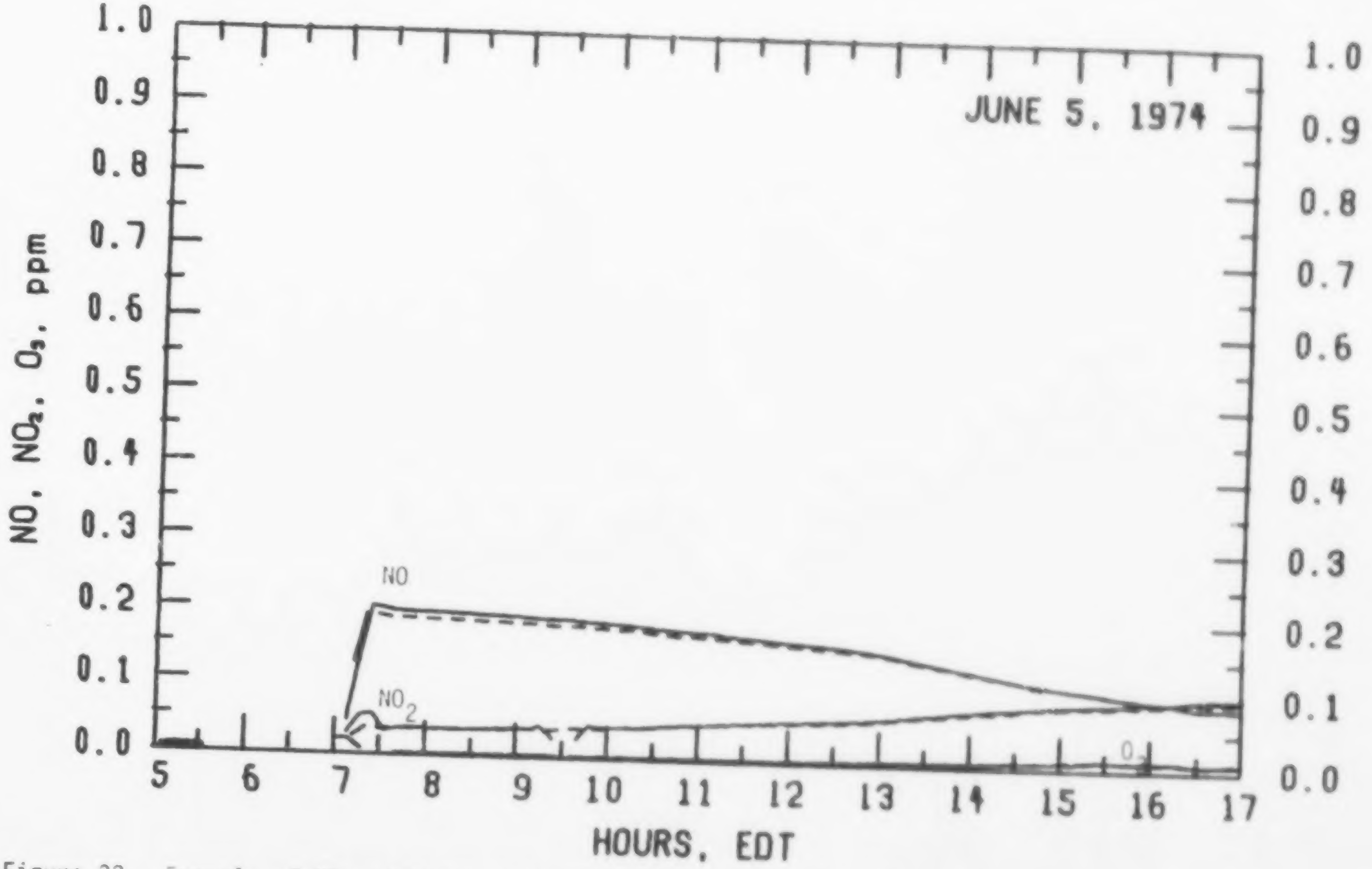

Figure 22. Example of NO oxidation dual run in background air. Initial conditions: NO_x(—) 0.240, (---) 0.230 ppm; NO_2(—) 0.037, (---) 0.035 ppm; NMHC(—) 0.15, (---) 0.15 ppmC.

Table 10. RATES OF NO LOSS AND NO_2 FORMATION IN UNC OUTDOOR CHAMBER USING BACKGROUND AIR

Nov. 3, 1973

Time Period EDT	NO Concentration at Start of Interval, ppm	NO_2 Concentration at Start of Interval, ppm	NO Rate ppb/min	NO_2 Rate ppb/min
0703-1000	0.454	0.056	-0.090	+0.096
1000-1207	0.438	0.073	-0.157	+0.142
1207-1451	0.418	0.091	-0.305	+0.116
1451-1755	0.368	0.110	-0.245	+0.065
1755	0.323	0.122		
Average	---	----	-0.199	+0.105

May 1, 1974

Time Period EDT	NO Concentration at Start of Interval, ppm	NO_2 Concentration at Start of Interval, ppm	NO Rate ppb/min	NO_2 Rate ppb/min
1252-1400	0.636	0.105	-0.162	+0.220
1400-1500	0.625	0.120	-0.366	+0.250
1500-1600	0.603	0.135	-0.350	+0.216
1600-1700	0.582	0.148	-0.367	+0.266
1700-1800	0.560	0.164	-0.367	+0.000
1800-1900	0.538	0.164	-0.183	+0.066
1900-2000	0.527	0.168	-0.183	-0.050
2000-2100	0.516	0.165	-0.216	-0.033
2100-2200	0.503	0.163	-0.100	-0.000
2200-2300	0.497	0.163	----	----
Average			-0.229	0.095

NO_2 was being converted into other nitrogen compounds, probably $HONO_2$, by either OH, O, or O_3.

Side-to-Side Performance

Before useful comparisons could be made between sides, it was important to demonstrate that each side could perform almost identically with the same initial chemical conditions. Figures 22 to 25 show the side-to-side behavior at various IHC and INOX. As can be seen, almost no difference exists between the chamber halves over the variety of initial conditions tested. Figures 23 and 24 are propylene runs and Figure 25 is a mix run.

Day-to-Day Comparisons

The effect of some possible day-to-day variation in physical conditions on the same chemical system at two different hydrocarbon levels (4 and 2 ppmC) and 0.5 ppm initial NO_x was illustrated by the propylene experiments of October 15 and 16, 1973. (Figures 26 and 27). The initial conditions on October 15 were the same as in the runs on October 16 except that the chamber halves were used in reverse. The solar radiation on these two days is given in Figure 28. There was more ozone formed in the high IHC side on October 16 than the high IHC side on October 15. This corresponded, however, to a higher morning temperature (the rate of reaction between NO and O_3 is slightly temperature dependent) and also to choppiness in solar radiation (see detailed discussion of the effects of temperature and solar radiation in subsequent sections).

After 1230 hours, the solar radiation on October 16 decreased significantly due to cumulus cloud formation. The high IHC side, which had almost twice as much propylene as the low IHC side on October 16, was essentially unaffected by the reduction in solar radiation; its NO had converted to NO_2 and the maximum O_3 had already been reached before the solar radiation reduction. In contrast, the low IHC side on October 16 was only at the initial stage of ozone generation at 1230 hours. Hence, the peak O_3 concentration for this side was less than would normally be expected on this day (see Figures 24 and 26) and corresponds to the drop off in solar radiation.

Comparison Experiments with Aromatics

Because there were certain questions as to the use of aromatics in the mix, experiments were designed to show the importance of including or excluding aromatics on the overall hydrocarbon mix behavior. Table 11 summarizes some of the critical data from these comparison experiments. The NO, NO_2 and O_3 profiles are given in Figures 29, 30, 31 and 32.

As long as the same carbon concentration was injected in both sides and toluene did not make up more than 27 to 40% of the total mixture, little difference in the NO, NO_2 and O_3 behavior could be observed. According to the Jackson reactivity scale,[31] the UNC mix has a mole fraction weighted reactivity of 2.61 and toluene alone has a reactivity of 2.2. When injections of equal ppmC were used, the side with toluene had 12 to 18% fewer hydrocarbon molecules initially available for reaction. Also the Jackson molar reactivity of the mix plus 40% toluene by carbon is slightly less than that of the mix without toluene. Hence, it is difficult to completely explain the excellent side-to-side agreement between the mix runs with and without toluene that were conducted on the same day with the same initial carbon concentrations.

The mix/toluene/m-xylene experiments on September 13, 1974, and September 14, 1974 (Figures 31 and 32), on the other hand, did indicate that if m-xylene was substituted for a portion of the toluene, the smog reactions proceeded at a slightly faster rate. The shift in rate, however, was small and would not greatly affect the trends presented in this report.

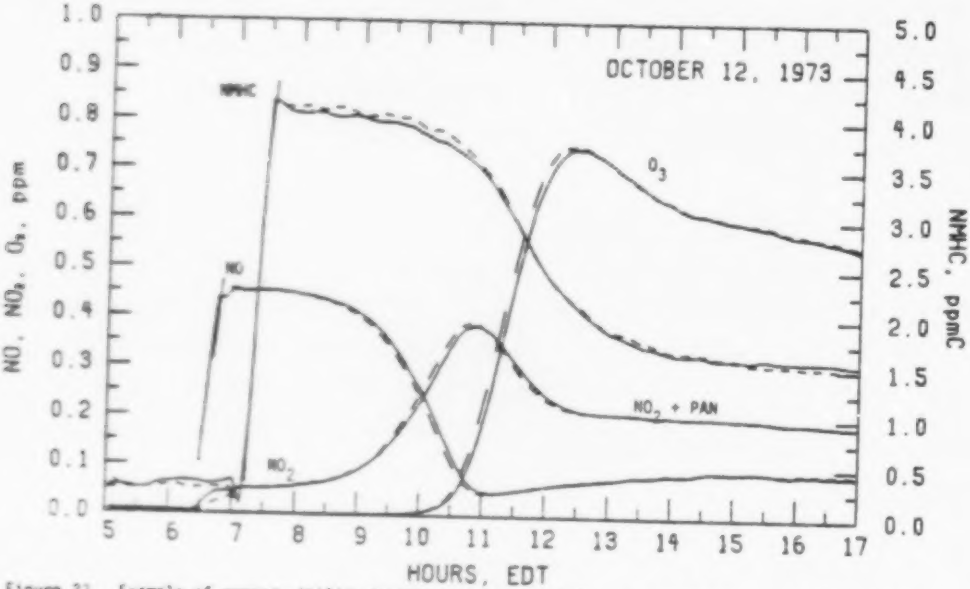

Figure 23. Example of reproducibility between two chamber halves for propylene. Initial conditions: NO_x (—) 0.503, (---) 0.503 ppm; NO_2 (—) 0.052, (---) 0.054 ppm; NMHC (—) 4.05, (---) 4.09 ppmC propylene in UNC outdoor smog chamber.

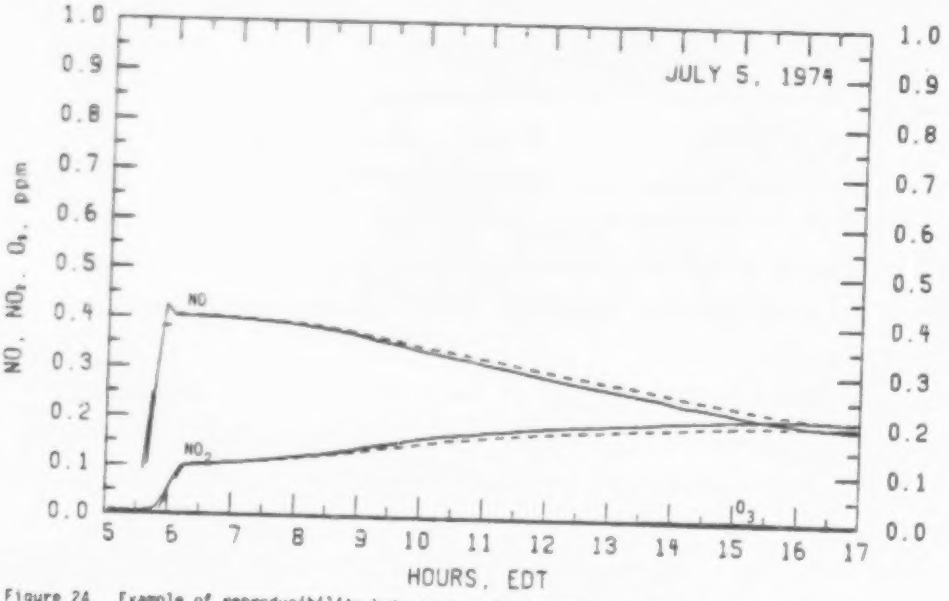

Figure 24. Example of reproducibility between two chamber halves for urban hydrocarbon mix. Initial conditions: NO_x (—) 0.500, (---) 0.500 ppm; NO_2 (—) 0.120, (---) 0.122 ppm; NMHC (—) 0.877, (---) 0.876 ppmC urban mix in UNC outdoor smog chamber.

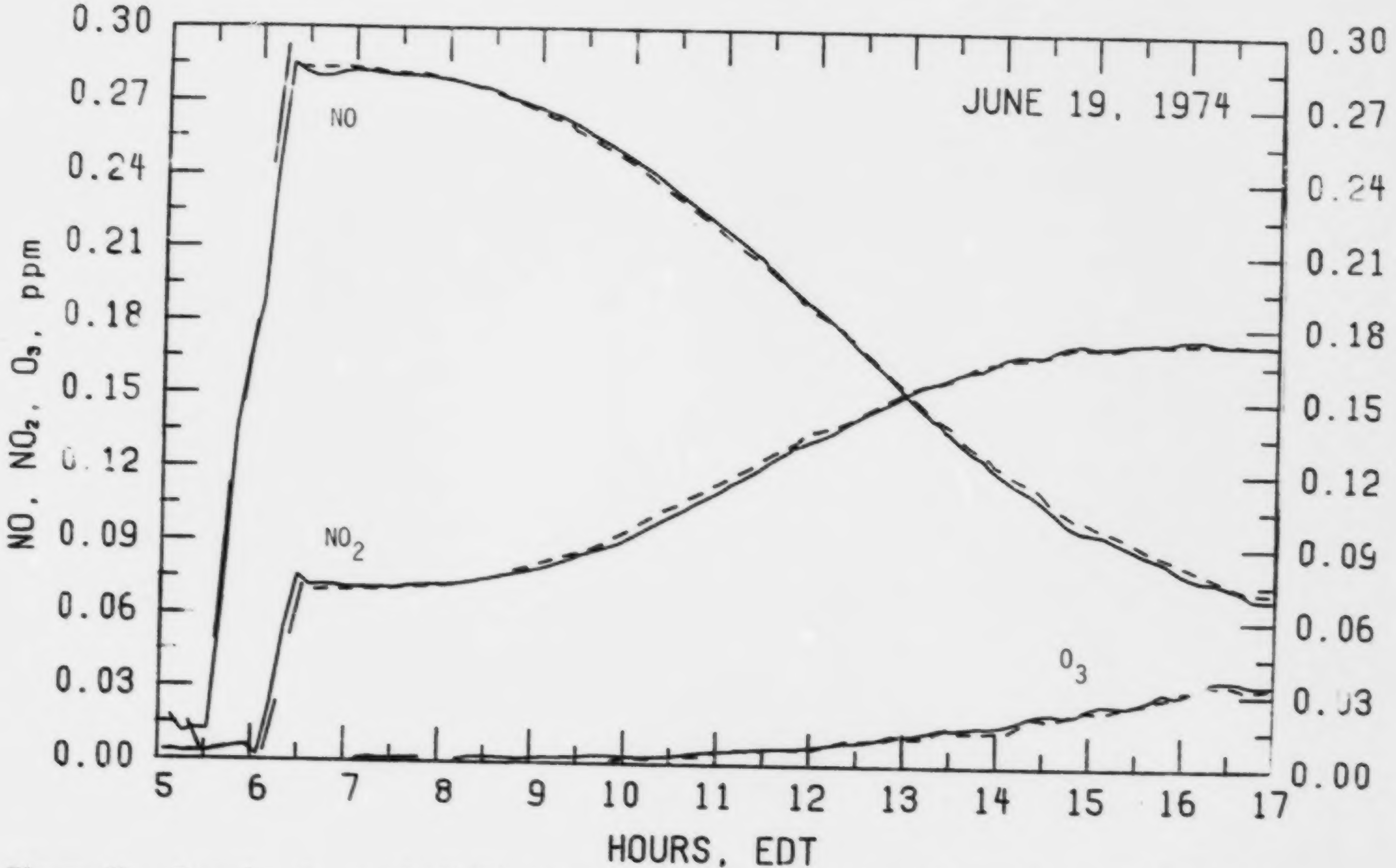

Figure 25. Example of reproducibility between two chamber halves for urban hydrocarbon mix. Initial conditions: NO_x (—)0.353, (---) 0.355 ppm; NO_2 (—) 0.072, (---) 0.070 ppm; NMHC (—) 1.29, (---) 1.29 ppmC urban hydrocarbon mix in UNC outdoor smog chamber.

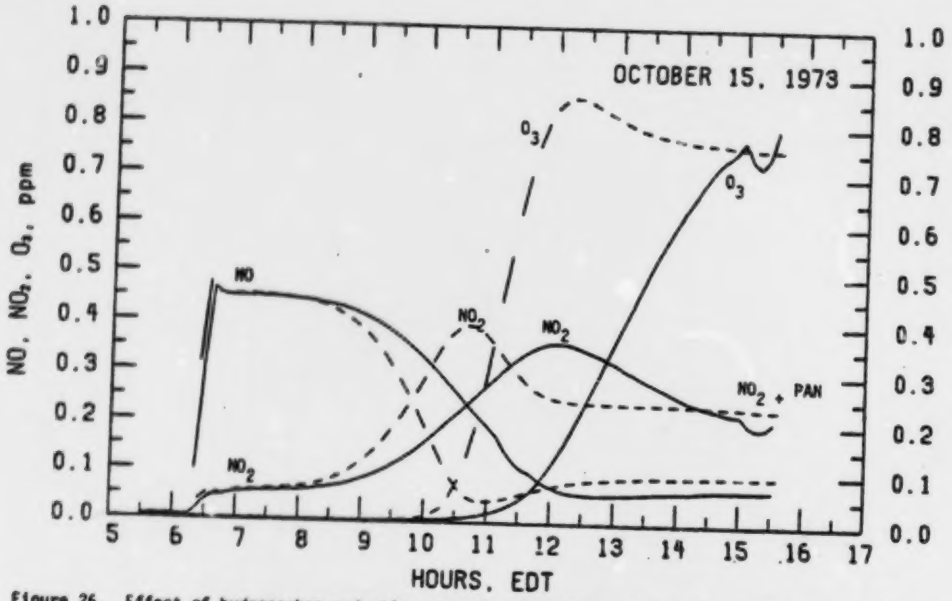

Figure 26. Effect of hydrocarbon reduction and solar radiation. Initial conditions: NO_x(—) 0.505, (---) 0.512 ppm; NO_2 (—) 0.058, (---) 0.064 ppm; NMHC (—) 1.98, (---) 3.88 ppmC propylene in UNC outdoor smog chamber.

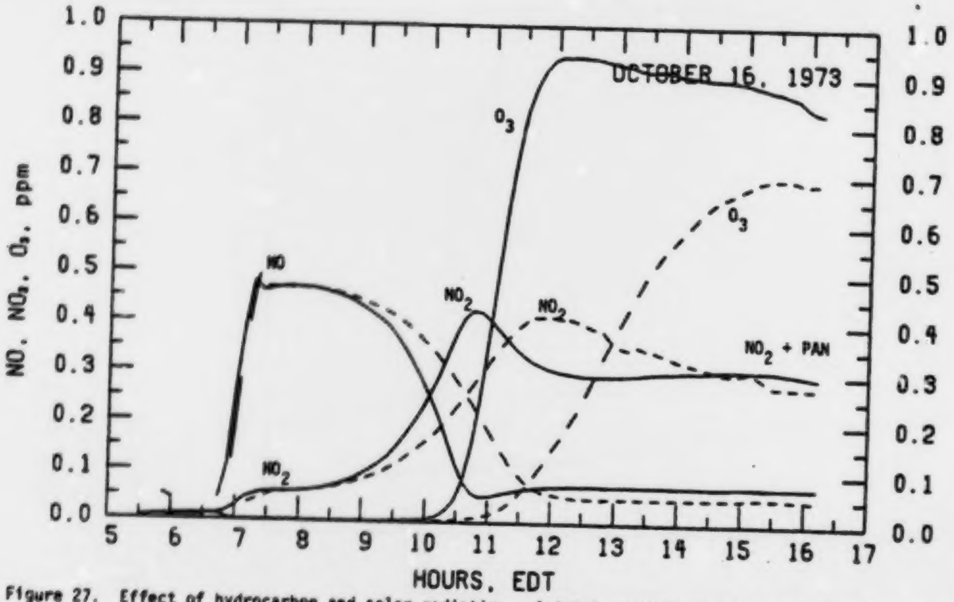

Figure 27. Effect of hydrocarbon and solar radiation. Initial conditions: NO_x(—) 0.527, (---) 0.528 ppm; NO_2(—) 0.059, (---) 0.059 ppm; NMHC (—) 3.89, (---) 2.05 ppmC propylene in UNC outdoor smog chamber.

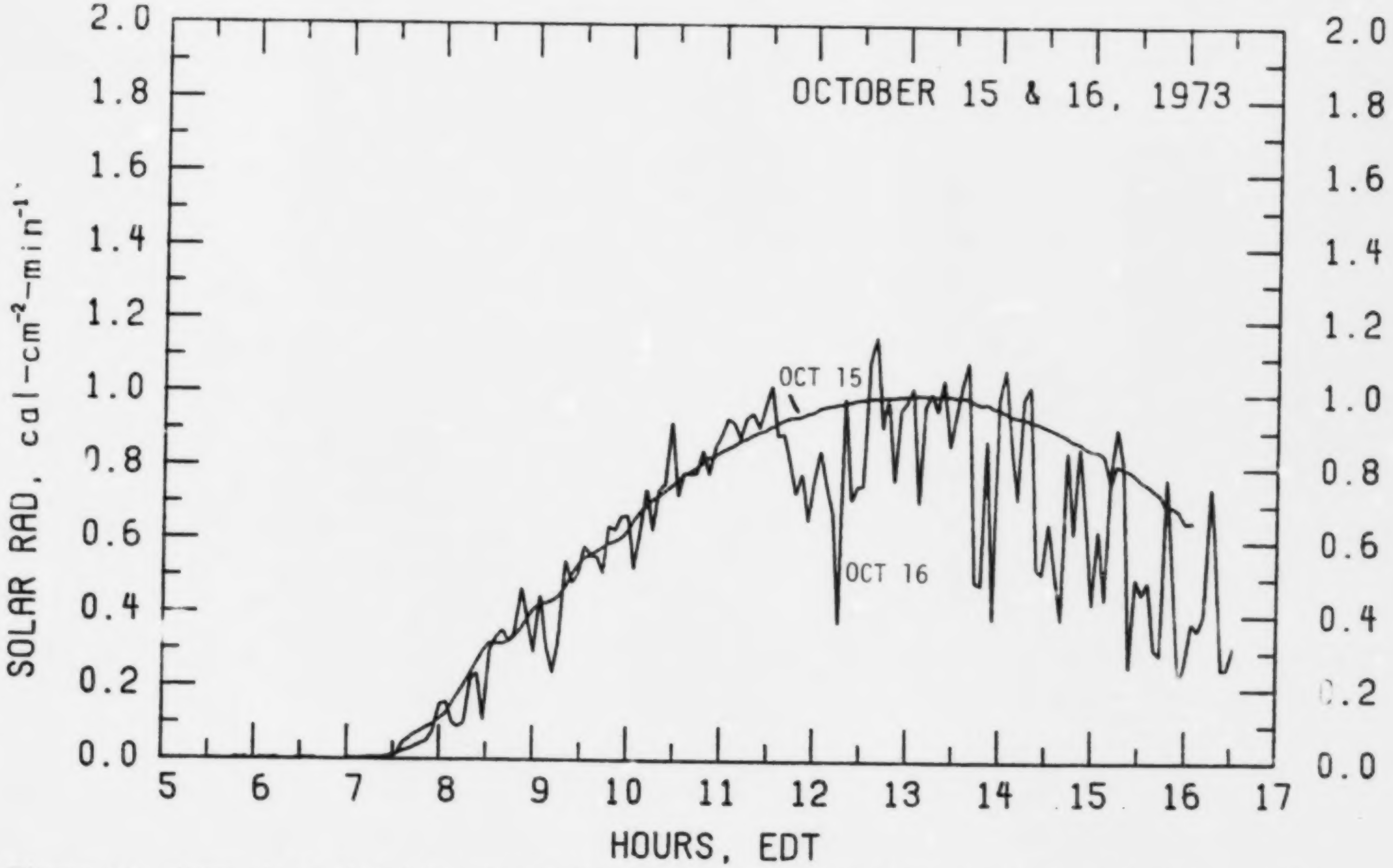

Figure 28. Comparison of total solar radiation for a totally clear day (Oct. 15) and a partly cloudy day (Oct 16).

Table 11. MIX PERFORMANCE WITH AND WITHOUT AROMATICS
(Side to Side Comparison)

Date	IHC, ppmC	INOX ppm	Mix[a], ppmC,	Toluene %Carbon	M-xylene %Carbon	NO2M, ppm	O3M, ppm	Comments
11/16/73	0.84	.201	0.84	0.0	0.0	.116	0.032	almost no difference in profiles
11/16/73	0.88	.200	0.64	27.2	0.0	.116	0.036	
11/19/73	2.28	.208	2.28	0.0	0.0	.115	0.227	no difference in profiles
11/19/73	2.34	.209	1.41	39.7	0.0	.114	0.215	
9/13/74	2.84	0.188	1.92	17.7	13.1	.134	.453	side with xylene is faster and displaced by ∿15 minutes
9/13/74	3.04	0.198	1.92	36.2	0.0	.132	.430	
9/14/74	1.98	.155	1.98	0.0	0.0	.098	.340	side with xylene slower but also had lower IHC
9/14/74	1.51	.153	1.13	0.0	24.5	.093	.372	

[a] Paraffins and olefins only

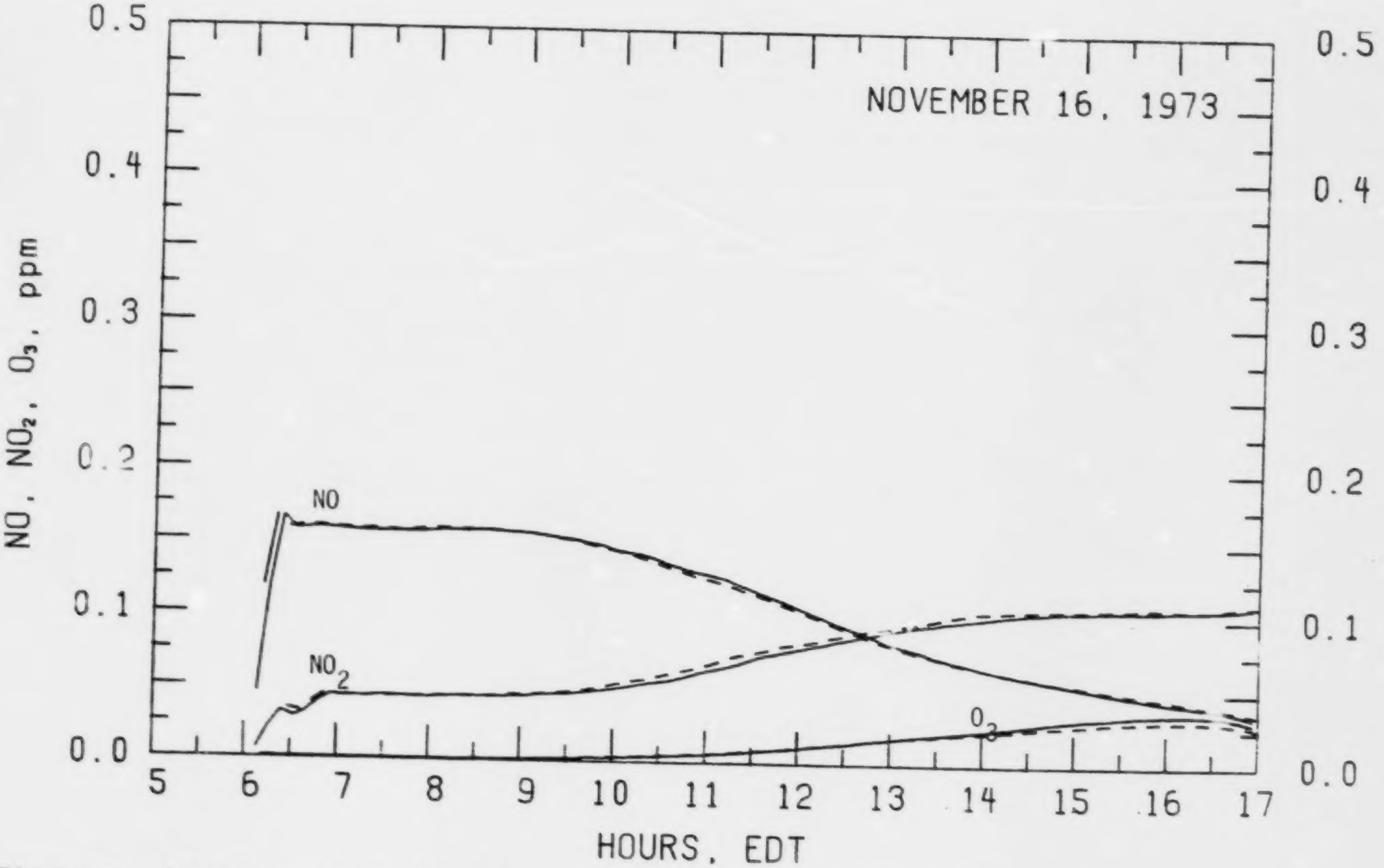

Figure 29. Comparison of mix (olefins and paraffins) and mix with toluene. Initial conditions: NO_x(—) 0.201, (---) 0.201 ppm; NO_2(—) 0.043, (---) 0.043 ppm; NMHC(—) 0.84 ppmC mix including 24 percent carbon toluene, (---) 0.84 ppmC mix in UNC outdoor smog chamber.

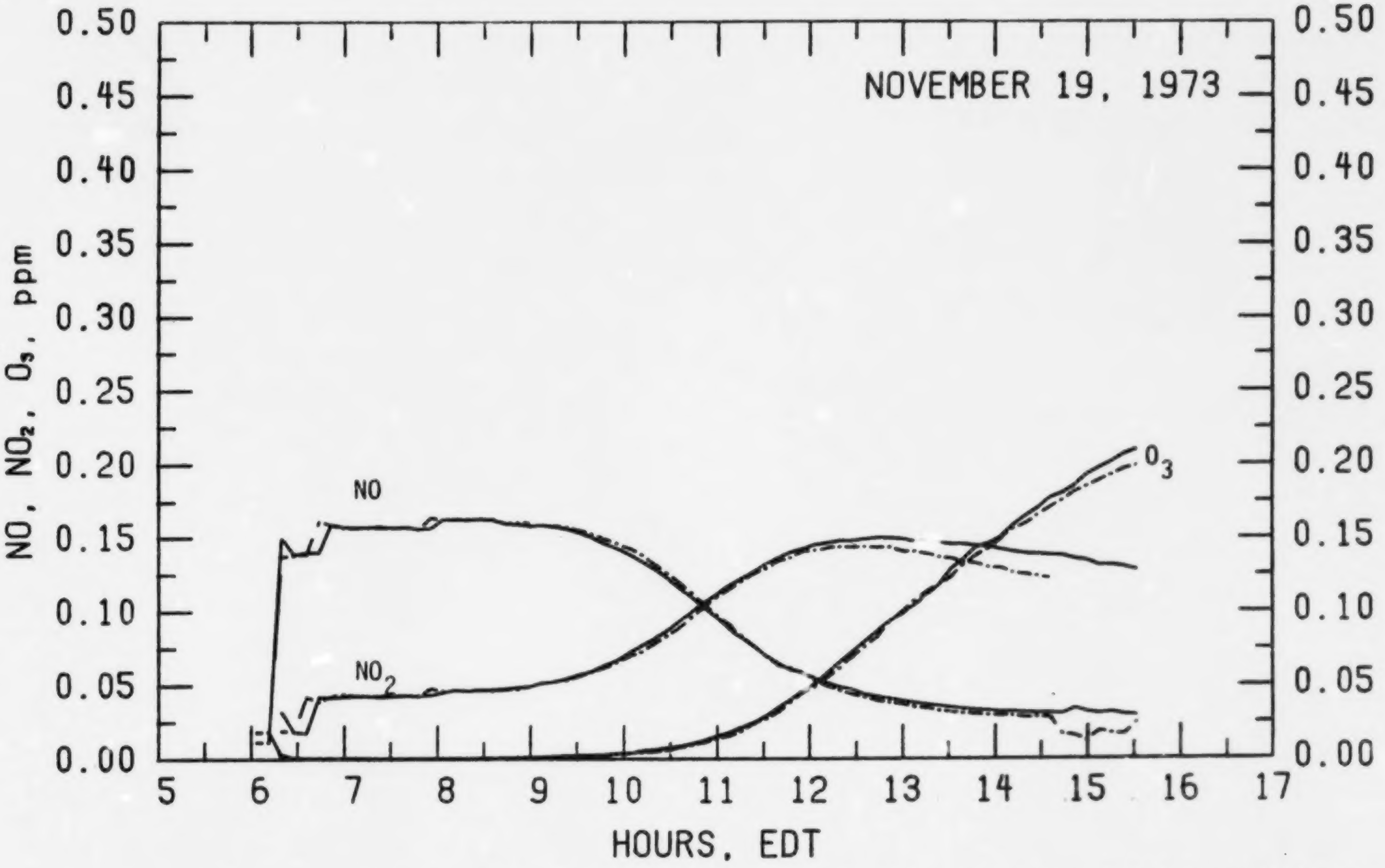

Figure 30. Comparison of mix (olefins and paraffins) and mix with toluene. Initial conditions: NO_x(—) 0.199, (---) 0.199 ppm; NO_2(—) 0.043, (---) 0.043 ppm; NMHC(—) 2.28 ppmC mix, (---) 2.34 ppmC mix including 39.7 percent carbon toluene in UNC outdoor chamber.

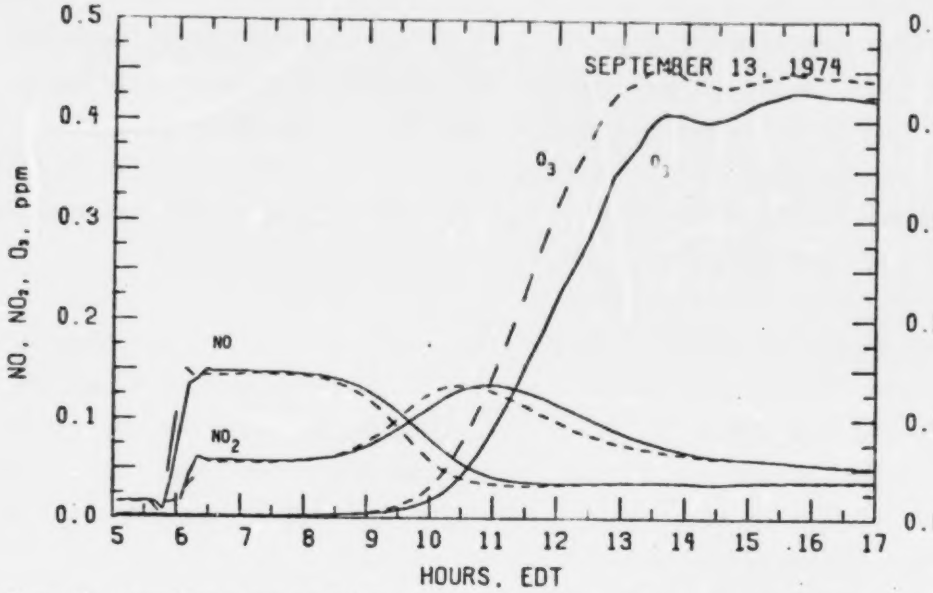

Figure 31. Comparison of mix and toluene with mix,toluene,and m-xylene. Initial conditions; NO_x(—) 0.198, (---) 0.188 ppm, NO_2(—) 0.057, (---) 0.054 ppm; NMHC(—) 3.04 ppmC mix including 36.2 percent carbon as toluene, (---) 2.84 ppmC mix including 17.7 percent carbon as toluene and 13.1 percent carbon m-xylene in the UNC outdoor chamber.

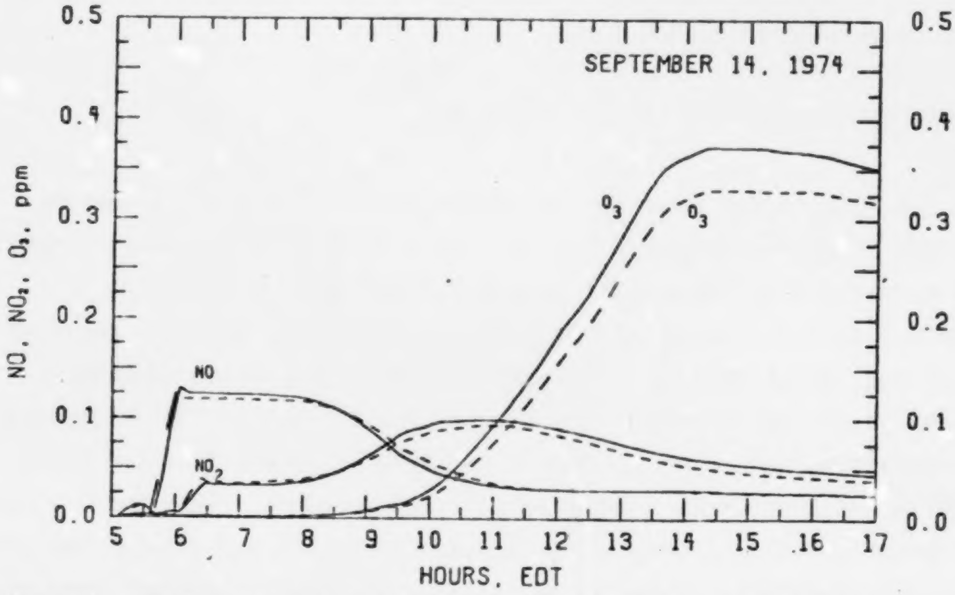

Figure 32. Comparison of mix and mix with m-xylene. Initial conditions: NO_x(—) 0.150, (---) 0.150 ppm; NO_2(—) 0.032, (---) 0.034 ppm; NMHC(—) 1.98 ppmC mix, (---) 1.51 ppmC mix including 24.5 percent m-xylene in UNC outdoor smog chamber.

Comparison Experiments Between Propylene and Mix

To assess the relative reactivity of the mix and propylene, two dual runs in which the mix was used as the NMHC in one chamber side and the same ppmC of propylene was used as the NMHC in the other side were run. In one dual run, 0.5 ppm NO_x and 4.05 ppmC NMHC was used in both sides and in the other run 0.21 ppm NO_x and 1.02 ppmC NMHC was used in both sides (see Figure 33 and 34).

In the propylene and mix sides of the 0.51 ppm NO_x runs, the time to NO2M was 224 mins and 376 mins and the NO2M values were .406 ppm and 0.365 ppm. The times to O3M were 328 mins and 560 mins and the values were 0.888 ppm and 0.274 ppm. The maximum NO_2 rates were 3.83 ppb/min and 1.70 ppb/min and the O_3 maximum rates were 12.87 ppb/min and 1.36 ppb/min for propylene and mix.

Thus, propylene was 225% faster than the mix in forming NO_2, 946% faster in forming O_3 and propylene formed 11% more NO_2 and 224% more ozone. Overall, it appeared that the reactivity of the mix, relative to propylene (5.5) on the Jackson scale, was 2.4.

COMPARISON WITH OTHER CHAMBERS: MODELING

The only meaningful technique to compare the performance of the UNC outdoor chamber with that of artificially illuminated (indoor) chambers was by means of photochemical kinetics modeling. We felt that if a chemical mechanism based on fundamental chemical principles, could be developed, which offered a reasonable explanation of the chemical events in the UNC chamber, it could be used to explore the differences in results between the UNC chamber and other chambers that are more familiar to smog chamber experimenters and modelers. This model would be specific for propylene and would use "generally acceptable" reactions and rate constants. It would be "validated" against several propylene runs from the UNC chamber. This in itself would lead to an increased

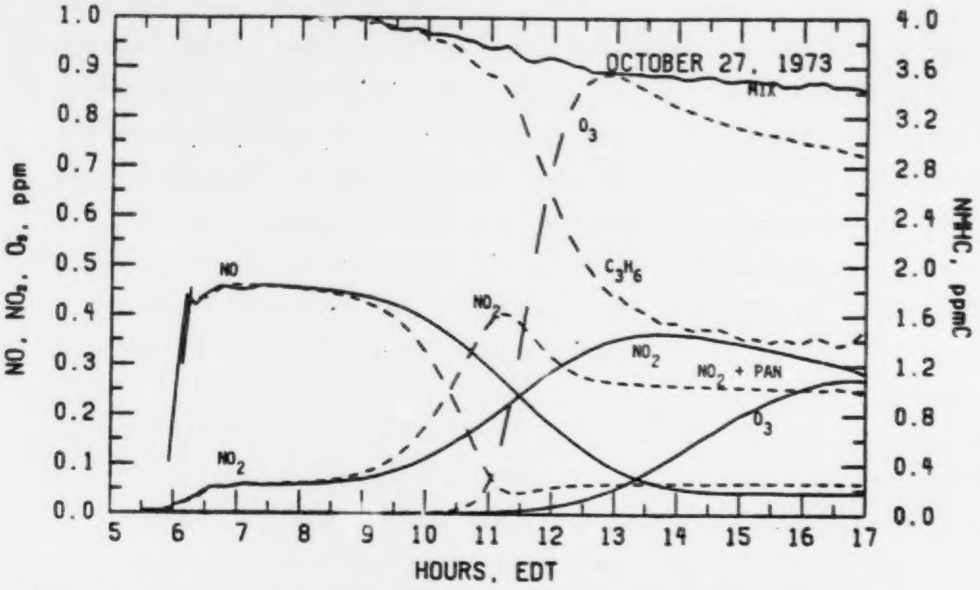

Figure 33. Comparison of mix and propylene as nonmethane hydrocarbon. Initial conditions: NO_x(—) 0.505, (---) 0.513 ppm; NO_2(—) 0.052, (---) 0.057 ppm; NMHC(—) 4.03 ppmC mix, (---) 4.05 ppmC propylene in UNC outdoor smog chamber.

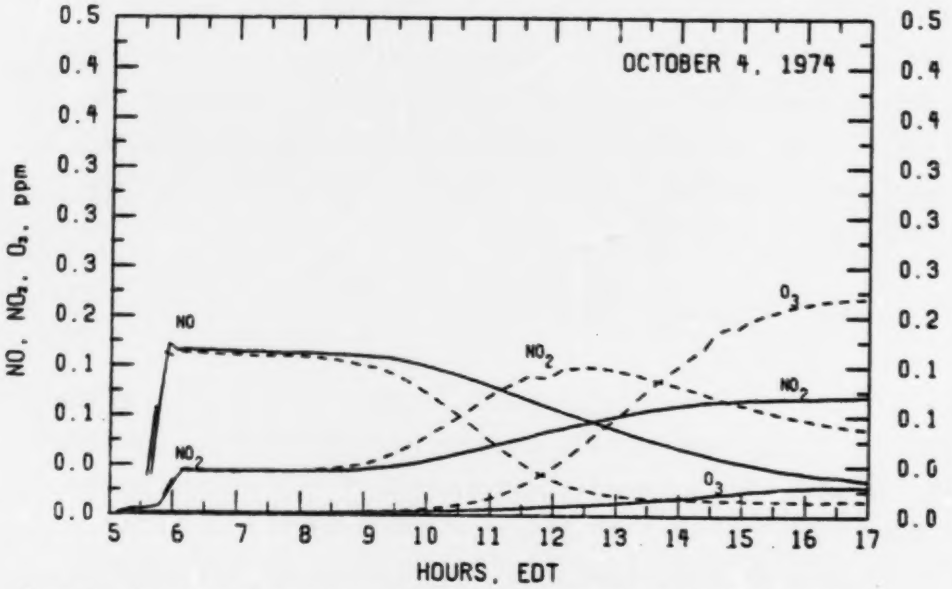

Figure 34. Comparison of mix and propylene as nonmethane hydrocarbon. Initial conditions: NO_x(—) 0.208, (---) 0.204 ppm; NO_2(—) 0.043,(---) 0.042 ppm; NMHC(—) 0.93 ppmC mix, (---) 1.02 ppmC propylene in UNC outdoor smog chamber.

understanding of the events taking place in the chamber. The same model would then be used to model runs from several indoor constant light intensity chambers. If the agreement was reasonably good in the models of these indoor chambers, then we could feel reasonably assured that nothing anomalous was happening in the UNC chamber. If the models of the indoor chambers were poor, then no real conclusion could be drawn, since we would not know whether it was the model or some factor in one or more of the chambers that was responsible for the poor results.

Propylene was chosen as the test hydrocarbon because it is the simplest hydrocarbon that exhibits essentially all the characteristics of photochemical smog and it is the most studied hydrocarbon in smog chambers. Propylene smog chamber data have been obtained from the EPA Cincinnati smog chamber, the Lockheed smog chamber, and the Statewide Air Pollution Research Center (SAPRC) smog chamber at Riverside, California. Auto exhaust smog chamber data from the BOM study of Dimitriades were also obtained for comparison with mix runs. All of these have been replotted on the same time scale axis (and where feasible on the same concentration axis); runs from the UNC outdoor chamber and from the modeling results have also been plotted on this scale to facilitate comparison.

Photochemical Model for Propylene

A thirty-five to fifty-five step mechanism (model) for the photochemistry of propylene (C_3H_6), NO and NO_2 was developed by Jeffries, Sickles and Gantner at UNC. The derivation and details of this mechanism are given in Appendix C. A modified version of the kinetic simulation program (which "solves" the chemical mechanism using the Gear differential equation solving subroutine) developed by Overton and Dodge at EPA was used to simulate the behavior of various photochemical mechanisms. The modifications were to increase the utility of the program by allowing for varying light intensity, for any reaction's rate constant to be changed at selected times during the run to simulate temperature changes or flow systems, for example, and for improved analysis of the contribution of each reaction in the output. The model used in this section was the ninth version written and tested. It had been reduced to the most important elements necessary to give an adequate representation of the events in several actual runs. Selection of rate constants is discussed in Appendix C. In general, either values recommended or adopted by the National Bureau of Standards[32,33] or by Demerjian, Kerr, and Calvert[34] were used; except for reactions which were suspected of having major heterogeneous character these rate constants were adjusted only within the range of uncertainity recommended by the above investigators.

Φka for Nitrogen Dioxide

To model the outdoor runs, it was necessary to specify actinic light intensity as a function of time. The continuous quartz chemical actinometer for NO_2 (see Appendix D) was used to generate two days of Φka (k_1) data which was compared to standard solar radiation sensor data (Eppley total solar radiation sensor (TSR) and Eppley ultraviolet radiation sensor (UV) data). These data were presented in Figures 16 and 17 earlier in this report. It appeared reasonable to assume that there was a general linear relationship between TSR and k_1 and that the slope of this relationship would be approximately 0.3575 $\text{min}^{-1}/\text{cal-cm}^{-2}\text{-min}^{-1}$. The data also suggested that this slope might vary somewhat from day-to-day depending upon upper atmospheric conditions of water vapor content, O_3 concentration, and thin, high cirrus clouds. For purposes of the calculations in this section however, the numerical relationship stated above was used to scale TSR readings for the individual day that was to be modeled and this k_1 profile was then used as the NO_2-specific rate in the modeling program. Other light-dependent rate constants were expressed as sub-multiples of k_1.

Model Validation

The dual matched propylene run of May 25, 1974, was one of the validation runs. The actual profiles of NO, NO_2, O_3, and TSR and the model profiles are given in Figures 35, 36, and 37. The agreement among actual and model profiles was quite good except for the more rapid conversion of NO to NO_2 by the model from the point of NO-NO_2 crossover to the NO_2 peak. This acceleration of conversion led to an increased O_3 production in the model in contrast with the actual data, but the later stages of O_3 formation were in closer agreement. It is not known if this was caused by some unknown physical behavior in the chamber (such as light intensity differences between the chamber and the model), or by some misrepresentation of the chemistry in the model.

It was not necessary to include the small variations in the actual TSR profile in the model because NO was very low at the time of occurrence and the duration of the cloud cover was not sufficient to allow O_3/NO_2 dark phase reactions to predominate.

A second day, May 7, 1974, with different initial conditions, and its model are given in Figures 38, 39 and 40. There were significant variations in the TSR for this day which occurred at critical times in the course of the run; it was necessary to approximate these variations in the model k_1 values as shown in Figure 38. The model profiles show rapid response to these abrupt light intensity changes which are discernible in the actual data profiles for O_3 even after the high-frequency filtering that occurred in data processing. The actual NO and NO_2 profiles do not appear to exhibit these rapid changes. The NO_x analyzer required a 30 second integration period to take a sample and each side was only sampled every eight minutes. It is quite possible that the combination of integration and low sampling rate missed these events.

The model of May 7, 1974, suffers from the same type of deviation from the experimental NO, NO_2 and O_3 profiles that characterized the May 25, 1974 model. In addition, the fact that the NO_2 readings of the chemiluminescent NO_x analyzer also included PAN in the actual data is clearly shown by comparison of the post-peak NO_2 model with actual data profiles for both of the runs modeled. The higher propylene concentration of May 25, 1974 led to a more rapid consumption of the NO_2 which, in turn led to a longer flat portion on the NO_2 post-peak profile due to the quasi-conservative nature of NO_2 + PAN and the NO_x chemiluminescent meter response.

Other outdoor runs were modeled with approximately the same degree of success. The k_1/TSR relationship used for the May 7 and 25 runs was too large for October 1974 runs, but was somewhat more satisfactory for October 1973 runs. This was apparently due to increased haze and high cirrus clouds that occurred more frequently during October 1974; no k_1 data was taken during this period.

The propylene model can apparently provide an adequate representation of the most significant chemical events that occurred in the outdoor chamber propylene runs and can thus serve as a tool for exploring some of the behavioral characteristics of the outdoor chamber in relation to the other indoor chamber work with propylene. Before examining these indoor chamber runs and their models, some of the detailed characteristics of the outdoor chamber model should be discussed.

Relative Rate of Outdoor Chamber Reactions

Relative to indoor smog chamber profiles, the UNC outdoor chamber appears to be slow. That is, the time required to convert the initial NO to NO_2 appears to be long. Some of this long time interval can be accounted for by the fact that the initial light intensity is zero, followed by a sine-wave-type increase. Figures 41 and 42 show the behavior of the same propylene model and initial conditions used in

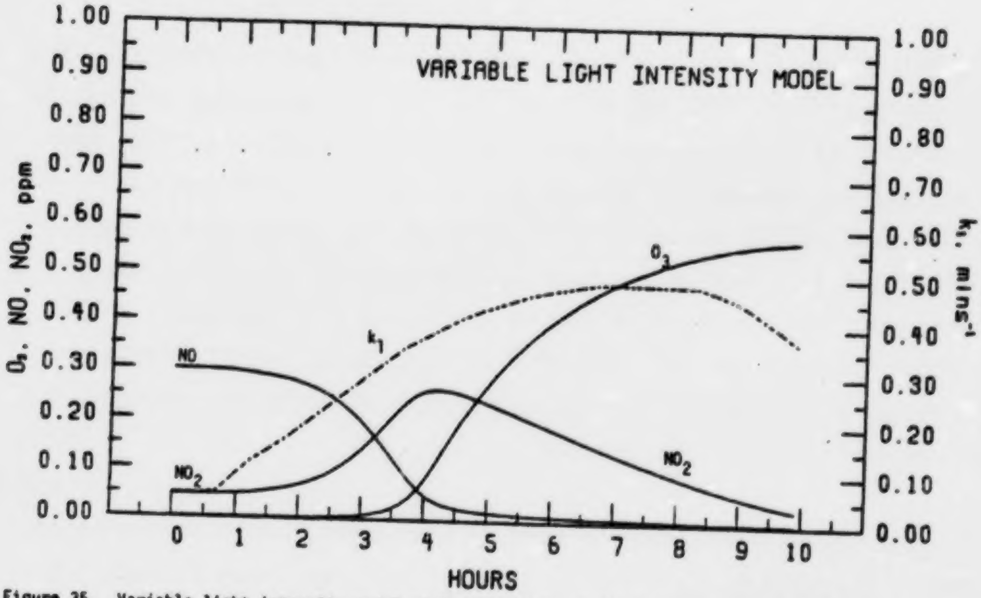

Figure 35. Variable light intensity model of May 25, 1974. Initial conditions: NO_x 0.345 ppm, NO_2 0.045 ppm, NMHC 1.10 ppmC propylene. The k_1 profile was scaled from total solar radiation shown in Figure 37.

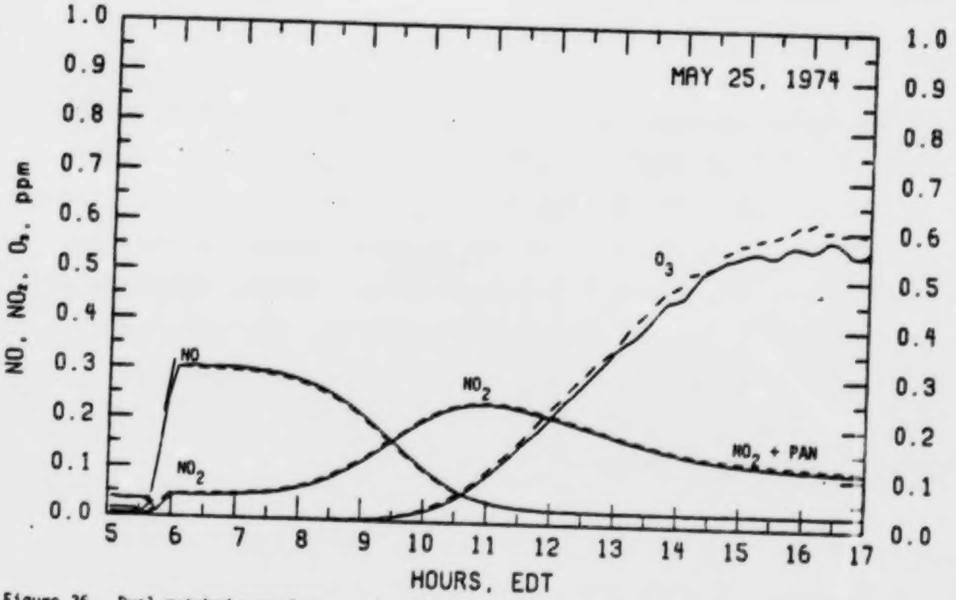

Figure 36. Dual matched propylene run in UNC outdoor smog chamber. Initial conditions: NO_x(—) 0.351, (---) 0.348 ppm; NO_2(—) 0.044, (---) 0.047 ppm; NMHC (—) 1.10, (---) 1.10 ppmC propylene

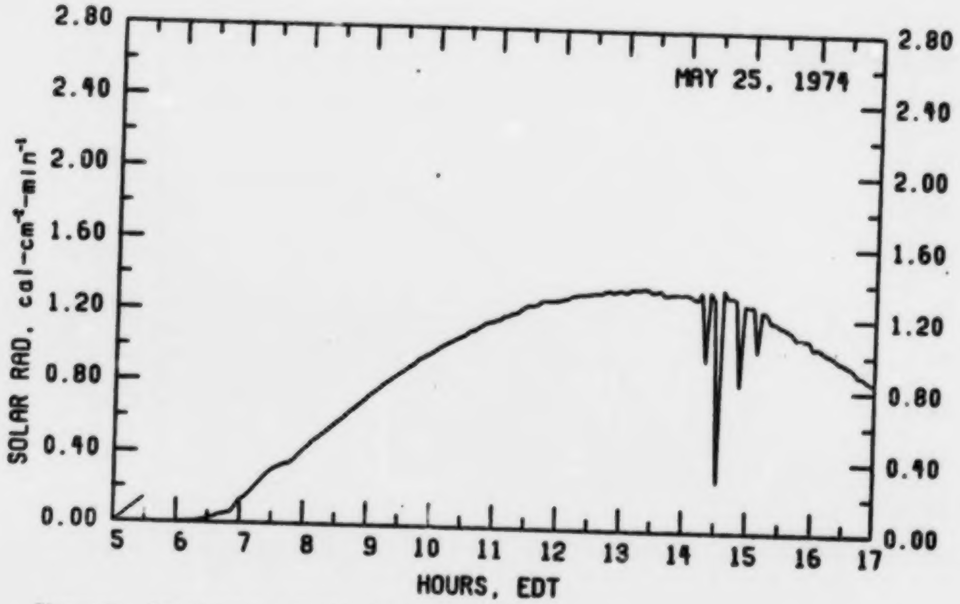

Figure 37. Actual solar radiation for May 25, 1974.

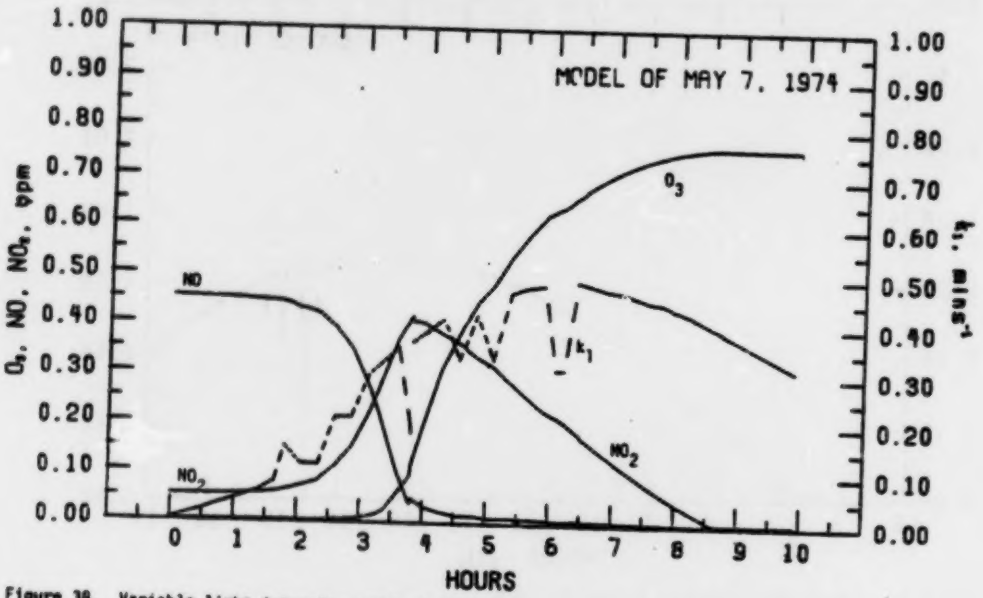

Figure 38. Variable light intensity model of May 7, 1974. Initial conditions: NO_x 0.502 ppm, NO_2 0.049 ppm, NMHC 2.09 ppmC propylene. The k_1 profile was scaled for total solar radiation shown in Figure 40.

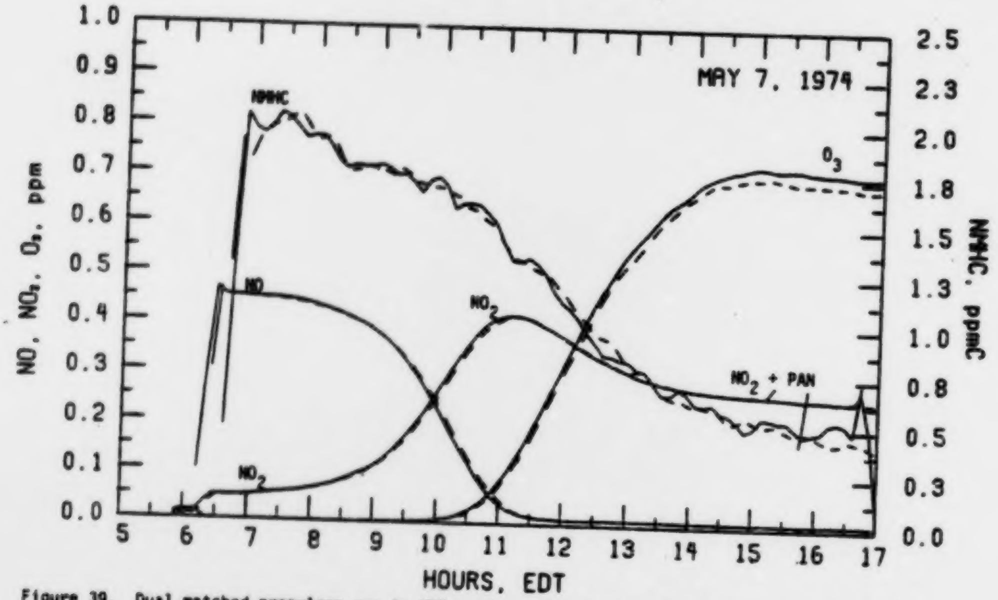

Figure 39. Dual matched propylene run in UNC outdoor smog chamber. Initial conditions: NO_x(—) 0.503, (---) 0.503 ppm; NO_2(—) 0.048 (---) 0.047 ppm; NMHC(—) 2.09, (---) 2.05 ppmC propylene in UNC outdoor smog chamber.

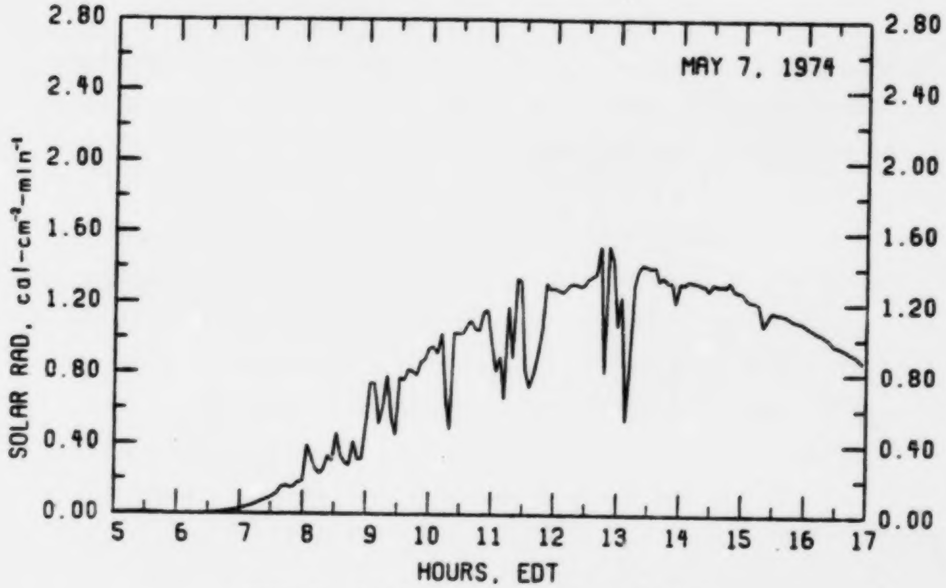

Figure 40. Actual solar radiation for May 7, 1974.

the May 25 simulation but under a) constant light intensity conditions typical of indoor chambers, and b) an increasing ramp of light intensity such that the average k_1 = 0.300 min^{1}.

The constant light intensity model (Figure 41) still required over 1.3 hours to reach NO-NO_2 crossover and 2 hours to reach the NO_2 maximum concentration, but these times are considerably shorter that those in the model of May 25. The final O_3 concentration is somewhat lower than the variable light intensity model of May 25 (Figure 35). The ramping k_1 simulation required 4 hours to reach crossover, longer than the model of May 25, but the final O_3 was approximately the same as the constant k_1 model, even though the *average* value for k_1 was less.

The long times reflect the slow initiation processes in the propylene model that was validated on the outdoor chamber runs. It was necessary in modeling the UNC chamber to set the rate constant for Reaction 25 (see Appendix D) at the upper limit of the *homogeneous* rate suggested by Garvin[32], a very low value.

$$25:\quad NO_2 + NO \overset{H_2O}{\rightleftarrows} 2HNO_2 \qquad K_{25} = \quad 3.2 \times 10^{-5}\,\text{ppm}^{-1}\,\text{min}^{-1}$$

$$\text{rate} = K[NO_2]\,[NO]\,[H_2O]^2\ ;\ K = 9 \times 10^{-14}\ ;\ [H_2O] = 18{,}000\ \text{ppm}$$

This reaction apparently has a major *heterogeneous* component, and its rate constant is used by most modelers to adjust the initial speed of the photochemical system based on the individual surface characteristics of each chamber. The photolysis of HNO_2 provides an early source of OH radicals which can initiate the $OH/C_3H_6/HO_2/NO/OH$ chain. Without this source of OH, initiation in the model must depend upon products of the $O_3 + C_3H_6$ reaction or upon the photolysis of aldehydes. The $O_3 + C_3H_6$ reaction is slow initially because of the high NO to NO_2 ratio. Aldehydes are not present initially in the smog systems modeled but do increase as the reaction proceeds.

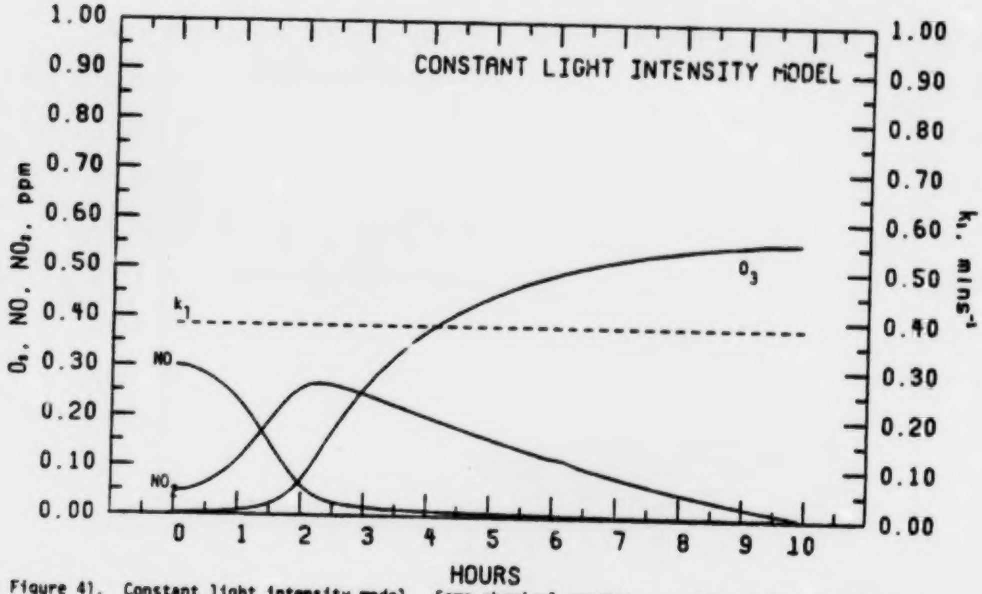

Figure 41. Constant light intensity model. Same chemical conditions as Figure 35. Constant k_1 = 0.38 min^{-1}.

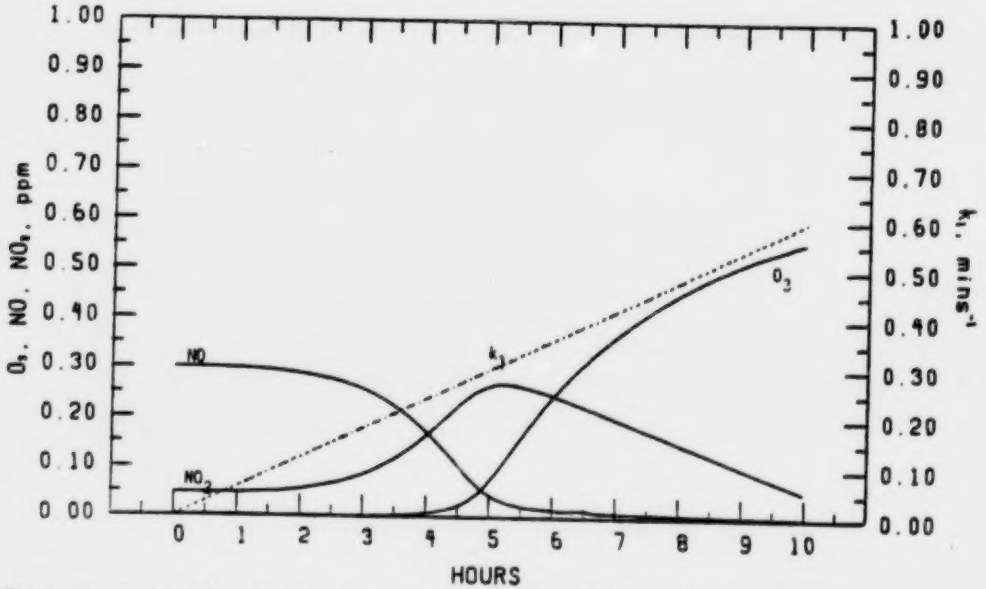

Figure 42. Ramping light intensity model. Same chemical conditions as Figures 35 and 41. The average k_1 = 0.30 min^{-1}.

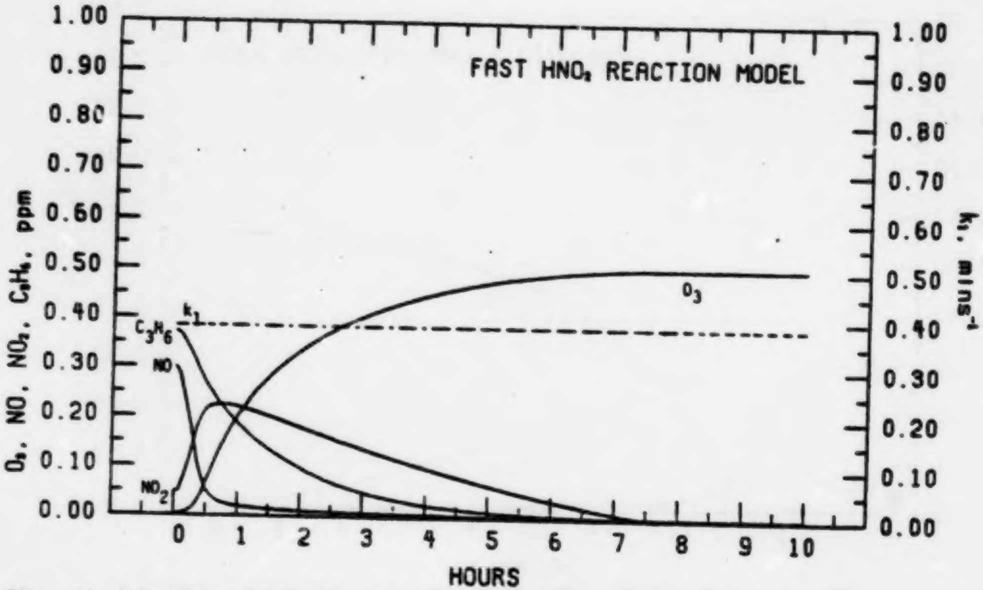

Figure 43. Fast HNO_2 reaction model. Same chemical conditions as 35,41,42. Constant k_1 = 0.38 min^{-1}.

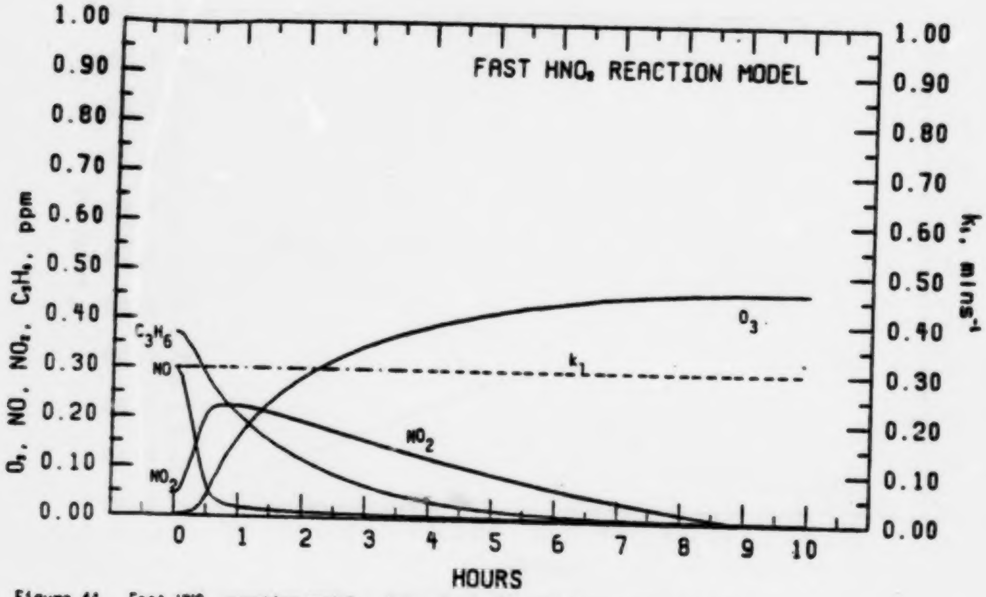

Figure 44. Fast HNO_2 reaction model. Same chemical conditions as 35, 41-43. Constant k_1 = 0.30 min^{-1}.

To examine the effect of using rates for Reaction 25 that have been commonly used in indoor smog chamber simulations, the model used to produce the profiles in Figure 41 was re-run with a rate constant for Reaction 25 of 1.5 x $10^{-2}ppm^{-1}min^{-1}$, the value used by Hecht, Seinfeld, and Dodge[35] in modeling the EPA chamber data and it includes both the heterogeneous and homogeneous reactions. The results are shown in Figures 43 and 44 for k_1 = 0.3835 min^{-1} and k_1 = 0.300 min^{-1}. Other conditions were the same as in Figures 35, 41, and 42.

The reaction systems in these simulations are much faster than those using the rate constant that fits the UNC outdoor chamber. The higher light intensity (Figure 43) produced a higher ozone concentration. The UNC outdoor chamber had a surface to volume ratio of 1.31 m^2/m^3 (0.40 ft^2/ft^3) which was less than that in the EPA chamber (1 ft^2/ft^3) modeled by Hecht, et al., but this does not seem sufficient to account for the differences above. In the comparisons performed by Lockheed[36], Teflon surfaces exhibited the slowest behavior of the four surfaces tested (Teflon, glass, aluminum, and stainless steel) and perhaps the fact that more than 98% of the UNC chamber's surface was Teflon could partially explain why it was slow relative to indoor chambers.

There was ample water available for reaction since at the cool morning starting conditions, the dewpoint temperature often approached the air temperature, and frequently surface water was available from condensation. Perhaps the HNO_2 formed in this condensed water, but did not evaporate back into the gas phase until later in the reaction sequence when its impact would not be noticeable. The NO/Background test runs however, showed no significant loss of NO_x to the walls at night nor did relative humidity show any significant correlation across a wide range of experimental conditions.

Comparison of Outdoor Chambers with Indoor Chambers

Smog chamber data for propylene from three indoor smog chambers were collected and replotted on the same scale and time axis as the UNC outdoor chamber profiles and the previous model profiles presented above. Dr. Marcia Dodge (Chemistry and Physics Laboratory, USEPA, Research Triangle Park, N.C.) kindly supplied the numerical data for EPA run 325 which was published by Hecht, et al.[35] Data from the SAPRC Smog Chamber operated by Pitts at Riverside and the Lockheed Smog Chamber were digitized from 8.5 x 11 in. plots in publications by Hecht[37] and by Jaffe[38].

In the simulations of these indoor chambers, presented below, only the light intensity (k_1) and the rate of Reaction 25 were changed from the rate constant values used in the modeling of UNC chamber runs of May 7 and 25, 1974. The rate of Reaction 25 was used to account for the individual surface characteristics of each chamber. The potential surface chemistry of N_2O_5 was ignored.

Model of EPA-325

Nitric oxide, NO_2, and O_3 profiles of EPA-325 and the UNC model of this run are given in Figures 45 and 46. The k_1 value used in this simulation was 0.4 min^{-1} and the rate constant for Reaction 25 was 1.5×10^{-2} ppm^{-1} min^{-1}. These values were the same as those used by Hecht et al. in their model of this run. Although Hecht, et al. stated that the potassium iodide oxidant data, which was 50% higher than the Mast data, was probably more accurate than the Mast oxidant data, both their model and the UNC model predicted the Mast data quite reasonably. This suggests that the potassium iodide data had a positive interference that was not accounted for in the corrections applied by the chamber operators.

The UNC model of EPA-325 has the same deviation of NO_2, NO, and O_3 after NO-NO_2 crossover that was exhibited by the models of UNC runs on May 7 and 25, 1974. The slowness of the UNC chamber makes this deviation more obvious than the much faster indoor chamber runs. The fact that the models of both chambers show this difference implies that the difficulties are within the chemical representation in the model and not in some unrecognized physical behavior in the chambers.

One possible cause of the problem discussed above may be Reaction 27. Recent work[32] has suggested a much higher rate constant (100-400 ppm^{-1} min^{-1}) for Reaction 27 than was used in this work. This rate constant is still subject to review and validation by NBS.

$$HO_2 + NO_2 \rightarrow HNO_2 + O_2 \qquad (27)$$

A large rate constant for Reaction 27 followed by

$$HNO_2 \xrightarrow{h\nu} NO + OH \qquad (30)$$

would compete effectively with

$$HO_2 + NO \rightarrow NO_2 + OH \qquad (3)$$

since the chain carrier, OH, is regenerated in each sequence. Larger values for Reaction 27 would bring the model NO_2 into closer agreement near the peak NO_2. Large ratios of k_{27} to k_3 however, can make it difficult to sustain large ratios of NO_2 to NO needed for high O_3 production after the NO_2 peak. Also a large rate constant for Reaction 27 followed by Reaction 30 would make the NO_2 maximum concentration light intensity dependent. Further research will be required to clarify the role of Reaction 27.

Models of SAPRC Chamber

The UNC model of run EC-17 from the Riverside Chamber again shows remarkable agreement for NO, NO_2, O_3, PAN, and C_3H_6 profiles at a very low concentration of starting reactants. The original data for alde-

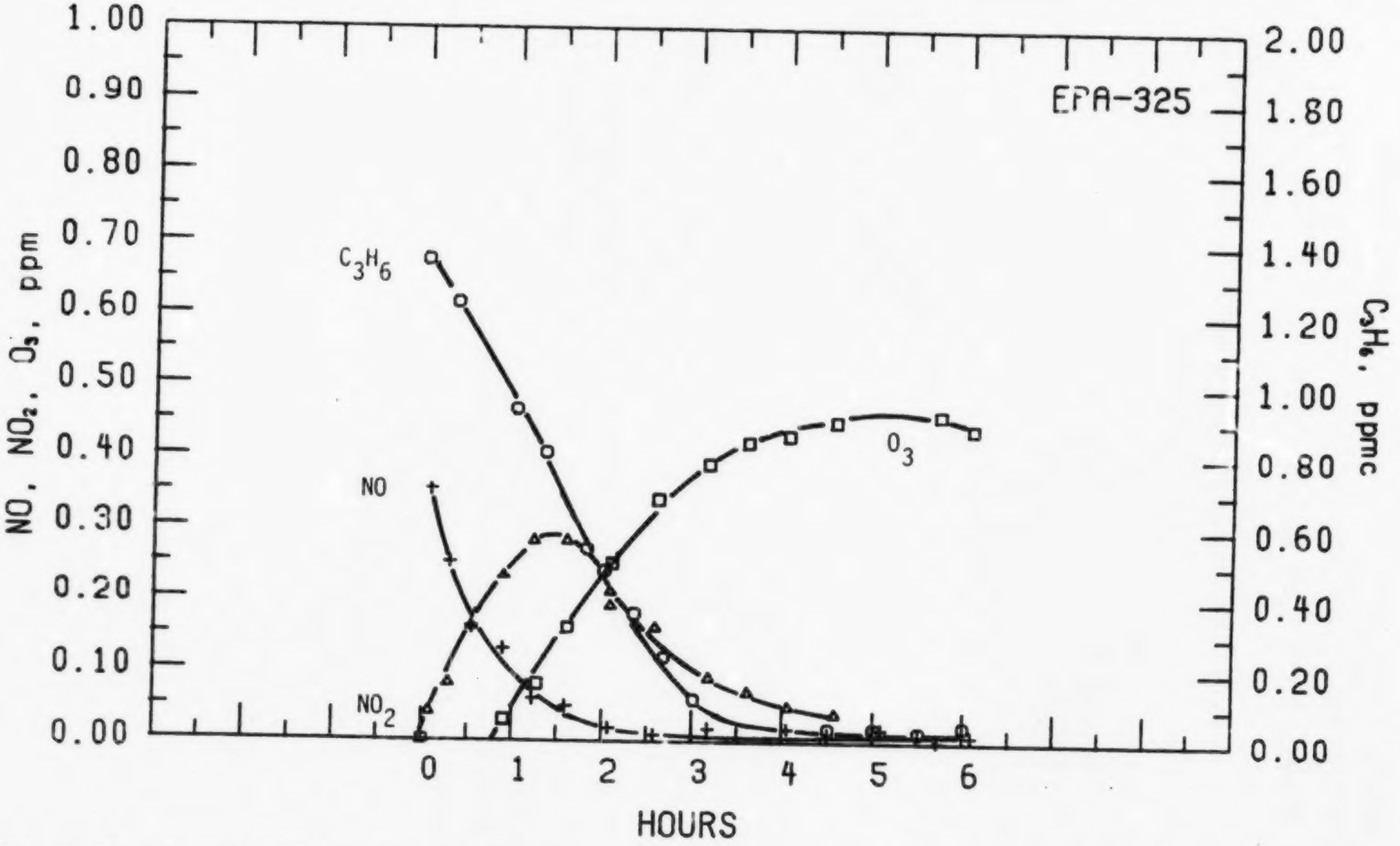

Figure 45. Actual profiles for run EPA-325. Initial conditions: 0.40 ppm NO_x, 0.04 ppm NO_2, and 1.35 ppmC propylene.

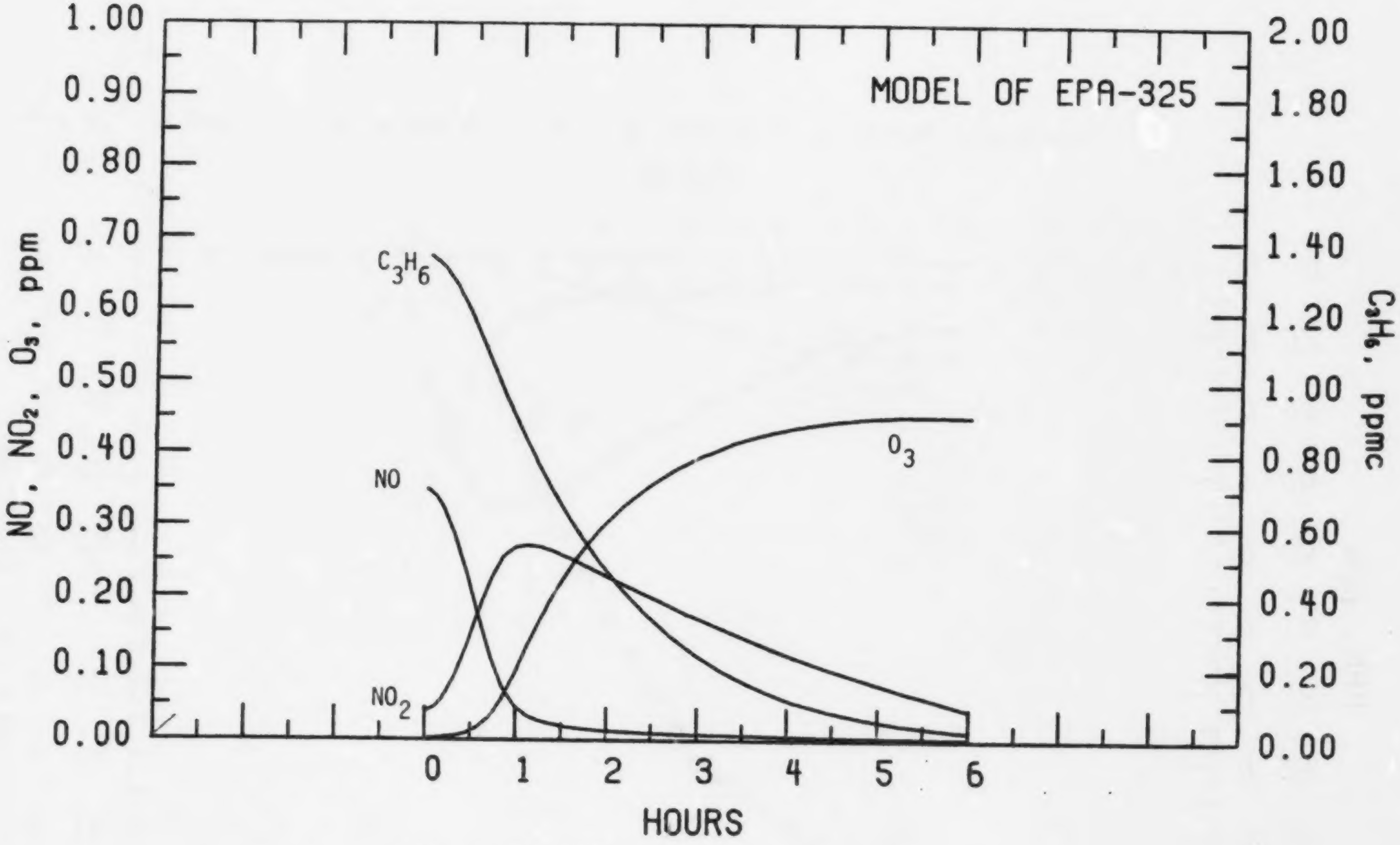

Figure 46. UNC model of run EPA-325.

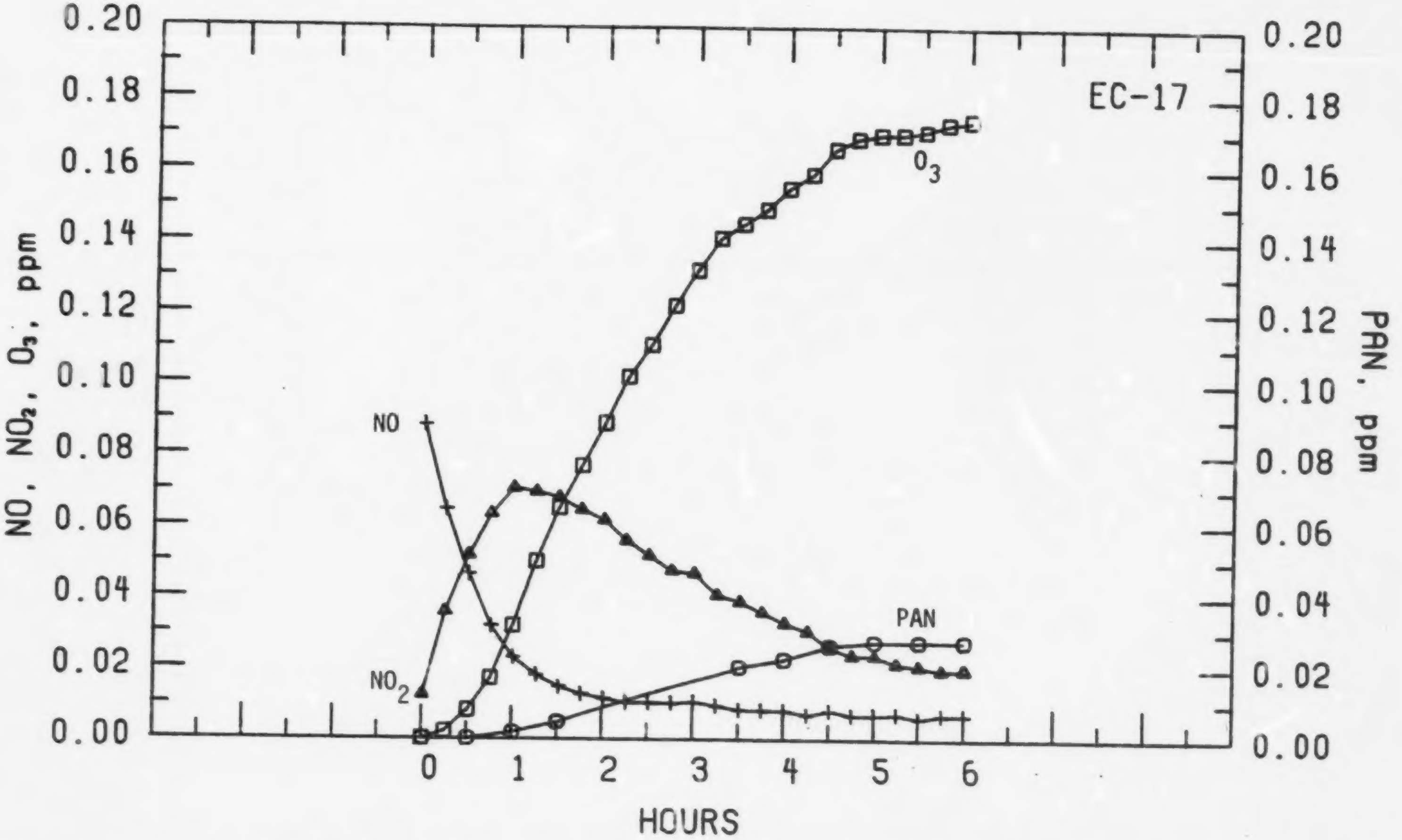

Figure 47. Actual profiles of run EC-17 in SAPRC chamber at Riverside, California.

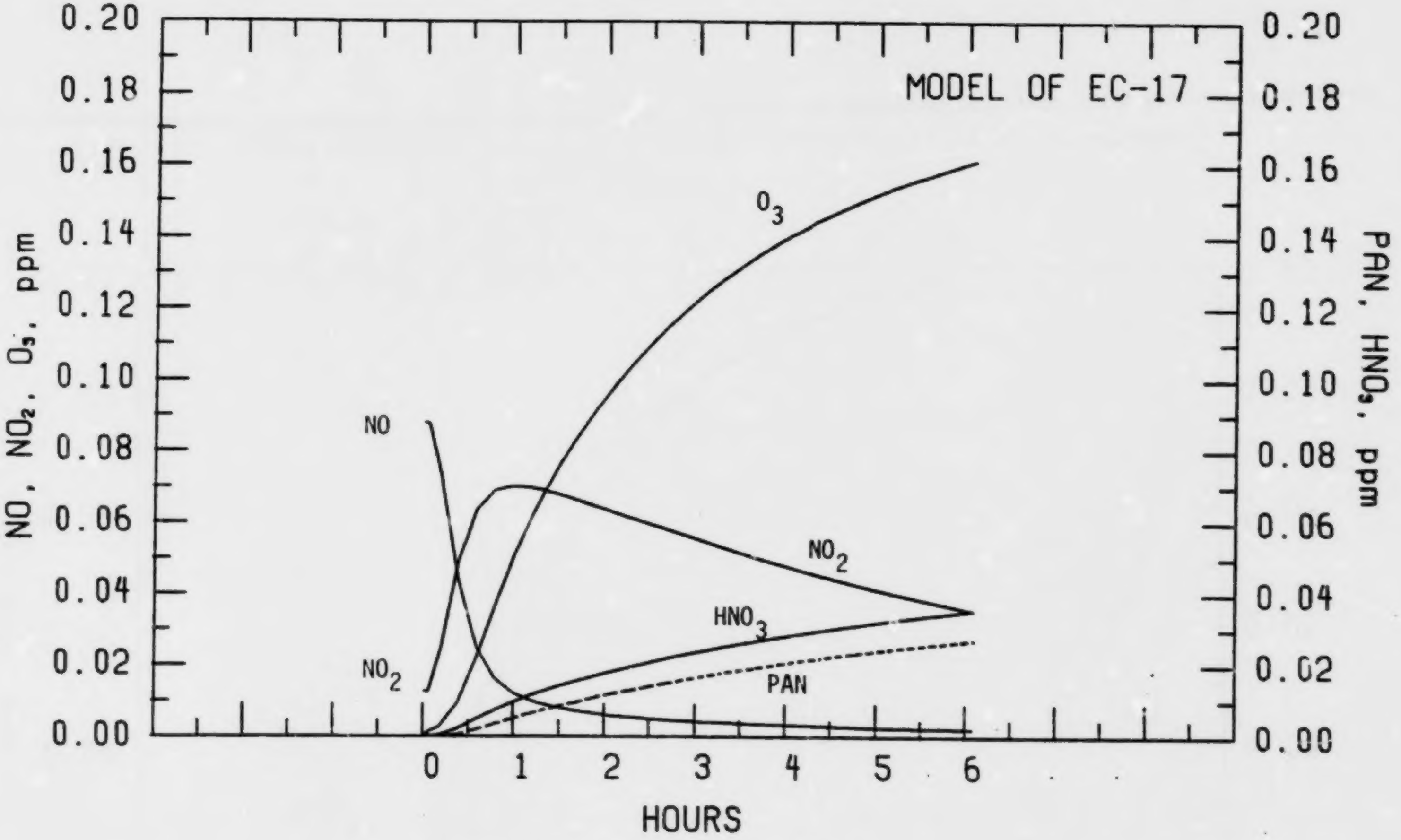

Figure 48. UNC model of run EC-17.

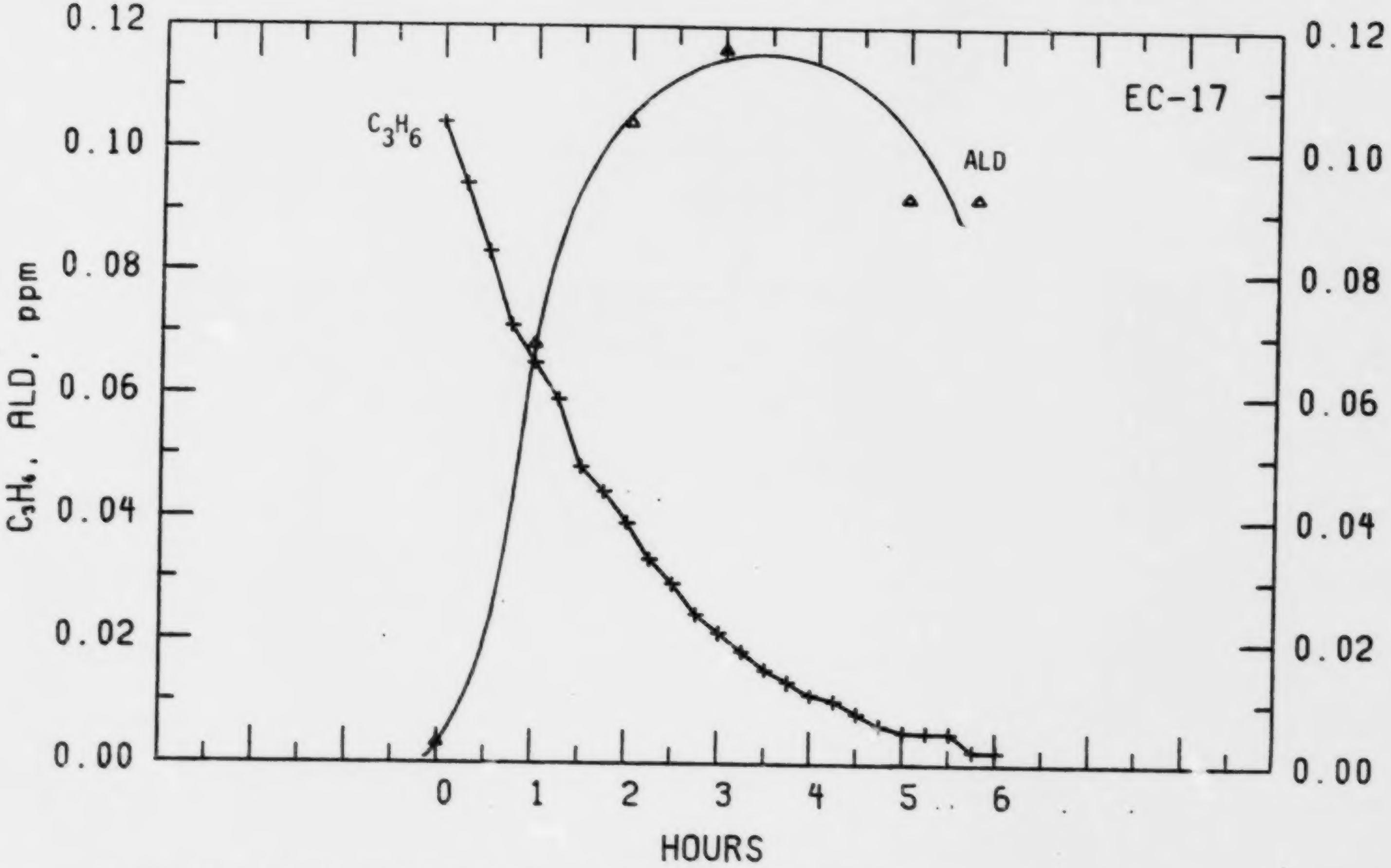

Figure 49. Actual profiles of run EC-17 in SAPRC chamber at Riverside, California.

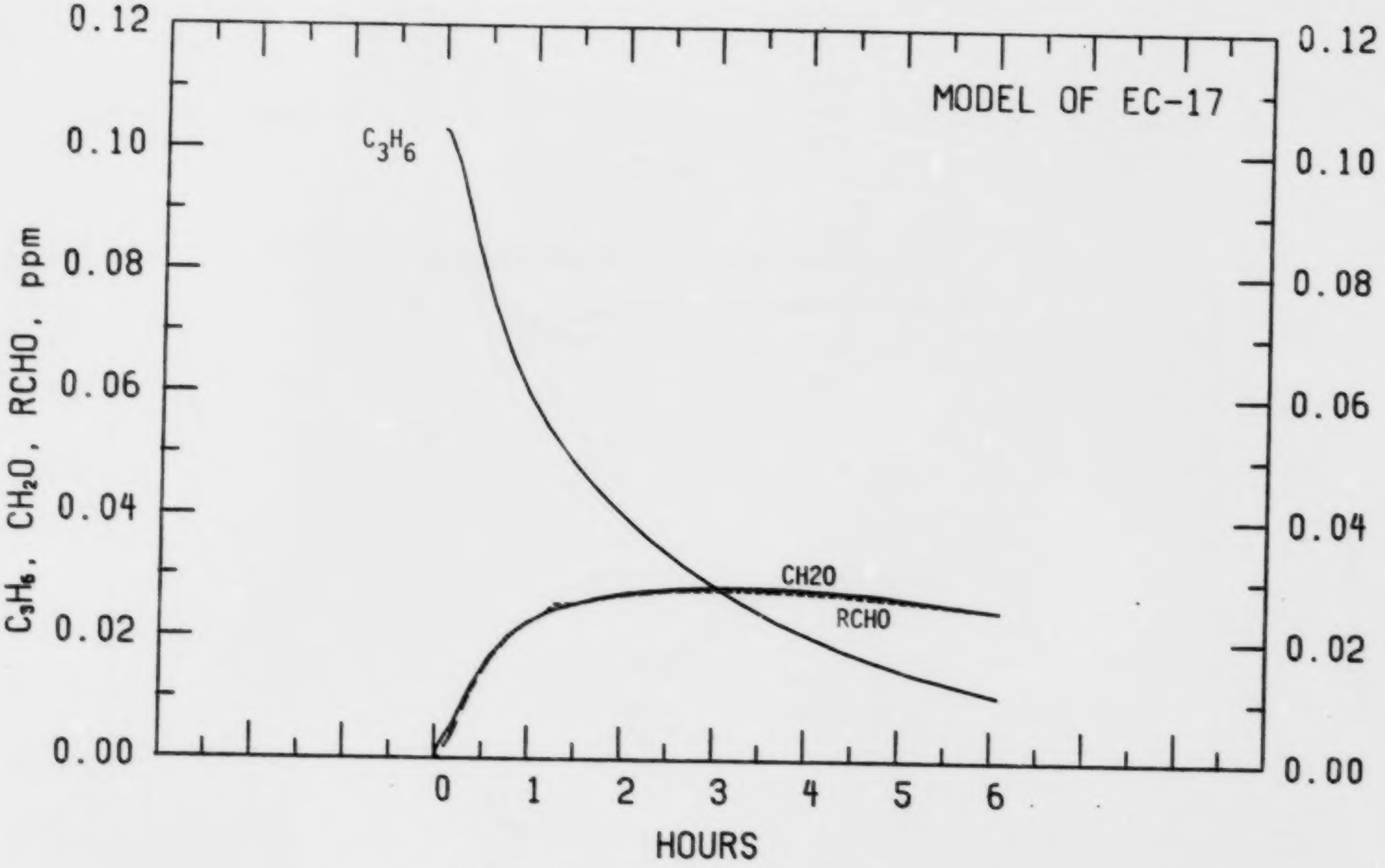

Figure 50. UNC model of run EC-17.

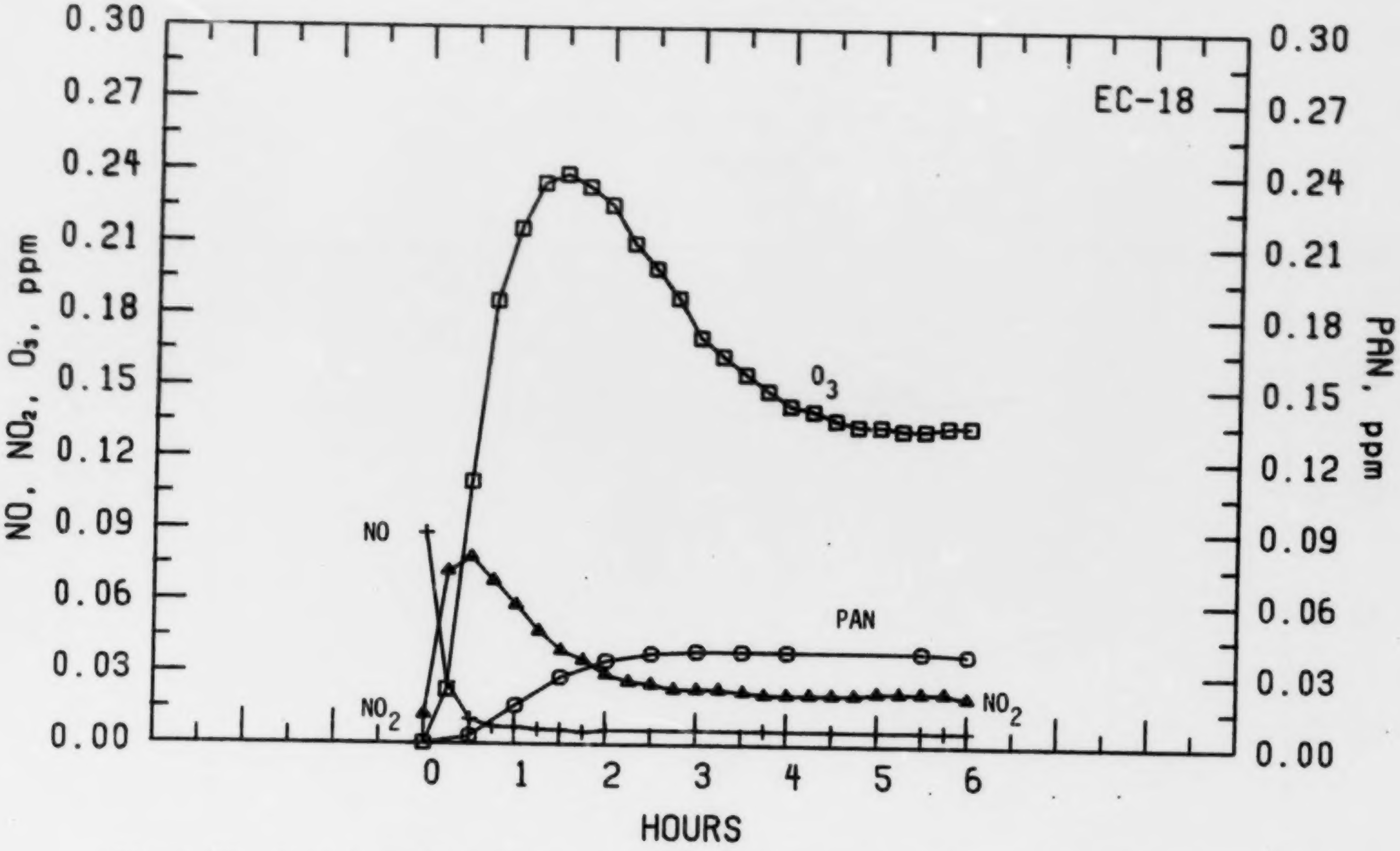

Figure 51. Actual profiles of run EC-18 in SAPRC chamber at Riverside, California.

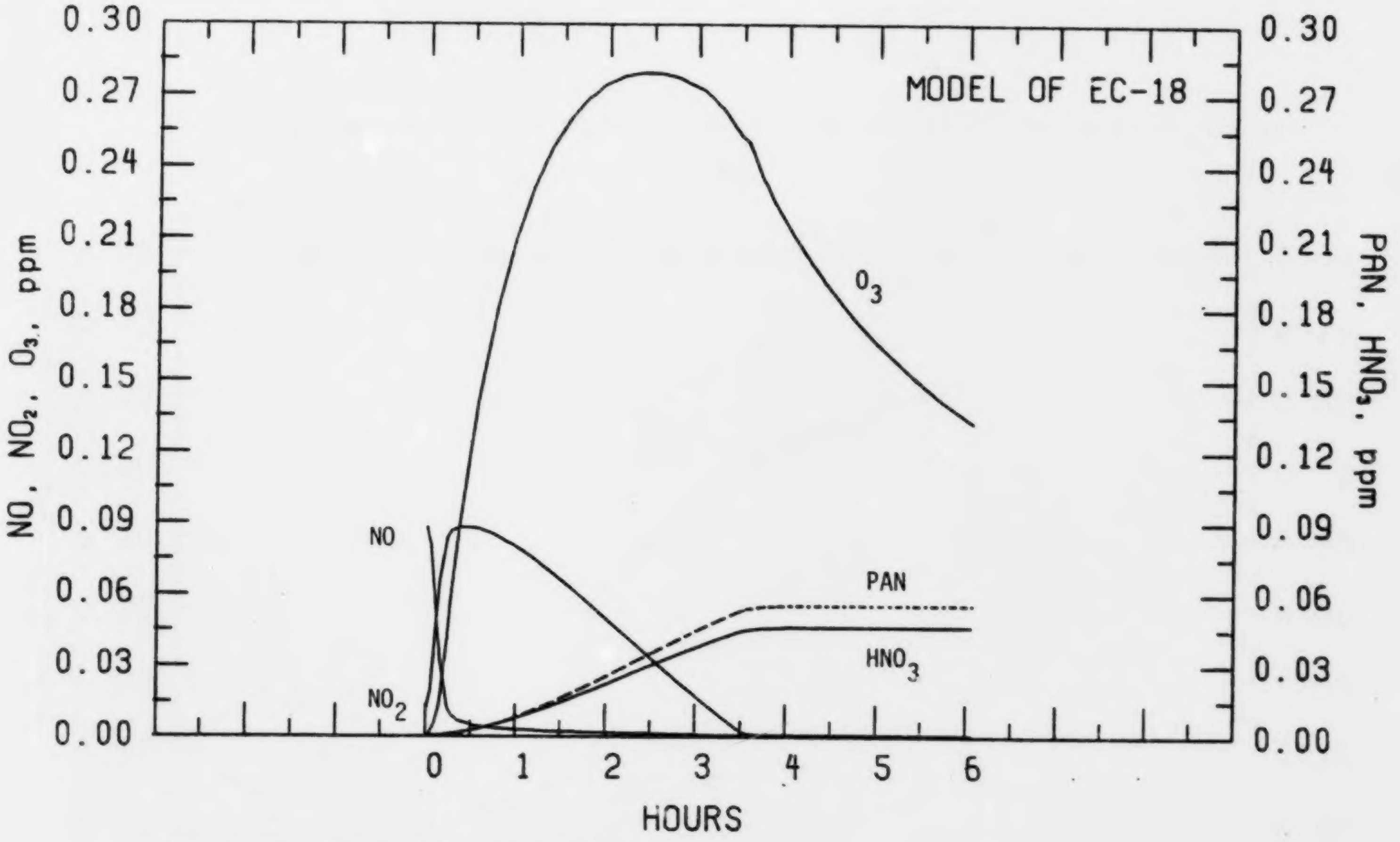

Figure 52. UNC model of run EC-18.

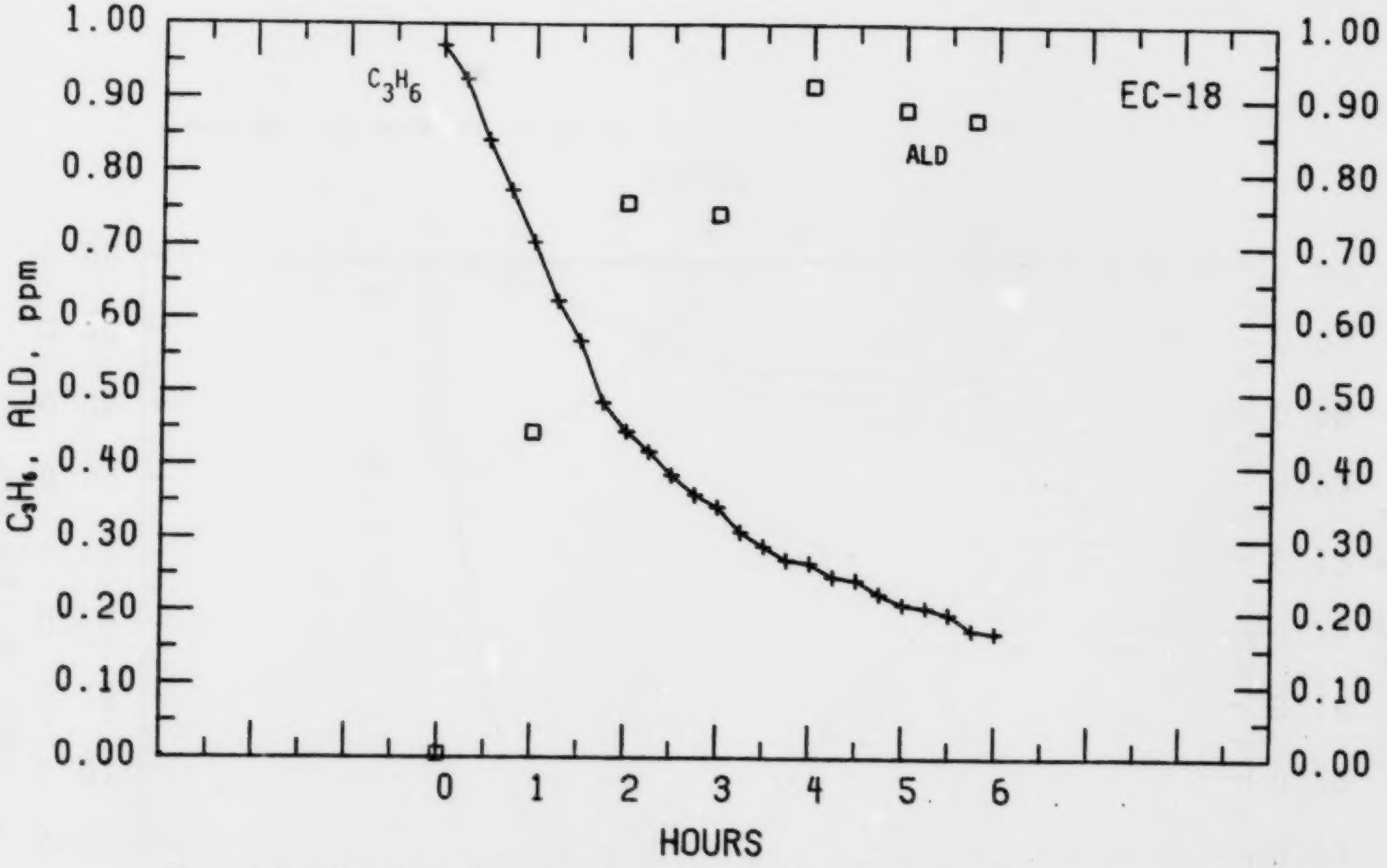

Figure 53. Actual profiles of run EC-18 in SAPRC chamber at Riverside, California.

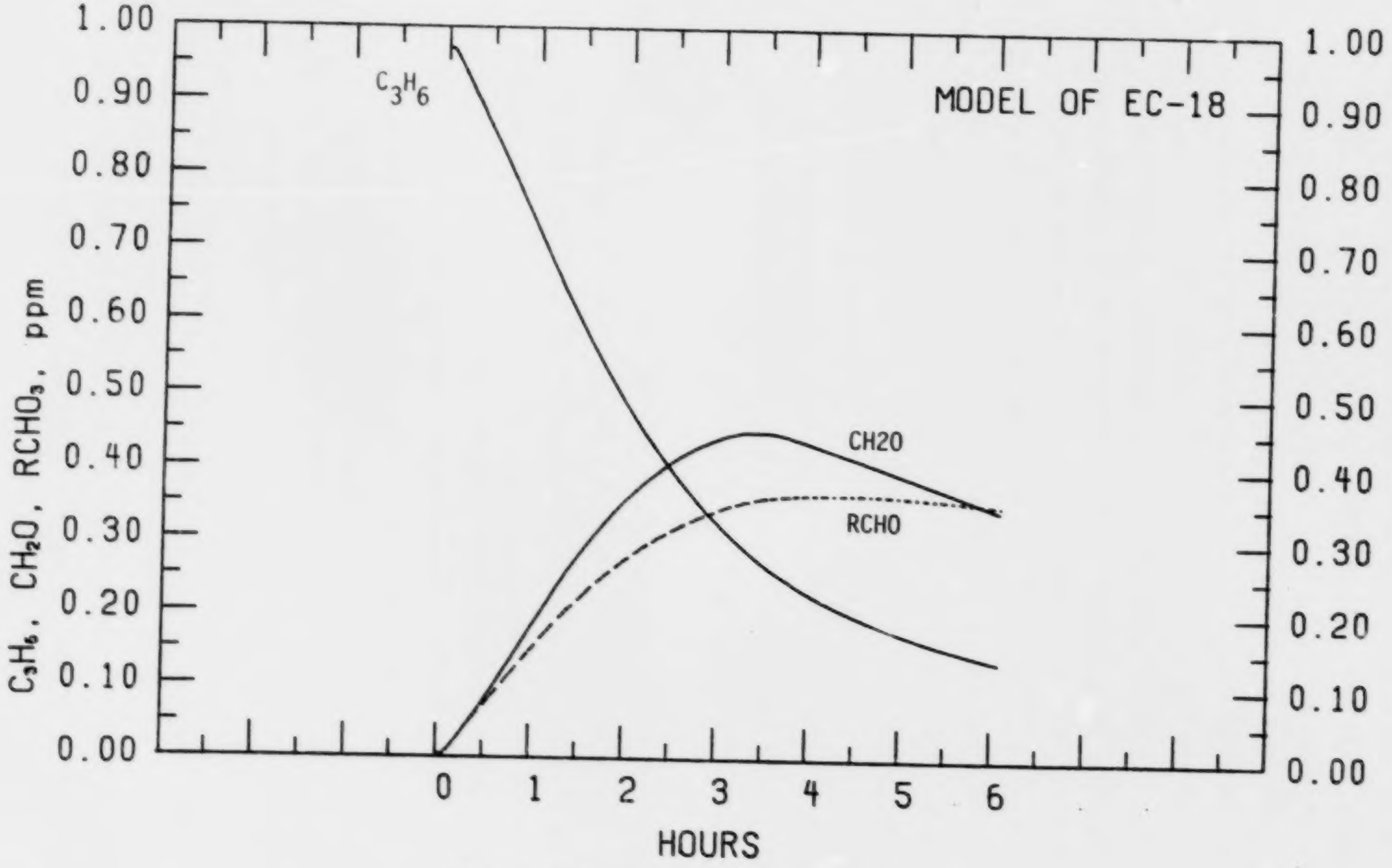

Figure 54. UNC model of run EC-18.

hydes was labeled only "Aldehyde" (represented by ◘ in Figure 49) and the simple sum of formaldehyde and acetaldehyde predicted by the model would be somewhat less than the original "Aldehyde" data. The NO_2 data for this chamber was taken by a chemiluminescent NO_x analyzer and subsequently corrected for PAN and HNO_3 interference[37]. The model predicts slightly higher NO_2 concentrations beginning at approximately 2.5 hours. Since the PAN data in the model agrees with the actual PAN data quite well, the difference between the model NO_2 and the actual NO_2 data would presumably be due to HNO_3 formation or this difference might have resulted from the correction applied to the raw NO_2 data. The k_1 value used in EC-17 and EC-18 was 0.223 min^{-1}. The rate constant for Reaction 25 that produced the best results in the model was the highest of any of the four chambers modeled, being 8.6×10^{-2} ppm^{-1} min^{-1}, implying a very high heterogeneous rate of formation of HNO_2 and therefore very rapid initiation of the photochemical conversion process. Since Reaction 35 also has a heterogeneous component its rate probably should have been higher which would have produced more HNO_3 in the model, thus leading to a better NO_2 fit.

In the UNC model of EC-18, the agreement for NO_2 and O_3 is poorer than in EC-17, but the model profiles of C_3H_6, CH_2O + RCHO ("Aldehydes"), and NO, are as good as or better than those for EC-17. The observed NO_2 profile for EC-18 is somewhat strange, since it decays to a plateau level of 0.02 ppm for approximately 4 hours, even though it was supposedly corrected for PAN and HNO_3 interference. Because the model maintains a higher NO_2 concentration during the 1.5 to 2 hour period, the O_3 concentration in the model is higher than that in the actual data. From 3.5 hours to the end of the simulation, the model O_3 decay is due almost exclusively to ozone reacting with the remaining propylene.

Model of Lockheed Chamber

The last chamber/reaction system modeled was a very high concentration propylene run in the Lockheed chamber[37] which was mostly Pyrex glass for this run. Although no actual data points were shown in the original plot of the Lockheed data, solid lines were drawn which exhibited rapid changes in slope. These were reproduced in the digitizing of the original plot and are present in Figure 55, the replotting of the Lockheed data on the standard axis box for this report. The NO data in the Lockheed study was from a chemiluminescent instrument and the NO_2 data from an automated Saltzman instrument[38]. There may be some calibration or response problem associated with this combination, since, as shown in Figure 55, there was a gain in NO_x of 0.5 ppm from start to crossover ($NO=NO_2=1.00$ ppm, therefore $NO_x=2.00$ ppm) and the NO_2 maximum concentration exceeded the initial NO concentration. The Lockheed data was taken at a k_d (pseudo-first-order rate constant for NO_2 photolysis) of 0.40 min^{-1} which for modeling must be translated into k_1, the actual first order rate constant.

Three model simulations were run in which the rate constant for Reaction 25 and k_1 were varied to obtain a reasonable fit to the actual data. Figure 56 is the last run of these three and used a value of 8×10^{-4} ppm^{-1}-min^{-1} for Reaction 25, well below that of EPA-325 and EC-17 and 18 but larger than the UNC chamber rate. The k_1 value used was 0.256 min^{-1} which is similar to that in the SAPRC chamber, but much lower than the value of 0.40 min^{-1} in the EPA-325 simulation and the peak value of approximately 0.55 min^{-1} which occurs in the UNC outdoor chamber. Since O_3 concentration is a function of the light intensity under which it forms, both the SAPRC and Lockheed chambers would probably yield O_3 concentrations which are less than those that would be found for the same concentrations of starting materials in the older EPA chamber or the UNC chamber on clear days.

The model and Lockheed data show reasonable agreement as to time of events and agree well in profiles for NO and C_3H_6, but the post-peak NO_2 behavior differs substantially and no clear ozone peak and decay were exhibited by the model data. This difference might be attributed

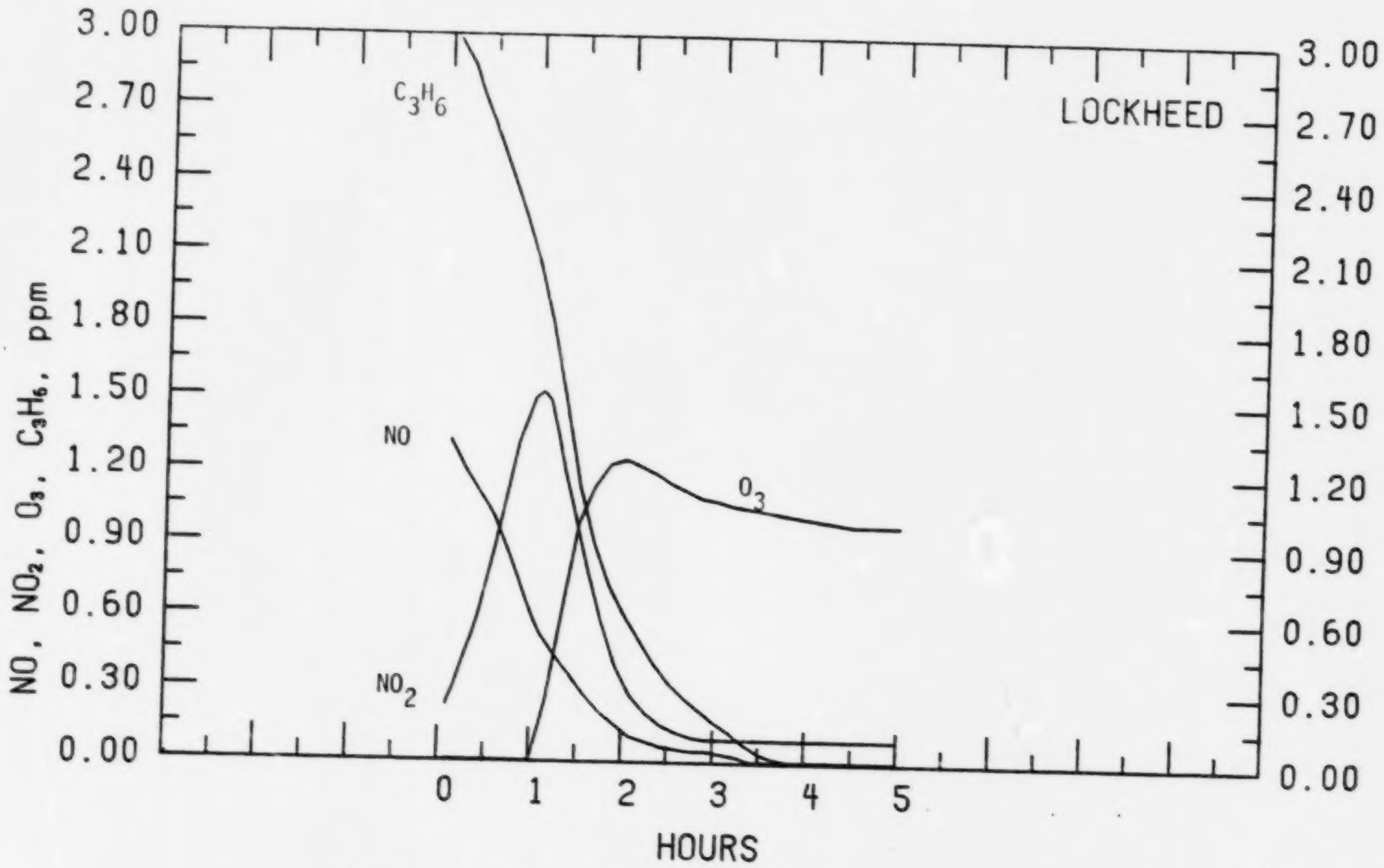

Figure 55. Actual profiles of a Lockheed run.

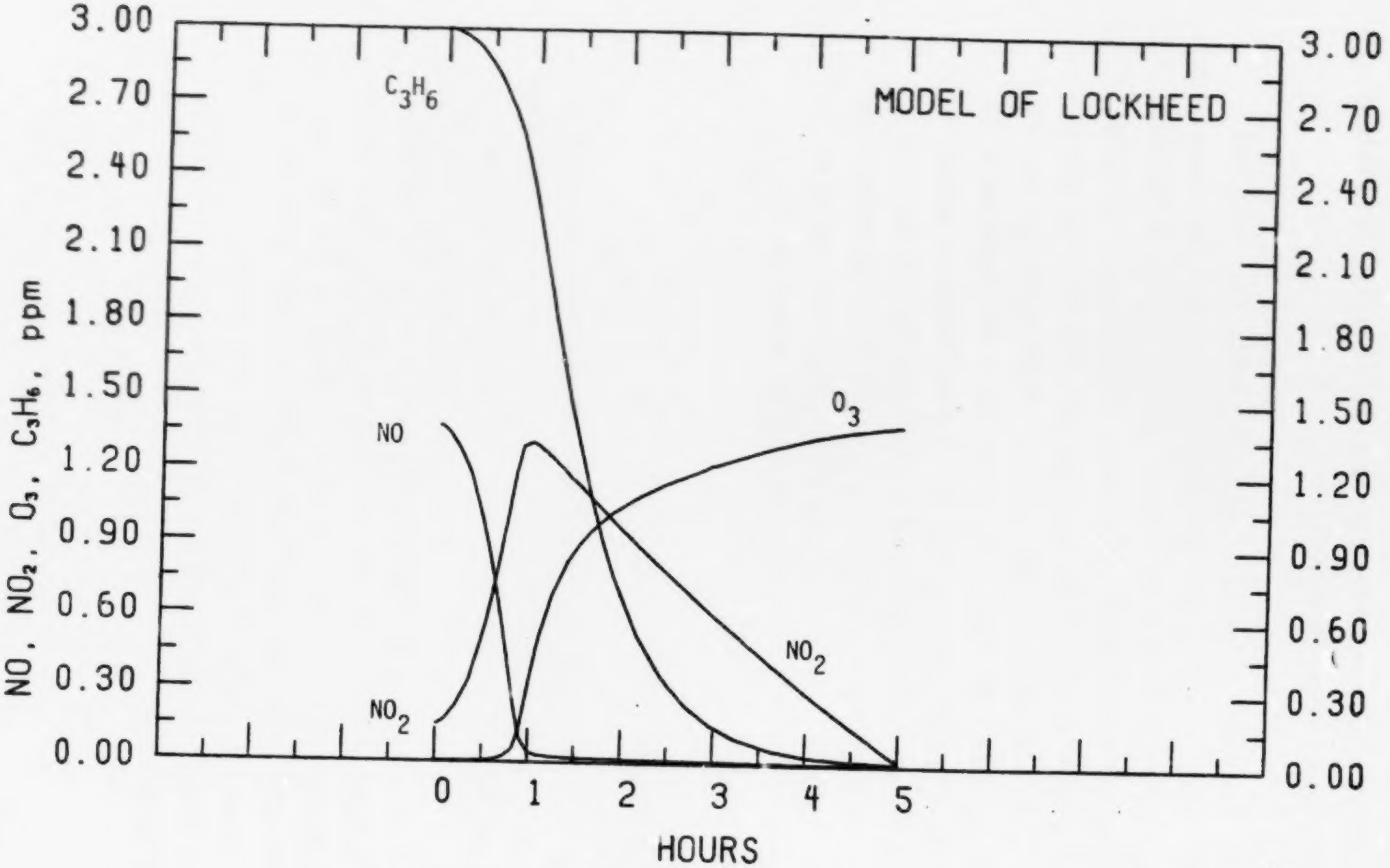

Figure 56. UNC model of a Lockheed run.

to a poor representation of the Lockheed N_2O_5 surface chemistry in the UNC model. Although the O_3 profiles differ substantially, the maximum O_3 concentrations agree reasonably well.

Considering that the model consists of only 35 steps, that only two parameters (the light intensity and the rate constant for HNO_2 formation from NO and NO_2 which represents individual surface chemistry of each chamber) were changed from chamber to chamber, and that a wide range of physical and chemical conditions were modeled, the results above speak well for both the model and the chemical performance of the UNC outdoor chamber on which the model was validated. The differences in behavior of propylene runs between the UNC chamber and more conventional indoor chambers can be simply and readily explained on the basis of differences in selected surface chemistry (which primarily affect the speed of the system) and light intensity magnitudes and time distribution (which primarily affect the detailed profile shape and the maximum concentration of ozone).

Bureau of Mines and UNC Chamber Comparison

One final comparison was made between a NO_x/auto exhaust run in the BOM smog chamber from data supplied by Dimitriades and a NO_x/simulated urban mix run in the UNC outdoor chamber. Figures 57 and 58 show these two runs. The BOM run had 0.05 ppm more NO and approximately the same IHC. The UNC run was slower than the BOM run, but the BOM run was at constant light intensity. Accounting for the light difference effects, these two runs are in general agreement. The UNC run formed 0.2 ppm more ozone, but the light intensity under which this formation occurred was higher than that in the BOM Chamber. An adequate hydrocarbon mix model has not yet been developed to allow a more detailed comparison.

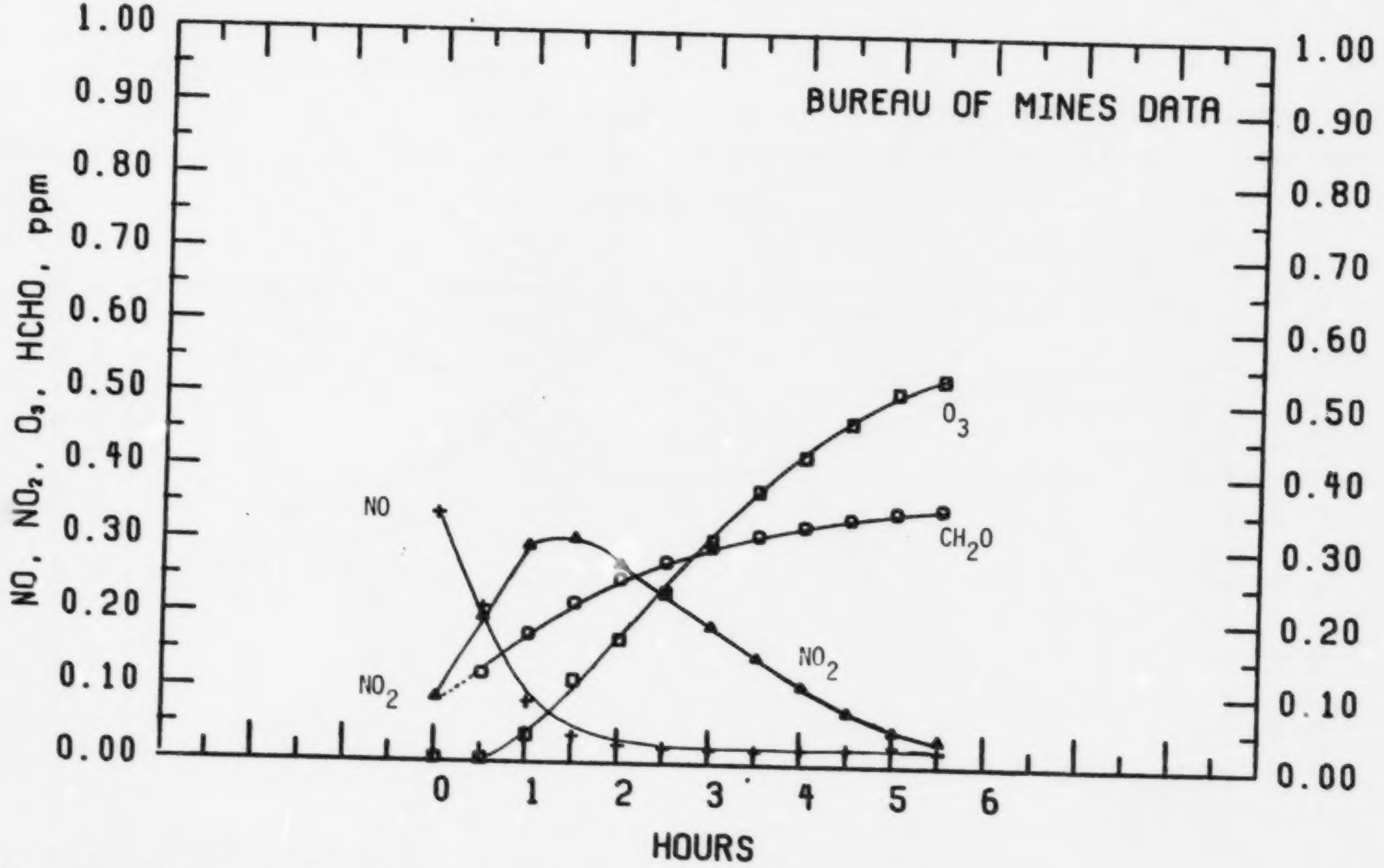

Figure 57. Actual profiles of Bureau of Mines run. Initial conditions: 0.414 ppm NO_x,0.082 ppm NO_2, and 3.3 ppmC auto-exhaust.

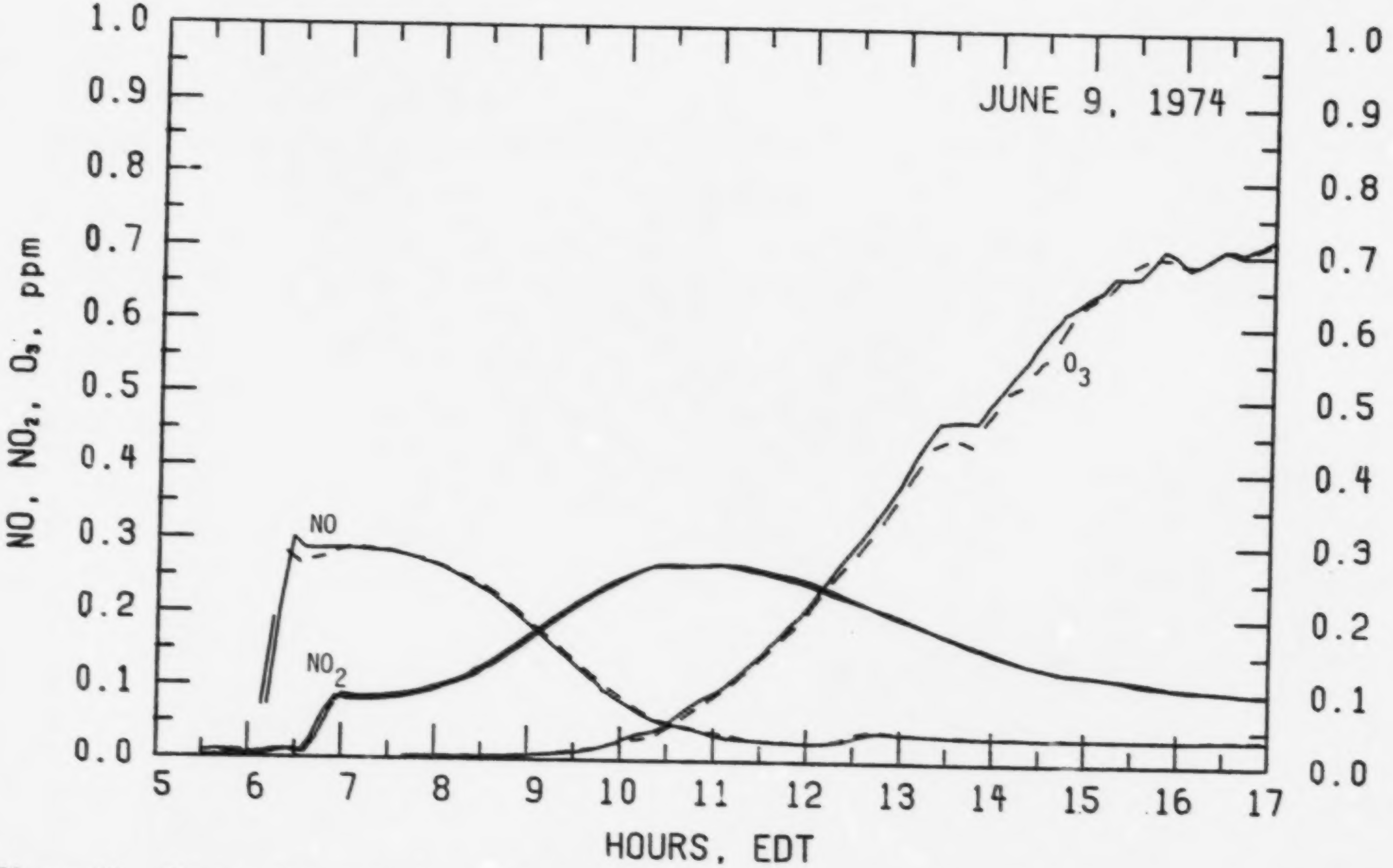

Figure 58. Mix run for comparison with BOM run. Initial conditions: NO_x(—) 0.369, (---) 0.368 ppm; NO_2(—) 0.083, (---) 0.079 ppm; NMHC(—) 3.60, (---) 3.60 ppmC urban hydrocarbon mix in UNC outdoor smog chamber.

SECTION VII

RESULTS AND DISCUSSION, PART II:

EFFECTS OF HYDROCARBON REDUCTION ON NITROGEN DIOXIDE CONCENTRATIONS

GENERAL

Of primary concern in this project was the effect of reducing NMHC concentrations (for the purpose of reducing oxidant) on the behavior of NO_2. The data generated by 130 mix runs in the outdoor chamber were examined to determine the effect of hydrocarbon reduction on: NO_2 maximum concentrations (NO2M), NO_2 ten-hour daytime dosages (DNO2DIFT), NO_2 ten-hour daytime average concentrations (NO2AVT), and the nighttime disappearance of any residual NO_2 at the end of runs. A nonlinear regression model that expressed NO2M as a function of initial NO_x (INOX), initial NMHC concentration (IHC), and average measures of solar radiation at various intervals (SRAV1 and SRAV3) was generated and explored. Data were also obtained and examined for possible effects on NO2M by factors such as initial NO_2/NO_x, dilution, and repeated irradiation.

RESULTS

Computer listings of data profiles and the summary listings of the significant measures for all runs are not included in this report, but are available as separate appendices.

For the purpose of discussion, mean values of clusters of data and plots of significant variables will be used. Selected individual profiles or exemplary runs will be used to illustrate specific points in the discussion.

Table 12 gives the mean values, standard deviations, and number of

TABLE 12. MEAN VALUES OF NITROGEN DIOXIDE MAXIMUM CONCENTRATION, NITROGEN DIOXIDE AVERAGE CONCENTRATION AND AVERAGE DAILY SOLAR RADIATION BROKENDOWN BY MEAN INITIAL HYDROCARBON AND MEAN INITIAL NITROGEN OXIDES

INOX $\bar{X} \pm \sigma$ / IHC $\bar{X} \pm \sigma$	0.007 4 Cases	0.122 ± 0.019 AVE SR TOT: 0.667 ± 0.280 AVE SR 13: 0.574 ± 0.273 AVE TEMP TOT: 81.7 ± 4.7 8 Cases	0.222 ± 0.023 AVE SR TOT: 0.699 ± 0.157 AVE SR 13: 0.699 ± 0.151 AVE TEMP TOT: 71.1 ± 12.2 30 Cases	0.311 ± 0.004 AVE SR TOT: 0.797 ± 0.00[illegible] AVE SR 13: 0.807 ± 0.026 AVE TEMP TOT: 76.4 ± 0.06 2 Cases	0.361 ± 0.008 AVE SR TOT: 0.719 ± 0.191 AVE SR 13: 0.707 ± 0.360 AVE TEMP TOT: 73.9 ± 7.7 51 Cases	0.433 ± 0.016 AVE SR TOT: 0.796 ± 0.013 AVE SR 13: 0.777 ± 0.038 AVE TEMP TOT: 85.0 ± 0.9 4 Cases	0.510 ± 0.008 AVE SR TOT: 0.672 ± 0.188 AVE SR 13: 0.635 ± 0.170 AVE TEMP TOT: 74.2 ± 11.0 23 Cases	0.707 ± [illegible] AVE SR TOT: 0.7[illegible]6 ± 0.03 AVE SR 13: 0.745 ± 0.16 AVE TEMP TOT: 69.5 ± 0.06 4 Cases
0.211 ± 0.071 5 Cases	0.007 NO$_x$ 0.21 HC 4 cases	CAPTION: INOX IHC NO2M NO2AVT SRAVT	0.243 ± 0.014 NO$_x$ 0.211 ± 0.071 HC 0.118 ± 0.030 0.076 ± 0.021 0.788 ± 0.132 5 cases					
0.794 ± 0.077 14 Cases			0.223 ± 0.025 NO$_x$ 0.832 ± 0.048 HC 0.138 ± 0.022 0.099 ± 0.022 0.608 ± 0.165 9 cases		0.373 NO$_x$ 0.721 HC 0.205 0.150 0.736 1 case	0.435 ± 0.021 NO$_x$ 0.706 ± 0.118 HC 0.186 ± 0.004 0.152 ± 0.009 0.790 ± 0.018 2 cases	0.516 ± 0.005 NO$_x$ 0.748 ± 0.074 HC 0.218 ± 0.004 0.167 ± 0.005 0.754 ± 0.093 2 cases	
1.059 ± 0.082 15 Cases			0.224 ± 0.020 NO$_x$ 1.006 ± 0.060 HC 0.138 ± 0.018 0.099 ± 0.026 0.746 ± 0.157 7 cases		0.358 ± 0.004 NO$_x$ 1.119 ± 0.067 HC 0.165 ± 0.031 0.122 ± 0.014 0.669 ± 0.222 7 cases	0.441 NO$_x$ 1.010 HC 0.195 0.150 0.800 1 case		
1.407 ± 0.117 19 Cases		0.131 ± 0.026 NO$_x$ 1.525 ± 0.035 HC 0.084 ± 0.013 0.059 ± 0.006 0.821 ± 0.215 2 cases	0.206 ± 0.011 NO$_x$ 1.392 ± 0.177 HC 0.149 ± 0.011 0.104 ± 0.003 0.625 ± 0.120 3 cases		0.358 ± 0.005 NO$_x$ 1.369 ± 0.102 HC 0.199 ± 0.042 0.144 ± 0.026 0.759 ± 0.223 11 cases		0.509 NO$_x$ 1.390 HC 0.303 0.241 0.681 1 case	0.710 ± 0.004 NO$_x$ 1.528 ± 0.057 HC 0.302 ± 0.095 0.183 ± 0.796 ± 0.051 2 cases

1.992 ± 0.160 22 Cases		0.121 ± 0.022 NO_x 1.926 ± 0 118 HC 0.084 ± 0.014 0.062 ± 0.006 0.664 ± 0.300 4 cases	0.222 ± 0.028 NO_x 1.967 ± 0.252 HC 0.156 ± 0.015 0.116 ± 0.013 0.810 ± 0.181 3 cases		0.362 ± 0.009 NO_x 2.083 ± 0.110 HC 0.229 ± 0.019 0.164 ± 0.025 0.724 ± 0.106 7 cases	0.419 NO_x 1.927 HC 0.258 0.216 0.806 1 case	0.507 ± 0.008 NO_x 1.959 ± 0.184 HC 0.332 ± 0.034 0.231 ± 0.028 0.749 ± 0.219 7 cases	
2.475 ± 0.055 15 Cases			0.106 ± 0.012 NO_x 2.464 ± 0.030 HC 0.125 ± 0.011 0.078 ± 0.003 0.682 ± 0.015 2 cases		0.355 ± 0.004 NO_x 2.485 ± 0.047 HC 0.218 ± 0.022 0.159 ± 0.018 0.592 ± 0.228 8 cases		0.511 ± 0.006 NO_x 2.462 ± 0.078 HC 0.281 ± 0.058 0.215 ± 0.045 0.738 ± 0.064 5 cases	
2.705 ± 0.069 5 Cases					0.366 ± 0.012 NO_x 2.699 ± 0.078 HC 0.242 ± 0.009 0.175 ± 0.009 0.658 ± 0.126 4 cases			0.704 NO_x 2.729 HC 0.365 ---- 0.768 1 case
2.900 ± 0.036 12 Cases		0.107 NO_x 2.925 HC 0.077 0.057 0.252 1 case	0.197 NO_x 3.095 HC 0.134 0.082 0.661 1 case		0.365 ± 0.010 NO_x 2.887 ± 0.080 HC 0.249 ± 0.010 0.188 ± 0.022 0.773 ± 0.167 9 cases		0.510 NO_x 2.800 HC 0.305 0.234 0.654 1 case	
3.444 ± 0.166 5 Cases					0.367 ± 0.002 NO_x 3.450 ± 0.191 HC 0.271 ± 0.007 0.158 ± 0.016 0.880 ± 0.071 4 cases			0.703 NO_x 3.420 HC 0.407 ---- 0.806 1 case
4.120 ± 0.183 10 Cases		0.122 NO_x 4.200 HC 0.089 0.060 0.789 1 case		0.311 ± 0.004 NO_x 4.408 ± 0.206 HC 0.265 ± 0.001 0.143 ± 0.032 0.797 ± 0.002 2 cases			0.509 ± 0.010 NO_x 4.062 ± 0.064 HC 0.342 ± 0.058 0.225 ± 0.034 0.526 ± 0.200 7 cases	

cases for the variables of most interest at each initial condition cluster. The standard deviation of initial conditions represents the spread of the data around each of the target initial conditions designated in the experimental design. Table 12 does not present the pairing of runs that occurred in the experiments; this will be taken up in other tables and plots.

EFFECTS ON NITROGEN DIOXIDE MAXIMUM CONCENTRATIONS

The NO2M data were examined by several types of analysis, beginning at mean values for the entire data set and proceeding to an examination of individual paired runs (dual runs with different hydrocarbon concentrations). IHC concentration was found to have a significant effect on NO2M concentrations, but other factors such as solar radiation conditions also caused variation in NO2M values at constant IHC and INOX. These other factors were not related in any simple manner to NO2M concentrations and required a detailed examination. This was performed on the 51 runs at INOX = 0.36 ppm. Nitrogen dioxide profiles for different IHC from individual runs (different days) at three constant INOX values were compared. Nitric oxide, NO_2, and O_3 profiles were compared for several dual runs and the percentage reduction in NO2M for a reduction in IHC at different INOX was computed for several dual runs.

Mean Values

If the mean NO2M ($\overline{\text{NO2M}}$) for each INOX cluster is computed without regard for the conditions under which the value occurred (i.e., ignoring effects of IHC, SR, Temp, and PCTNO2; across rows in Table 12) and it is plotted as a function of the mean value in each INOX cluster ($\overline{\text{INOX}}$), (Figure 59), the values of $\overline{\text{NO2M}}$ for cases INOX <0.7 ppm can be fitted by

$$\overline{NO_2M} = 0.5788\ \overline{INOX} + 0.0071 \qquad (1)$$

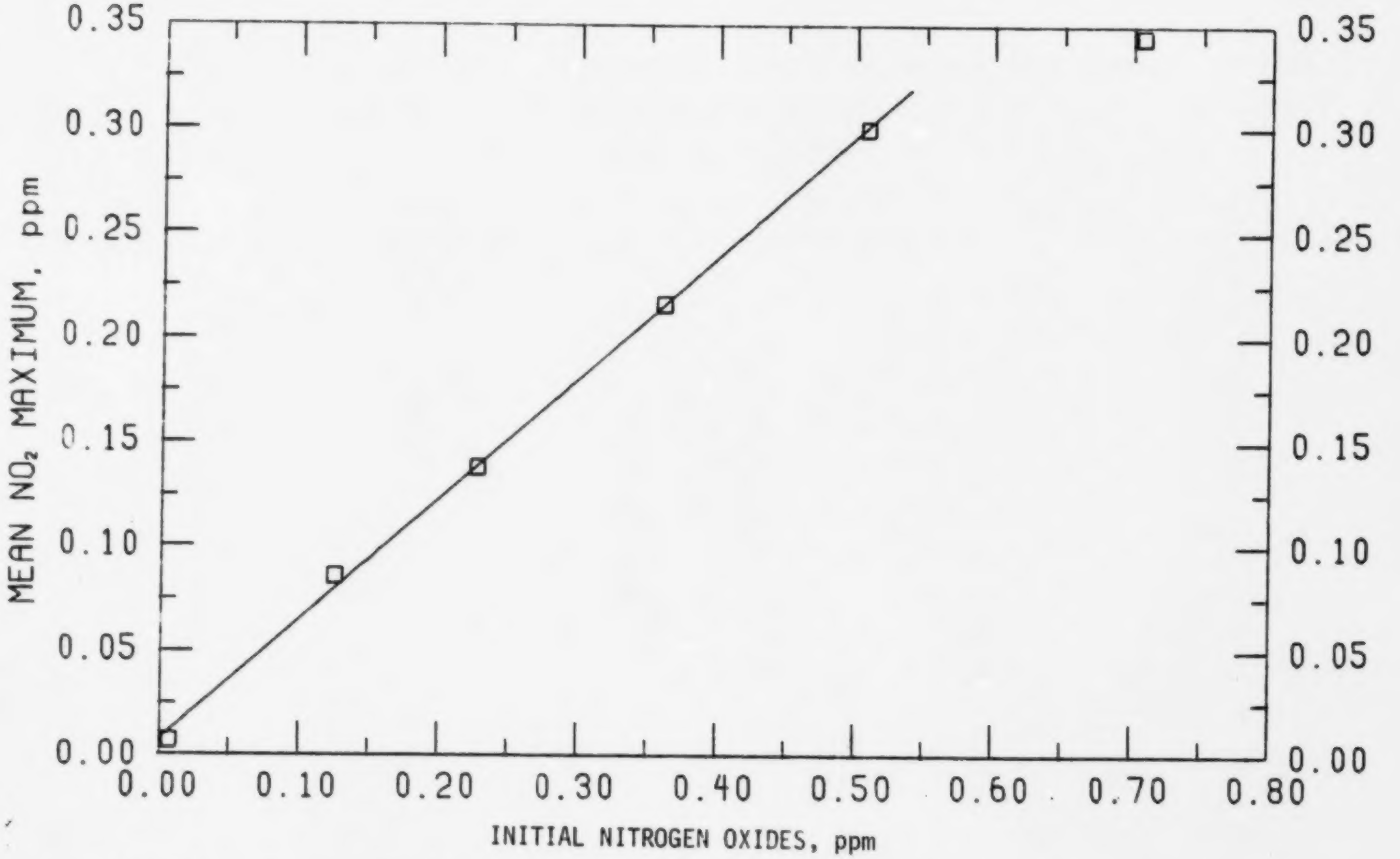

Figure 59. Mean nitrogen dioxide maximum concentration as a function of mean initial oxides of nitrogen for urban hydrocarbon mix in UNC outdoor smog chamber. Equation of line is NO_2 max = 0.5788 NO_x + 0.007.

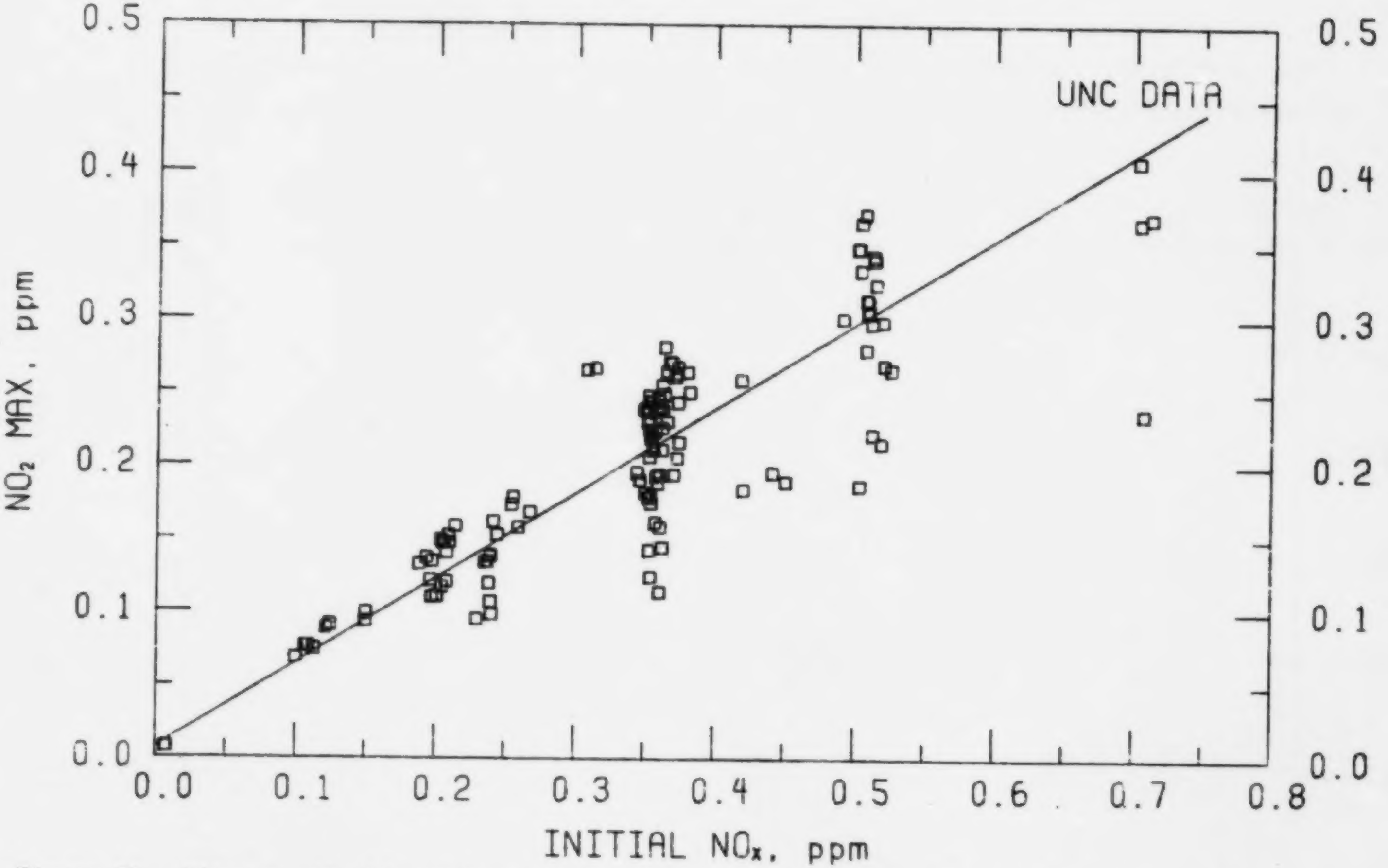

Figure 60. Nitrogen dioxide maximum concentration as a function of initial oxides of nitrogen for individual runs for urban hydrocarbon mix in UNC outdoor smog chamber. Equation of line is the same as Fig. 59.

with an r^2 of 0.9988. Equation 1 implies that over the range of conditions that occurred in the experimental series, the $\overline{\text{NO2M}}$ was primarily dependent upon INOX.

A plot of individual NO2M values as a function of individual INOX (Figure 60) however, reveals not only the scatter around each target INOX, but also a large range of NO2M values which tend to cluster near the upper end of each range. It is also evident that the INOX cluster at $\overline{\text{INOX}}$ = 0.7 ppm might also be consistant with the line from Equation 1 if sufficient runs had been made to give a representative mean.

Individual Values at Constant INOX

To investigate the factors which might be responsible for the scatter of cases around the $\overline{\text{NO2M}}$, the 51 cases for $\overline{\text{INOX}}$ = 0.361 ppm were examined in detail. In Table 13, the individual $\overline{\text{NO2M}}$ values and associated information have been classified according to the $\overline{\text{IHC}}$ and ranked in ascending order. In Table 13, NO2M values increase with increasing $\overline{\text{IHC}}$, with two exceptions ($\overline{\text{IHC}}$ = 2.48 and 2.70), but there was sufficient scatter at each $\overline{\text{IHC}}$ to cause an overlap in NO2M values from one $\overline{\text{IHC}}$ value to another.

Several factors were investigated to determine if they were associated with the scatter in NO2M at each IHC. The most important of these are also listed in Table 13. A number of observations relevant to the scatter in NO2M can be made from the data in Table 13:

1) The total average solar radiation (SRAVT) for a day is not a strong predictor of NO2M given constant INOX and IHC and neither is the average solar radiation from the start until the occurrence of NO2M (SRAV13),
2) Although some values of $\overline{\text{IHC}}$ exhibit a trend in time to NO2M, time to NO2M is also not a good predictor of NO2M,

Table 13. NITROGEN DIOXIDE MAXIMUM CONCENTRATIONS, TIME TO NO-NO_2 CROSSOVER, NET NO_2 FORMED, AVERAGE SOLAR RADIATION AT INITIAL NO_x AVERAGE CONCENTRATION OF 0.361 ppm BROKEN DOWN BY INITIAL HYDROCARBON AVERAGE CONCENTRATIONS AVERAGE SOLAR RADIATION VALUES.

IHC, ppmc	RUN[a] NO	NO2M,[b] ppm	NO2M-INO_2,[c] ppm	SRAVT,[d] cal-cm^{-2}-min^{-1}	TIMDIF13[e] mins	SR-RANGE[f] cal-cm-$^{-2}$-min^{-1}	Comment[g]
0.79	740629 R	0.205	0.126	0.736	528	0.36-1.4	10 peaks
1.06	740922 R	0.114[h]	0.032	0.198	464	- - - -	heavy overcast
	741001 B	0.144[h]	0.061	0.831	432		clear day
	740923 R	0.158	0.081	0.785	440	0.41-1.2	6 dips
	741022 B	0.161	0.082	0.755	456	0.40-0.84	choppy
	741010 B	0.182	0.110	0.731	528	0.46-1.0	mostly clear
	741006 R	0.192	0.121	0.793	520	0.50-1.08	partly clear
	741008 B	0.206	0.133	0.589	592	0.26-1.06	choppy
1.41	740927 B	0.124	0.056	0.400	472	0.32-1.16	4 dips
	740924 B	0.142	0.071	0.071	536	- - - -	- - - -
	740619 B	0.176	0.105	0.869	548	0.43-1.40	8 spikes in 1/2 hr
	740920 B	0.194	0.105	0.604	568	0.30-1.25	6 spikes,choppy
	740611 R	0.211	0.133	0.067	344	0.81-1.36	clear after 1.5 hrs.
	741012 R	0.231	0.160	0.578	552	0.54-1.00	choppy
	740612 B	0.236	0.156	0.764	392	0.48-1.42	4 spikes, choppy

Table 13. Cont'd.

IhC, ppmC	RUN[a] NO	NO2M,[b] ppm	NO2M-INO$_2$,[c] ppm	SRAVT,[d] cal-cm^{-2}-min^{-1}	TIMDIF13[e] mins	SR-RANGE[f] cal-cm^{-2}-min^{-1}	Comment[g]
1.99	740919 B	0.210	0.129	0.858	408	1.04-1.15	clear
	741005 R	0.224	0.151	0.857	368	0.94-1.10	mostly clear
	741025 B	0.230	0.154	0.640	360	0.56-0.98	very choppy, 1 hr. dip
	741022 R	0.237	0.157	0.748	376	0.60-1.02	mod. choppy
	740629 B	0.267	0.187	0.731	320	0.40-1.41	6 spikes, with peaks
2.48	740927 R	0.180	0.111	0.386	368	0.3-1.3	many clouds
	740922 B	0.188	0.108	0.193	464	0.1-0.2	overcast
	740924 R	0.221	0.150	0.444	512	- - - -	
	740923 R	0.223	0.149	0.763	400	0.45-1.4	8 spikes
	741001 R	0.226	0.144	0.825	408	0.93-1.14	clear
	741008 R	0.230	0.158	0.595	432	0.68-1.08	3 dips, choppy
	741010 R	0.238	0.164	0.733	368	0.88-1.0	clear
	741006 B	0.239	0.168	0.785	344	0.79-1.07	3 dips, slightly choppy
2.70	740919 R	0.230	0.147	0.843	352	0.97-1.15	clear
	741012 B	0.239	0.168	0.589	392	0.62-1.0	2 mod. dips
	741029 R	0.249	0.163	0.567	312	0.73-0.85	partly clear
	740920 R	0.250	0.158	0.633	368	0.35-1.33	very spikey

Table 13. Cont'd.

IHC, ppmC	RUN[a] NO	NO2M,[b] ppm	NO2M-INO$_2$,[c] ppm	SRAVT,[d] cal-cm^{-2}-min^{-1}	TIMDIF13[e] mins	SR-RANGE[f] cal-cm^{-2}-min^{-1}	Comment[g]
2.90	740611 B	0.238	0.164	1.064	264	0.81-1.34	clear
	741029 B	0.240	0.158	0.583	280	0.73-0.85	partly clear
	741025 R	0.244	0.167	0.639	312	0.56-0.98	1 large dip, choppy
	741005 B	0.247	0.175	0.856	272	0.90-1.10	clear
	740612 R	0.264	0.183	0.779	296	0.95-1.23	small freq dips
3.44	740609 R	0.270	0.189	0.857	224		

a The run number is given as YYMMDDS where YY = year, MM = month, DD = day, S = side (RED or BLUE).

b The maximum NO_2 concentration during a run.

c The net ppm NO_2 formed. NO_2 maximum minus the initial NO_2 injected.

d The average total solar radiation from the hydrocarbon injection until 17:00.

e The time difference between the hydrocarbon injection and the occurrence of the NO_2M.

f The range in total solar radiation from NO-NO_2 crossover to the NO2M.

g Qualitative description of solar radiation in the range given.

h Did not cross over.

3) At every $\overline{\text{IHC}}$ value which contained a June run, a June run exhibited the maximum NO2M for the category,

4) The September and October 1974 runs tend to occur near the lower values of NO2M at each $\overline{\text{IHC}}$ value and the two $\overline{\text{IHC}}$ which have only runs from these months have lower maximum NO2M values than would be expected from the trend discussed above,

5) The October runs of 1974 with lower SRAVT than a typical clear October day ($\sim$0.8 cal-cm^{-2}-min^{-1}) have higher NO2M values than clear October and September days.

6) The maximum NO2M at a $\overline{\text{IHC}}$ value is never associated with the maximum SRAVT or SRAV13 for that $\overline{\text{IHC}}$ value.

The explanation for all of these observations can be related to the effects of variable, sometimes "choppy", solar radiation and to the method of reporting solar radiation measurements used in this study. The values of SRAVT are computed from the total integrated solar radiation for the day (ISRDIFT) and the total time difference (TIMEDIFT) and represent the true average over the period. If a dip or "hole" occurs in solar radiation due to clouds, the ISRDIFT reflects this, but it does not indicate when it occurred. The same is true for SRAV13 (which is computed from the integrated solar radiation from start until the time the NO2M occurs, i.e., ISRDIF13/TIMEDIF13) except that if SRAV13 is low then the dip or hole occurred before the NO2M. Thus, very low values of SRAVT indicate a fairly cloudy or overcast day and very high values of SRAVT indicate a very clear day. Intermediate values probably indicate some choppiness but not when this choppiness occurred.

From Table 13, and observation (6) above it appears that the maximum NO2M in each HC category occurred on choppy days. Since a clear day in June yields a SRAVT value $\sim$0.2 cal-cm^{-2}-min^{-1} higher than a clear October day, the SRAVT for a choppy June day can be nearly equal to the value for a clear October day and furthermore, the June day will have peak values that greatly exceed the values for the clear October day. In addition, the actual solar radiation peak values for a choppy day exceed the peak values for a total clear day as was shown in Figure 28. Since this phenomenon occurs in the readings from both the Eppley total solar radiation radiometer and the Eppley ultraviolet radiometer, which operate on different sensing principles, it is apparently real and probably results from the cloud increasing the forward scatter of radiation into the direct solar beam just before and just after it passes over the sun.

Furthermore, comparisons of closely spaced runs, for clear days and choppy days with otherwise identical chemical and temperature conditions indicates that choppy days are faster, have larger maximum NO oxidation rates, higher NO_2 maximum values, larger O_3 formation rates and frequently higher final O_3 concentrations depending upon the degree of choppiness (see for example Figures 23, 26, and 27).

The above discussion suggests that the effects of solar radiation on photochemical systems is not solely dependent on the dosage or average value, but also on the maximum value that occurs during an interval.

The effect of rapidly changing solar radiation depends upon the state of the photochemical system at the time the change occurs. Two examples of this are shown in Figure 61 and 62. In Figure 61, the short, small burst of solar radiation at 0910 hours was able to initiate the system sufficiently so that a large change in the NO and NO_2 rate occurred, which was sustained for the rest of the run even though the solar radiation never again reached the peak value during the run. The dual run shown in Figure 62 was a test of the effect of changing the initial percentage NO_2 for constant NO_x and HC. The expected effect of different NO_2/NO_x did not occur in this dual run after 1030 hours due to the difference in response of each chemical system to the rapid decrease and then increase in solar radiation at 0900 and 1000 hours.

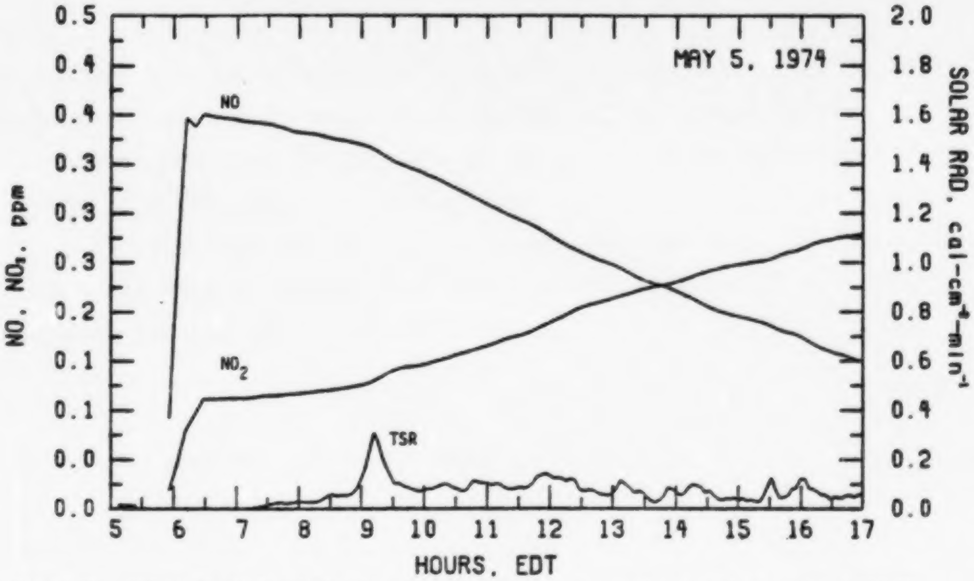

Figure 61. Effect of single light pulse on nitrogen oxides conversion rate in a system initially containing 0.511 ppm NO_x, 0.114 ppm NO_2 and 1.89 ppmC propylene in UNC outdoor smog chamber.

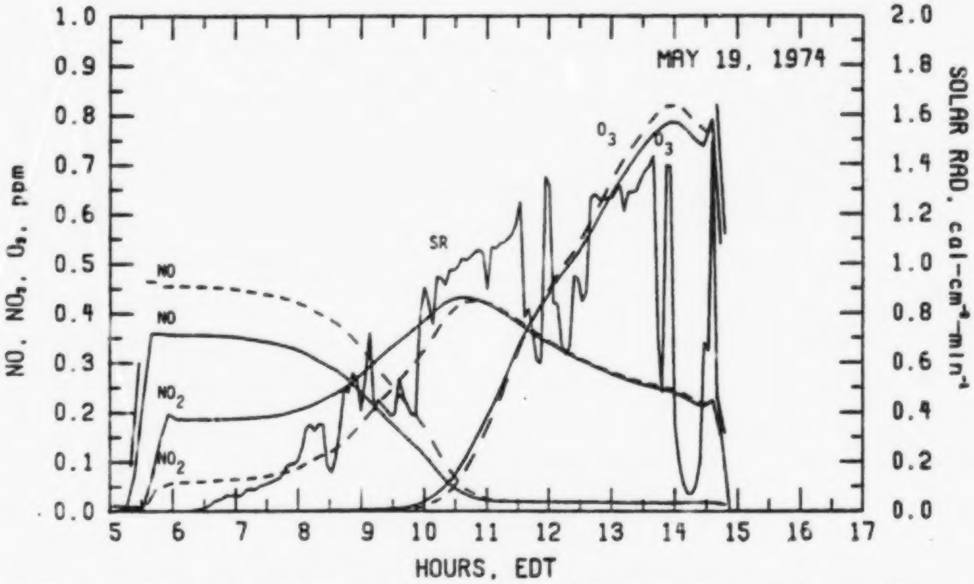

Figure 62. Example of rapid changes in solar radiation accelerating occurrence of nitrogen dioxide maximum. Compare with clear day behavior shown in Figure 77. Initial hydrocarbon concentration 1.95 ppmC propylene in both sides.

Individual Runs on Different Days and at Different INOX

Comparison of runs conducted on different, essentially totally clear days which had the same INOX but different IHC does show a decrease in NO2M with a decrease in IHC. Figures 63, 64, and 65 depict only the NO_2 time profiles at different IHC for INOX = 0.5, 0.35, and 0.22 ppm respectively. In Figure 66, the NO_2 profiles for two dual October runs of INOX = 0.36 and four different IHC are shown. Figure 67 shows typical solar radiation profiles for the runs in summer and the October runs.

From these figures, the effect of HC reduction on NO_2 maximum concentration, NO_2 dosage, and dosage distribution, is clearly discernible. Thus, 52% and 56% reduction in IHC at INOX = 0.36 ppm, cause reductions in maximum concentrations of approximately 7% and 20%. The October runs in Figure 66 exhibit much longer times to NO_2 maximum due to the lower total solar radiation available and the shorter solar day (Figure 67). October 1974 also had more haze and thinly overcast days than October 1973 reducing further the amount of actinic radiation available during this period. The effects of reducing IHC, however, are clearly evident in Figure 66.

Dual Runs at Different IHC

Pairwise determination of the effects of reducing IHC was accomplished by running differential runs in the dual chamber with all conditions identical except IHC on the two sides. Thus, unlike the data in Figure 63, a comparison of NO_2 behavior can be made for the same solar radiation or temperature conditions. The NO_2, NO, and O_3 profiles from two of these dual runs are shown in Figures 68 and 69.

In Table 14, the differential percentage reduction in NO2M is given as a function of IHC differential reduction. The NO2M reduction also appears to be a function of the INOX; higher INOX yields a greater percentage NO2M reduction for approximately the same IHC reduction.

Table 14. PAIRWISE COMPARISON OF EFFECTS OF REDUCING INITIAL HYDROCARBON CONCENTRATION ON NITROGEN DIOXIDE MAXIMUM CONCENTRATIONS FOR SELECTED DUAL RUNS WITH URBAN HYDROCARBON MIX IN UNC OUTDOOR CHAMBER

Initial NOX, ppm	Run No.	Initial HC, ppmC			NO_2 maximum, ppm		
		High Side	Low Side	% Reduction	High Side	Low Side	% Reduction
0.261	741013	0.71	0.32	54.9	0.1781	0.1680	5.7
0.257	740622	1.87	0.85	54.5	0.1731	0.1577	8.9
0.358	740611	2.80	1.40	50.0	0.2385	0.2110	11.5
0.369	740612	2.90	1.30	55.2	0.2638	0.2362	10.5
0.373	740629	2.11	0.72	65.9	0.2669	0.2053	23.1
0.513	740616	2.58	0.70	72.9	0.3427	0.2213	35.4
0.520	740620	2.50	0.80	68.0	0.2979	0.2152	27.8
0.508	740702	4.00	2.29	42.8	0.3713	0.3129	15.7

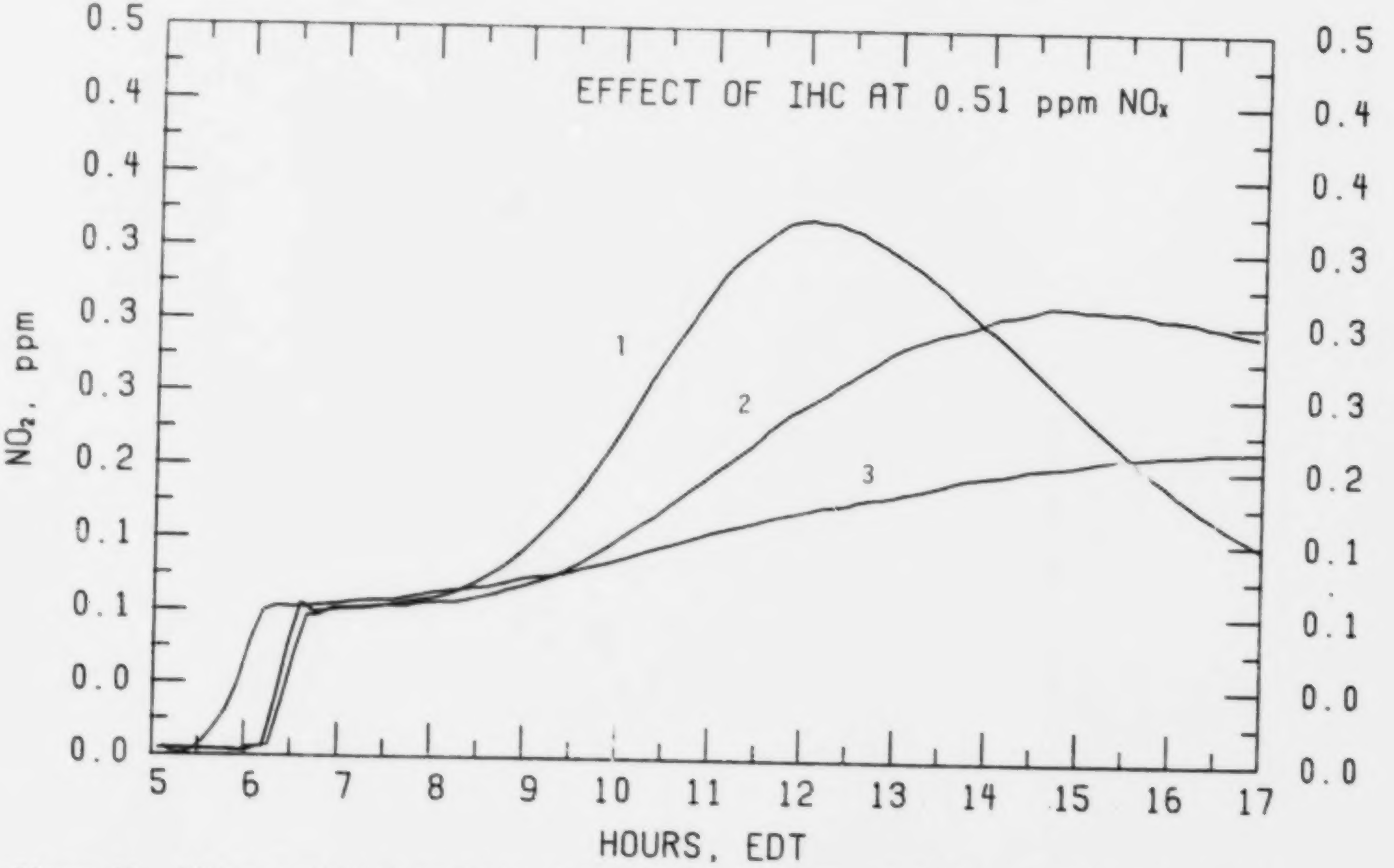

Figure 63. Nitrogen dioxide profiles at constant initial NO$_x$ of 0.51 ppm and initial NMHC of 4.00 ppmC(7/2/74, curve 1), 2.29 ppmC (7/2/74, curve 2) and 0.80 ppmC (6/20/74, curve 3) urban hydrocarbon mix in UNC outdoor smog chamber.

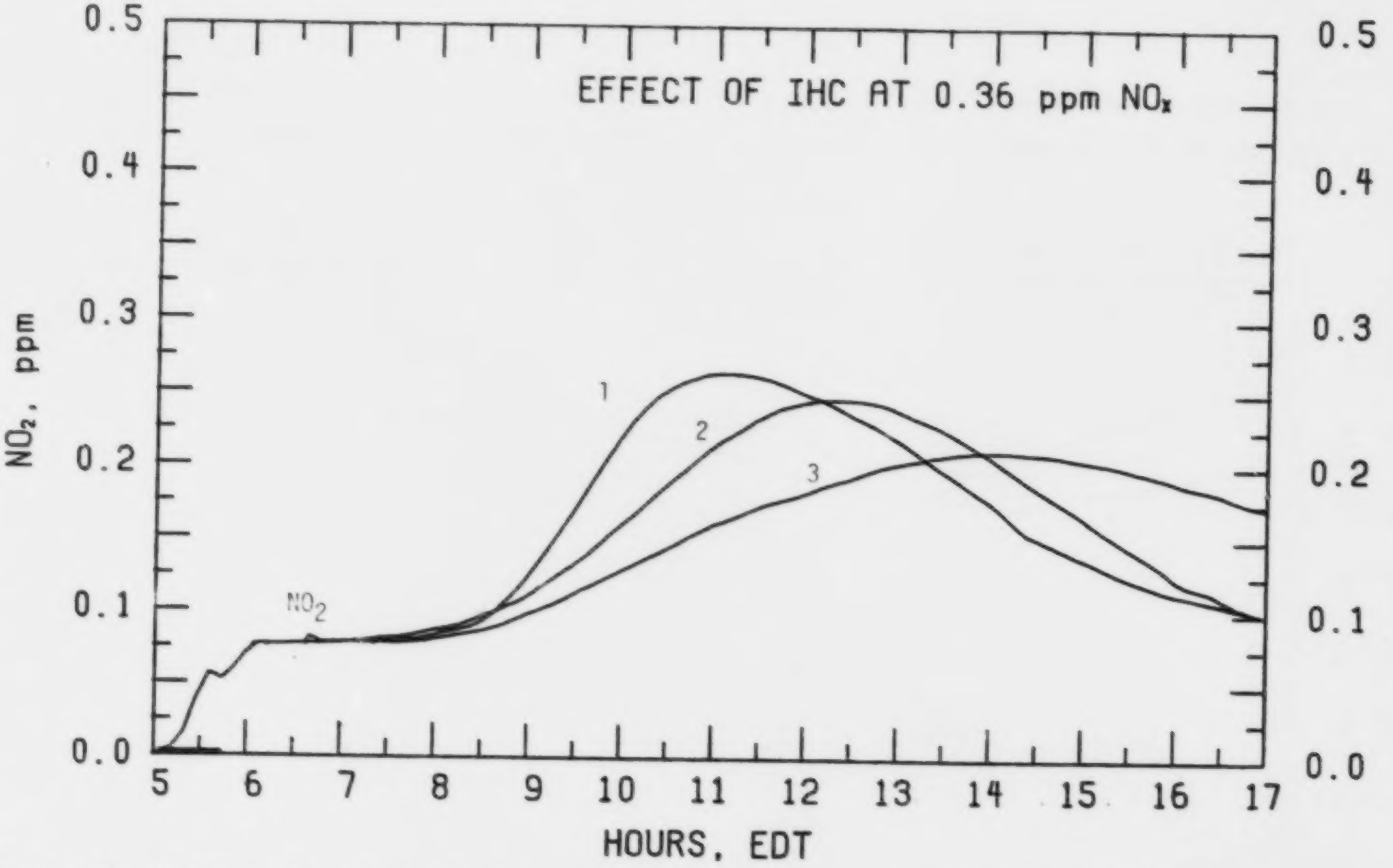

Figure 64. Nitrogen dioxide profiles at constant initial NO$_x$ of 0.36 ppm and initial NMHC of 3.2 ppmC (5/8/74, curve 1), 1.53 ppmC (7/15/74, curve 2) and 1.40 ppmC (6/11/74, curve 3) for urban hydrocarbon mix in UNC outdoor smog chamber.

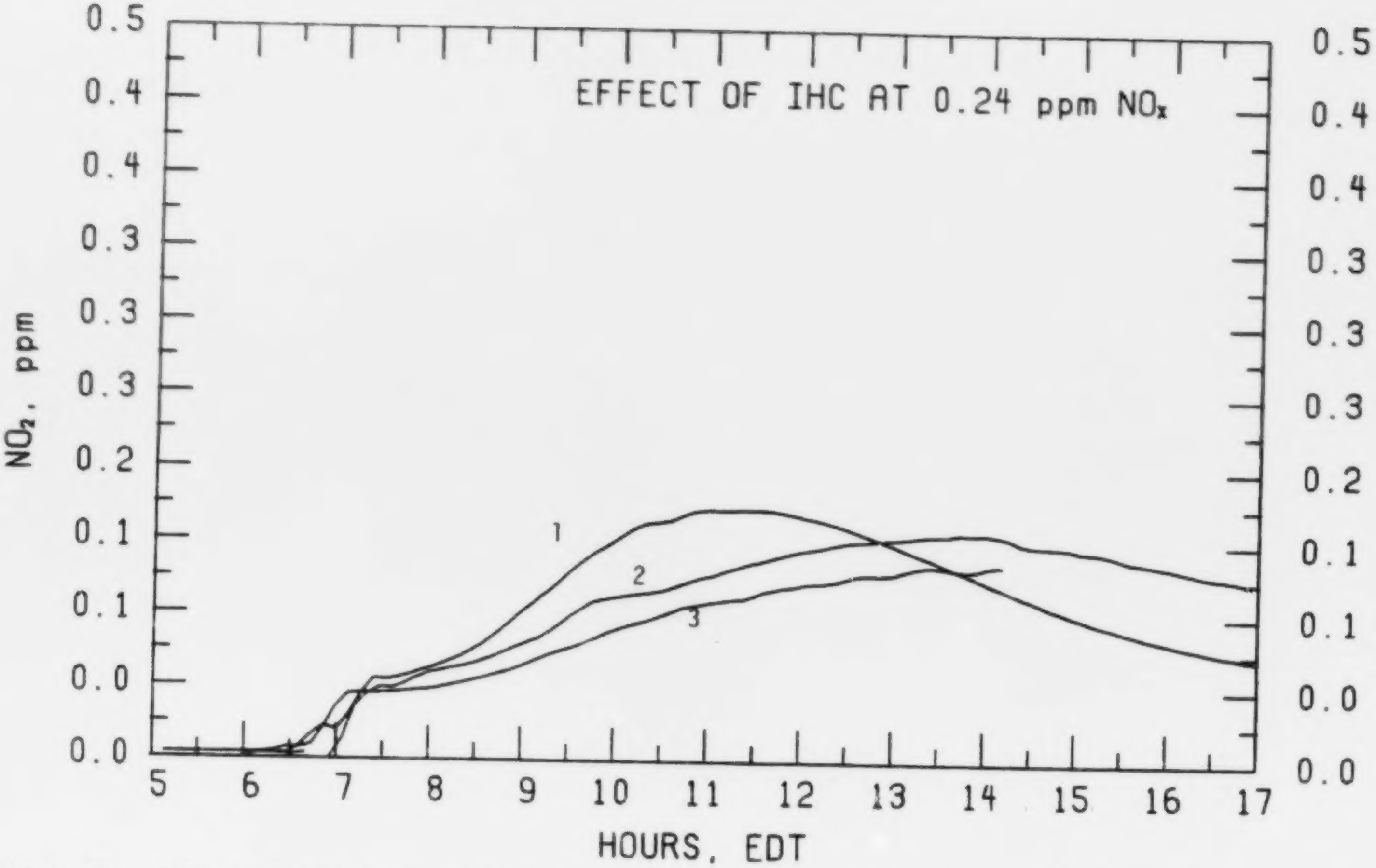

Figure 65. Nitrogen dioxide profiles at constant initial NO_x of 0.24 ppm and initial NMHC of 1.87 ppmC (6/22/74, curve 2), and 1.08 ppmC (6/25/74, curve 3) urban hydrocarbon mix in UNC outdoor smog chamber.

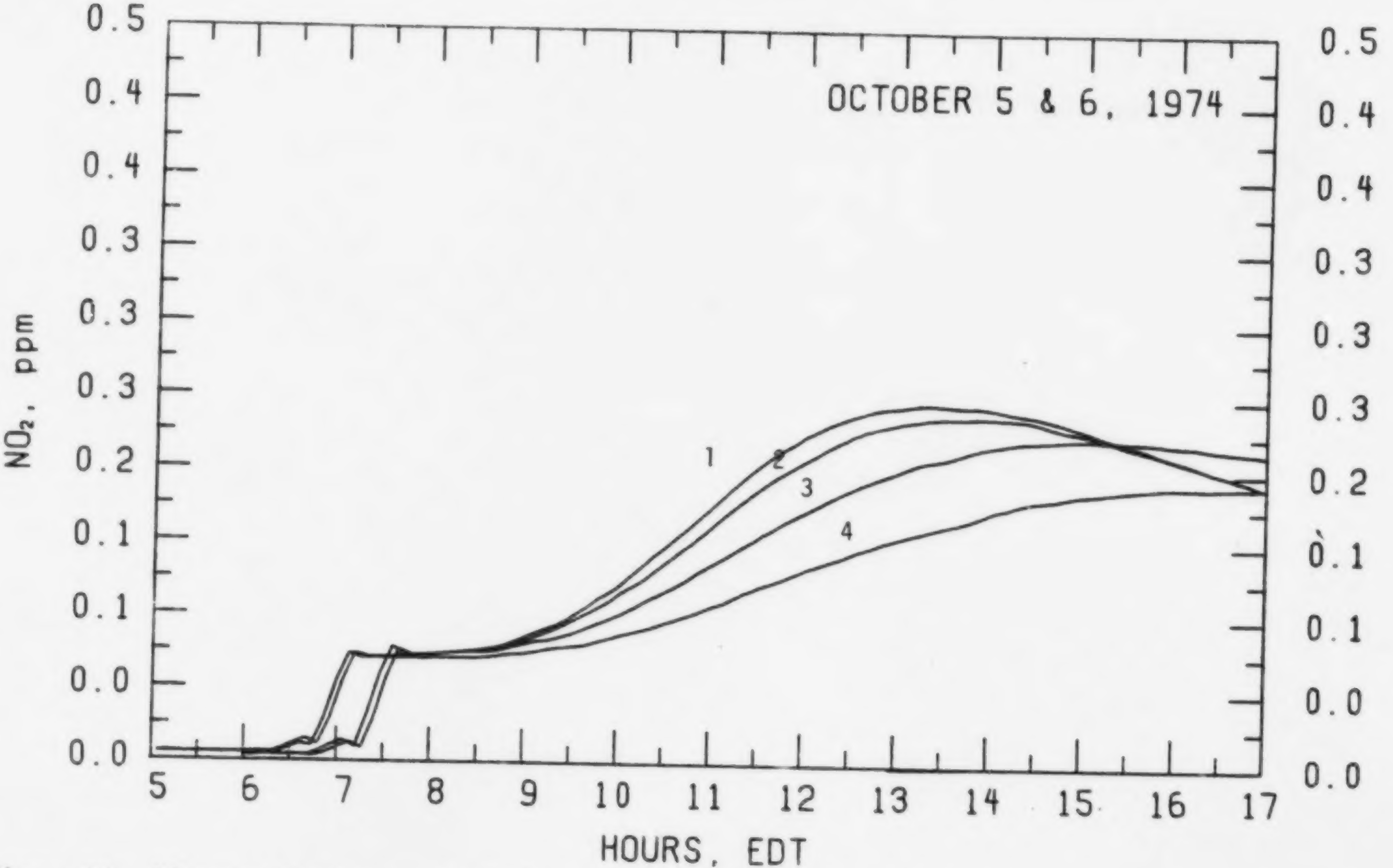

Figure 66. Nitrogen dioxide profiles for October 5 and 6,1974 at initial NO_x of 0.36 ppm and initial NMHC of 3.00 ppmC (10/5/74, curve 1), 2.48 ppmC (10/6/74, curve 2), 1.98 ppmC (10/5/74, curve 3), and 1.20 ppmC (10/6/74, curve 4) urban hydrocarbon mix in UNC outdoor smog chamber.

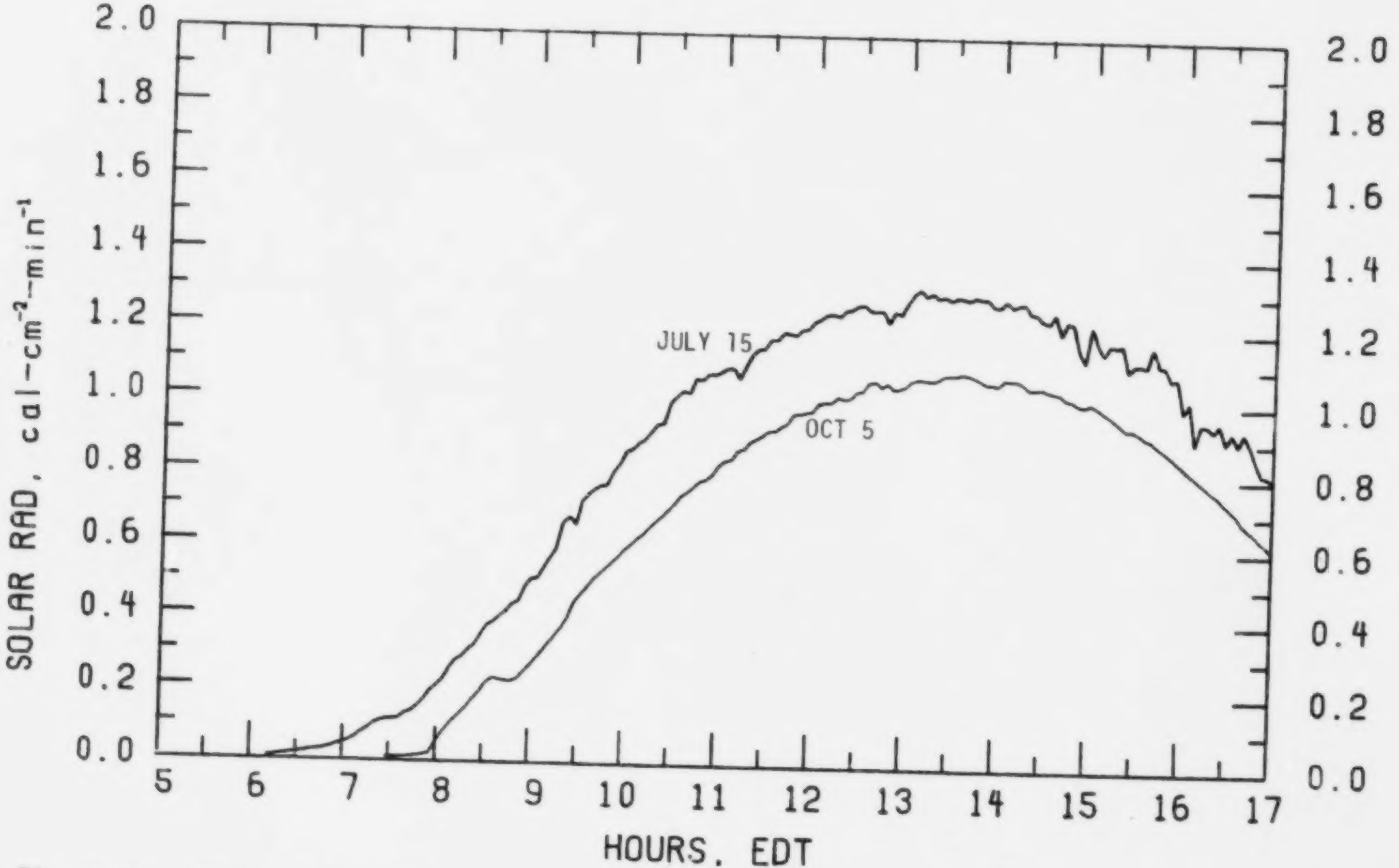

Figure 67. Total solar radiation for a clear summer and a clear fall day. Solar noon occurs at a nominal 1320 hours Eastern Daylight Time at the UNC outdoor smog chamber. (Longitude 79.0°W, latitude 35.72°N).

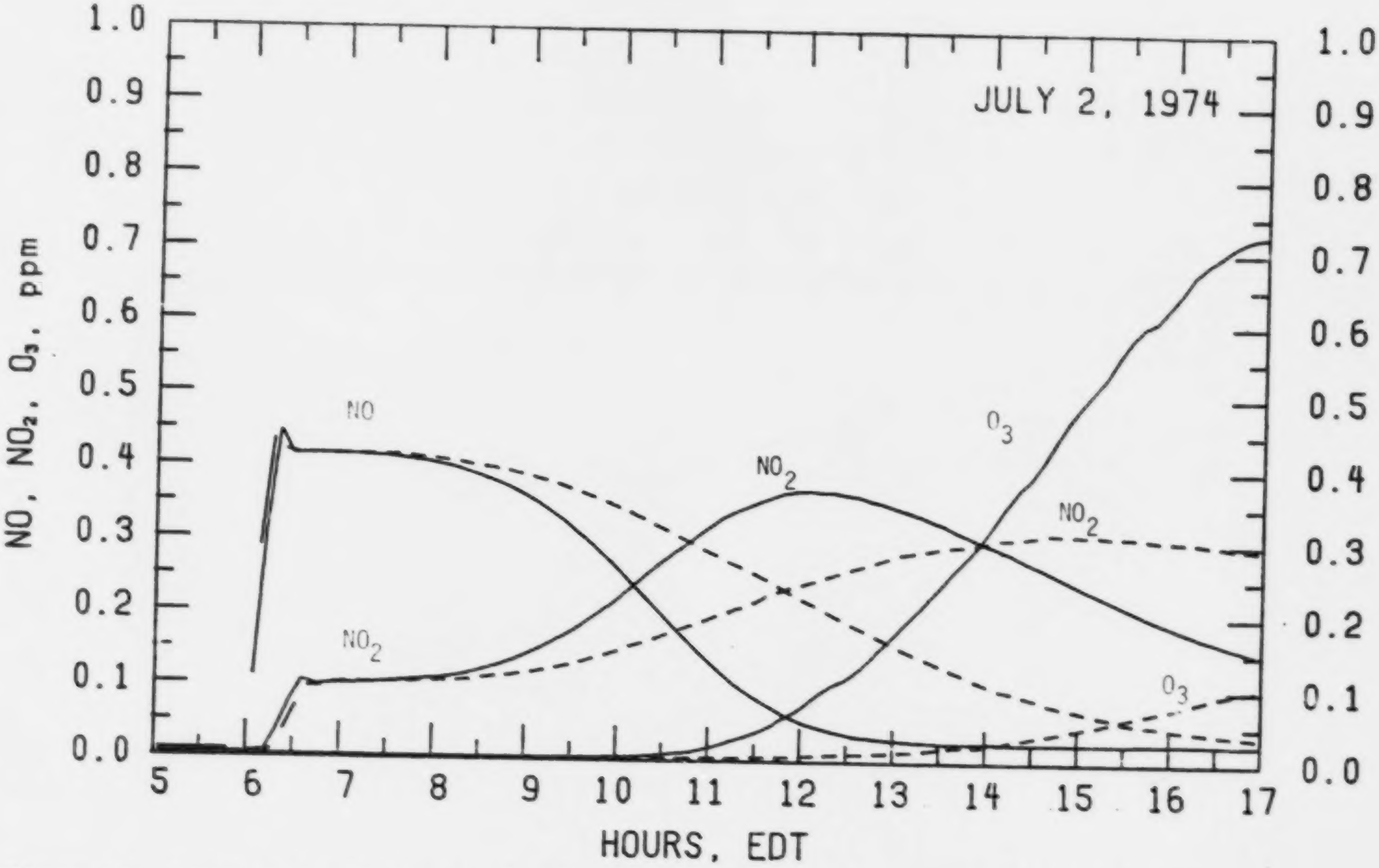

Figure 68. Profiles for dual run. Initial conditions: NO_x(—) 0.507, (---) 0.510 ppm; NO_2(—) 0.100, (---) 0.102 ppm; NMHC(—) 4.00, (---) 2.29 ppmC urban hydrocarbon mix in UNC outdoor smog chamber.

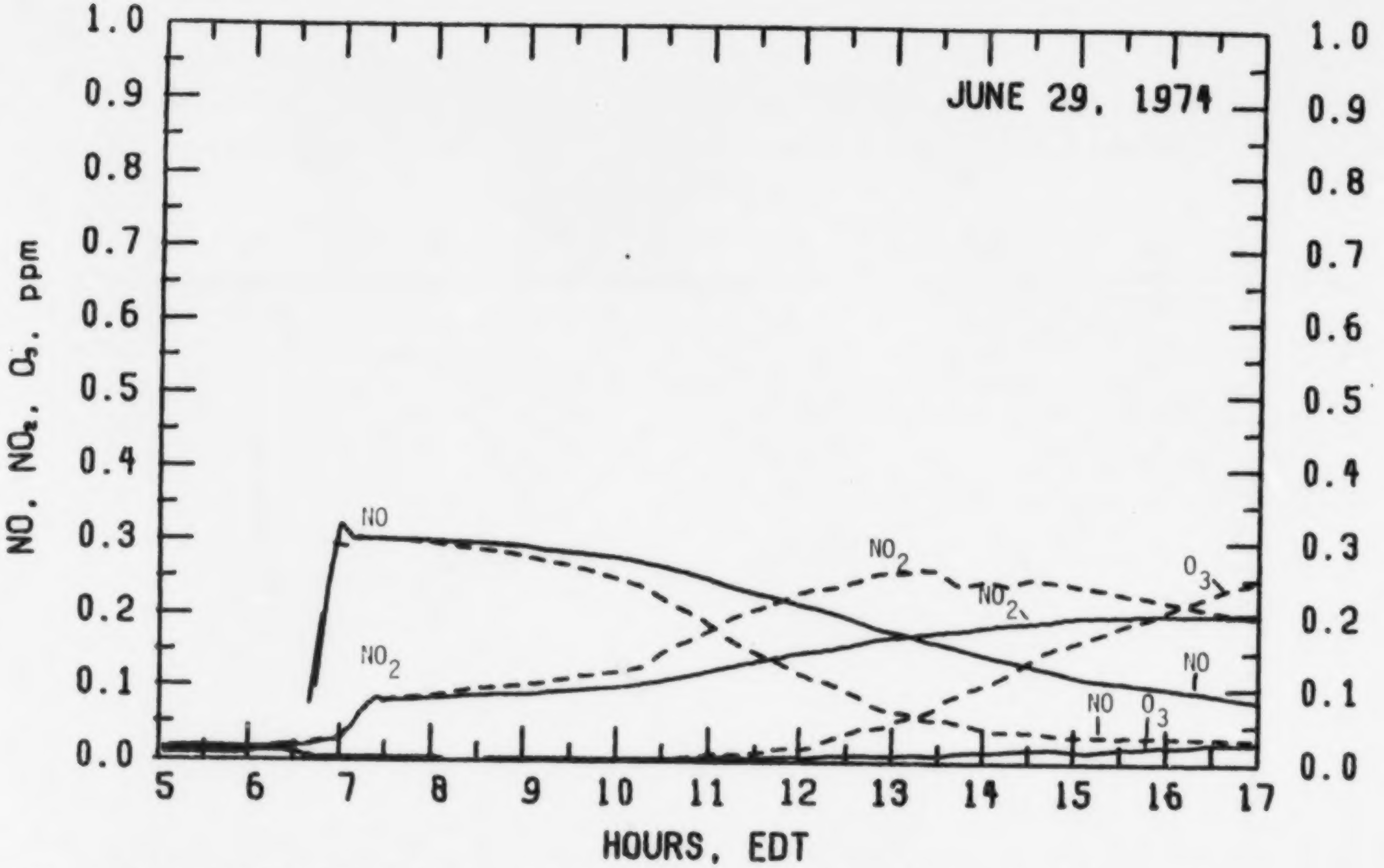

Figure 69. Profiles for dual run. Initial conditions: NO_x(—) 0.373, (---) 0.374 ppm; NO_2(—) 0.080, (---) 0.080 ppm; NMHC (—) 0.72, (---) 2.11 ppmC urban hydrocarbon mix in UNC outdoor smog chamber.

EFFECTS OF HYDROCARBON CONTROL ON NO_2 DOSAGE AND AVERAGE CONCENTRATION

Dosage may be treated as dosage or, in equivalent terms, as the average concentration that would be required to achieve the same dosage over the same time period. The latter is somewhat easier to deal with conceptually and is easier to relate to maximum values. The time period over which total dosage was computed in these outdoor runs was approximately 10-11 hours. Both measures, the total NO_2 dosage (DNO2DIFT) and the 10 hour average NO_2 concentration (NO2AVT), will be used, somewhat interchangably, in the following discussion.

If the mean NO2AVT ($\overline{\text{NO2AVT}}$) is computed for each INOX cluster in Table 12 without regard to the conditions under which the value occurred (i.e., ignoring the effects of IHC, SR, Temp, and PCTNO2; across rows in Table 12) and plotted as a function of the mean INOX in each class (Figure 70), the values of $\overline{\text{NO2AVT}}$, except for $\overline{\text{INOX}}$ = 0.7 and the 4 cases in which $\overline{\text{INOX}}$ = 0.433, can be fitted by

$$\overline{\text{NO2AVT}} = 0.4246\ \overline{\text{INOX}} + 0.0042 \qquad (2)$$

with an $r^2 = 0.9989$ for 114 cases. Equation 2 is similar to Equation 1 and would suggest that, in the mean, the 10 hour average NO_2 concentration was primarily dependent upon INOX. Since both the $\overline{\text{NO2M}}$ and $\overline{\text{NO2AVT}}$ can be reasonably fitted by equations in which the independent variable is INOX only, the ratio between average and maximum NO_2 can be found by a ratio of the slopes of Equations 1 and 2, neglecting the small difference in intercepts.

$$\frac{\text{NO2AVT}}{\text{NO2M}} = \frac{0.4246}{0.5788} = 0.7337 \qquad (3)$$

This value is to be compared with the mean value of the ratio of $\overline{\text{NO2AVT}}$ to $\overline{\text{NO2M}}$ for each INOX, IHC cluster which is 0.7252.

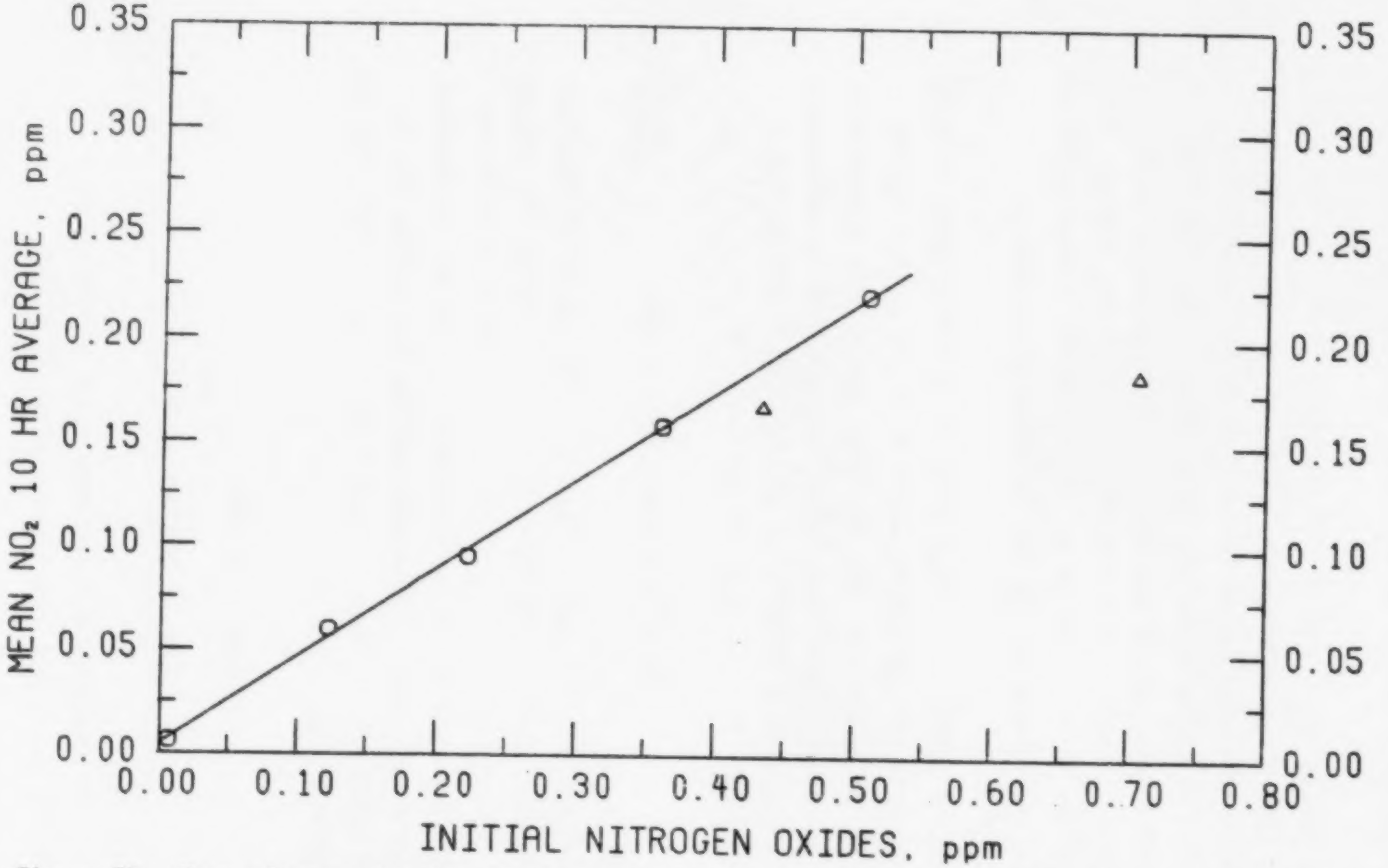

Figure 70. Mean nitrogen dioxide 10-hour average concentration as a function of mean initial oxides of nitrogen for urban hydrocarbon mix in UNC outdoor smog chamber. Equation of line is $NO_2AVE = NO_x + 0.004$. Points designated by had only 4 cases for both 0.44 and 0.71 ppm.

In Table 15, the mean NO2AVT and mean NO2AVT to NO2M ratio across all other conditions of SR, TEMP, PCTNO2 are broken down by INOX and IHC cluster mean values. There appears to be an upward trend, a maximum and then a decline in $\overline{\mathrm{NO2AVT}}$ with increasing $\overline{\mathrm{IHC}}$ in each $\overline{\mathrm{INOX}}$ cluster. The trend is relatively small and the data exhibits noise apparently due to solar radiation effects and the small number of runs in a given class. The IHC at which the maximum $\overline{\mathrm{NO2AVT}}$ occurs appears to be an increasing function of INOX. Overall, the NO2AVT constituted a relatively fixed percentage of the NO2M (72%), but it does appear that the ratio is somewhat smaller at lower INOX and higher IHC.

Examination of Figures 63, 64, 65 and 66 in terms of NO_2 dosage indicates that even though the total dosage (DNO2DIFT) might have been fairly close over a 10 hour period, the distribution of dosage was not. In Figure 64, curve 1 (IHC = 3.2 ppm) resulted in a higher dosage before solar noon and curve 3 (IHC = 1.40 ppmc) resulted in essentially the same dosage at the end of the run, but had a much smaller dosage before noon. The behavior of NO_2 concentration and dosage after 1700 hours will be discussed later.

The pairwise comparison of runs conducted on the same day with the same INOX, but different IHC is given in Table 16. There was a strong effect of reducing IHC on the total NO_2 dosage and 10 hr. average NO_2 concentration which parallels the reduction in NO2M. This is not unexpected given the near constant ratio of 10 hr. average NO_2 (NO2AVT) to NO2M discussed above. A 72% reduction in IHC from 2.58 ppmC to 0.70 ppmC resulted in a 35% reduction in both NO2M and DNO2DIFT and thus in NO2AVT by approximately the same amount. It should also be noted that reducing IHC generally leads to a higher final NO_2 concentration, if the NO_2 maximum actually occurs (i.e., $dNO_2/dt = 0$). This means that the evening and nighttime periods will begin with a sometimes much larger (up to 100% higher) NO_2 concentration in the case of hydrocarbon reduction versus no reduction. The implications of this condition will be discussed in detail in a subsequent section.

Table 15. MEAN NITROGEN DIOXIDE 10 HOUR AVERAGE CONCENTRATION AND MEAN AVERAGE TO MAXIMUM NITROGEN DIOXIDE RATIO BROKEN DOWN BY MEAN INITIAL OXIDES OF NITROGEN AND MEAN INITIAL HYDROCARBON FOR URBAN HYDROCARBON MIX IN UNC OUTDOOR SMOG CHAMBER[a]

	INOX = 0.222 ppm			INOX = 0.361 ppm			INOX = 0 510 ppm		
IHC ppmC	NO2AVT ppm	Ratio %	No. Cases	NO2AVT ppm	Ratio %	No. Cases	NO2AVT ppm	Ratio %	No. Cases
0.21	0.076	64.5	5	--	--	--	--	--	--
0.79	0.099	70.4	9	0.150	73.5	1	0.167	76.3	2
1.06	0.099	69.4	5	0.122	74.1	7	--	--	--
1.41	0.104	69.4	3	0.144	73.0	11	0.241	79.4	1
1.99	0.116	74.1	3	0.164	70.9	7	0.231	69.0	7
2.48	0.078	62.9	2	0.159	72.5	8	0.215	76.3	5
2.70	--	--	--	0.175	72.5	4	--	--	--
2.90	0.082	61.3	1	0.188	74.6	9	0.234	76.9	1
3.44	--	--	--	0.158	57.5	4	--	--	--
4.12	--	--	--	--	--	--	0.225	65.8	7
Across all IHC	0.095	68.5	28	0.158	71.8	51	0.221	71.0	23

[a]The entire population mean values are NO2AVT = 0.155 ppm, Ratio - 72.5%, and 102 cases.

Table 16. PAIRWISE COMPARISON OF EFFECTS OF REDUCING INITIAL HYDROCARBON CONCENTRATION ON NITROGEN DIOXIDE AVERAGE CONCENTRATION AND DOSAGE FOR SELECTED DUAL RUNS WITH URBAN HYDROCARBON MIX IN UNC OUTDOOR CHAMBER

Initial NOX, ppm	Run No.	Initial HC, ppmC			NO_2 Dosage, ppm min.			Average Daily NO_2, ppm		
		High Side	Low Side	% Reduction	High Side	Low Side	% Reduction	High Side	Low Side	% Reduction
0.261	741013	0.71	0.32	54.9	70.8	63.0	11.0	0.125	0.111	11.2
0.257	740622	1.87	0.85	54.5	61.5	63.9	-3.9	0.130	0.135	-3.8
0.358	740611	2.80	1.40	50.0	96.2	89.9	6.5	0.179	0.168	6.1
0.369	740612	2.90	1.30	55.2	100.9	96.2	4.7	0.168	0.160	4.8
0.373	740629	2.11	0.72	65.9	103.6	80.7	22.1	0.193	0.150	22.3
0.513	740616	2.58	0.70	72.9	155.2	100.7	35.1	0.262	0.170	35.1
0.520	740620	2.50	0.80	68.0	137.7	101.7	26.1	0.224	0.163	27.2
0.508	740702	4.00	2.29	42.8	137.8	126.8	8.0	0.246	0.230	6.5

FUNCTION RELATIONSHIPS

A search was made for meaningful functional relationships among nitrogen dioxide measures, initial conditions and meteorological factors by multivariate regression analysis. A combination of preselection (a variable is forced into equation on a particular step) and stepwise (program chooses the variable that will contribute the most to the r^2 from a list of variables available) techniques were used to build the equations. Testing was performed on various model equations by linear least squares curve fitting techniques. The variables that were treated as dependent were: NO2M, DNO2AVT, and NO2AVT. The independent variables were INOX, IHC, PCTNO2, all solar radiation averages (SVRAV1-T), various combinations of SR averages, and all temperatures and temperature averages.

Various sets and subsets of the entire data set (130 cases) were analyzed as well as the entire set. Given the information presented in Figures 59 and 60, and the fitting of Equation 1 to the mean conditions of only the 0.51, 0.36, 0.222, 0.122, and 0.007 ppm INOX classes it seemed reasonable to form a subset consisting only of data in these classes (the limited number of runs in the other classes probably do not form a representative data base for those conditions). In addition, dilution runs, runs in which the percentage INO2 fell outside of the range 18 to 24% and of course, runs with one or more of the desired independent variable missing were also excluded. This resulted in a data set with 110 runs.

Models consisting of simple linear combinations of initial conditions and meteorological variables gave relatively poor fits to data. Since most chemical systems exhibit multiplicative behavior (i.e., rate = k[NO] [HC]), models involving the logarithmic transformation of the chemical variables were explored.

In the simple case of the mean values of each INOX class (Figure 59), the logarithmic transformed variables gave an equation with a slightly greater r^2 than the simple linear Equation 1.

$$\overline{NO2M} = 0.5336\ (\overline{INOX})^{0.8864} \qquad r^2 = 0.9997 \qquad (4)$$

When the same functional form was fitted to the individual points of Figure 60, slightly different coefficients were found (Equation 5): a much lower r^2 indicated a large amount of scatter around the fitted line.

$$NO2M = 0.5631\ (INOX)^{0.9199} \qquad r^2 = 0.846 \qquad (5)$$

Equation 6 resulted from a linear least squares fit of the logarithmically transformed chemical variables and untransformed meteorological variables for 110 cases.

$$NO2M = 0.4927\ (INOX)^{0.844}\ (IHC)^{0.143}\ EXP\ (0.144\ SRAV3 - 0.270\ SRAV1)$$

$$r^2 = 0.9244 \qquad (6)$$

The magnitude of various components of Equation 6 are given in Table 17. As suggested by Equation 4 and 5, the NO2M is dependent primarily on INOX. The values of IHC ranged from 0.2 to 4.2 ppmC in these runs and, as indicated in Table 17-B, this range can introduce a ±20% variation in the NO2M predicted by Equation 6 at constant INOX and constant SRAV3/ SRAV1. At constant INOX and IHC, the typical variations in solar radiation can lead to a ±5% variation in predicted NO2M.

There was unavoidable confoundment between IHC and solar radiation and solar radiation averages, with higher IHC leading to faster reaction. Thus, events occur earlier in the solar day. Furthermore, the average values of solar radiation used in this study are computed between events in the chemical system (such as between maximum NO_2 rate and

Table 17. MAGNITUDES OF TERMS IN NITROGEN DIOXIDE MAXIMUM REGRESSION EQUATION

$$[NO_2]_{max} = 0.4927\ \underbrace{([NO_x]_o)^{0.844}}_{\text{Part A}^a}\ \underbrace{([HC]_o)^{0.143}}_{\text{Part B}^b}\ \underbrace{EXP(0.144\overline{SR}_3-0.270\overline{SR}_1)}_{\text{Part C}^c}$$

Table 17-A

$[NO_x]_o$ ppm	Part A ppm
0.007	0.006
0.122	0.0837
0.222	0.1383
0.361	0.2085
0.510	0.2791

Table 17-B

$[HC]_o$ ppmC	PART B
0.31	0.846
0.79	0.967
1.06	1.01
1.41	1.05
1.99	1.10
2.48	1.13
2.70	1.15
2.90	1.16
3.44	1.19
4.00	1.21

Table 17-C

$\overline{SR}_3/\overline{SR}_1$[d]	PART C
1.804	0.931[e]
1.8575	1.000
1.928	1.055[e]

[a] Part A expresses the dependence of $[NO_2]_{max}$ on $[NO_x]_o$ for $[HC]_o$ = 1.0 ppmC and a ratio of $\overline{SR}_3/\overline{SR}_1$ = 1.8575. Use $[NO_x]_o$ to look up Part A in Table 17-A

[b] Part B is the multiplier factor for $[HC]_o$ other than 1.0 ppmC. Use Table 17-B and $[HC]_o$ to find multiplier. $[NO_2]_{max}$ = (Part A) x (Part B) at $\overline{SR}_3/\overline{SR}_1$ = 1.8575

[c] Part C is the multiplier factor for solar radiation variation. Use ratio in Table 17-C to find multiplier factor.

[d] SR_1 is the average solar radiation from the hydrocarbon injection until the NO-NO_2 crossover. SR_3 is the average solar radiation from the occurrence of the NO_2 maximum formation rate to the occurrence of the NO_2 maximum concentration. Since the latter events usually occur close together, SR_3 is a good measure of solar radiation conditions near the peak

[e] The 0.931 value is typical of October solar radiation conditions. The 1.055 value is typical of June solar radiation conditions.

NO_2 maximum concentration) and not at fixed time intervals. The average solar radiation values, therefore, have a time confoundment that is related to the IHC value. Other methods of expressing solar radiation are under investigation, but no entirely suitable method has yet been found.

NIGHTTIME BEHAVIOR OF RESIDUAL NITROGEN DIOXIDE

Previous discussion has indicated that some runs with lower IHC have final NO_2 concentrations (FNO2), that is, NO_2 concentrations at 1700 hours EDT, that are higher than those with higher IHC (see Figures 68 and 69). Table 18 is a pairwise (side-to-side) comparison of FNO2 values for various INOX and IHC and is a companion table to Table 14 (the same dual runs were used). As indicated in Table 18, the FNO2 on the low IHC side was usually higher than the high IHC side and sometimes was slightly lower. In those cases where FNO2 was lower, the NO_2 did not reach a true peak, that is, there was incomplete conversion of NO to NO_2 by 1700 hours.

Daytime Conditions and Nighttime NO_2

In a few runs, the chamber was not exhausted after 1700 hours and the instruments continued to record data on strip chart recorders (the computer stopped at 1700 hours). Figure 71 shows the NO_x and O_3 profiles from the June 16, 1974 dual run in which NO_2 was recorded during the night. Ink problems with the O_3 strip chart prevented the recovery of O_3 data for the nighttime period. Figure 72 shows the solar radiation profile for this day, and although it was not a very clear day, there are periods of very high SR, approximately equivalent to ϕka for NO_2 of 0.57 min^1. At 1630 hours, there was a rapid decrease in SR due to a summer squall (intense, short rainstorm) which rapidly lowered temperatures and light.

The NO_2 behavior exhibited by the dual run of June 16, 1974 was not

Table 18. PAIRWISE COMPARISON OF EFFECTS OF REDUCING INITIAL HYDROCARBON CONCENTRATION ON FINAL NITROGEN DIOXIDE CONCENTRATION FOR SELECTED DUAL RUNS WITH URBAN HYDROCARBON MIX IN UNC OUTDOOR CHAMBER

Initial NOX ppm	Run No.	Initial HC, ppmC High Side	Low Side	% Reduction	Final No_2, ppm[a] High Side	Low Side	Increase %
0.261	741013	0.71	0.32	54.9	0.1583	0.1652	4.4
0.257	740622	1.87	0.85	54.5	0.0708	0.1237	74.7
0.358	740611	2.80	1.40	50.0	0.1169	0.1724	47.5
0.369	740612	2.90	1.30	55.2	0.1030	0.1906	85.0
0.373	740629	2.11	0.72	65.9	0.1980	0.2033	2.7
0.513	740616	2.58	0.70	72.9	0.2535	0.2213	-12.7
0.520	740620	2.50	0.80	68.0	0.2752	0.2152	-21.8
0.508	740702	4.00	2.29	42.8	0.1468	0.2935	100

[a] The remaining concentration at 1700 hours EDT.

unique. Another dual differential IHC run on June 12, 1974, Figure 73 showed the expected high FNO_2 in the lower IHC run. Unlike the low IHC run on June 16, however, the June 12 low IHC run exhibited a significant deterioration in NO_2 after 1700 hours. See Figure 74 for solar radiation for June 12.

Analysis of the two lower hydrocarbon runs for June 12 and 16 indicated that the major difference was the concentrations of O_3 and NO in the afternoon. The lower IHC side on June 16 produced only 0.02 ppm ozone and had elevated evening NO_2 concentrations while the lower IHC side on June 12 generated about 0.10 ppm of ozone and experienced a decline in NO_2 after 1700 hours.

Several other runs of this type were made and these followed the same trends as the June 12 and 16 runs. Data for these runs are given in Table 19. Two of the runs listed in Table 19 had very similar initial conditions (June 12 BLUE and September 20 BLUE, Figures 73 and 75) and yet one of these (June 12) had relatively low nighttime NO_2 while the other (September 20) had high evening NO_2. Examination of the solar radiation conditions for these days reveals that much more favorable reaction conditions were present on June 12. The total integrated solar radiation values were 466 and 364 $cal\text{-}cm^{-2}$ for June 12 and September 20.

It seems apparent that different combinations of meteorological and chemical conditions can result in high nighttime NO_2 in outdoor smog chambers. These conditions have in common low afternoon concentrations of ozone and fairly high afternoon NO_2 and NO. The contribution of nighttime NO_2 to the total NO_2 dosage can be very substantial in certain cases. In most of these experiments nighttime NO_2 constitutes from 25 to 35% of the total 22 hour NO_2 dosages. In the runs with high evening NO_2, the contribution of the nighttime NO_2 to the total 22 hour dosage was of the order of 60%. These days also had significantly higher overall NO_2 dosages.

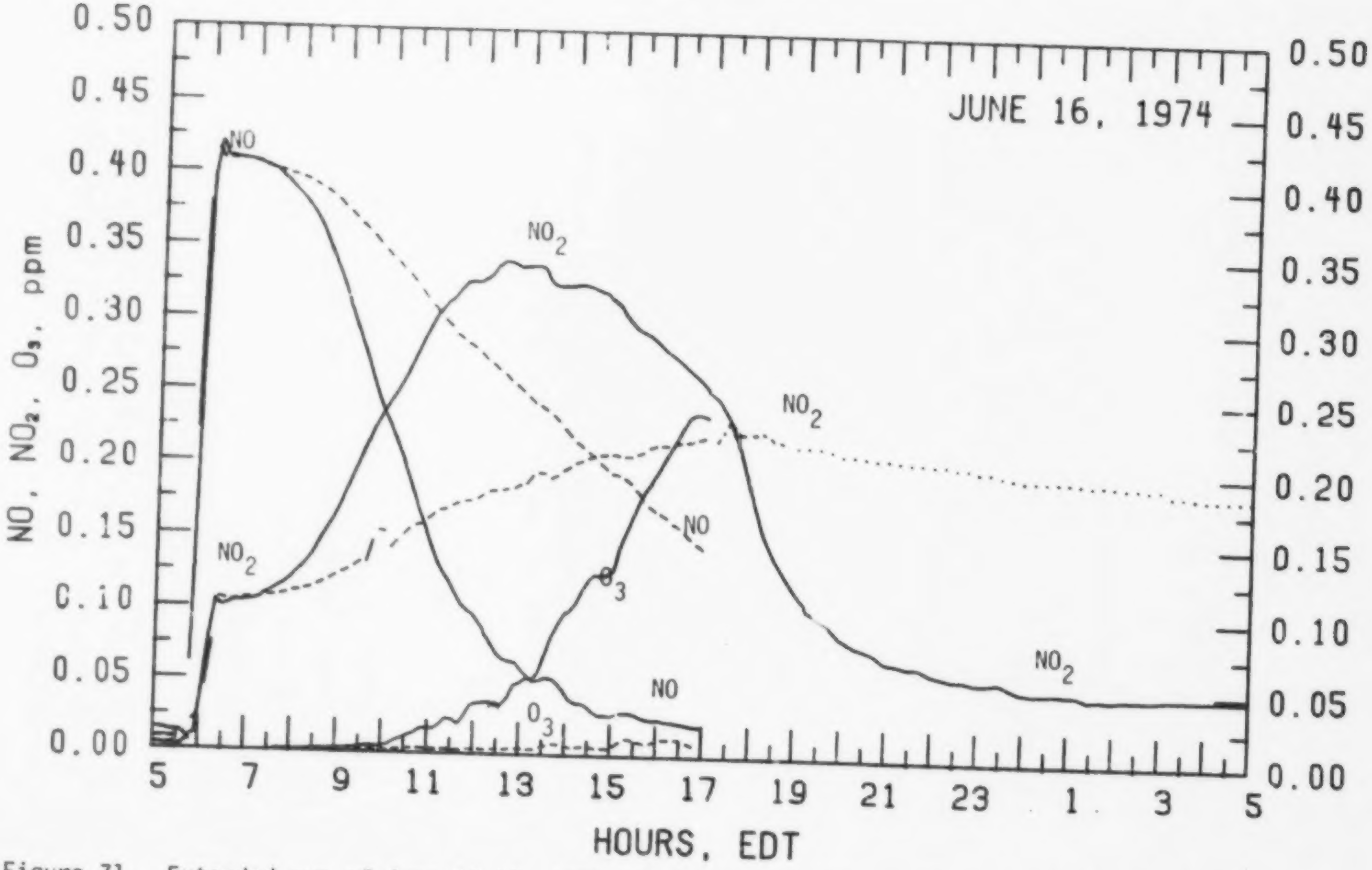

Figure 71. Extended run of June 16-17, 1974. Initial conditions: NO_x(—) 0.513, (---) 0.513 ppm; NO_2(—) 0.103, (---) 0.105 ppm; NMHC (—) 2.58, (---) 0.70 ppmC urban hydrocarbon mix in UNC outdoor smog chamber.

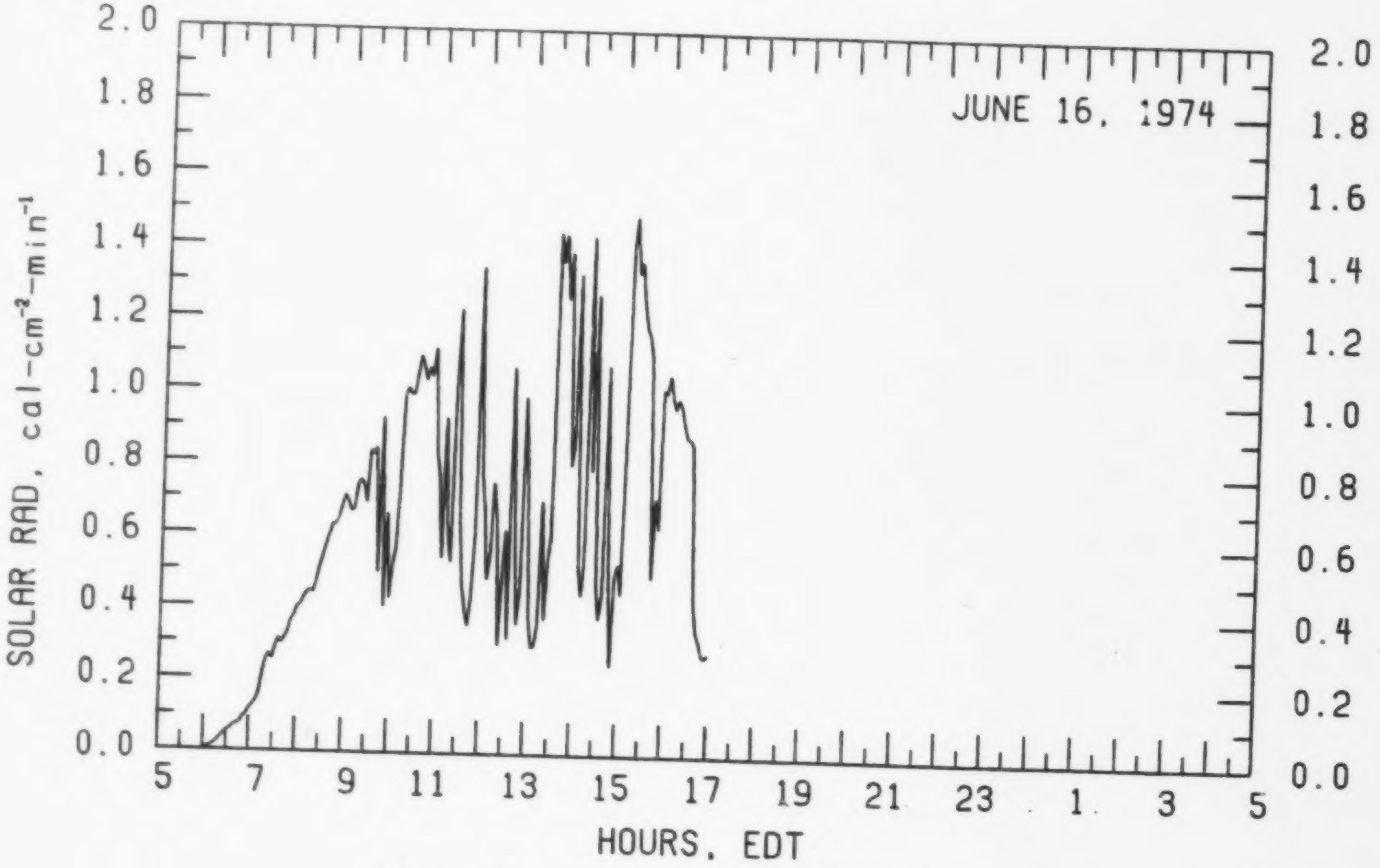

Figure 72. Total solar radiation for June 16, 1974.

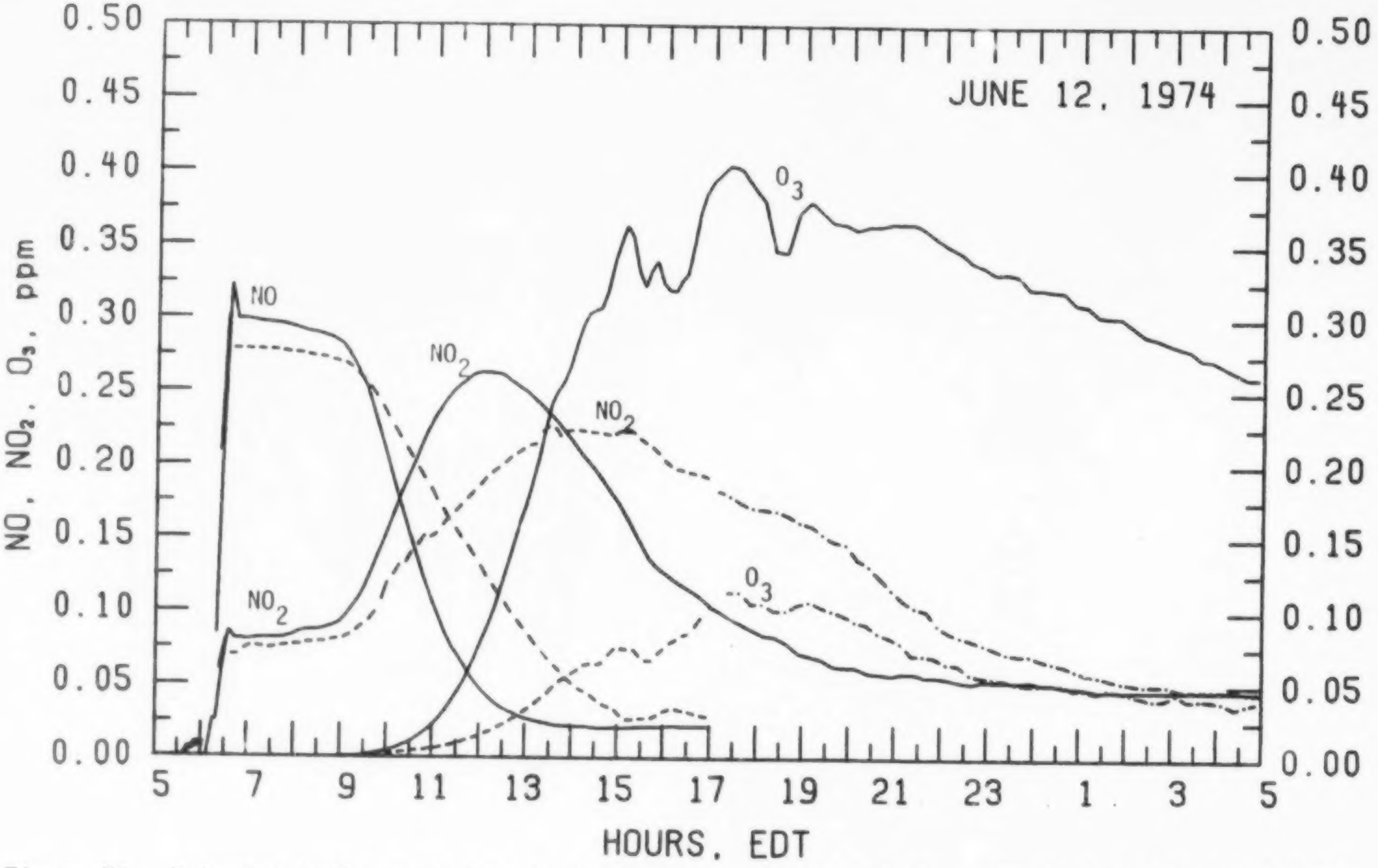

Figure 73. Extended dual run of June 12-13, 1974. Initial conditions: NO_x(—) 0.380, (---) 0.357 ppm; NO_2(—) 0.081, (---) 0.080 ppm; NMHC (—) 2.90, (---) 1.30 ppmC urban hydrocarbon mix in UNC outdoor smog chamber.

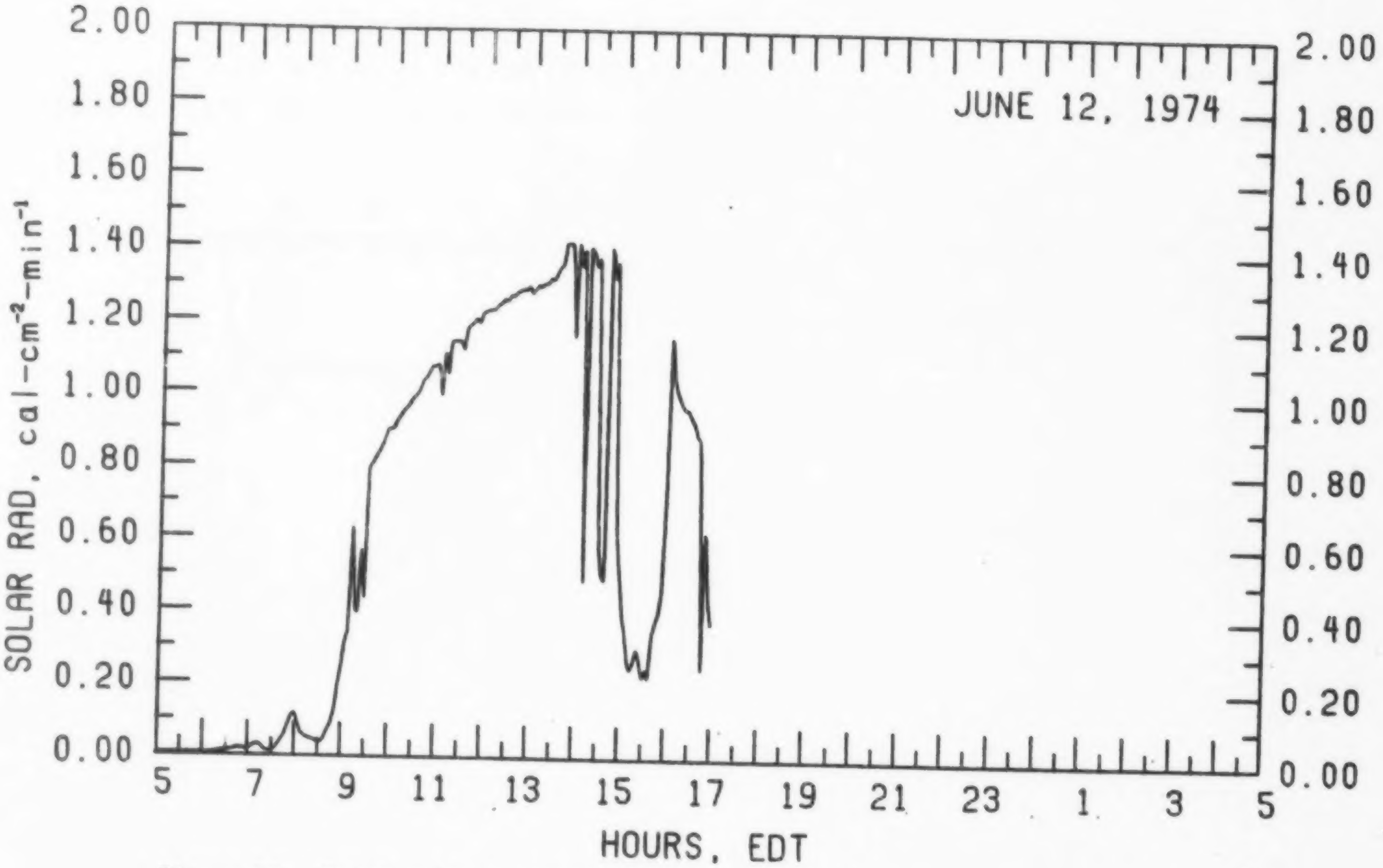

Figure 74. Total solar radiation for June 12, 1974.

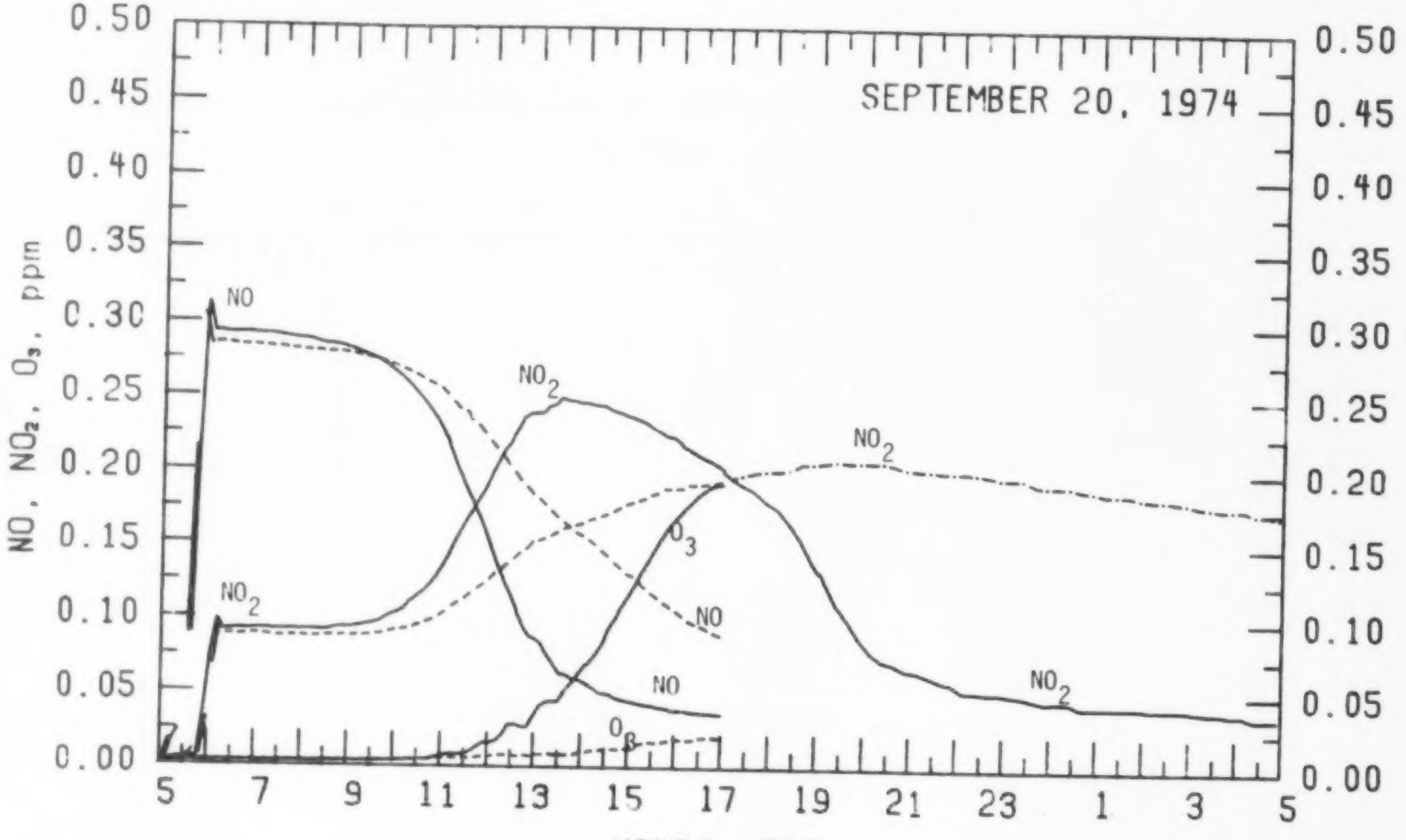

Figure 75. Extended dual run of September 20-21, 1974. Initial conditions: NO_x(—) 0.382, (---) 0.371 ppm; NO_2(—) 0.092, (---) 0.089 ppm; NMHC (—) 1.31, (---) 1.07 ppmC urban hydrocarbon mix in UNC outdoor smog chamber.

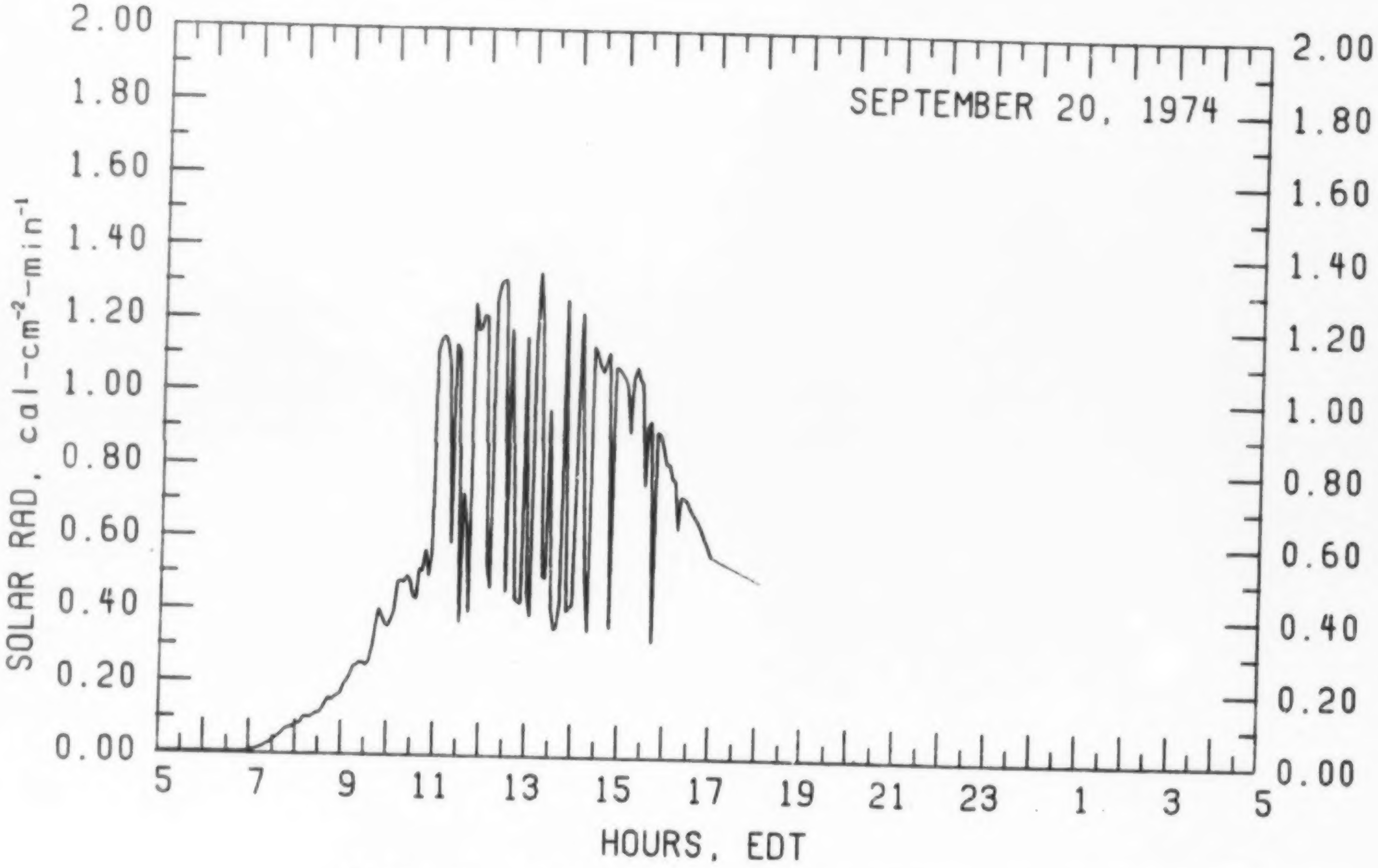

Figure 76. Total solar radiation for September 20, 1974.

Table 19. COMPARISON OF DAYTIME AND NIGHTTIME NITROGEN DIOXIDE DOSAGES FOR EXTENDED DUAL RUNS WITH URBAN HYDROCARBON MIX IN UNC SMOG CHAMBER

Date* & Side	Initial NO_x, ppm	Initial NMHC ppmC	Max NO_2 ppm	Ozone conc at 5 p.m. ppm	NO_2 dosage at 5 p.m., ppm-hr	NO_2 dosage at 5 a.m. next morning ppm-hr	Ratio of nighttime dosage to total dosage %
Jun 9, Red	0.386	3.5	0.270	0.72	1.734	2.443	29.0
Jun 9, Blue	0.386	3.5	0.271	0.72	1.726	2.406	28.3
Jun 12, Red	0.381	2.9	0.264	0.39	1.689	2.269	25.6
Sep 20, Red	0.382	2.6	0.250	0.22	1.759	2.611	32.6
Jun 12, Blue	0.357	1.3	0.235	0.40	1.613	2.556	36.9
Sep 20, Blue	0.371	1.3	0.194	0.02	1.322	3.571	63.0
Jun 16, Red	0.513	2.7	0.342	0.24	2.584	3.501	26.2
Jun 16, Blue	0.513	0.7	0.221	0.01	1.694	4.025	57.9

* all 1974 runs

NO_2 Removal Process

It seems reasonable that a partial explanation for the consumption or disappearance in nighttime NO_2 on June 12 (in the lower IHC side) could be the reaction between O_3 and NO_2.

In order to assess the importance of the O_3 and NO_2 reaction in a competitive situation, a photochemical model was run using the residual concentrations of all products from two variable sunlight simulations as starting conditions in two nighttime simulations. The two daylight simulations were designed to yield different concentrations of end products so as to demonstrate the variation typically occurring in the ambient atmosphere at the end of the day. In the first sunlight simulation the final (600 minutes) concentrations were NO_2 = 0.209 ppm and O_3 = 0.468 ppm with a minimal amount of NO, 0.006 ppm. In the second sunlight simulation the concentrations were NO_2 = 0.331 ppm, NO = 0.081 ppm and O_3= 0.059.

The only reactions having any significant effect in the second nighttime simulation were:

2: $NO + O_3 \rightarrow NO_2 + O_2$ $k = 24.0\ ppm^{-1}\text{-}min^{-1}$

31: $NO_2 + O_3 \rightarrow NO_3 + O_2$ $k = 0.046\ ppm^{-1}\text{-}min^{-1}$

For NO_2 and NO to have a similar demand for O_3, the NO_2/NO ratio must be greater than 500 : 1. The model NO_2/NO ratio was only 4.09, indicating that most of the available O_3 would react with NO to form NO_2. In this simulation, all of the O_3 and NO combined to form NO_2 by 6 minutes into the dark phase run with virtually no reaction between NO_2 and O_3.

The dark phase reaction using the first set of concentrations showed somewhat different results. Since very little NO was available, a substantial concentration of O_3 remained after all the NO had reacted. The remaining O_3 therefore, reacted with NO_2 as shown below.

$$\begin{array}{llll}
31: & NO_2 + O_3 \rightarrow NO_3 + O_2 & & K_{31} = .046\ ppm^{-1}\text{-}min^{-1} \\
 & NO_3 + NO_2 \rightleftarrows N_2O_5 & & K_f = 5600\ ppm^{-1}\text{-}min^{-1} \\
 & & & K_r = 17.1\ min^{-1} \\
 & N_2O_5 \xrightarrow{H_2O} 2HNO_3 & & K_{35} = .01\ min^{-1}
\end{array}$$

Within 100 minutes into the run 95% of the NO_2 disappeared to form NO_3, N_2O_5, and HNO_3. The remaining amount went to N_2O_5 (0.12%) and NO_3 (5.62%). During the entire 600 minute dark phase run, a total of 169 ppm N_2O_5 was formed. Most of this decomposed by the back reaction, but ample opportunity was available to form HNO_3.

Hydrocarbon Reduction and NO_2 Dosages

Hydrocarbon reduction had a tendency to lower, broaden and extend NO_2 peak concentrations. The June 12 run (Fig. 73) had NO_2 peak values above 0.24 ppm for 2 hours on the higher IHC side while no NO_2 concentrations on the lower IHC side exceeded this level. The lower IHC side had 8 hours in excess of 0.15 ppm compared to about 5 1/2 hours on the higher IHC side. The number of hours in these runs exceeding selected concentrations are given in Table 20. The September 20 BLUE run had high evening NO_2 and the highest overall dosage. Although there were not any NO_2 concentrations above 0.24 ppm in this run, there were almost twice the number of hours above 0.19 ppm and 0.15 ppm NO_2 than in the others.

Differences can also be observed between runs which had approximately the same overall NO_2 dosage. Due to day-to-day variations in solar radiation, however, it is useful to look at hydrocarbon reduction from

Table 20. NUMBER OF HOURS EXCEEDING VARIOUS NO_2 CONCENTRATIONS

Run	Initial NMHC	Initial NO_x, ppm	NO_2 max, ppm	Total 22 hr. NO_2 Dosage, ppm-hrs.	Hours for which NO_2 was above				
					0.22 ppm	0.19 ppm	0.17 ppm	0.15 ppm	0.13 ppm
June 9-Red	3.5	.387	0.270	2.432	2.87	3.86	4.52	5.07	5.83
June 9-Blue	3.5	.387	0.271	2.406	2.83	3.73	4.47	4.93	5.80
June 12-Red	2.9	.357	0.220	2.269	2.12	4.13	4.80	5.46	6.10
June 12-Blue	1.3	.381	0.264	2.556	--	4.76	6.47	8.02	9.37
Sept. 20-Red	2.6	.382	0.256	2.611	3.40	5.26	6.17	7.40	7.83
Sept. 20-Blue	1.3	.371	0.194	3.571	--	8.46	14.60	16.07	16.73

dual runs (i.e., performed on the same day) as opposed to a comparison across all days based on initial hydrocarbon values. The dual run on June 12 is suitable for such a comparison. Reduction of initial NMHC from 2.9 to 1.3 ppmC (under the same solar radiation and final NO_2 dosage) was associated with a 28% increase in concentrations above 0.17 ppm and a 50% increase in NO_2 above 0.13 ppm.

SECTION VIII

OTHER RESULTS AND OBSERVATIONS

EFFECT OF INITIAL PERCENTAGE NITROGEN DIOXIDE

The ratio of NO_2 to NO_x (PCTNO2) at the initiation of an experiment is an important parameter to investigate in terms of the effects of NMHC on NO to NO_2 conversion. Most experiments discussed in this report have a constant ratio of NO_2 to NO_x equal to 0.20 (that is, 20%). In a few selected runs however, the PCTNO2 was varied to determine its effect on NO to NO_2 conversion. In these differential runs, each side had the same IHC and INOX but had a different initial PCTNO2 (e.g., 20% and 40%). Experiments on May 8, 1974 (Figure 77) and July 15, 1974 (Figure 78) were differential PCTNO2 runs that occurred on clear days; runs on May 4, 1974 (Figure 79) and October 14, 1974 (Figure 80) occurred on days with erratic solar radiation.

Higher PCTNO2s in differential runs on clear days appear to provide more optimum conditions for O_3 formation; chemical events occurred earlier in the day and O_3 formation therefore occurred under higher light conditions in the higher PCTNO2 run, thus leading to higher ozone concentrations.

In differential PCTNO2 runs conducted on days that had choppy solar radiation conditions, the outcomes were very much a function of the detailed light-history (see discussion of Figure 62 in NO2M discussion). Figure 79 shows a PCTNO2 run in which the more typical O_3 behavior of May 8 and July 15 was reversed and the lower PCTNO2 run formed approximately 2.5 times more ozone than the higher PCTNO2 run.

In the October 14 experiment, the higher PCTNO2 run was slower than would be expected based on the clear day run results. Both October 14 and May 4 had erratic solar radiation conditions; the exact effect of

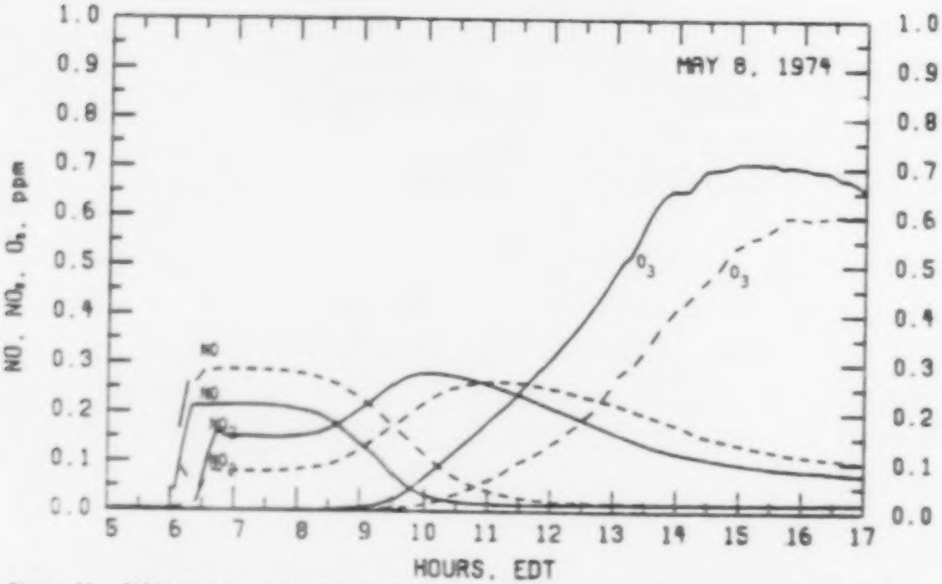

Figure 77. Differential percentage NO_2 run under clear sky. Initial conditions: NO_x(—) 0.364, (---) 0.366 ppm; NO_2(—) 0.151, (---) 0.079 ppm; NMHC(—) 3.40, (---) 3.20 ppmC urban hydrocarbon mix in UNC outdoor smog chamber.

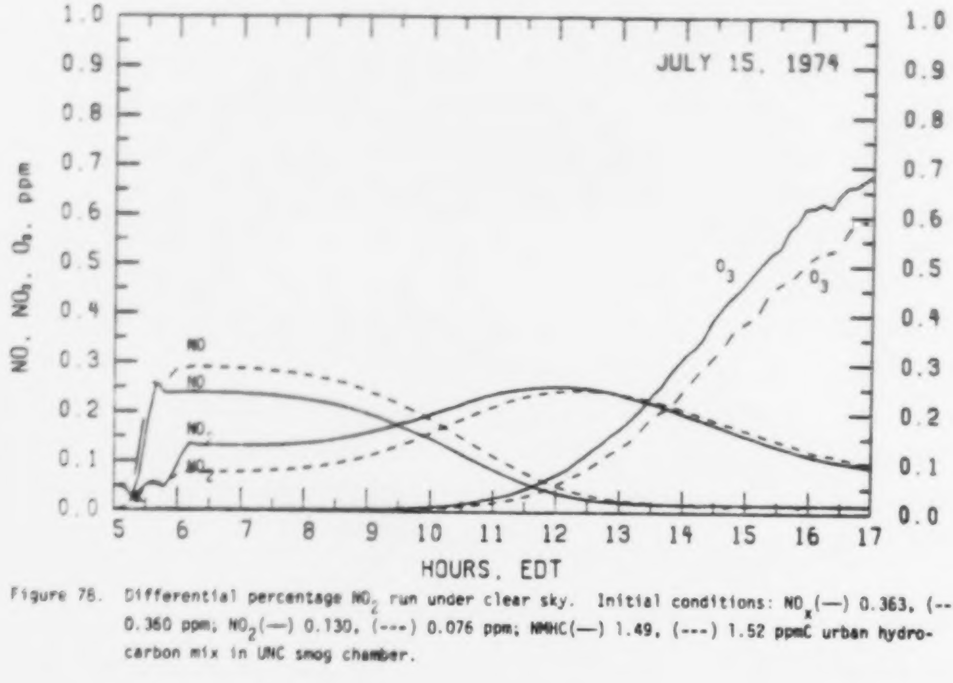

Figure 78. Differential percentage NO_2 run under clear sky. Initial conditions: NO_x(—) 0.363, (---) 0.360 ppm; NO_2(—) 0.130, (---) 0.076 ppm; NMHC(—) 1.49, (---) 1.52 ppmC urban hydrocarbon mix in UNC smog chamber.

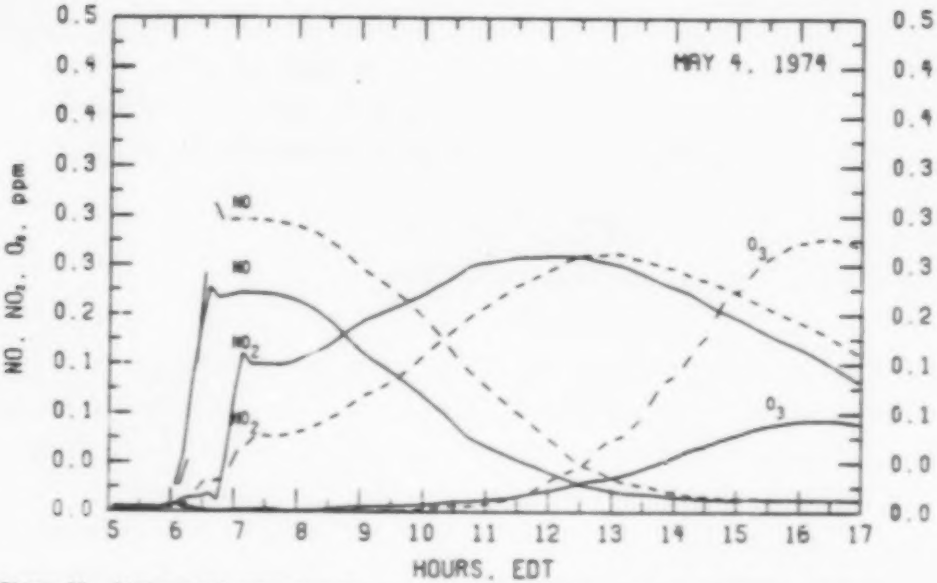

Figure 79. Differential percentage NO_2 run under erratic solar radiation conditions. Initial conditions: NO_x(—) 0.372, (---) 0.372 ppm; NO_2(—) 0.151, (---) 0.076 ppm; NMHC (—) 2.82, (---) 2.82 ppmC urban hydrocarbon mix in UNC outdoor smog chamber.

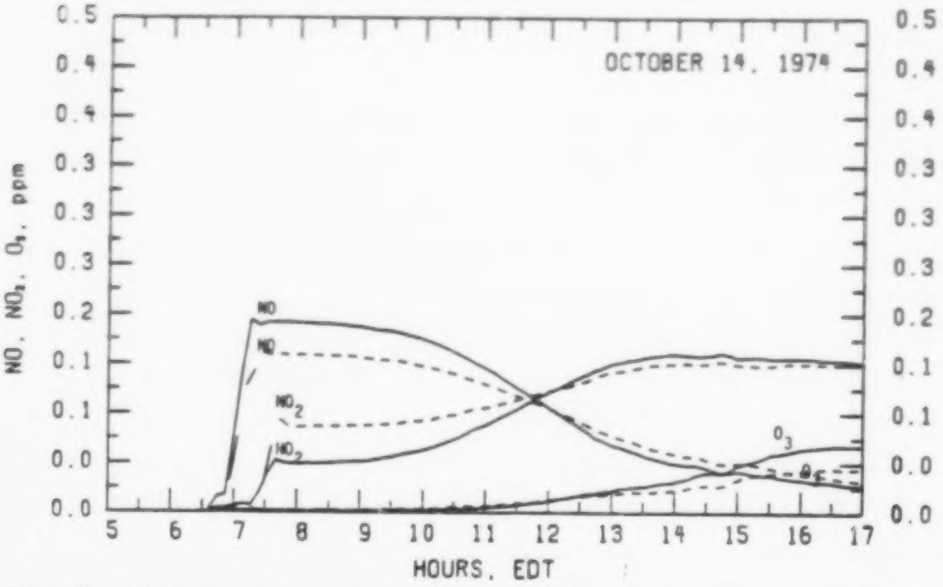

Figure 80. Differential percentage NO_2 run under erratic solar radiation conditions. Initial conditions: NO_x(—) 0.241, (---) 0.244 ppm; NO_2(—) 0.049, (---) 0.086 ppm; NMHC(—) 1.05, (---) 0.92 ppmC urban hydrocarbon mix in UNC outdoor smog chamber.

these conditions appears to be a function of when in the chemical system the light intensity changes and the direction in which it changes. Additional investigation of PCTNO2 will further clarify its participation in NO to NO_2 conversion under different physical conditions.

EFFECT OF DILUTION ON NO_2 AND OZONE FORMATION

Selected experiments were conducted to investigate the effect of dilution on NO to NO_2 conversion and ozone formation. These experiments were designed such that the same initial concentrations of nonmethane hydrocarbons (NMHC) and oxides of nitrogen (NO_x) were introduced into both sides of the outdoor chamber. One side remained sealed off from the ambient atmosphere while the other side was slowly diluted with background air starting in the morning. Two different dilution vs static smog runs will be discussed: a) using propylene as the hydrocarbon which was relatively fast, and b) another system which used the urban hydrocarbon mix.

In the propylene experiments, both chamber sides had identical reactant profiles until 0705, when dilution began in the BLUE side. Propylene NO_2 and NO were then slowly removed from the BLUE chamber by the dilution system. At the same time however, NO_2 was being generated at a faster rate than it was being removed by dilution, and actually appeared almost as fast as NO_2 in the RED (undiluted) chamber. This created a situation in which the ratio of NO_2/NO was higher in the BLUE chamber than the RED. If one assumes that pseudo photostationary equilibrium can be used to approximate the instantaneous O_3 concentration (Equation 1) then the ratio of NO_2/NO governs O_3 concentration at a given light intensity.

$$\frac{[NO_2]}{[NO]} = \frac{k_3}{k_1}[O_3] \qquad (7)$$

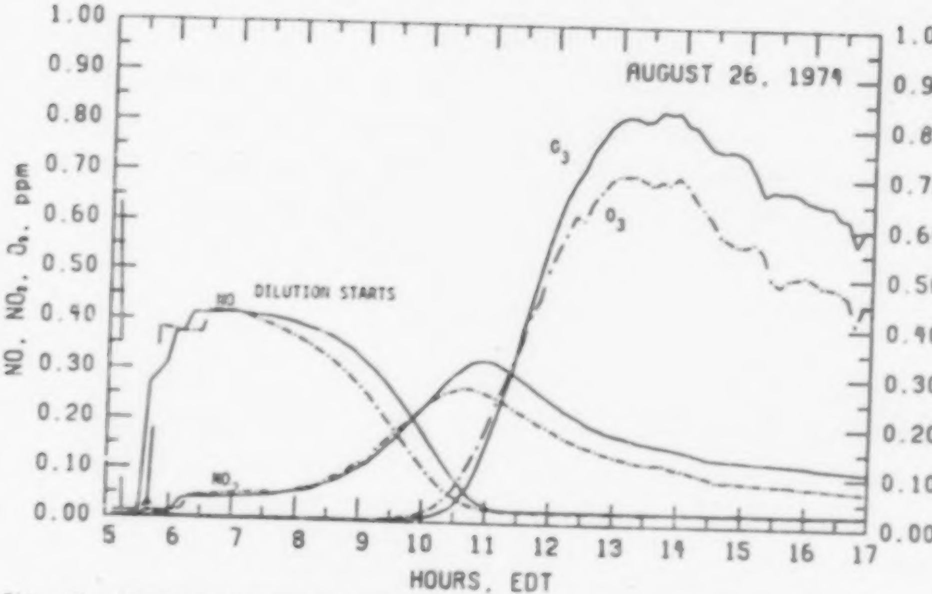

Figure 81. Example of dilution in a reactive system. Initial conditions: NO_x(—) 0.450, (---) 0.460 ppm; NO_2(—) 0.043, (---) 0.050 ppm; NMHC(--) 2.76, (---) 2.63 ppmC propylene in UNC outdoor smog chamber.

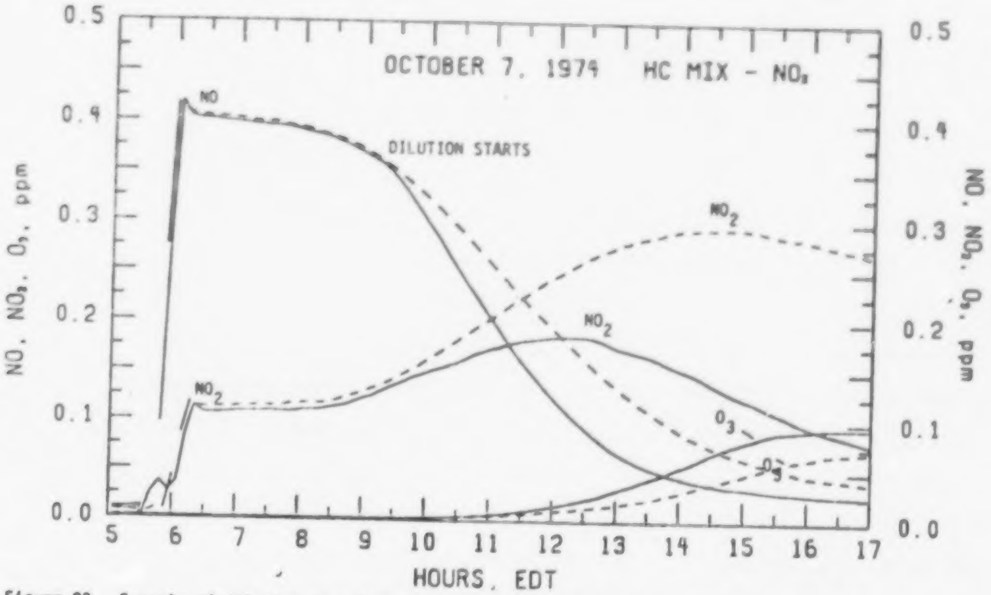

Figure 82. Example of dilution in a less reactive system. Initial conditions: NO_x(—) 0.504, (---) 0.512 ppm; NO_2(—) 0.106, (---) 0.111 ppm; NMHC(—) 2.39, (---) 2.43 ppmC urban hydrocarbon mix in UNC outdoor smog chamber.

Where k_1 is the photolysis rate constant for NO_2 and k_3 is the rate constant for the reaction of NO and O_3.

In the reactive system (Figure 81), ozone was initially generated more quickly in the diluted side. However, NO_x was being removed by dilution and the potential NO_2 peak was therefore greater in the undiluted side during a period of the day when the solar intensity was greatest (i.e., greater value for k_1) and was accompanied by a faster ozone generation rate and higher ozone concentrations.

Analysis of the less reactive smog system can be made in a similar manner. Both sides initially contained 2.4 ppmC of urban hydrocarbon mix and 0.5 ppm NO_x (20% NO_2). Dilution began in the RED side about 0900 hours (Figure 82) and soon after, this side was generating ozone faster than the static side. The major difference between this less reactive system and the reactive propylene system was, for the less reactive system, a higher ratio of NO_2/NO was not reached in the undiluted side until the sun was beginning to go down. The net effect was lower and lower values of k_1 during the greatest period of potential ozone generation for the undiluted side.

In summary, the effect of different dilution rates and time at which dilution begins on O_3 cannot be presently quantified. From the two runs discussed however, extrapolation to the general case may be possible. Reactive systems, which would normally achieve maximum oxidant values during the early afternoon, may initially go faster under dilution conditions but probably will not reach the oxidant levels generated by static systems. By contrast, less reactive systems under certain dilution conditions may actually generate more oxidant. In the experiment considered (Figure 82), the diluted side actually exceeded the National Ambient Air Quality Standard for oxidant while the undiluted side did not. Greater hydrocarbon reduction compared to NO_x reduction will have the tendency to shift the urban atmosphere to one containing less reactive mixtures. Dilution in smog chamber experiments with these less reactive mixtures may prove to be important in assessing the worst case "condition".

SECOND DAY IRRADIATION

The dual run of June 13, 1974, discussed previously under nighttime behavior of NO_2, actually was a 36 hour run which included two daylight periods. The results on the second day were not expected. The 36-hour profiles for NO_2 and O_3 are given in Figure 83. The NO profiles are also given, but only for the first 12 hours and the last 7 hours. The values for NO_2 and O_3 between 1700 hours June 12 and 1000 hours June 13 were from digitized strip chart ; NO was not recorded on strip charts.

The experiment of June 12 represented a situation in which hydrocarbon control of ~50% occurred (from 2.9 ppmC to 1.3 ppmC) at constant INOX of 0.36 ppm. This hydrocarbon control affected both the NO_2 and O_3 maximum concentrations; approximately a 10% reduction in NO2M and 74% reduction in O3M resulted during the first daylight period. Because both sides had $O_3 > 0.1$ ppm , the NO_2 concentrations decayed throughout the nighttime period to values slightly below the NAAQS of 0.05 ppm.

During the second daylight period, the O_3 increased in both sides while the NO_2 remained relatively constant at 0.045 to 0.050 ppm. The peak O_3 values in this second daylight period, with no additional material added, were 0.40 and 0.37 ppm. Thus, the reduced NMHC run, which barely exceeded the NAAQS for O_3 in the first daylight period, exceeded the standard for ozone in the second daylight period by a factor of four. The higher NMHC run produced essentially the same O_3 in both daylight periods, also exceeding the NAAQS for ozone by a factor of four. This occurred even though the NO_2 concentration was below the NAAQS for NO_2 and the "reactive" hydrocarbon compounds had presumably been consumed the previous day.

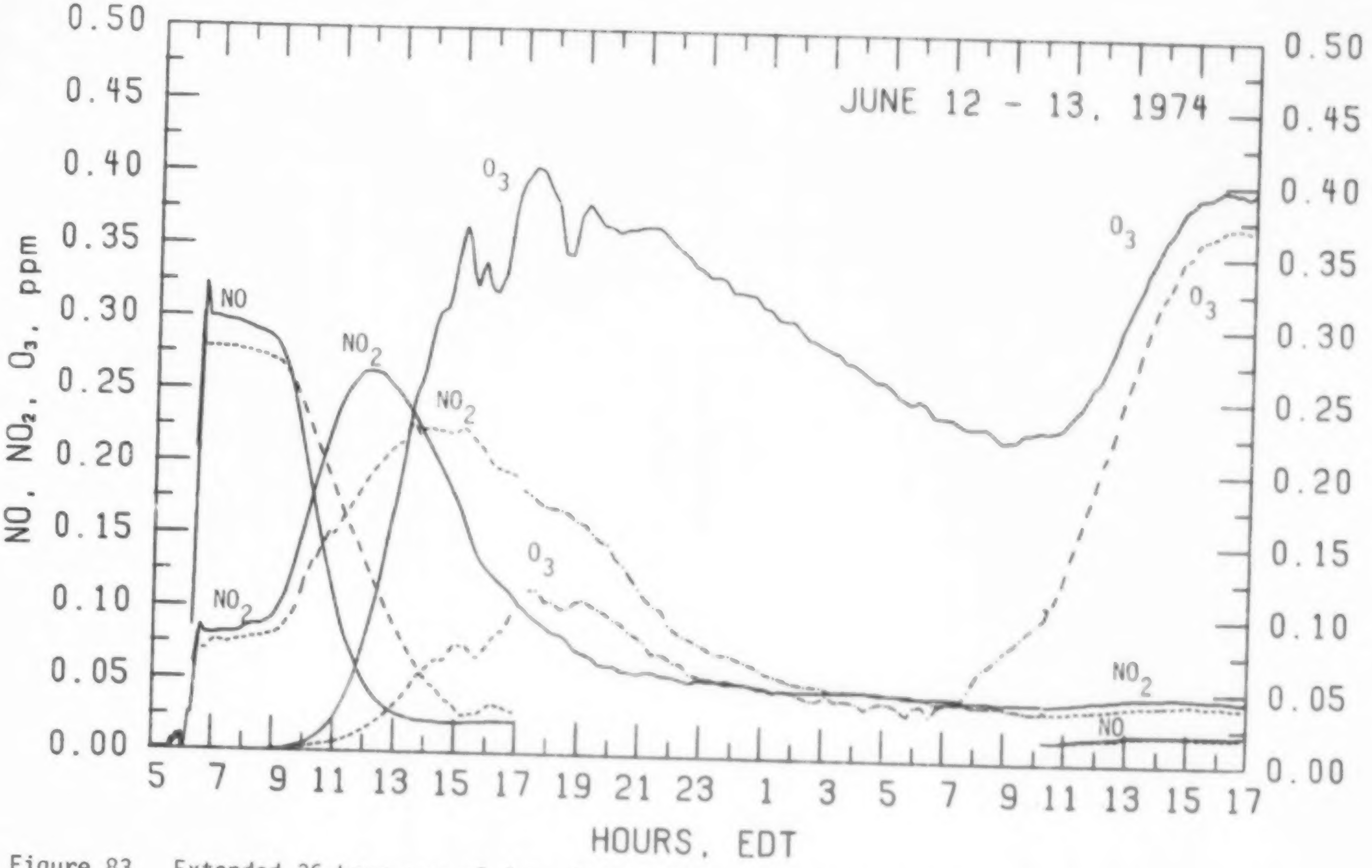

Figure 83. Extended 36-hour run of June 12-13, 1974. Initial conditions: NO_x(—) 0.380, (---) 0.357 ppm; NO_2(—) 0.081, (---) 0.080 ppm; NMHC (—) 2.90, (---) 1.30 ppmC urban hydrocarbon mix in UNC outdoor smog chamber.

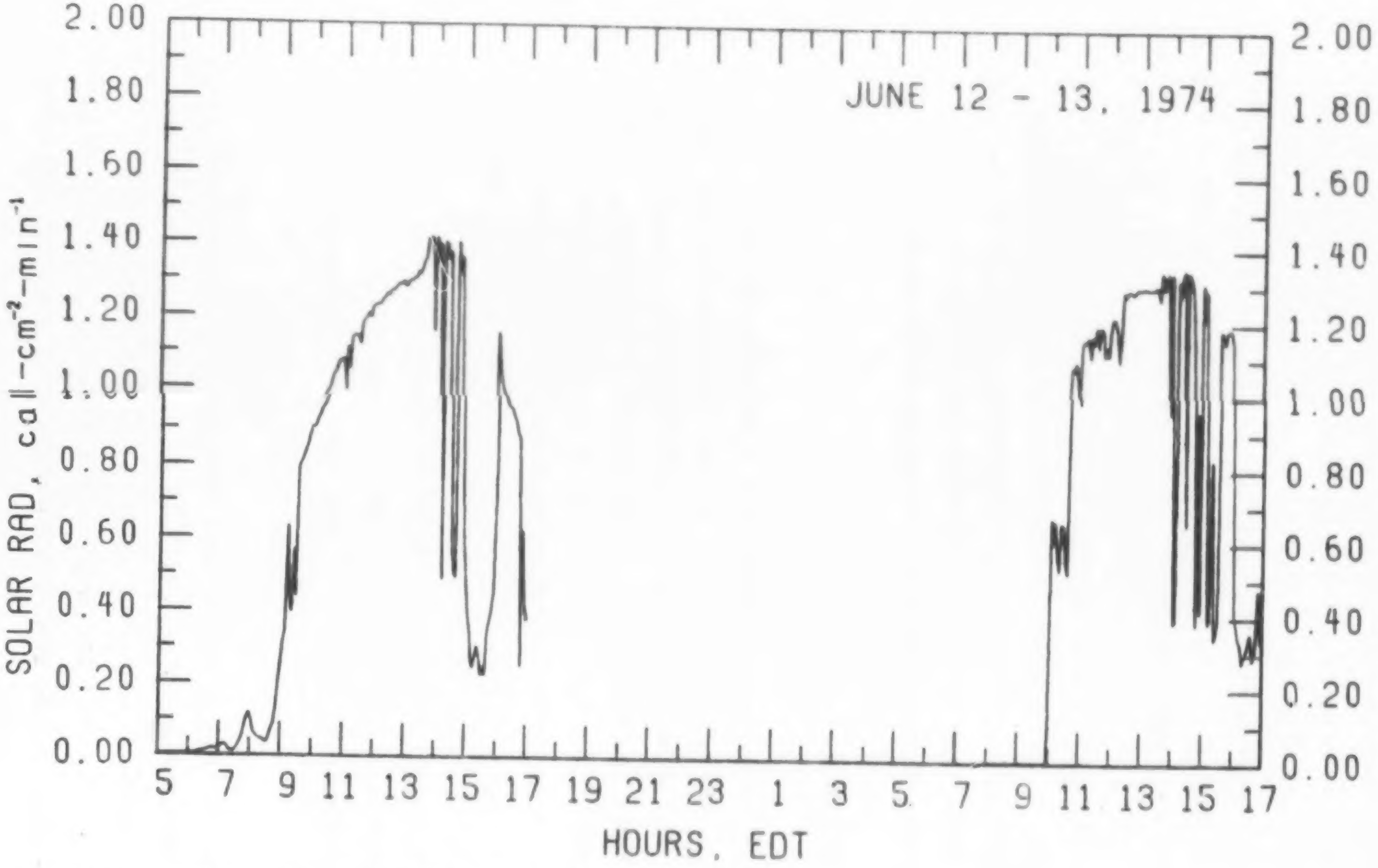

Figure 84. Total solar radiation for June 12-13, 1974.

This system might represent the behavior of a stagnant air mass which could give rise to the so called "Sunday effect" in which O_3 concentrations on Sundays are often as high as those on weekdays. It would be interesting to determine if fresh material were injected into the system that existed on the second day, would the O_3 concentration have been any higher than what occurred?

This system might also give insight into transport effects on O_3 concentrations. If one assumes that dilution would have only linear effects on the concentrations, the results shown in Figure 84 indicate that the air mass, even on the reduced NMHC side, might be capable of generating O_3 in excess of the NAAQS, downwind on the second day.

TEMPERATURE AND HUMIDITY EFFECTS

Table 21 contains average air temperature information at various events during a run. The mean values across the table provide some indication of the degree of temperature variation that occurs during a run in the outdoor chamber. The maximum and minimum values illustrate the wide seasonal range that occurs from early spring to late fall. There is some confoundment between solar radiation and temperature, in that, as solar radiation increases during a day, so does air temperature, and although solar radiation decreases fairly rapidly toward sunset, the back radiation of the earth tends to maintain the air temperature. The coolest part of a 24 hour day is usually just before sunrise and the initial temperatures in Table 21 are near the minimum daily air temperature.

Wide variations in initial temperature have no clearly discernible effects on the reaction profiles, provided the midday temperatures are above ∿ 70°F. Cases in which the temperature at the NO and NO_2 maximum rate (usually near the NO-NO_2 crossover and always before the NO2M) is less than 70°F do show a temperature effect on the rate of NO

Table 21. Air Temperature Statistics at Various Chemical Events in Outdoor Chamber

	Air Temperature, °F						
Statistic	Initial	$NO-NO_2$ Crossover	NO_2 max Rate	NO_2 maximum	O_3 maximum	Final	Daily Average
MEAN	55.9	76.4	74.8	79.3	80.4	79.4	74.3
Std.Dev.	15.0	8.9	8.9	9.1	8.4	9.2	9.7
Min	17.3	51.0	48.6	49.9	53.8	49.9	44.4
Max	81.5	92.6	93.3	91.9	92.7	92.5	88.8
# Cases	122	114	118	120	120	120	120

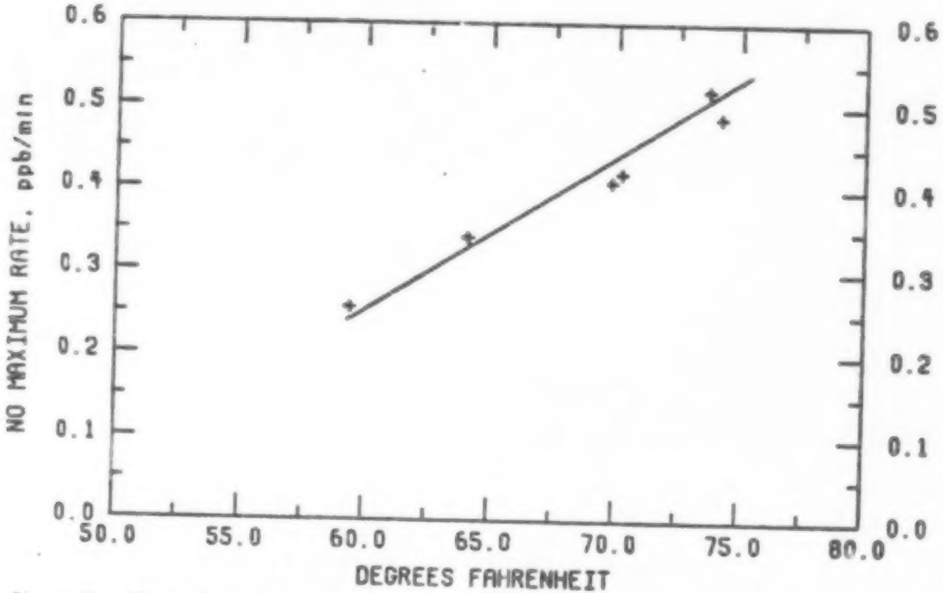

Figure 85. Effect of air temperature at maximum rate on maximum nitric oxide disappearance for clear days for November 1973 and initial conditions of 0.20 ppm NO_x, 0.04 ppm NO_2 and 0.80 ppmC urban hydrocarbon mix in UNC outdoor smog chamber.

disappearance and on the O_3 maximum. Figure 85 shows a 50% reduction in the rate of NO oxidation for a 14°F drop in temperature. These cases are from closely spaced replicate runs under clear skies in November, 1973. The coldest run is approaching the NO oxidation rate of hydrocarbon background runs (0.2-0.3 ppb/min). A 0.24 ppm NO_x/background hydrocarbon (<0.2 ppmc) run in June had a NO oxidation rate of 0.31 ppb/min and made 0.007 ppm O_3 at a temperature of 89.9°F. As the NO oxidation rate decreased in the runs shown in Figure 85, a reduction in the O_3 maximum occurred. The same chemical conditions in June produced O_3 maximum values of 0.17, 0.10, and 0.06 ppm O_3 at temperatures of 90, 84, and 89°F respectively. The runs in Figure 85 produced 0.06, 0.05, 0.03, 0.03, 0.014, and 0.012 ppm O_3 at O_3 maximum temperatures of 80, 80, 70, 69, 53.8, and 53.4°F respectively. These data suggest that there might be a lower temperature limit (∿55°F) at which the O_3 formation rate is so low as to preclude ambient concentrations from reaching the National Ambient Air Quality Standard of 0.08 ppm. This could be due to the very slow oxidation rate of NO at lower temperatures. These observations have been supported by an examination of field data collected by the Research Triangle Institute.

No effects of relative humidity have been observed in the range of 40% to ∿ 85% relative humidity. The data exhibits no perceptible trends with relative humidity including those runs that have essentially the same chemical, temperature and solar radiation conditions, but different relative humidity.

REFERENCES

1. "National Primary and Secondary Ambient Air Quality Standards," Environmental Protection Agency, Fed. Register, 36, No. 84, p. 8187 (April 30, 1971).

2. Shy, C., et al., "The Chattanooga School Study, Effects of Community Exposure to Nitrogen Dioxide," J. Air Pollution Contr. Assoc., 20, p. 539 (1970).

3. "Air Quality Criteria for Nitrogen Oxides," Air Pollution Control Office, Publication No. AP-84. Environmental Protection Agency, U. S. Government Printing Office, Washington D. C., 1971.

4. Korth, W., Rose, A., and Stahman R., "Effects of Hydrocarbon to Oxides of Nitrogen Ratios on Irradiation Auto Exhaust," J. Air Pollution Contr. Assoc., 14, p. 168 (1964).

5. Dimitriades, B., "Oxidant Control Strategies. Part I. An Urban Oxidant Control Strategy Derived from Existing Smog Chamber Data". Paper submitted for publication in Environ. Sci. and Technol.

6. "Proceedings of the Conference on Health Effects of Air Pollution," Committee on Public Works, United States Senate, U. S. Government Printing Office, Washington, D. C. Stock No. 5270-02105 (1973).

7. Altshuller, A. P., "Relationship of HC and NO_x Concentrations and Reactants Ratios to Federal Air Quality Standards for Photochemical Oxidant and Nitrogen Dioxide," Presented to Committee on Motor Vehicle Emissions, Panel 1, National Academy of Sciences. (1972).

8. Dupont Technical Information Bulletin T-5, "Optical Properties."

9. Dimitriades B., "Methodology in Air Pollution Studies Using Irradiation Chambers," J. Air Pollution Contr. Assoc., 17, pp. 460-6 (1967).

10. Dupont Technical Information Bulletin T-3D, "Chemical Properties."

11. Dupont Technical Information Bulletin T-6B, "Weatherability Performance."

12. Relme, K. A., Martin, B. F., and Hodgeson, J. A., "Tentative Method for the Calibration of Nitric Oxide, Nitrogen Dioxide and Ozone Analyzers by Gas Phase Titration." EPA, No. 2-73-246 (March, 1974).

13. Saltzman, B. F., Burg, W. R., and Ramswany, G., "Performance of Permeation Tubes as Standard Gas Sources," Environ. Sci. and Technol., 5, pp. 1121-1128 (1971).

14. Saltzman, B. F., "Determination of Nitrogen Dioxide and Nitric Oxide," In: Selected Methods for the Measurement of Air Pollutants, U. S. Dept. of H.E.W., Public Health Service Publication No. 999-AP-11 (1967).

15. Coordinating Research Council, CAPI-6 Committee, New York, CRC Report No. 398, "Individual Hydrocarbon Reactivity Measurements: State-of-the-Art" (June, 1966).

16. Dimitriades, B., "Effects of Hydrocarbon and Nitrogen Oxides on Photochemical Smog Formation," Environ. Sci. and Technol., 6, p. 253 (1972).

17. "A Critique of the 1975-1976 Federal Automobile Emissions Standards for Hydrocarbons and Oxides of Nitrogen," Report of Panel 1 on Standards to Committee on Motor Vehicle Emissions, National Academy of Sciences, Washington D. C., pp. 11-12 (1973).

18. Larsen, R. I., "A Mathematical Model for Relating Air Quality Measurements to Air Quality Standards," Preliminary Publication, Environmental Protection Agency, Office of Air Programs, No. AP-89, Research Triangle Park, N. C. (1971).

19. Kopczynski, S. L., Personal communication to Harvey Jeffries, National Environmental Research Center, Research Triangle Park, North Carolina, June, 1972.

20. Petterssen, S., Introduction to Meteorology. McGraw-Hill Book Company, New York, pp. 286-7 (1958).

21. "Local Climatological Data," U. S. Department of Commerce, National Climatic Center, Asheville, N. C. (1974).

22. Sellers, W. D., Physical Climatology, University of Chicago Press, Chicago, pp. 26-7 (1965).

23. Sickles, J. and Jeffries, H. E.,"Development and Operation of a Device for the Continuous Measurement of Photolysis Rate of Nitrogen Dioxide," Univ. of North Carolina, Dept. of Environ. Sci. and Eng. Publication No. 396. (1975).

24. Joshi, S. D., "Comparison of Several Techniques for Determining NO_x," Univ. of North Carolina, Dept. of Environ. Sci. and Eng., Master's Thesis (1974).

25. Leighton, P. A., *Photochemistry of Air Pollution*, Academic Press, New York (1961).

26. Dimitriades, B., *Proceedings of the Smog Chamber Conference*. (In press). U.S. Environmental Protection Agency, National Environmental Research, Research Triangle Park, N. C. (1975)

27. Winer, A. W., *et al*., "Response of Commercial Chemiluminescent NO-NO_2 Analyzers to Other Nitrogen-Containing Compounds," *Environ. Sci. and Technol.* *8*, pp. 1116-21 (1974).

28. Miller, D. F., "NO_2 Measurements in Smog Chambers," *Proceedings of the Smog Chamber Conference*, Research Triangle Park, N. C. (1975).

29. Miller, D. F., and Spicer, C., "A Continuous Analyzer for Determining Nitric Acid," Presented at Air Pollution Control Association Metting, Denver (1974).

30. Jeffries, H. E., "An Experimental Method for Measuring the Rate of synthesis, Destruction and Transport of Ozone in the Lower Atmosphere," Univ. of North Carolina, Ph.D. Thesis. Dept. of Environ. Sci. and Eng., Publication No. 285 (1971).

31. Bonamassa, F. and Wong-Woo, H., "Composition and Reactivity of Exhaust Hydrocarbons from 1966 California Cars," Presented at American Chemical Society Meeting, New York (1966).

32. Hampson, R. F., ed., "Chemical Kinetics Data Survey VI, Photochemical Data for Twelve Gas Phase Reactions of Interest for Atmospheric Chemistry," NBS Report, NBSIR 73-207 (1974).

33. Garvin, D., and Hampson, R. F., "Chemical Kinetics Data Survey VII. Tables of Rate and Photochemical Data for Modeling the Stratosphere (revised)," NBS Report, NBSIR 74-430 (1974).

34. Demerjian, K., Kerr, J. A., and Calvert, J., "Mechanism of Photochemical Smog Formation," In: Advances in Environmental Sciences and Technology, Vol. 4, Pitts, J. N. and Metcalf, R. L., ed., John Wiley and Sons, Inc. New York (1974).

35. Hecht, T. A., Seinfeld, J. H., and Dodge, M. C., "Further Development of Generalized Kinetic Mechanism for Photochemical Smog," Environ. Sci. and Technol., 8, pp. 327-39 (1974).

36. Jaffee, R. J., and Smith, F. C., "Factors Affecting Reactions in Smog Chambers," Presented at 67th Air Pollution Control Association Meeting, Denver (1974).

37. Hecht, T. A., Liu, M. K., and Whitney, D. C., "Mathematical Simulation of Smog Chamber Photochemical Experiments," Environmental Protection Agency, Publication No. EPA-650/4-74-040 (1974).

38. Jaffe, R. J., "Lighting Effects in Smog Simulations I. Constant Intensity vs. Diurnal Variation," Presented at 68th Annual Air Pollution Control Association Meeting, Boston (1975).

39. Shuck, E. A., Stephens, E. R., and Schrock, R. R., "Rate of Constant Ratios During Nitrogen Dioxide Photolysis," J. of Air Pollution Contr. Assoc., 16, p. 1965 (1966).

SECTION X

GLOSSARY

Aerometric data - Data resulting from measurements of pollutant concentrations in the ambient air.

ARB - California Air Resources Board.

Background run - A run in which the chamber was charged with only rural, ambient air just prior to sunrise.

BLUE or BLUE side - see "side".

BOM - Bureau of Mines

Calibration equations - Equations used to calculate the substance values in physical units from instrument voltage output and/or substance values.

Crossover - The time at which the NO_2 concentration equals the NO concentration. (Runs for which the initial NO_2 exceeded the initial NO do not have a crossover. Also, crossover does not occur in extremely slow runs).

DAS - Data acquisition system.

.DAT files - Computer files at TUCC containing measurement data as collected during a run plus comments of operator made during the run.

Dilution run - A run in which the contents of the chamber are diluted with rural ambient air after the injection at a constant flowrate. Chamber is run as a continuous - flow stirred - tank reactor (CFSTR) with very low reactant concentrations in the incoming dilution air.

Dosage - The area under a concentration versus time graph for some specific time interval, in units of concentration x time.

Dual run - An experiment using both sides of the chamber to compare the effects of differences in controlled variables (such as initial concentrations) under identical solar radiation and temperature conditions.

Greenhouse effect - (With respect to a smog chamber) the heating of the gas within a chamber due to the transmission of shortwave radiation into the chamber and absorption of long-wave (infra red) radiation by the chamber walls preventing radiative cooling of chamber contents.

HC/NOX - The ratio of non-methane hydrocarbons to oxides of nitrogen present in the chamber initially, ppmC/ppm.

HP - Hewlett-Packard 9810A Programmable calculator with plotter.

IHC (initial hydrocarbon) - non-methane hydrocarbon concentration at the time of completion of the hydrocarbon injection.

Injection - The process by which the chamber is charged with reactants. A solenoid valve is opened for a specified time allowing gas to flow at a known rate from cylinders, through precision needle valves, and into the return line of the sampling manifold. The return link transports injected material to the chamber just below a mixing fan for rapid dispersal of material.

INO (initial nitric oxide) - The nitric oxide concentration at the time of completion of the hydrocarbon.

INOX (initial nitrogen oxides) - The concentration of NO_x (essentially NO and NO_2) at the time of completion of the hydrocarbon injection.

k_1 - see "ϕka"

ϕka - The first order rate constant of NO_2 photo-dissociation.

Molar reactivity - The Jackson reactivity of a hydrocarbon mixture computed by weighing the reactivities of the individual compounds by their mole fractions in the mixture.

NAAQS - National Ambient air quality standard(s).

NMHC - Non-methane hydrocarbons; total hydrocarbons minus methane as measured by a flame ionization detector times an empirical efficiency factor.

O_x - Photochemical oxidants

Oxidant standard - National air quality standard for photochemical oxidants, measured as ozone. The primary and secondary standards are both 0.08 ppm, a 1-hour average not to be exceeded more than once per year.

PCT NO_2 - see "percentage NO_2"

Percentage NO_2 or PCT NO_2 - The initial NO_2 divided by the initial NO_x, multiplied by 100.

Percentage NO_2 run - A dual run in which the only difference between chamber sides initially is the percentage NO_2 -- the initial NO_x and hydrocarbons being nearly identical.

pphm - Parts per hundred million; moles of pollutant per 10^8 moles of gas.

ppm - Parts per million; moles of pollutant per 10^6 moles of gas.

QGA - Quartz globe actinometer; device for measuring the rate constant of NO_2 photo-dissociation.

RED or RED side - See "side".

Run - An experiment performed in one side of the chamber with data collection from 0500 to 1700 Eastern Daylight Savings Time.

Run identification - For the purpose of data processing each run has been assigned a 7-digit alphanumeric word of the form: YYMMDDS where YY is the last two digits of the year in which run was performed, MM is the number of the month in which run was performed, DD is the day of the month on which run was performed, S is the side of the chamber on which run was performed, either R for red or B for blue.

SAS - Statistical Analysis System, a collection of statistical computer programs.

S.C.O.T. - Supported column, open, tubular.

Side - The chamber is divided into two 6000 ft^3 compartments, which are arbitrarily designated as the "BLUE" side and the "RED" side.

.SMTH files - Computer files at TUCC containing smooth estimates of raw data, the derivatives and integrals of smoothed estimates plus operator comments.

SPSS - Statistical Package for the Social Sciences, a collection of statistical computer programs.

Static run or static operation - A run in which the chamber is operated as a batch reactor: reactants are charged before sunrise, the chamber is then closed, and reaction takes place without further input of material.

Substance - (With respect to data acquistion) any of the chemical quantities or physical properties being measured.

THC - Total hydrocarbons, i.e., methane plus non-methane corrected by an empirical efficiency factor measured by a flame ionization detector.

TSO - Time Sharing Option; an interactive system for on-line computation.

TSR - Total solar radiation.

TUCC - Triangle Universities Computation Center.

UNC - University of North Carolina at Chapel Hill.

SECTION XI

APPENDICES

Page

A. Standard Nomenclature Conventions Adopted 187

B. Equations Used in Computer Programs 190

C. Photochemical Model for Propylene 194

D. Statistical Assessment of Ozone Calibration Procedure 200

E. Device for the Continuous Measurement of ϕk_a for Nitrogen Dioxide 204

Appendix A

STANDARD NOMENCLATURE CONVENTIONS ADOPTED

The following conventions were used to name variables considered in data analysis:

Main Components

NOX - total nitrogen oxides (NO + NO$_2$), ppm

NO - nitric oxide, ppm

NO$_2$ - nitrogen dioxide, ppm

HC - nonmethane hydrocarbon, ppmC

TIME - mins after 0500 EDT

TEMP - air temperature, °F

SR_ - total solar radiation (2800°A-25,000°A), langleys/min = cal/cm^2/min

UV_ - ultraviolet radiation, millilangleys/min = millical/cm^2/min (2800°A-3900°A)

I_TP - integrated temp, °F-mins

I_SR - integrated total solar radiation, Langley = gmcal/cm^2

I_UV - integrated ultraviolet radiation, millilangleys = milligmcal/cm^2

D_ccc - dosage of species ccc, concentration · time

Prefixes & Suffixes (main component indicated by ccc)

ICCC - initial, e.g. INOX - initial NO$_x$, INO$_2$ - initial NO$_2$

Xccc - crossover where NO = NO$_2$, e.g. XNOX - NO$_x$ crossover conc, XHC-HC conc
or
ccc_X at NO$_x$ crossover point

cccR - rate, ppb/min; with no other modifier, indicates a max value
e.g. NOR - maximum NO rate O3R - maximum O$_3$ rate

cccM - maximum concentration, ppm; e.g. NO_2M - maximum concentration when a main component name is used as a prefix it indicates "at the time of"

ccc_INT - initial, just after the HC injection is completed

ccc_FIN - final, the time of the last recorded data or 1700 which ever is earlier

ccc_DIF1 - delta or difference between initial state and crossover condition

ccc_DIF2 - delta or difference between cross condition and NO_2 max rate

ccc_DIF3 - delta or difference between NO_2 max rate condition and NO_2 max conc

ccc_DIF4 - delta or difference between NO_2 max conc condition and O_3 max rate condition

ccc_DIF5 - delta or difference between O_3 max rate condition and O_3 max conc condition

ccc_DIF_F - delta or difference between init and final
or
ccc_DIF_T

ccc_AV1 - same as DT1 thru DT5, except average condition between events
or
ccc_AVE1

thru
ccc_AV5
or
ccc_AVE5

ccc_A23 or ccc_AV23 - average across events 2 and 3 as defined in DT1 definitions i.e., from crossover event to max NO_2 event

ccc_A45 to ccc_AV45 - average across events 4 and 5 as defined in DT4 and DT5 definition i.e., from NO_2 max conc to O_3 max concentration

ccc_NOR - at the time of maximum rate of change of the NO concentration

ccc_NO2R - at the time of maximum rate of change of the NO_2 concentration

ccc_NM - at the time of the maximum NO_2 concentration
or
ccc_NO2M

ccc_O3R - at the time of the maximum rate of change of the O_3 concentration

ccc_O3M - at the time of the maximum O_3 concentration

APPENDIX B

EQUATIONS USED IN COMPUTER PROGRAMS

TRANSFER EQUATIONS:

All underlined constants can be modified during run, and represent default values. S represents physical units and V represents measured voltages.

Ozone: $S_{O3} = \underline{1.0}\,(V_{O3}) + \underline{0.0}$

Nitric Oxide: $S_{NO} = \underline{1.0}\,(V_{NO}) + \underline{0.0}$

Nitrogen Dioxide: $S_{NO2} = \underline{1.0}\,(V_{NO2}) + \underline{0.0}$

Oxides of Nitrogen: $S_{NOX} = \underline{1.0}\,(V_{NOX}) + \underline{0.0}$

Humidity (Dew Point): $S_{DP} = \underline{4.724}\,(V_{DP}) + 0.0185\,(V_{DP})^2 + 0.000242(V_{DP})^3 - \underline{40.0}$

Methane: $S_{CH4} = \{\underline{1.0}[S_{CH4}(n-1) + \underline{1.0}(V_{CH4}) + 0.0]/n\} + \underline{0.0}$

where n is number of readings; n can be reset to 0 during the run

Non-Methane Hydrocarbons: $S_{NMHC} = \underline{1.613}^{*}\,[1.0(V_{THC}) + \underline{0.0} - S_{CH4}] + \underline{0.0}$

Total Hydrocarbons: $S_{THC} = \underline{1.0}\,[S_{CH4} + S_{NMHC}] + \underline{0.0}$

Carbon Monoxide: $S_{CO} = \underline{2.0}\,(V_{CO}) + \underline{0.0}$

Temperature: $S_T = \underline{100.00}\,(V_T) + \underline{0.0}$

Solar Radiation: $S_{SR} = \underline{123.0}\,(V_{SR}) + \underline{0.0}$

UV Radiation: $S_{UV} = \underline{12195.122}\,(V_{UV}) + \underline{0.0}$

* This is the default value of multiplier which corresponds to an average sampling efficiency of 62% and was adjusted by operator, if necessary, based on daily or weekly calibration.

COMPUTATIONS USED IN SMOOTH PROGRAM

Given that $x_1 < x_2 < x_3 < x_4 < x_5$ and

$$x_2 - x_1 = x_3 - x_2 = x_4 - x_3 = x_5 - x_4 ,$$

the parabola that fits the points

$$(x_1,y_1),\ (x_2,y_2),\ (x_3,y_3),\ (x_4,y_4),\ (x_5,y_5)$$

in a least squares fashion has the following form:

$$y = a_o + a_1x + a_2x^2$$

where

$$a_o = (-6y_1 + 24y_2 + 34y_3 + 24y_4 - 6y_5)/70$$
$$a_1 = (-2y_1 - y_2 + y_4 + 2y_5)/10$$
$$a_2 = (2y_1 - y_2 - 2y_3 - y_4 + 2y_5)/14$$

thus, to compute S_t, a smoothed estimate of D_t, a data value at time t, the following equation is used:

$$S_t = a_o$$

where

$$a_o = (-6D_{t-2} + 24D_{t-1} + 34D_t + 24D_{t+1} - 6D_{t+2})/70$$

and

$\{D_{t-2}, D_{t-1}, D_t, D_{t+1}, D_{t+2}\}$ is a set of data points equally spaced in time

To compute a measure of fit, r^2, the squared correlation coefficient is computed between the sets

$$\{D_{t-2}, D_{t-1}, D_t, D_{t+1}, D_{t+2}\}$$

and

$$\{S_{t-2}, S_{t-1}, S_t, S_{t+1}, S_{t+2}\}.$$

The derivative with respect to time $\frac{dS_t}{dt}$, of a smoothed estimate at time t is given by the following equation:

$$\frac{dS_t}{dt} = a_1/I$$

where

$$a_1 = (-2D_{t-2} - D_{t-1} + D_{t+1} + 2D_{t+2})/10$$

and

I = Number of time units between time t and time t+1; in the UNC data, this was 8 minutes

To derive smoothed estimates of the first two points in a data set, the following equations are used:

$$S_1 = a_0 - 2a_1 + 4a_2$$

$$S_2 = a_0 - a_1 + a_2$$

where

$$a_0 = (-6D_1 + 24D_2 + 34D_3 + 24D_4 - 6D_5)/70$$

$$a_1 = (-2D_1 - D_2 + D_4 + 2D_5)/10$$

$$a_2 = (2D_1 - D_2 - 2D_3 - D_4 + 2D_5)/14$$

To derive smoothed estimates of the last two points in a data set with n readings, the following equations are used:

$$S_{n-1} = a_0 + a_1 + a_2$$

$$S_n = a_0 + 2a_1 + 4a_2$$

where

$$a_0 = (6D_{n-4} + 24D_{n-3} + 34D_{n-2} + 24D_{n-1} - 6D_n)/70$$

$$a_1 = (-2D_{n-4} - D_{n-3} + D_{n-1} + 2D_n)/10$$

$$a_2 = (2D_{n-4} - D_{n-3} - 2D_{n-2} - D_{n-1} + 2D_n)/14$$

For the first two points and the last two points, the derivative is not computed.

To compute the integral, $\int_1^t S_t$, of a set of smooth estimates up to and including time t, the following equation is used:

$$\int_1^t S_t = \sum_{i=2}^{t} \{(S_i + S_{i-1})/2\} * I$$

where

I = number of time units between time t and time t+1; in the UNC data, this was 8 minutes.

APPENDIX C

PHOTOCHEMICAL MODEL FOR PROPYLENE

INTRODUCTION

The model described in this appendix was based primarily upon a simplification of the more than 250-step mechanism used by Demerjian, Kerr, and Calvert[34] and the work of Hecht, et al.[35] Dr. Dodge also supplied a copy of EPA's kinetic simulation program developed by J. Overton which uses the Gear differential equation solving subroutine for stiff differential equations. The Overton program was modified by Dr. Baker of UNC to allow for a time-varying light intensity profile, for rate constant changes for any reaction in the course of a simulation, for variable dilution rates, and for improved output to allow better assessment of the importance of an individual reaction step.

DEVELOPMENT

The propylene mechanism presented below was the ninth version written and tested. It has 35 steps, fifteen of which are "lumped" or net reaction steps which represent the results of a sequence of very fast radical rearrangement or radical-oxygen reactions. Earlier versions had up to 60 steps and 24 species, the present limit of the kinetic simulation program. Each reaction was tested for its importance to the time profile shape of the major species during the course of the 10-hour simulation and was eliminated if its contribution was found not to be significant in this time period. For example, the model was frequently run without the N_2O_5 chemistry. These reactions were found to be not very significant in the daylight simulations in the UNC chamber, but merely served as a cyclic process with little net effect in relation to other, more important, reactions such as $OH+NO_2 \rightarrow HNO_3$.

Mass balances in the model were not maintained for such species as H_2O, O_2, and CO_2 and were not completely maintained for CO. The concentration of H_2O and O_2 were lumped into the necessary rate constants and CO_2, formic acid, acetic acid, and other low concentration products were not quantified (that is, they were allowed to "disappear" from the mechanism). Since $O + C_3H_6$ resulted in the same reaction products as $O_3 + C_3H_6$ and the primary fate of atomic oxygen (O) is $O + O_2 \rightarrow O_3$, atomic oxygen reactions were lumped into Reactions 1 and 15. Other atomic oxygen reactions were found not to be competitive and were deleted.

ORGANIC RADICAL SYMBOLS

The mechanism contains seven organic radical symbols which represent the radicals that result after rearrangement and reaction with oxygen. The original radicals are the initial products of $O_3 + C_3H_6$, $OH + C_3H_6$, $HO_2 + C_3H_6$, $OH + CH_2O$, and OH + RCHO, where C_3H_6 represents a propylene molecule, CH_2O represents a formaldehyde molecule, and RCHO represents an acetaldehyde molecule. The seven organic radicals and the stoichiometry used in the mechanism resulted from summarizing the more specific reaction sequences of Demerjian et al.[34] An example of such a summarization is shown in Figure 87. Table 21 gives, for each organic radical symbol in the mechanism, the proposed molecular configuration suggested by Demerjian. In addition, Table 21 also gives the molecular structure assumed for other organic species in the mechanism.

45a) $CH20 \xrightarrow{h\nu} H + HCO \quad (2 \times 10^{-3} \text{ when } k_1 = 0.48)$

44) $H + O_2 \rightarrow HO_2 \quad (1.7 \times 10^{-3})$

47a) $HCO + O_2 \rightarrow CO + HO_2 \quad (250)$

48a) $HCO + O_2 \xrightarrow{m} HCO_3 \quad (100)$

49a) $HCO_3 + NO \rightarrow HCO_2 + NO_2 \quad (1500)$

52) $HCO_2 \rightarrow H + CO_2 \quad (1.5 \times 10^{10})$

44) $H + O_2 \rightarrow HO_2 \quad (1.7 \times 10^{-3})$

51a) $HCO_3 + NO_2 \rightarrow HCO_3NO_2$ [PFN] (490)

53a) $HCO_3NO_2 \rightarrow CO_2 + HNO_3 \quad (4.2 \times 10^{8})$

- -

$CH20 \xrightarrow{h\nu} (1 + 250/350)\, HO2 + (100/350) HCO_3 + (250/350) CO \quad (2.0 \times 10^{-3} \text{ when } k_1 = 0.48)$

$HCO_3 + NO \rightarrow NO_2 + HO_2 + CO_2 \quad (1500)$

$HCO_3 + NO_2 \rightarrow HNO_3 + CO_2 \quad (490)$

Figure 86. Formaldehyde photolysis chemistry. Top: elementary steps proposed by Demerjian et al., 34; Bottom: Lumped equations used in propylene model in this report. Equation numbers and rates on top portion are those adopted by Demerjian et al.

Table 22. ORGANIC SYMBOLS USED IN MECHANISM

Mechanism Symbol	Molecular Formula
RHO_3	$CH_3CH(O_2)CH_2OH$
RHO_2	$CH{=}CHCH_2O_2$
RHO_4	$CH_3CH(O_2)CH_2O_2H$
RCO_3	CH_3OO_2
HCO_3	$HCOO_2$
ROO	CH_3OO
RO_3	$CH_2(O_2)OH$
RCHO	CH_3CHO
CH_2O	$H_2C{=}O$
C_3H_6	$CH_3CH{=}CH_2$
PAN	$CH_3COOONO_2$

PHOTOCHEMICAL MODEL FOR PROPYLENE

No.	Reaction	Rate constant[a,e]
Nitrogen Dioxide Photolysis:		
1:	$NO_2 \rightarrow 1.00\ NO + 1.00\ O_3$	k_1
Nitric Oxide Oxidation:		
2:	$O_3 + NO \rightarrow 1.00\ NO_2$	2.4×10^{1}G
3:	$HO_2 + NO \rightarrow 1.00\ NO_2 + 1.00\ OH$	2.9×10^{2}G
4:	$RHO_2 + NO \rightarrow 1.00\ NO_2 + 2.00\ CH_2O + 0.72\ HO_2 + 0.28\ HCO_3 + 0.72\ CO$	4.7×10^{2}D
5:	$RHO_3 + NO \rightarrow 1.00\ NO_2 + 1.00\ RO_3 + 0.96\ RCHO + 0.04\ CH_2O + 0.04\ CO$	4.7×10^{2}D
6:	$RO_3 + NO \rightarrow 1.00\ NO_2 + 1.00\ HO_2 + 1.00\ CO$	4.9×10^{3}D
7:	$RHO_4 + NO \rightarrow 1.00\ NO_2 + 1.00\ OH + 1.00\ RCHO + 1.00\ CH_2O$	4.7×10^{2}D
8:	$RCO_3 + NO \rightarrow 1.00\ NO_2 + 1.00\ ROO$	1.5×10^{3}D'
9:	$HCO_3 + NO \rightarrow 1.00\ NO_2 + 1.00\ HO_2 + 1.00\ CO$	1.5×10^{3}D'
10:	$ROO + NO \rightarrow 1.00\ NO_2 + 1.00\ HO_2 + 1.00\ CH_2O$	1.5×10^{3}D'
11:	$PAN + NO \rightarrow 2.00\ NO_2 + 1.00\ ROO$	1.6×10^{-1}D
Major Nitrogen Dioxide Losses:		
12:	$OH + NO_2 \rightarrow 1.00\ HNO_3$	8.5×10^{3}G
13:	$RCO_3 + NO_2 \rightarrow 1.00\ PAN$	4.9×10^{2}D
14:	$HCO_3 + NO_2 \rightarrow 1.00\ HNO_3 + 1.00\ CO_2$	5.0×10^{2}D
Propylene Oxidation:		
15:	$O_3 + C_3H_6 \rightarrow 1.50\ HO_2 + 0.50\ RCHO + 0.50\ CH_2O + 0.50\ ROO + 1.00\ CO$	1.8×10^{-2}G
16:	$OH + C_3H_6 \rightarrow 0.61\ RHO_3 + 0.39\ RHO_2$	2.1×10^{4}G
17:	$HO_2 + C_3H_6 \rightarrow 0.95\ RHO_4 + 0.02\ H_2O_2 + 0.02\ RHO_2$	1.1×10^{0}D

Aldehyde Chemistry:

18:	CH_2O	→	$1.71\ HO_2$	$+\ 0.29\ HCO_3$	$+\ 0.71\ CO$	$0.004k_1$ b
19:	$OH + CH_2O$	→	$0.71\ HO_2$	$+\ 0.29\ HCO_3$	$+\ 0.71\ CO$	2.1×10^4 G
20:	$RCHO$	→	$0.71\ HO_2$	$+\ 0.29\ HCO_3$	$+\ 1.00\ ROO$	$0.00175k_1$ b
21:	$OH + RCHO$	→	$1.00\ RCO_3$			2.2×10^4 D

Hydrogen Peroxide Chemistry:

22:	$HO_2 + HO_2$	→	$1.00\ H_2O_2$		4.0×10^3 G
23:	H_2O_2	→	$2.00\ OH$		$0.01k_1$ b
24:	$OH + H_2O_2$	→	$1.00\ HO_2$		1.2×10^3 G

Nitrous Acid Chemistry:

25:	$NO_2 + NO$	→	$2.00\ HNO_2$		3.2×10^{-5} d,c
26:	$HNO_2 + HNO_2$	→	$1.00\ NO_2$	$+\ 1.00\ NO$	1.7×10^{-3} D
27:	$HO_2 + NO_2$	→	$1.00\ HNO_2$		5.0×10^{-2} D
28:	$OH + NO$	→	$1.00\ HNO_2$		4.9×10^3 H
29:	$OH + HNO_2$	→	$1.00\ NO_2$		1.0×10^4
30:	HNO_2	→	$1.00\ OH$	$+\ 1.00\ NO$	$0.1k_1$ b

Ozone- Nitrogen Dioxide Dark Phase Chemistry:

31:	$O_3 + NO_2$	→	$1.00\ NO_3$		4.6×10^{-2} G
32:	$NO_3 + NO$	→	$2.00\ NO_2$		1.3×10^4 G
33:	$NO_3 + NO_2$	→	$1.00\ N_2O_5$		5.6×10^3 G
34:	N_2O_5	→	$1.00\ NO_2$	$+\ 1.00\ NO_3$	1.7×10^1 b G
35:	N_2O_5	→	$2.00\ HNO_3$		1.0×10^{-2} b,c,d,

[a] units are ppm^{-1}-min^{-1} unless otherwise stated

[b] units are min^{-1}

[c] water concentration included in rate constant

[d] heterogeneous and homogeneous rate combined

[e] reference for rate constant; G = Garvin, et al., D = Demerjian, et al., D' = Dodge, H = Hampson, et al.

APPENDIX D

STATISTICAL ASSESSMENT OF OZONE CALIBRATION PROCEDURE

The use of analytical instruments to measure low concentration of air contaminants often leads to data of uncertain quality. One measure of data quality is the confidence interval for a measured volume of concentration. The confidence interval is the range of concentrations believed to contain the true concentration with a certain level of confidence. The level of confidence is related to the probability that the actual value is within the interval, but it is not a true probability since the actual concentration is a constant for any given measurement.

The calibration procedure for the chemiluminescent ozone instrument was studied in order to calculate the confidence intervals for measurements of ozone and to determine which factors in the calibration have the greatest effects on data quality. The ozone instrument itself is very precise, but its accuracy depends on the calibration procedure. The calibration technique employs a neutral buffered potassium iodide as a reference standard to measure a concentration of ozone from an ozone generator. The instrument is adjusted to agree with the result of the NBKI determination.

The relationship between absorbance, X, and equivalent ozone collected, Y', was determined by a weighted regression using five sets of serial dilutions. It was found that the greatest source of error was in the titration and dilution of standard I_2 solutions. Thus, several sets of data for different I_2 solutions must be considered to minimize bias. The slope was calculated by the following equation:

$$b = \frac{\sum_{i=1}^{n} Y'_i}{\sum_{i=1}^{n} X_i}$$

This yields the following least squares fit:

$$Y'(\text{pphm-liters}) = 262.806\ X\ (\text{absorbance})$$

The confidence interval for the biased ozone measurements after calibration may be determined by the following equations:

$$[L,U] = \left[Y_p \pm t_{(1-\alpha/2)(n-1)} \left[\frac{\text{Var}(Y_n)}{k} + S_e{}^2 \frac{X^2}{\sum_{i=1}^{n} X_i} \right]^{1/2} \right] \frac{1}{V}$$

$$S_e{}^2 = \frac{1}{n-1} \sum_{i=1}^{n} \frac{(Y_i - Y_{pi})^2}{X_i}$$

Where Y_p is the estimated value of ozone concentration in pphm; t is the Students' -t statistic with a cumulative probability density of $(1 - \alpha/2)$ and n - 1 degrees of freedom; Y_n is a new value of ozone collected from an actual NBKI bubbler run; k is the number of replicate bubbler runs; X is the absorbance correcponding to the mean of the concentrations determined by NBKI; $\sum_{i=1}^{n} x_i$ is the sum of all absorbances used in the weighted regression; Y_i and Y_{pi} are the actual and predicted values of O_3 collected at each point used in the weighted regression; V is the volume of air from the ozone generator that is sampled in each bubbler run. The quantity $\text{Var}(Y_n)$ must be determined empirically and ranges between 0.69 and 6.75 in the procedure studied. The $S_e{}^2 x^2/\Sigma x_i$ term was $5.2x^2$.

The most critical factor is the number of replicates. Table 22 illustrates the effect of the number of replicate NBKI measurements on the confidence interval on bias for measuring ozone at the Federal air quality standard -- 8 pphm.

The best-case and worst-case figures represent uncertainty in $Var(Y_n)$. As k is increased the term $S_e^2 x^2 / \Sigma X_i$ becomes more significant; this is related to the ability of the analyst to consistently produce standard I_2 solutions. This term also has increasing importance at higher concentrations.

Initial calibrations performed in the previous first year grant period were with 7 to 8 replicates. Later, weekly calibrations were done with 4 replicates. The long-term average slope of $[I_2]$ versus absorbance was used in the O_3 concentration prediction. Project personnel feel that the accuracy of O_3 determinations at the National Ambient Air Quality standard of 0.08 ppm was valid to within less than ± 0.01 ppm (0.95 confidence limit).

Since the ozone meter was used to measure ozone concentration and change in concentration for the O_3-NO gas phase titration used as a claibration for the NO_x meter, the NO_x meter accuracy would probably have been less than the O_3 meter accuracy because of further transfer and measurement errors. Therefore the best-case estimate of the NO_x accuracy would be ± 0.01 ppm.

Table 23. CONFIDENCE INTERVALS ON ACCURACY OF MEASUREMENT OF OZONE AT 8 PPHM

Number of Replicates	Confidence Intervals	
	Best Case[a]	Worst Case[b]
1	8 ± 1.4 pphm	8 ± 4.4 pphm
2	8 ± 1.1	8 ± 3.1
4	8 ± 0.83	8 ± 2.2
6	8 ± 0.73	8 ± 1.8
8	8 ± 0.68	8 ± 1.6

[a] Data taken by skilled operator in constant practice

[b] Data taken by students performing technique for first time

APPENDIX E

DEVICE FOR THE CONTINUOUS MEASUREMENT OF ϕk_a FOR NITROGEN DIOXIDE

A quartz globe actinometer (QGA) utilizing NO_2 in N_2 as the sensing gas was developed by Sickles and Jeffries[23] in the fall of 1974. The QGA is illustrated schematically in Figure 87. It is operated as a continuous stirred tank reactor (CSTR) and can be used in either steady-state or nonsteady-state light conditions. The solution of a simple equation utilizing the inlet and outlet NO_2 concentrations gives ϕk_a directly.

The kinetics of NO_2 photolysis in N_2 were orginally derived by Shuck et al.[39] and are expressed in Equation 8:

$$r = -2k_1\left[\frac{1}{[NO_2]} + \frac{R_1}{[NO_2]} + \frac{R_2[NO]}{[NO_2]^2} + \frac{R_3[O_2]}{[NO_2]^2}\right]^{-1} \tag{8}$$

where $k_1 = \phi k_a$ for NO_2

$R_1 = k_6[M]/k_5 = 0.268$

$R_2 = k_7[M]/k_5 = 0.25$

$R_3 = k_2[M]/k_5 = 1.55 \times 10^{-3}$

$[NO_2]$ = NO_2 concentration in ppm

r has units of ppm-min^{-1} and

k_5 is the rate constant for $O + NO_2 \rightarrow NO + O_2$

k_6 is the rate constant for $O + NO_2 + (M) \rightarrow NO_3$

k_7 is the rate constant for $O + NO + (M) \rightarrow NO_2$

k_2 is the rate constant for $O + O_2 + (M) \rightarrow O_3$

Several assumptions are embodied in Equation 8. These are $[O_2]_o$,

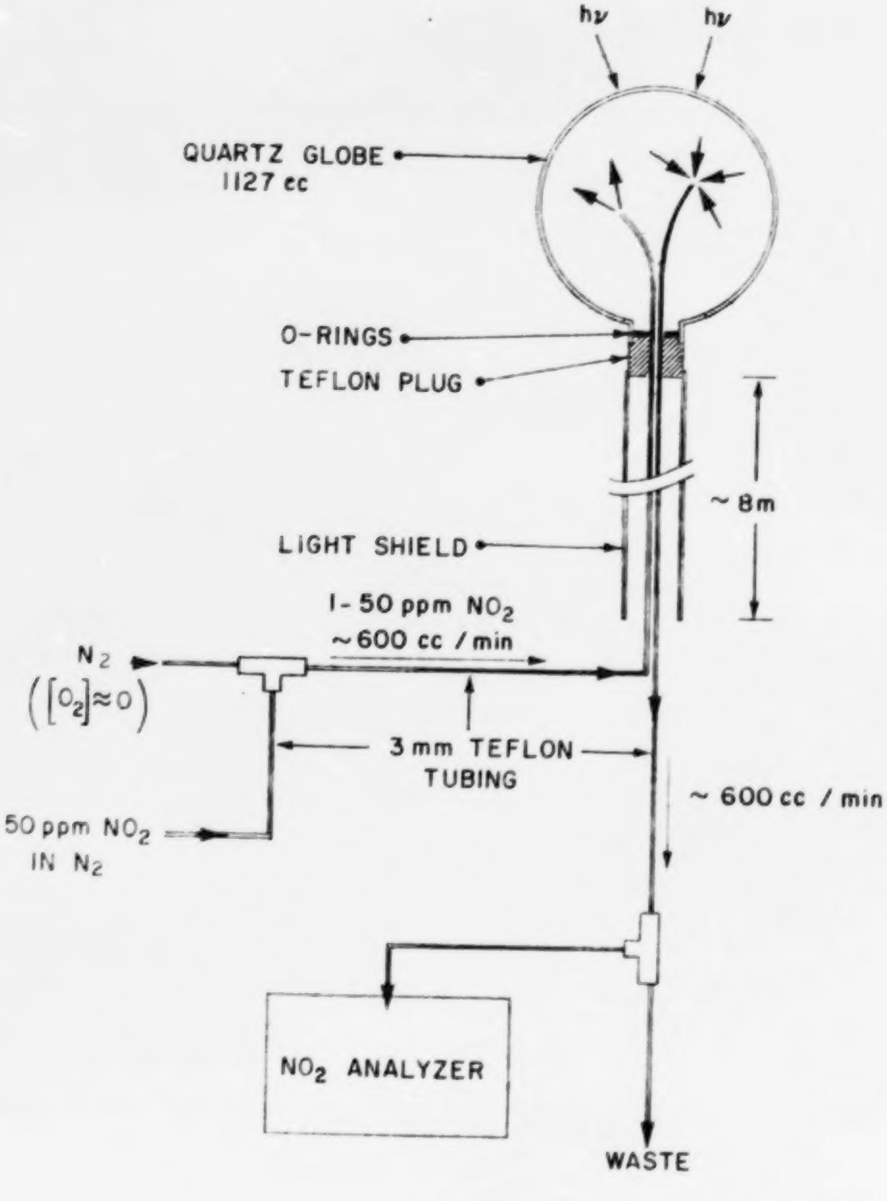
hν
hν
QUARTZ GLOBE
1127 cc
O-RINGS
TEFLON PLUG
~ 8m
LIGHT SHIELD
1-50 ppm NO2
~600 cc / min
N2
([O2]≈0)
3 mm TEFLON TUBING
~ 600 cc / min
50 ppm NO2 IN N2
NO2 ANALYZER
WASTE

Figure 87. Flow Diagram of One Liter Quartz Globe CSTR for Nitrogen Dioxide Photolysis Rate Measurements.

$[NO_3]$, and $[N_2O_5]$ are small, and that pseudo-steady-state exists for O, O_3, NO_3, and N_2O_5. The most serious assumption is that of steady-state for N_2O_5 which is not achieved for nearly 40 seconds at typical conditions.

If the necessary condition for CSTR operation (ideal mixing) is assumed to hold in the QGA, then a mass balance yields:

$$V\frac{dC}{dt} = QC_o - QC + Vr \qquad (9)$$

where V = volume of globe
Q = flow rate
C_o = NO_2 concentration at inlet
C = NO_2 concentration at outlet and inside the globe
t = time
r = reaction net rate = $d[NO_2]/dt = f(NO_2,\text{light})$

Rearrangement gives:

$$-r = \frac{[NO_2]_o - [NO_2]}{\tau} = \frac{\Delta[NO_2]}{\tau} \qquad (10)$$

where τ = Q/V and steady flow and light intensity are assumed
and $t > 7\tau$

Substitution of Equation 8 in Equation 10 yields:

$$k_{1_{ss}} = \frac{\Delta[NO_2]}{2\tau[NO_2]}\left[1 + R_1 + \frac{R_2([NO]_o + \Delta[NO_2]) + R_3[O_2]}{[NO_2]}\right] \qquad (11)$$

which is the basic equation for the QGA.

If $[O_2]_o$ and $[NO]_o$ are negligible, then Equation 11 may be simplified to:

$$k_{1_{ss}} = \frac{\Delta[NO_2]}{2\tau[NO_2]}\left[1 + R_1 + R_2\frac{\Delta[NO_2]}{[NO_2]}\right] \qquad (12)$$

If the light intensity is not constant, Equation 8 may be substituted in Equation 9 directly to yield:

$$k_{1_{nss}} = \frac{1}{2[NO_2]}\left[\frac{\Delta[NO_2]}{\tau} - \frac{d[NO_2]}{dt}\right]$$

$$\left[1 + R_1 + \frac{R_2([NO]_o + \Delta[NO_2]) + R_3[O_2]}{[NO_2]}\right] \qquad (13)$$

which for $[NO]_o$ and $[O_2]_o$ nearly zero can also be simplified to:

$$k_{1_{nss}} = \frac{1}{2[NO_2]}\left[\frac{\Delta[NO_2]}{t} - \frac{d[NO_2]}{dt}\right]\left[1 + R_1 + \frac{R_2\Delta[NO_2]}{[NO_2]}\right] \quad (14)$$

The derviative of the NO_2 outlet may be approximated numerically, however, for outdoor conditions, only a small error occurs by assuming that it is zero and using Equation 11.

The QGA has been extensively evaluated by experiment and by computer simulation studies and these are reported elsewhere[23]. These results indicate a 95% confidence limit on precision at $k_1 = 0.50$ mins^{-1} of $^{+}$3.25 % and on accuracy of ± 10.2%. The limit on accuracy is largely due to uncertainties in the values of the rate constant ratios R_1, R_2, and R_3. In actual use in an indoor smog chamber, the standard deviation of nine replicates readings at $k_1 = 0.496$ min^{-1} was ± 0.01 min^{-1} over a three hour period.